MycoKeys 83: 1–37 (2021)
doi: 10.3897/mycokeys.83.68926
https://mycokeys.pensoft.net

RESEARCH ARTICLE

A peer-reviewed open-access journal
MycoKeys
Launched to accelerate biodiversity research

New contributions to Diatrypaceae from karst areas in China

Sihan Long[1,2], Lili Liu[3], Yinhui Pi[1], Youpeng Wu[1], Yan Lin[1], Xu Zhang[1], Qingde Long[1], Yingqian Kang[4], Jichuan Kang[5], Nalin N. Wijayawardene[1,6], Feng Wang[7], Xiangchun Shen[1,2], Qirui Li[1,2]

1 *State Key Laboratory of Functions and Applications of Medicinal Plants, Guizhou Medical University, Guiyang 550004, China* **2** *The High Efficacy Application of Natural Medicinal Resources Engineering Center of Guizhou Province (The Key Laboratory of Optimal Utilization of Natural Medicine Resources), School of Pharmaceutical Sciences, Guizhou Medical University, University Town, Guian New District, Guizhou 550025, China* **3** *Immune Cells and Antibody Engineering Research Center of Guizhou Province/ Key Laboratory of Biology and Medical Engineering, Guizhou Medical University, Guiyang 550004, China* **4** *Key Laboratory of Environmental Pollution Monitoring and Disease Control, Ministry of Education of Guizhou and Guizhou Talent Base for Microbiology and Human Health, School of Basic Medical Sciences, Guizhou Medical University, Guiyang, China* **5** *Engineering and Research Center for Southwest Bio-Pharmaceutical Resources of National Education Ministry of China, Guizhou University, Guiyang, Guizhou 550025, China* **6** *Center for Yunnan Plateau Biological Resources Protection and Utilization, College of Biological Resource and Food Engineering, Qujing Normal University, Qujing, Yunnan 655011, China* **7** *Guizhou Provincial Academician Workstation of Microbiology and Health, Guizhou Academy of Tobacco Science, Guiyang, Guizhou, 550000, China*

Corresponding author: Qirui Li (lqrnd2008@163.com)

Academic editor: Andrew Miller | Received 20 May 2021 | Accepted 20 July 2021 | Published 20 August 2021

Citation: Long S–H, Liu L–L, Pi Y–H, Wu Y–P, Lin Y, Zhang X, Long Q–D, Kang Y–Q, Kang J–C, Wijayawardene NN, Wang F, Shen X–C, Li Q–R (2021) New contributions to Diatrypaceae from karst areas in China. MycoKeys 83: 1–37. https://doi.org/10.3897/mycokeys.83.68926

Abstract

In this study, fungal specimens of the family Diatrypaceae were collected from karst areas in Guizhou, Hainan and Yunnan Provinces, China. Morpho-molecular analyses confirmed that these new collections comprise a new genus *Pseudodiatrype*, three new species (*Diatrype lancangensis*, *Diatrypella pseudooregonensis* and *Eutypa cerasi*), a new combination (*Diatrypella oregonensis*), two new records (*Allodiatrype thailandica* and *Diatrypella vulgaris*) from China and two other known species (*Neoeutypella baoshanensis* and *Paraeutypella citricola*). The new taxa are introduced, based on multi-gene phylogenetic analyses (ITS, β-tubulin), as well as morphological analyses. The new genus *Pseudodiatrype* is characterised by its wart-like stromata with 5–20 ascomata immersed in one stroma and the endostroma composed of thin black

outer and inner layers of large white cells with thin, powdery, yellowish cells. These characteristics separate this genus from two similar genera *Allodiatrype* and *Diatrype*. Based on morphological as well as phylogenetic analyses, *Diatrype lancangensis* is introduced as a new species of *Diatrype*. The stromata of *Diatrype lancangensis* are similar to those of *D. subundulata* and *D. undulate*, but the ascospores are larger. Based on phylogenetic analyses, *Diatrype oregonensis* is transferred to the genus *Diatrypella* as *Diatrypella oregonensis* while *Diatrypella pseudooregonensis* is introduced as a new species of *Diatrypella* with 8 spores in an ascus. In addition, multi-gene phylogenetic analyses show that *Eutypa cerasi* is closely related to *E. lata*, but the ascomata and asci of *Eutypa cerasi* are smaller. The polyphyletic nature of some genera of Diatrypaceae has led to confusion in the classification of the family, thus we discuss whether the number of ascospores per asci can still be used as a basis for classification.

Keywords
Five novel taxa, phylogeny, systematics, taxonomy, Xylariales

Introduction

Diatrypaceae is an important family of higher ascomycetes, belonging to Xylariales (Maharachchikumbura et al. 2016). In the latest compilation, Hyde et al. (2020a) revised the family Diatrypaceae and included several new genera (i.e. *Allodiatrype* Konta & K.D. Hyde, *Halocryptovalsa* Dayar. & K.D. Hyde and *Neoeutypella* M. Raza et al.). This was followed by Wijayawardene et al. (2020) in which 20 genera were accepted into Diatrypaceae. The Diatrypaceae is characterised by perithecial ascomata embedded in a poor or well-developed, brown or black-coloured stroma, long-stalked and 8-spored or numerous-spored asci and allantoid, unicellular ascospores (Glawe and Rogers 1984; Rappaz 1987; Mehrabi et al. 2015; de Almeida et al. 2016).

Members of Diatrypaceae occur on a wide range of hosts in terrestrial and marine environments worldwide, some of which are important plant pathogens (Moyo et al. 2018a; Mehrabi et al. 2019; Dayarathne et al. 2020; Konta et al. 2020). For many decades, canker diseases on grapevine have been attributed to the species of Diatrypaceae worldwide, for example in China *Cryptovalsa* Ces. & De Not., *Cryptosphaeria* Ces. & De Not, *Diatrype* Fr., *Diatrypella* (Ces. & De Not.) De Not., *Eutypa* Tul. & C. Tul. And *Eutypella* (Nitschke) Sacc., are responsible for canker diseases in grapevine (Trouillas et al. 2011; Gao et al. 2013; Moyo et al. 2018b). Besides cankers of grapevine, some species have been reported as the causal pathogentic agents of fruit trees and woody plants in Europe and the USA (Trouillas et al. 2011; Gao et al. 2013).

Thirteen species of *Cryptosphaeria* and *Diatrype* were introduced by Vasiljeva and Ma (2014) from north-eastern China, which includes two new species and four new records. China has the largest range of karst distribution in the world. The landform of karst can be found in almost all Provinces of China, with the most extensive distribution in Guizhou and Yunnan Provinces (Miao et al. 2007). Karst virgin forest is a relatively stable ecosystem with rich biological resources, highly primitive and maintaining stable biological diversity (Dong et al. 2002). The special karst and ecological environment is home to a rich diversity of diatrypaceous fungi.

In this study, we revisit species of Diatrypaceae collected from karst areas in Guizhou, Hainan and Yunnan Provinces of China. Based on morpho-molecular analyses, one new genus and three new species are introduced; in addition, a new combination and two new records from China are reported. Descriptions and illustrations of new taxa and new records are provided.

Materials and Methods

Fungi collection, isolation and identification

Samples of decaying wood were collected from October 2019 to November 2020 in forests and nature reserves of Guizhou, Hainan and Yunnan Provinces in China. The specimens were observed with a stereomicroscope while microscopic images of the samples were taken using a Nikon ECLIPSE Ni compound microscope, with a Canon EOS 700D digital camera. Measurements were taken with Tarosoft (R) Image Frame Work (v.0.9.7). More than 30 asci and ascospores were measured for each specimen examined. Photoplates were arranged and improved by using Adobe Photoshop CS6 software. Isolations of fungi were made by single spore isolation (Chomnunti et al. 2014) and germinated spores were transferred to potato dextrose agar (**PDA**) medium for purification. The specimens were deposited at the Herbarium of Cryptogams, Kunming Institute of Botany Academia Sinica (**KUN-HKAS**) and Herbarium of Guizhou Medical University (**GMB**). Strains of the new genus and new species are maintained in the Guizhou Medical University Collection Centre (**GMBC**).

DNA extraction, Polymerase Chain Reaction (PCR) and phylogenetic analyses

Genomic DNA was extracted from fungal mycelium following the manufacturer's protocol of the BIOMIGA Fungal gDNA isolation Kit (BIOMIGA, Hangzhou City, Zhejiang Province, China). Extracts of DNA were stored at –20 °C.

PCR was carried out in a volume of 25 µl containing 9.5 µl of ddH_2O, 12.5 µl of 2× Taq PCR Master Mix (2 × Taq Master Mix with dye, TIANGEN, China), 1 µl of DNA extracts and 1 µl of forward and reverse primers (10 µM each) in each reaction. Primers pairs, ITS4 and ITS5, fRPB2-7CR and fRPB2-5f, LROR and LR5, T1 and Bt2b, as well as Bt2a and Bt2b (Vilgalys and Hester 1990; White et al. 1990; Glass and Donaldson 1995; O'Donnell and Cigelnik 1997), were used to amplify internal transcribed spacer (ITS) sequences, RNA polymerase II second largest subunit (RPB2) sequences, large subunit ribosomal (LSU) sequences and β-tubulin (TUB2) sequences, respectively.

PCR profiles for the ITS and LSU are as follows: initially at 95 °C for 5 minutes, followed by 35 cycles of denaturation at 94 °C for 1 minute, annealing at 52 °C for 1 minute, elongation at 72 °C for 1.5 minutes and a final extension at 72 °C for 10 minutes. PCR profile for the RPB2 is as follows: initially at 95 °C for 5 minutes, followed by 35 cycles of denaturation at 95 °C for 1 minute, annealing at 54 °C for 2 minutes,

Table 1. Taxa used in the phylogenetic analyses and their corresponding GenBank accession numbers.

Taxa	Strain number	GenBank Accession number		Reference
		ITS	β-tubulin	
Allocryptovalsa elaeidis	MFLUCC 15-0707	MN308410	MN340296	Konta et al. (2020)
A. polyspora^{T}	MFLUCC 17-0364	MF959500	MG334556	Senwanna et al. (2017)
A. rabenhorstii	WA08CB	HQ692619	HQ692523	Trouillas et al. (2011)
Allodiatrype arengae^{T}	MFLUCC 15-0713	MN308411	MN340297	Konta et al. (2020)
A. elaeidicola	MFLUCC 15-0737a	MN308415	MN340299	Konta et al. (2020)
A. elaeidis	MFLUCC 15-0708a	MN308412	MN340298	Konta et al. (2020)
A. thailandica	MFLUCC 15-3662	KU315392	NA	Li et al. (2016)
A. thailandica	MFLUCC 15-0711	MN308414	NA	Konta et al. (2020)
A. thailandica	**GMB0050**	**MW797108**	**MW814880**	This study
Anthostoma decipiens^{T}	IPV-FW349	AM399021	AM920693	Unpublished.
A. decipiens^{T}	JL567	JN975370	JN975407	Luque et al. (2012)
Cryptosphaeria ligniota	CBS 273.87	KT425233	KT425168	Acero et al. (2004)
C. pullmanensis	ATCC 52655	KT425235	KT425170	Trouillas et al. (2015)
C. subcutanea	DSUB100A	KT425189	KT425124	Trouillas et al. (2015)
C. subcutanea	CBS 240.87	KT425232	KT425167	Trouillas et al. (2015)
Cryptovalsa ampelina	A001	GQ293901	GQ293972	Trouillas et al. (2010)
C. ampelina	DRO101	GQ293902	GQ293982	Trouillas et al. (2010)
Diatrype bullata	UCDDCh400	DQ006946	DQ007002	Rolshausen et al. (2006)
D. disciformis^{T}	GNA14	KR605644.1	KY352434.1	Senanayake et al. (2015)
D. disciformis^{T}	D21C, CBS 205.87	AJ302437	NA	Acero et al. (2004)
D. enteroxantha	HUEFS155114	KM396617	KT003700	de Almeida et al. (2016)
D. enteroxantha	HUEFS155116	KM396618	KT022236	de Almeida et al. (2016)
D. lancangensis	**GMB0045**	**MW797113**	**MW814885**	**This study**
D. lancangensis	**GMB0046**	**MW797114**	**MW814886**	**This study**
D. lancangensis	**GMB0047**	**MW797116**	**MW814887**	**This study**
D. palmicola	MFLUCC 11-0020	KP744438	NA	Liu et al. (2015)
D. palmicola	MFLUCC 11-0018	KP744439	NA	Liu et al. (2015)
D. spilomea	D17C	AJ302433	NA	Acero et al. (2004)
D. stigma	DCASH200	GQ293947	GQ294003	Trouillas et al. (2010)
D. undulata	D20C, CBS 271.87	AJ302436	NA	Acero et al. (2004)
Diatrypella atlantica	HUEFS 136873	KM396614	KR259647	de Almeida et al. (2016)
D. banksiae	CPC 29118	KY173402	NA	Crous et al. (2013)
D. delonicis	MFLUCC 15-1014	MH812994	MH847790	Hyde et al. (2019)
D. delonicis	MFLU 16-1032	MH812995	MH847791	Hyde et al. (2019)
D. elaeidis	MFLUCC 15-0279	MN308417	MN340300	Konta et al. (2020)
D. favacea	Islotate 380	KU320616	NA	de Almeida et al. (2016)
D. favacea	DL26C	AJ302440	NA	Unpublished
D. frostii	UFMGCB 1917	HQ377280	NA	Vieira et al. (2011)
D. heveae	MFLUCC 15-0274	MN308418	MN340301	Konta et al. (2020)
D. heveae	MFLUCC 17-0368	MF959501	MG334557	Senwanna et al. (2017)
D. hubeiensis	CFCC 52413	MW632937	NA	Zhu et al. (2021)
D. iranensis	KDQ18	KM245033	KY352429	Mehrabi et al. (2015)
D. macrospora	KDQ15	KR605648	KY352430	Mehrabi et al. (2016)
D. oregonensis (*Diatrype oregonensis*)	DPL200	GQ293940	GQ293999	Trouillas et al. (2010)
D. oregonensis (*Diatrype oregonensis*)	CA117	GQ293934	GQ293996	Trouillas et al. (2010)
D. pseudooregonensis	**GMB0039**	**MW797115**	**MW814888**	**This study**
D. pseudooregonensis	**GMB0040**	**MW797117**	**MW814889**	**This study**
D. pseudooregonensis	**GMB0041**	**MW797118**	**MW814890**	**This study**
D. pseudooregonensis	**GMB0042**	**MW797119**	**MW814891**	**This study**
D. pseudooregonensis	**GMB0043**	**MW797120**	**MW814892**	**This study**
D. pseudooregonensis	**GMB0044**	**MW797110**	**MW814882**	**This study**
D. pulvinata	H048	FR715523	FR715495	de Almeida et al. (2016)
D. pulvinata	DL29C	AJ302443	NA	Unpublished
D. tectonae	MFLUCC 12-0172a	KY283084	NA	Shang et al. (2017)
D. tectonae	MFLUCC 12-0172b	KY283085	KY421043	Shang et al. (2017)
D. verruciformis^{T}	UCROK1467	JX144793	JX174093	Lynch et al. (2013)

Taxa	Strain number	GenBank Accession number		Reference
		ITS	β-tubulin	
D. verruciformis^{T}	UCROK754	JX144783	JX174083	Lynch et al. (2013)
D. vulgaris	HVFRA02	HQ692591	HQ692503	Trouillas et al. (2011)
D. vulgaris	HVGRF03	HQ692590	HQ692502	Trouillas et al. (2011)
D. vulgaris	**GMB0051**	**MW797107**	**MW814879**	**This study**
D. yunnanensis	VT01	MN653008	MN887112	Zhu et al. (2021)
Eutypa armeniacae	ATCC 28120	DQ006948	DQ006975	Rolshausen et al. (2006)
E. astroidea	E49C, CBS 292.87	AJ302458	DQ006966	Rolshausen et al. (2006)
E. cerasi	**GMB0048**	**MW797104**	**MW814893**	**This study**
E. cerasi	**GMB0049**	**MW797105**	**MW814877**	**This study**
E. flavovirens	E48C, CBS 272.87	AJ302457	DQ006959	Rolshausen et al. (2006)
E. laevata	E40C CBS 291.87	AJ302449	NA	Acero et al. (2004)
E. lata^{T}	CBS290.87	HM164736	HM164770	Trouillas and Gubler (2010)
E. lata^{T}	EP18	HQ692611	HQ692501	Trouillas et al. (2011)
E. lata^{T}	RGA01	HQ692614	HQ692497	Trouillas et al. (2011)
E. leioplaca	CBS 248.87	DQ006922	DQ006974	Rolshausen et al. (2006)
E. leptoplaca	CBS 287.87	DQ006924	DQ006961	Rolshausen et al. (2006)
E. maura	CBS 219.87	DQ006926	DQ006967	Rolshausen et al. (2006)
E. microasca	BAFC 51550	KF964566	KF964572	Grassi et al. (2014)
E. sparsa	3802 3b	AY684220	AY684201	Trouillas and Gubler (2004)
E. tetragona	CBS 284.87	DQ006923	DQ006960	Rolshausen et al. (2006)
Eutypella caricae	EL51C	AJ302460	NA	Acero (2000)
E. cerviculata^{T}	M68	JF340269	NA	Arhipova et al. (2012)
E. cerviculata^{T}	EL59C	AJ302468	NA	Acero et al. (2004)
E. leprosa	EL54C	AJ302463	NA	Acero et al. (2004)
E. leprosa	Isolate 60	KU320622	NA	de Almeida et al. (2016)
E. microtheca	BCMX01	KC405563	KC405560	Paolinelli-Alfonso et al. (2015)
E. parasitica	CBS 210.39	DQ118966	NA	Jurc et al. (2006)
E. semicircularis	MP4669	JQ517314	NA	Mehrabi et al. (2016)
Halocryptovalsa salicorniae	MFLUCC 15-0185	MH304410	MH370274	Dayarathne et al. (2020)
Halodiatrype avicenniae	MFLUCC 15-0953	KX573916	KX573931	Dayarathne et al. (2016)
H. salinicola^{T}	MFLUCC 15-1277	KX573915	KX573932	Dayarathne et al. (2016)
Kretzschmaria deusta	CBS 826.72	KU683767	KU684190	U'Ren et al. (2016)
Monosporascus cannonballus^{T}	CMM3646	JX971617	NA	Unpublished
M. cannonballus^{T}	ATCC 26931	FJ430598	NA	Unpublished
Neoeutypella baoshanensis^{T}	**GMB0052**	**MW797106**	**MW814878**	**This study**
N. baoshanensis^{T}	LC 12111	MH822887	MH822888	Hyde et al. (2019)
N. baoshanensis^{T}	EL51C, CBS 274.87	AJ302460	NA	Acero et al. (2004)
N. baoshanensis^{T}	MFLUCC 16-1002	MT310662	NA	Phukhamsakda et al. (2020)
N. baoshanensis^{T}	GL08362	JX241652	NA	Gao et al.(2013)
Paraeutypella citricola	HVVIT07	HQ692579	HQ692512	Trouillas et al. (2011)
Pa. citricola	HVGRF01	HQ692589	HQ692521	Trouillas et al. (2011)
Pa. citricola	**GMB0053**	**MW797109**	**MW814881**	This study
Pa. guizhouensis^{T}	KUMCC 20-0016	MW039349	MW239660	Dissanayake et al. (2021)
Pa. guizhouensis^{T}	KUMCC 20-0017	MW036141	MW239661	Dissanayake et al. (2021)
Pa. vitis	UCD2291AR	HQ288224	HQ288303	Úrbez-Torres et al. (2012)
Pa. vitis	UCD2428TX	FJ790851	GU294726	Úrbez-Torres et al. (2009)
Pedumispora rhizophorae^{T}	BCC44877	KJ888853	NA	Klaysuban et al. (2014)
Pe. rhizophorae^{T}	BCC44878	KJ888854	NA	Klaysuban et al. (2014)
Peroneutypa alsophila	EL58C, CBS 250.87	AJ302467	NA	Acero et al. (2004)
Pe. curvispora	HUEFS 136877	KM396641	NA	de Almeida et al. (2016)
Pe. diminutispora	MFLUCC 17-2144	MG873479	NA	Shang et al. (2018)
Pe. mackenziei	MFLUCC 16-0072	KY283083	KY706363	Shang et al. (2017)
Pe. mangrovei	PUFD526	MG844286	MH094409	Phookamsak et al. (2019)
Pseudodiatrype hainanensis^{T}	**GMB0054**	**MW797111**	**MW814883**	**This study**
Ps. hainanensis^{T}	**GMB0055**	**MW797112**	**MW814884**	**This study**
Quaternaria quaternata	EL60C, CBS 278.87	AJ302469	NA	Acero et al. (2004)
Q. quaternata	GNF13	KR605645	NA	Mehrabi et al. (2016)
Xylaria hypoxylon	CBS 122620	AM993141	KX271279	Peršoh et al. (2009)

^{T}: Types species of the genus; **NA**: No sequence is available in GenBank; Newly generated sequences are indicated in **bold**.

elongation at 72 °C for 1.5 minutes and a final extension at 72 °C for 10 minutes (Konta et al. 2020). PCR profile for the TUB2 are as follows: initially at 95 °C for 5 minutes, followed by 35 cycles of denaturation at 94 °C for 1 minute, annealing at 52 °C for 1 minute, elongation at 72 °C for 1.5 minutes and a final extension at 72 °C for 10 minutes (de Almeida et al. 2016). PCR products were submitted to Sangon Biotech, Shanghai, China for purification and sequencing.

Phylogenetic analyses

Phylogenetic analyses were performed by searching homologous sequence data of the family Diatrypaceae in the GenBank database, selected from NCBI and recently published papers (Mehrabi et al. 2019; Dayarathne et al. 2020; Konta et al. 2020; Dissanayake et al. 2021; Zhu et al. 2021). After the preliminary identification results of the sequences, multiple sequence alignments (ITS and β-tubulin) were aligned using BioEdit v. 7.0 (Hall 1999). Alignments were converted from FASTA to PHYLIP format by using Alignment Transformation Environment online (https://sing.ei.uvigo.es/ALTER/, Glez-Peña et al. 2010). Maximum Likelihood (ML) analyses and Bayesian posterior probabilities (BYPP) were performed by using RAxML-HPC BlackBox (8.2.12) and MrBayes on XSEDE (3.2.7a) tools in the CIPRES Science Gateway platform, based on a combination of ITS and TUB2 sequence data (Miller et al. 2010). Both of the two methods use the GTR+I+G model of evolution (Nylander 2004). The Bootstrap supports of ML analyses were obtained by running 1,000 pseudo-replicates and BYPP using a simulation technique called Markov chain Monte Carlo (or MCMC) to approximate the posterior probabilities of trees. Six simultaneous Markov Chains were run for 3,000,000 generations and trees were sampled every 1,000th generation. Finally, the tree was visualised in FigTree v.1.4.4 (Rambaut 2012) and edited by using Adobe Photoshop CS6 software. The final alignment and phylogenetic trees were deposited in TreeBASE under the submission ID28176 (http://www.treebase.org/)

Result

Phylogenetic analyses

Based on RAxML and BYPP analyses, phylogenetic analyses were similar in overall tree topologies and did not differ significantly. The dataset consists of 105 taxa for representative strains of species in Diatrypaceae, including outgroup taxa with 1071 characters, including gaps (ITS: 1–486, β-tubulin: 486–1071). The RAxML analyses resulted in a best scoring likelihood tree selected with a final ML optimisation likelihood value of -15731.506304, which is shown in Fig. 1.

The phylogenetic tree, based on combining ITS and β-tubulin sequence data, is also shown in Fig. 1 and contains 17 clades within Diatrypaceae. Below, we list the placements of new taxa:

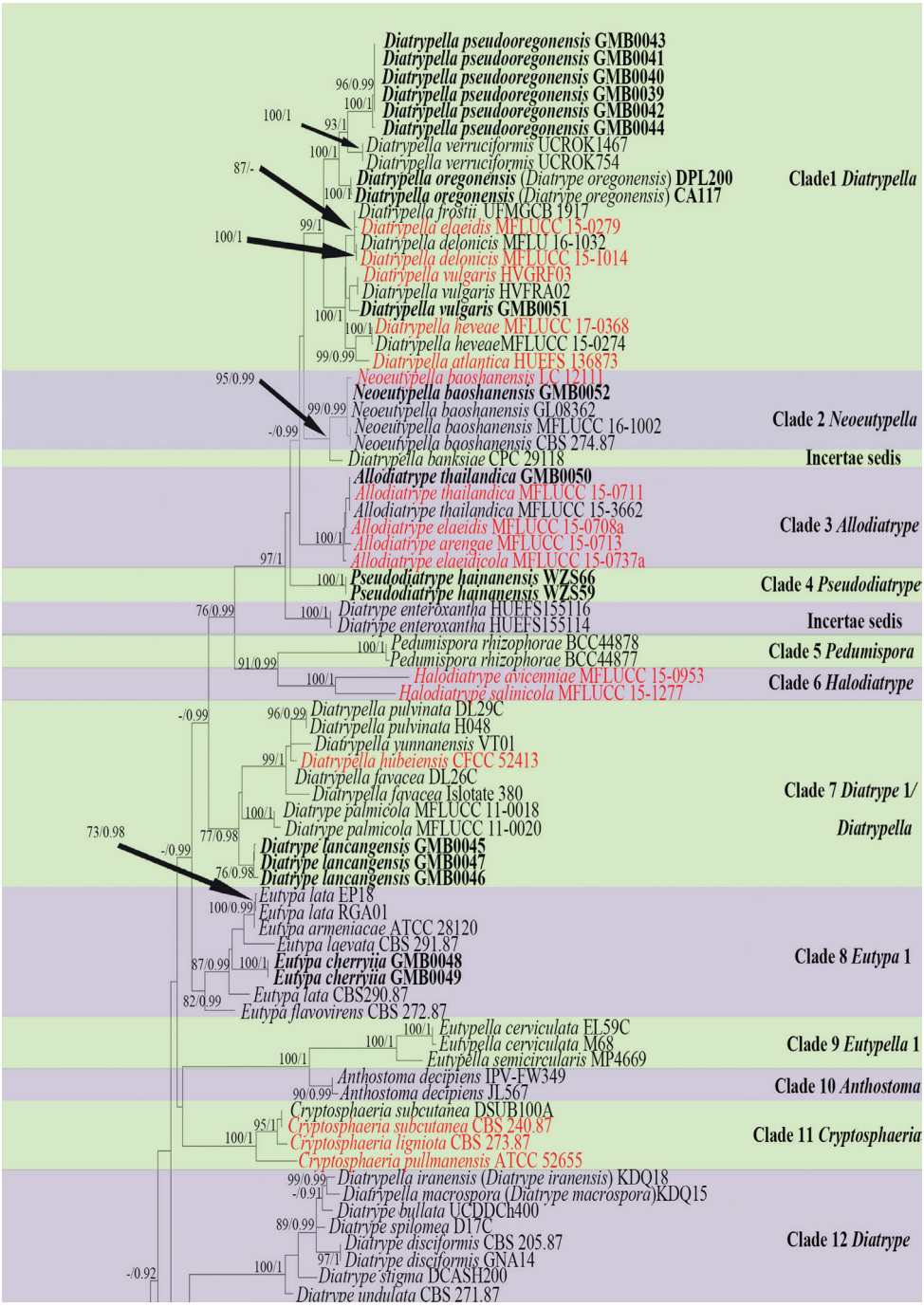

Figure 1. Phylogram generated from Maximum Likelihood (RAxML) analyses, based on ITS-β-tubulin matrix. ML bootstrap supports (≥ 70%) and Bayesian posterior probability (≥ 0.90) are indicated as ML/BYPP. The tree is rooted to *Kretzschmaria deusta* (CBS 826.72) and *Xylaria hypoxylon* (CBS 122620). Ex-type strains are in red. Newly generated strains are in black bold.

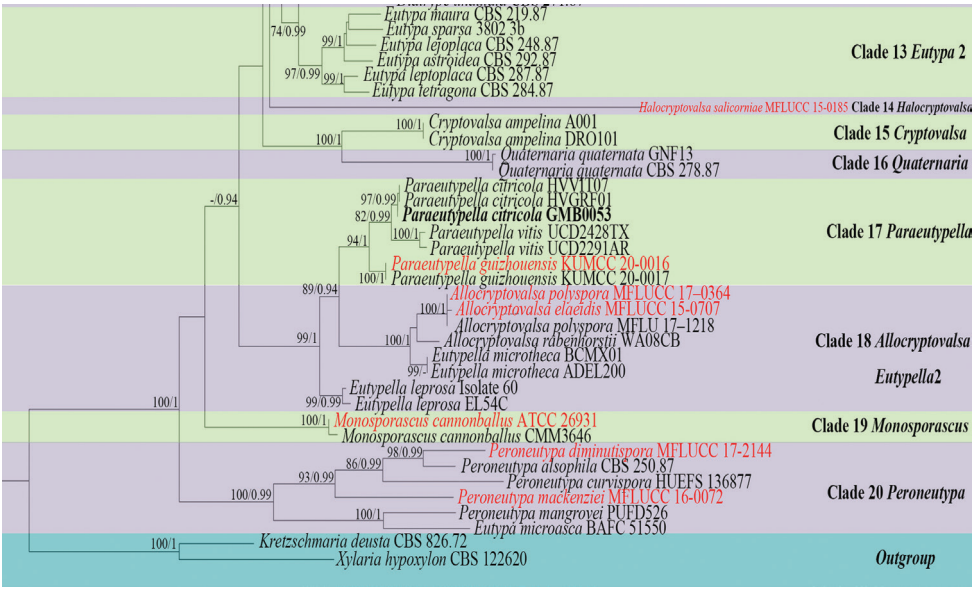

Figure 1. Continued.

Clade 1: *Diatrypella pseudooregonensis* and *Diatrypella oregonensis* clustered with the species of *Diatrypella* in Clade 1 with high bootstrap support, *Diatrypella pseudooregonensis* is introduced as an 8-spored new species of *Diatrypella* and *Diatrype oregonensis* is renamed as *Diatrypella oregonensis*.

Clade 4: *Pseudodiatrype* formed a separate branch in a clade (Clade 4) basal to the genus *Allodiatrype*.

Clade 7: *Diatrype lancangensis* clusters with the species of *Diatrypella* and *Diatrype* in an unresolved clade. However, *Diatrype* and *Diatrypella* have previously shown confused classification which is difficult to distinguish, based on phylogenetic aspects alone. Therefore, we introduce *Diatrype lancangensis* as a new species of *Diatrype*, based on phylogenetic analyses and morphological differences (Table 2).

Clade 8: *Eutypa cerasi* forms a distinct lineage which is sister to *Eutypa lata* (EP18, RGA01) (Fig. 1).

Taxonomy

Diatrype Fr.

Notes. The genus *Diatrype* was introduced by Fries (1849). The genus is characterised by stromata widely effuse or verrucose, flat or slightly convex, with discoid or sulcate ostioles at the surface, 8-spored and long-stalked asci and hyaline or brownish, allantoid ascospores. In this study, we introduce a new species of *Diatrype* from China.

Diatrype lancangensis **S.H. Long & Q. R. Li, sp. nov.**
MycoBank No: 839655
Fig. 2

Holotype. GMB0045.

Etymology. Refers to the name of the location, where the type specimen was collected.

Description. Saprobic on decaying branches of an unidentified plant. **Sexual morph:** *Stromata* immersed in bark, aggregated, irregular in shape, widely effused, flat, margin diffuse, surface dark brown to black, with punctiform ostioles scattered at surface, with tissues soft, white between perithecia. *Entostroma* dark with embedded perithecia in one layer. *Perithecium* semi-immersed in stroma, globose to subglobose, glabrous, with cylindrical neck, brevicollous or longicollous 283.5–343.5 µm high, 207–290 µm broad (av. = 315.5 × 248.0 µm, n = 10), ovoid, obovoid to oblong, monostichous, aterrimus. *Ostiole* opening separately, papillate or apapillate, central. *Peridium* 30–50 µm thick, dark brown to hyaline with *textura angularis* cell layers. *Asci* 90.5–160.5 × 7.0–15.0 µm (av. = 129.5 × 10.5 µm n = 30) 8-spored clavate, unitunicate, with rounded apex, apical rings inamyloid. *Ascospores* 11–18.5 × 2–4 µm (av. = 14.9 × 2.8 µm, n = 30), irregularly arranged, allantoid, slightly curved, brown to dark brown, smooth, aseptate, usually with oil droplets. Asexual morph: undetermined.

Culture characteristics. Ascospores germinating on PDA within 24 hours. Colonies on PDA, white when young, became luteous, dense but, thinning towards edge, margin rough, white from above, reverse white at margin, pale yellow to luteous at centre, no pigmentation produced on PDA medium, no conidia observed on PDA or on OA media.

Specimens examined. China, Yunnan Province, Baoshan City, Lancang River Nature Reserve (25°1'17.44"N, 99°35'10.05"E) on branches of an unidentified plant, 4 October 2019. Altitude: 2549 m., Y.H. Pi & Qiong Zhang, LC172 (GMB0045, ***holotype***, KUN-HKAS 112664, ***isotype***, ex-type living culture GMBC0045).

Additional specimens examined. China, Yunnan Province, Baoshan City, Lancang River Nature Reserve (25°1'17.44"N, 99°35'10.05"E) on branches of an unidentified plant, 4 October 2019. Altitude: 2549 m., Y.H. Pi and Qiong Zhang, LC173 (GMB0046, KUN-HKAS 112665, living culture GMBC0046); CHINA, Yunnan Province, Baoshan City, Lancang River Nature Reserve (25°1'15.48"N, 99°35'24.08"E) on branches of an unidentified plant, 5 October 2019. Altitude: 2623 m., Y.H. Pi and Qiong Zhang, LC262 (GMB0047, KUN-HKAS 112672, living culture GMBC0047).

Additional sequences. GMB0045 (LSU: MW797057, RPB2: MW81490); GMB00046 (LSU: MW797058); GMB0047 (LSU: MW797060, RPB2: MW814903)

Note. Our new strain, GMBC0045 falls into the unresolved clade (Clade 7) which comprises five *Diatrypella* and one *Diatrype* species (Fig. 1), this clade is consistent with the study of Konta et al. (2020). The taxonomic confusion of Diatrypaceae has led to difficulties in separating the genera. We consider that the new species belongs to the genus *Diatrype*, based on the stromata features mentioned above which closely resemble descriptions of *Diatrype subundulata* Lar. N. Vassiljeva & Hai X. Ma and *Diatrype undu-*

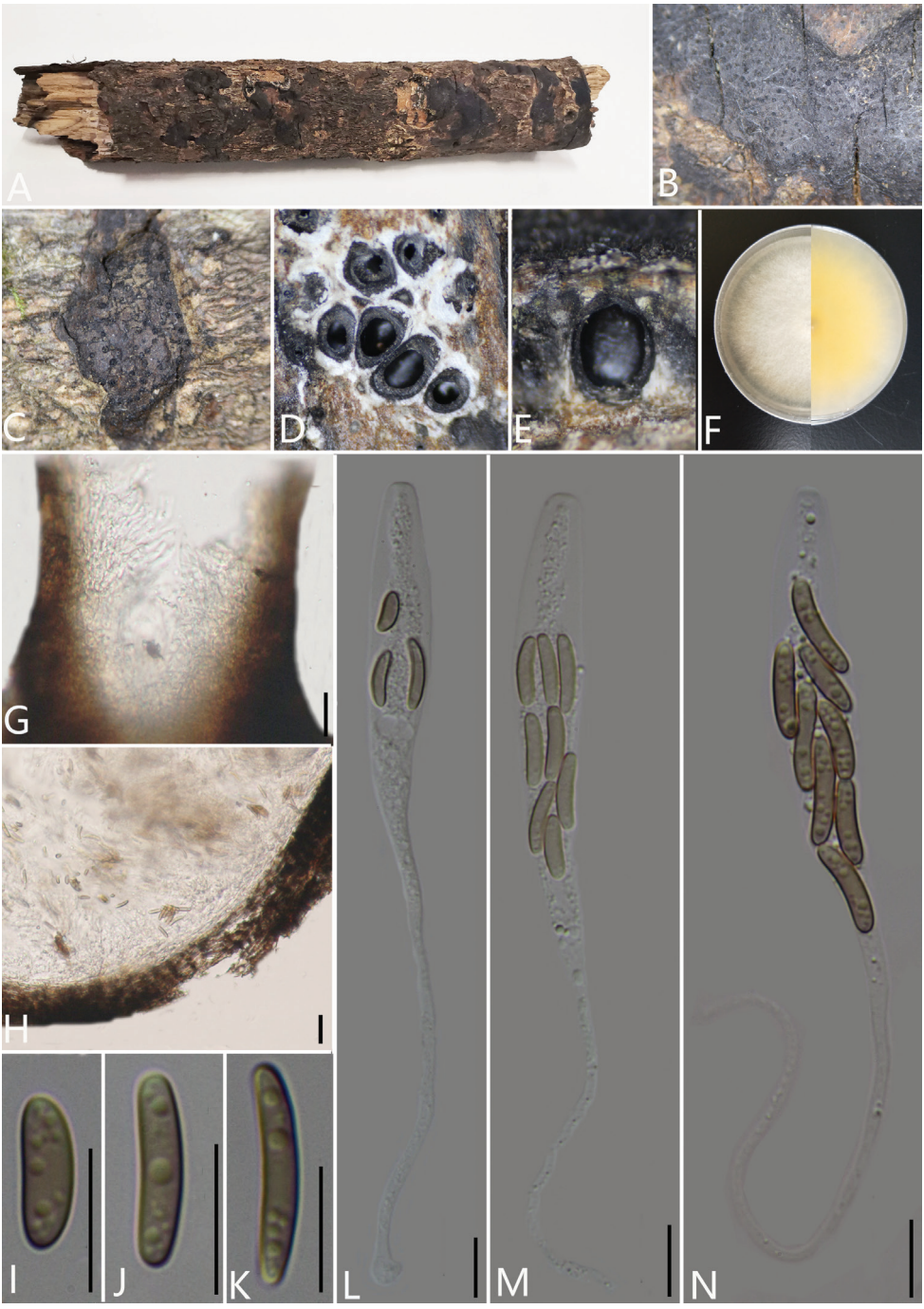

Figure 2. *Diatrype lancangensis* (GMB0045, **holotype**) **A** stromata on host substrate **B, C** stromata on host **D** transverse sections through ascostroma **E** vertical section through ascostroma **F** culture on PDA **G** ostiolar canal **H** peridium **I–K** ascospores **L–N** asci. Scale bars: 10 μm (**G–N**).

lata (Pers.) Fr. (Vasilyeva et al. 2014). However, the ascospores of these species are larger than the ascospores of *D. subundulata* and *D. undulata* (Table 2). Phylogenetic analyses also showed that *D. lancangensis* falls on a separate branch that clustered with species of *Diatrypella* and *Diatrype* (Fig. 1). Hence, by combining morphological characteristics and phylogenetic analyses, it seems appropriate to categorise this species as *Diatrype*.

In the phylogenetic analyses, it can be seen that Clade 7 can be defined as a new genus, but it is difficult to find the common morphological similarities among these species. More specimens and sequence or chemical composition analysis are needed in the future to determine whether Clade 7 can be a new genus. The characteristics of the stromata of *Diatrypella* spp. in clade 7 are solitary and scattered, which is distinctly different from widely effuse, flat and slightly convex stromata of *Diatrype lancangensis* and *Diatrype palmicola* (Liu et al. 2015; Hyde et al. 2020b; Zhu et al. 2021). And in the recent study, Zhu et al. (2021) proposed that the species of *Diatrypella* in Clade 7 were isolated from *Betula* spp., it may have host specificity. Because of the above two reasons, we think it is better to classify our strains into *Diatrype*.

***Pseudodiatrype* S.H. Long & Q.R. Li, gen. nov.**
MycoBank No: 839658

Etymology. Refers to this genus resembling *Diatrype* in morphology, but it is phylogenetically distinct.

Type species. *Pseudodiatrype hainanensis* S. H. Long & Q.R. Li sp. nov.

Description. *Saprobic* on decaying branches of an unidentified plant. **Sexual morph:** *Stromata* scattered or aggregated on host, wart-like, pustulate, visible as black, rounded to irregular in shape on host surface, erumpent through host bark, 5–20 ascomata immersed in one stroma. *Endostroma* consists of outer layer of black, small, dense, thin parenchymal cells and inner layer of white, large, loose parenchymal cells, thin, pale yellow, powdery near margin of the black cells. *Ostiole* opening through host bark and appearing as black spots, separately, papillate or apapillate, central. *Perithecium* immersed in stroma, globose to subglobose, glabrous, with cylindrical neck, brevicollous or longicollous. *Peridium* is composed of an outer layer of dark brown to black, thin-walled cells, arranged in *textura angularis*, the inner layer of hyaline thin-walled cells of *textura angularis*. *Asci* 8-spored, unitunicate, clavate, long-stalked, apically rounded, apical rings inamyloid. *Ascospores* irregularly arranged, allantoid, slightly or moderately curved, smooth, subhyaline, aseptate, usually with two oil droplets. **Asexual morph:** undetermined.

Note. The genus *Pseudodiatrype* is introduced to accommodate the new collection made from Hainan Province of China and typified by *Pseudodiatrype hainanensis*. *Pseudodiatrype* is monotypic and, morphologically, resembles *Diatrype* and *Allodiatrype* Konta & K.D. Hyde. However, *Pseudodiatrype* can be distinguished from *Diatrype* by its 5–20 ascomata immersed in a stroma, while the stroma of species of *Diatrype* is

distributed over large areas, sometimes covering the surface of the host (Vasilyeva and Ma 2014; Konta et al. 2020). *Pseudodiatrype* differs from *Alloiatrype* by having its 5–20 ascomata immersed in a stroma, whereas the stroma of *Allodiatrype* has only 1–10 ascomata. Moreover, the endostroma of *Allodiatrype* is composed of dark brown outer layer cells and yellow inner layer cells (Konta et al. 2020), which are different from the endostroma of *Pseudodiatrype* having black outer and inner cells surrounded by powdery, pale yellow cells. In addition, the sizes of stroma and ascospores are different from species of *Diatrype* and *Allodiatrype* (Table 2). In the phylogenetic analyses, species of *Pseudodiatrype* appeared in a separate branch which is distinct from other genera within *Diatrypaceae* (Fig. 1), thus, justifying the erection of the new genus *Pseudodiatrype*.

Pseudodiatrype hainanensis **S. H. Long & Q.R. Li, sp. nov.**
MycoBank No: 839659
Fig. 3

Holotype. GMB0054.

Etymology. Refers to the location of collections, Hainan Province.

Description. *Saprobic* on decaying branches of an unidentified plant. **Sexual morph:** *Stromata* wart-like, pustulate, 2–3.6 mm long and 1.6–3 mm broad (av. = 3.2 × 1.9 mm, n = 30), about 2 mm thick, 5–20 in single stroma, visible as black, rounded to irregular in shape on the host surface, erumpent through host bark, solitary to gregarious. *Endostroma* composed of an outer layer of dark brown to black, small, tightly packed, thin parenchymatous cells and an inner layer of white, large, loose parenchymal cells with powdery, thin, yellowish tissue. *Ostiole* opening separately, papillate or apapillate, central. *Perithecium* immersed in the stroma, globose to subglobose, glabrous, with cylindrical neck, brevicollous or longicollous, 193–347 µm high, 138–206 µm diam. (av. = 278 × 156 µm, n = 10). *Peridium* 30–50 µm thick, dark brown to hyaline with *textura angularis* cell layers. *Asci* 110–155.5 × 6–10 µm (av. = 132 × 8 µm, n = 30), 8-spored, unitunicate, clavate, long-stalked, apically rounded with inamyloid rings. *Ascospores* 8.5–13 × 1.5–2.5 µm (av. = 10.5 × 2 µm, n = 30), irregularly arranged, allantoid, slightly or moderately curved, smooth, subhyaline, aseptate, usually with two oil droplets. **Asexual morph:** undetermined.

Culture characteristics. Ascospores germinating on PDA within 24 hours. Colonies on PDA, white when young, became pale brown, dense, but thinning towards edge, fluffy to slightly fluffy, white from above, pale brown from below, no pigmentation produced on PDA medium, no conidia observed on PDAor on OA media.

Specimens examined. China, Hainan Province, Wuzhishan City, Wuzhishan Nature Reserve (18°54'21.81"N, 109°40'54.12"E) on branches of unidentified plant, 14 November 2020. Altitude: 775 m. Y.H. Pi & Q.R. Li, WZS59 (GMB0054, ***holotype***, KUN-HKAS 112700, ***isotype***, ex-type living culture GMBC0054).

Additional specimen examined. China, Hainan Province, Wuzhishan City, Wuzhishan Nature Reserve (18°54'21.81"N, 109°40'54.12"E) on branches of an uni-

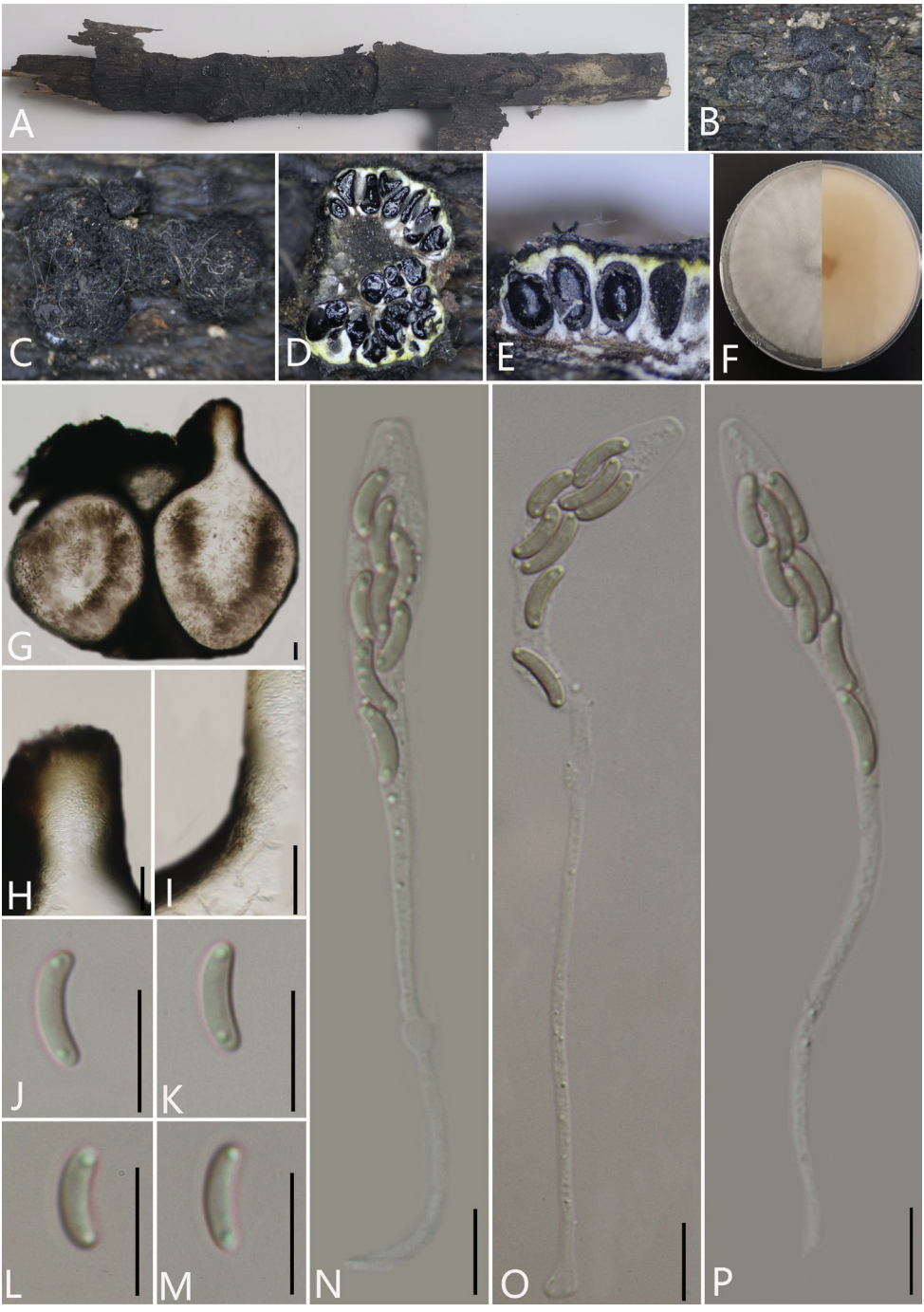

Figure 3. *Pseudodiatrype hainanensis* (GMB0054, **holotype**) **A** stromata on host substrate **B, C** stromata on host **D** transverse section through ascostroma **E** vertical section through ascostroma **F** culture on PDA **G** section through the ascostroma **H** ostiolar canal **I** peridium **J–M** ascospores **N–P** asci. Scale bars: 40 μm (**G**); 10 μm (**H–P**).

dentified plant, 14 November 2020. Altitude: 775 m, Y.H. Pi & Q.R. Li, WZS66 (GMB0055, living culture GMBC0055)

Additional sequences. GMB0054 (LSU: MW797055, RPB2: MW814900); GMB0055 (LSU: MW797056, RPB2 MW814901).

Note. A peculiar feature of *Pseudodiatrype hainanensis* is the composition of endostroma. There are black outer layer cells, white inner layer cells and powdery, yellowish cells that are smaller than the white cells at the edge of the endostroma near the black cells in endostroma.

Diatrypella (Ces. & De Not.) De Not.

Notes. The genus *Diatrypella* was introduced by Cesati & De Notaris (1863) and was typified with *Diatrypella verruciformis* (Ehrh.) Nitschke. This genus was characterized by pustule-like stromata erumpent through the host surface, polysporous asci and allantoid ascospores and libertella-like asexual morphs (Senanayake et al. 2015; Hyde et al. 2017; Shang et al. 2017). In this study, we introduce a new species, a new combination and a new record of *Diatrypella vulgaris* from Guizhou Province for China.

Diatrypella pseudooregonensis S.H. Long & Q.R. Li, sp. nov.

MycoBank No: 839656
Fig. 4

Holotype. GMB0041

Etymology. Refers to its similar species of *Diatrype oregonensis*.

Description. *Saprobic* on decaying branches of unidentified plant. **Sexual morph:** *Stromata* pustulate, with groups of 3–16 perithecia, rugose, visible as black, erumpent, scattered, surrounded by a thin, black line in host tissue, solitary to gregarious, 1–3 mm long and 0.5–2 mm broad (av. = 2 × 1.5 mm, n = 30), about 1 mm thick. *Endostroma* white to light yellow. *Ostiole* opening separately, papillate or apapillate, central. *Perithecium* immersed in stroma, globose to subglobose, glabrous, with cylindrical neck, brevicollous or longicollous 218.5–465 μm high, 112–257 μm diam. (av. = 306 × 164 μm, n = 10), globose to subglobose, glabrous, ostioles individual. *Peridium*: 30–50 μm thick, dark brown to hyaline with *textura angularis* cell layers. *Asci* 95–149 × 6.5–11.5 μm (av. = 120 × 10.5 μm, n = 30), 8-spored, unitunicate, clavate or cylindrical, long-stalked, apically rounded, apical rings inamyloid. *Ascospores* 11–16 × 1.5–3.5 μm (av. = 14 × 2.5 μm, n = 30), irregularly arranged, allantoid, slightly or moderately curved, subhyaline to slightly brown, smooth, aseptate, usually with two oil droplets. **Asexual morph:** undetermined.

Culture characteristics. Ascospores germinating on PDA within 24 hours. Colonies on PDA, white when young, became pale brown, dense, but thinning towards the edge, margin rough, white from above, white at margin and light brown at centre from

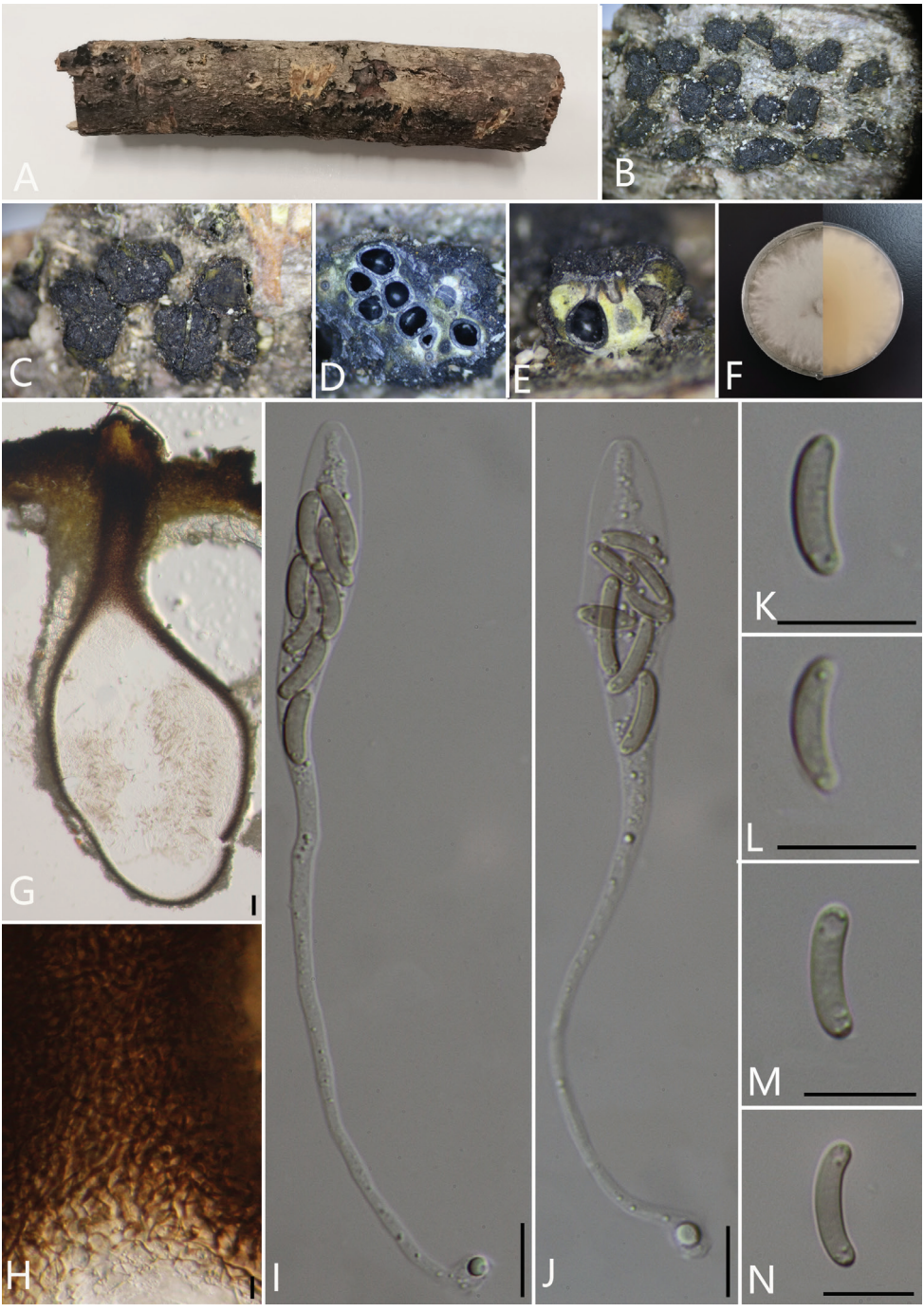

Figure 4. *Diatrypella pseudooregonensis* (GMB0041, **holotype**) **A** stromata on host substrate **B, C** stromata on host substrate **D** transverse section through ascostroma **E** vertical section through ascostroma **F** culture on PDA **G** section through the ascostroma **H** ostiolar canal **I, J** asci **K–N** ascospores. Scale bars: 20 μm (**G**); 10 μm (**H–N**).

below, no pigmentation produced on PDA medium, no conidia observed on PDA or on OA media.

Specimens examined. China, Yunnan Province, Baoshan City, Lancang River Nature Reserve (25°1'19.88"N, 99°35'30.68"E) on branches of an unidentified plant, 5 October 2019. Altitude: 2677 m, Y.H. Pi & Qiong Zhang, LC323 (GMB0041, ***holotype***, KUN-HKAS 112646, ***isotype***, ex-type living culture GMBC0041)

Additional specimens examined. China, Yunnan Province, Baoshan City, Lancang River Nature Reserve (25°1'13.51"N, 99°35'25.59"E) on branches of an unidentified plant, 6 October 2019. Altitude: 2630 m, Y.H. Pi & Qiong Zhang, LC384 (GMB0043, KUN-HKAS 112681, living culture GMBC0043); China, Yunnan Province, Baoshan City, Lancang River Nature Reserve (25°1'15.00"N, 99°35'39.73"E) on branches of an unidentified plant, 5 October 2019. Altitude: 2698 m, Y.H. Pi & Qiong Zhang, LC312 (GMB0040, KUN-HKAS 112674, living culture GMBC0040); China, Yunnan Province, Baoshan City, Lancang River Nature Reserve (25°35'19.09"N, 99°35'19.09"E) on branches of an unidentified plant, 5 October 2019. Altitude: 2569 m, Y.H. Pi & Qiong Zhang, LC193 (GMB0039, KUN-HKAS 112667, living culture GMBC0039); China, Yunnan Province, Baoshan City, Lancang River Nature Reserve (25°1'9.11"N, 99°35'24.80"E) on branches of an unidentified plant, 5 October 2019. Altitude: 2649 m, Y.H. Pi & Qiong Zhang, LC335 (GMB0042, KUN-HKAS 112647, living culture GMBC0042); China, Guizhou Province, Anshun City, Pingba District (26°25'9.65"N, 106°24'24.48"E) on branches of an unidentified plant, 1 August 2020. Altitude: 1250 m, Y.H.Pi, PB51 (GMB0044, KUN-HKAS 112693, living culture GMBC0044).

Additional sequences. GMB0041 (LSU: MW797062, RPB2: MW814906); GMB0043 (LSU: MW797064, RPB2: MW814907); GMB0040 (LSU: MW797061, RPB2: MW814905); GMB0039 (LSU: MW797059, RPB2: MW814904); GMB0042 (LSU: MW797063); GMLB0044 (LSU: MW979054, RPB2: MW814899).

Note. Morphologically, *Diatrype* has 8 ascospores in a single ascus, while *Diatrypella* has more than eight ascospores in each ascus (Senanayake et al. 2015). However, previous research (e.g. Acero et al. 2004 and Trouillas et al. 2011) suggested that both *Diatrypella* and *Diatrype* are polyphyletic within the family. In the phylogenetic analyses, *Diatrypella pseudooregonensis* grouped closely to the *D. verruciformis* and thus, we consider this new species to belong in the genus *Diatrypella*, because it is doubtful whether the number of ascospores per asci is useful as a basis for generic classification.

Diatrypella vulgaris **Trouillas, W.M. Pitt & Gubler, Fungal Diversity 49: 212 (2011)**

MycoBank No: 519404

Fig. 5

Description. *Saprobic* on decaying branches of an unidentified plant. **Sexual morph:** *Stromata* scattered on the host, 0.8–1.5 mm long and 0.8–2 mm broad (av. = 1.2 ×

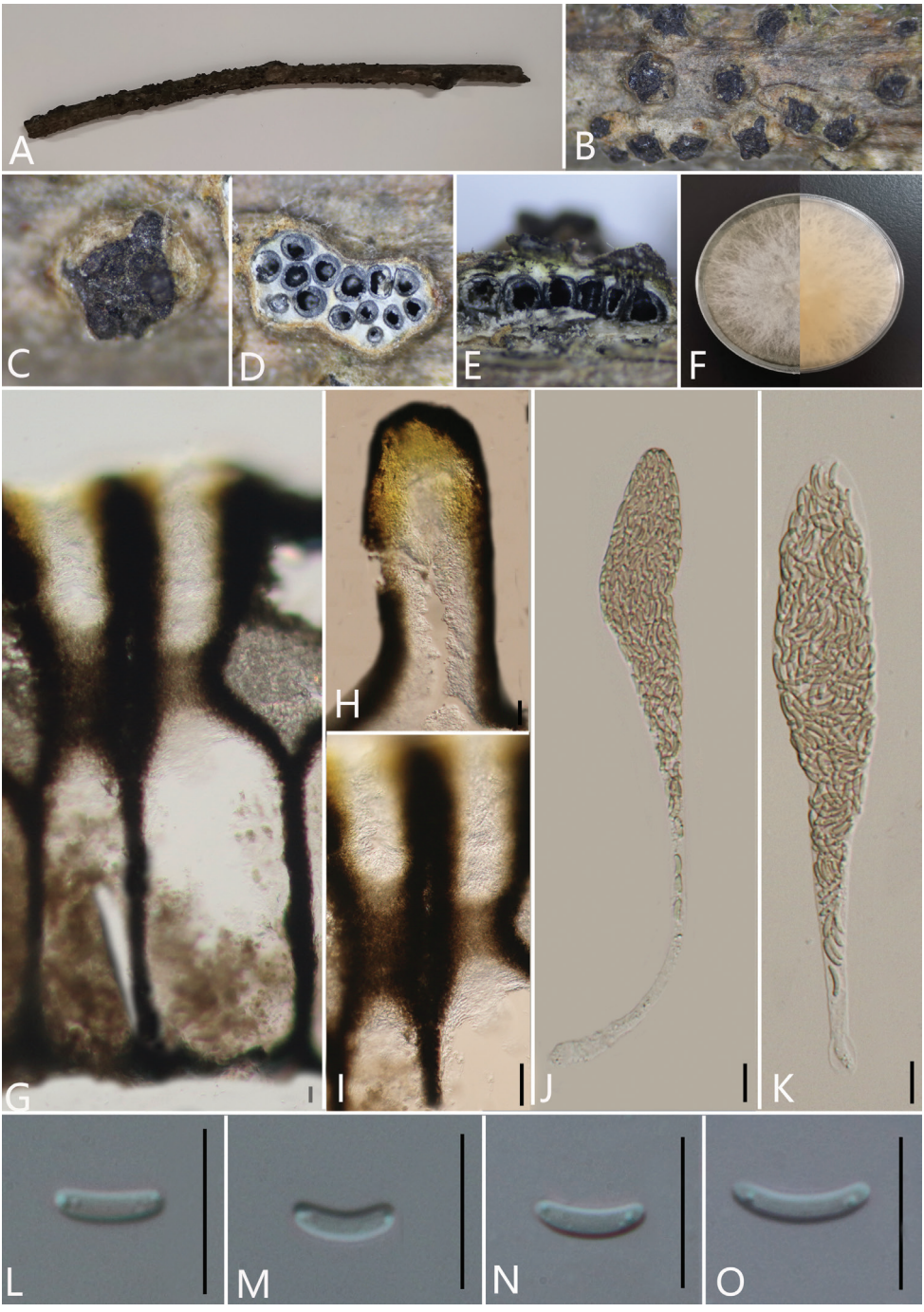

Figure 5. *Diatrypella vulgaris* (GMB0051, **new record for China**) **A** stromata on host substrate; **B, C** close-up of stroma **D** transverse sections through ascostroma **E** vertical section through ascostroma **F** culture on PDA **G** section through the ascostroma **H, I** ostiolar canal **J, K** asci **L–O** ascospores. Scale bars: 20 μm (**G**); 10 μm (**H–I**).

1.3 mm, n = 30) pustulate, visible as black, rounded to irregular in shape on host surface, semi-immersed, erumpent through host bark, with 2–8 ascomata immersed in one stroma. *Endostroma* consists of outer dark brown, small, dense, thin parenchymal cells and an inner layer of white, large, loose parenchymal cells. *Ostiole* opening separately, papillate or apapillate, central 710.7–787.2 μm high, 270.2–422 μm diam. (av. = 742 × 363 μm, n = 10). *Perithecium* immersed in stroma, round to oblong, with cylindrical neck, brevicollous or longicollous. *Peridium* composed of outer layer of dark brown to black, thin-walled cells, arranged in *textura angularis*, inner layer of hyaline thin-walled cells of *textura angularis*. *Asci* 111.4–152.9 × 10.6–17.5 μm (av. = 124.5 × 15.5 μm, n = 30), polysporous, clavate, long-stalked, apically rounded. *Ascospores* 8–11 × 1–2 μm (av. = 8.9 × 1.7 μm, n = 30), overlapping, crowded, allantoid, slightly or moderately curved, smooth, subhyaline, yellowish in mass, aseptate, usually with two oil droplets. **Asexual morph:** undetermined.

Culture characteristics. Ascospores germinating on PDA within 24 hours. Colonies on PDA, white when young, became pale brown, dense, but thinning towards edge, medium dense, white from above, reverse side white at margin, flesh to pale brown at centre, no pigmentation produced on PDA medium, no conidia observed on PDA or on OA media.

Specimens examined. China, Guizhou Province, Guiyang City, Gaopo Township (26°29'72.02"N, 106°29'55.57"E), on branches of unidentified plant, 30 October 2020. Altitude: 1589 m, S.H. Long, GP02 (GMB0051, KUN-HKAS 112697, living culture GMBC0051).

Additional sequences. GMB0051 (LSU: MW797051, RPB2: MW814897).

Note. The comparison of ITS sequences in NCBI showed that this isolate is 100% similar to the strain of *Diatrypella vulgaris* (HVGRF03), isolated from holotype specimens. Morphologically, GMB0051 shows the same features as *Diatrypella vulgaris*. The stromata of these specimens are similar, but ascospores of GMB0051 are thinner than those of the HVGRF03 (8–10 × 2–2.5 μm) and, when compared with the ascospores of strain MFLUCC 17-0128 (4.5–7.5 × 1–2 μm), they are shorter than GMB0051 (Trouillas et al. 2011; Hyde et al. 2017). Here, we use the ITS sequence similarity between the new collection and the type strain of *Diatrypella vulgaris* as the identification tool. *Diatrypella vulgaris* has been reported in Austria and Thailand (Trouillas et al. 2011, Hyde et al. 2017). This is the first report of *Diatrypella vulgaris* from China.

***Diatrypella oregonensis* (Wehm.) S.H. Long & Q.R. Li, comb. nov.**
MycoBank No: 839728

≡ *Eutypella oregonensis* Wehm. Pap. Mich. Acad. Sci. 11: 163 (1930)
≡ *Diatrype oregonensis* (Wehm.) Rappaz, Mycol. helv. 2(3): 420 (1987)

Description. See Trouillas et al. (2010).

Note. The strains of *Diatrype oregonensis* (DPL200, CA117) generated from Trouillas et al. (2010) grouped in *Diatrypella s. str. Diatrype oregonensis* was erected

in 1930 as *Eutypella oregonensis* (Kauffman 1930). No available sequences from type material were found. After re-examination of holotype specimen of *Diatrype oregonensis*, Trouillas et al. (2010) introduced two strains of *Diatrype oregonensis* (DPL200 and CA117). Although neither of these strains are ex-type, they are, the most authoritative strains. Here, we tentatively transfer *Diatrype oregonensis* to *Diatrypella* as *Diatrypella oregonensis*, based on the phylogenetic analyses (Fig. 1). *Diatrypella oregonensis* is similar to *D. pseudooregonensis* in having 8-spored asci (Rappaz 1987; Trouillas et al. 2011). Nevertheless, we consider that the number of ascospores as a basis for distinguishing *Diatrypella* from *Diatrype* is not useful.

Allodiatrype **Konta & K.D. Hyde Mycosphere 11(1): 247 (2020)**

Notes. The genus *Allodiatrype* was introduced by Konta et al. (2020), which was characterised by regular or irregular-shaped stromata, erumpent through host surface, asci with 8 spores and aseptate, allantoid ascospores. In this study, we introduce a new record of *Allodiatrype thailandica* (R.H. Perera et al.) Konta & K.D. Hyde collected from Yunnan Province in China.

Allodiatrype thailandica **(R.H. Perera et al.) Konta & K.D. Hyde, Mycosphere 11(1): 253 (2020)**
Mycobank No: 556932
Fig. 6

≡ *Diatrype thailandica* R.H. Pereraet al., Fungal Diversity 78: 1–237, [105] (2016)

Description. *Saprobic* on decaying branches of unidentified plant. **Sexual morph:** *Stromata* wart-like, pustulate, 0.5–1.8 mm long and 0.8–2.2 mm broad (av. = 1.2 × 1.3 mm, n = 30), about 1 mm thick, 1–18 in a single stroma, visible as black, rounded to irregular in shape on the host surface, erumpent through host bark, solitary to gregarious. *Endostroma* composed of an outer layer of dark brown to black, small, tightly packed, thin parenchymatous cells and an inner layer of white to yellow, large, loose parenchymal cells. *Ostiole* opening separately, papillate or apapillate, central. *Perithecium* immersed in stroma, globose to subglobose, glabrous, with cylindrical short neck, 377–447 μm high, 191–264 μm diam. (av. = 406 × 221 μm, n = 10). *Peridium* hyaline to dark brown with *textura angularis* cell layers. *Asci* 80–113.5 × 6.9–10 μm (av. = 109.3 × 8.5 μm, n = 30), 8-spored, unitunicate, clavate, long-stalked, upper part inflated, apically rounded to truncate, apical rings inamyloid. *Ascospores* 6–11 × 2–2.5 μm (av. = 8.9× 2.3 μm, n = 30), irregularly arranged, allantoid, slightly curved, smooth, subhyaline, aseptate, usually with two oil droplets. **Asexual morph:** undetermined.

Culture characteristics. Ascospores germinating on PDA within 24 hours. Colonies on PDA, white when young, became pale yellow, irregular in shape, medium dense, flat or effuse, slightly raised, with edge fimbriate, fluffy to fairly fluffy, white

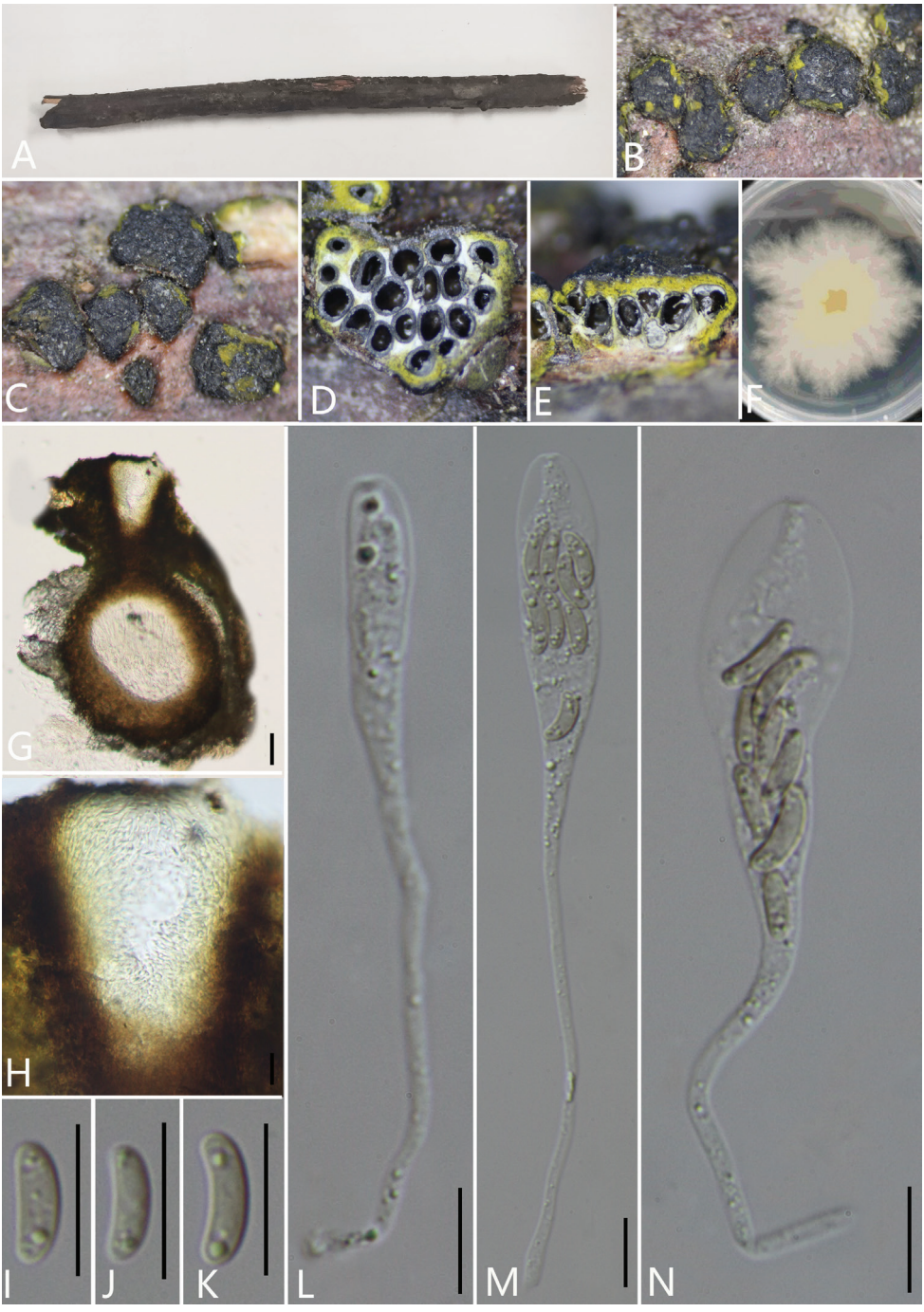

Figure 6. *Allodiatrype thailandica* (GMB0050, new record for China) **A** stromata on host substrate **B, C** close-up of stromata **D** transverse section through ascostroma **E** vertical section through ascostroma **F** culture on PDA **G** section through the ascostroma **H** ostiolar canal **I–K** ascospores **L–N** asci. Scale bars: 20 μm (**G**); 10 μm (**H–N**).

from above, reverse side white at margin, pale brown at centre, no pigmentation produced on PDA medium, no conidia observed on PDA or on OA media.

Specimens examined. China, Yunnan Province, Baoshan City, Lancang River Nature Reserve (24°57'25.35"N, 99°44'22.82"E), on branches of unidentified plant, 2 October 2019. Altitude: 1317 m, Y.H. Pi & Qiong. Zhang, LC103 (GMB0050, KUN-HKAS 112660, living culture GMBC0050).

Additional sequences. GMB0050 (LSU: MW797052).

Note. The ITS sequence data were subjected to BLAST in NCBI and the results showed that it is 100% similar to *Allodiatrype thailandica*. Additionally, based on morphological and phylogenetic analyses, this strain was identified as the *A. thailandica*. The stromata are similar, but the ascospores of GMB0050 are longer and wider than the ascospores of strain MFLUCC 15-3662 (3.8–6.9 × 1–1.4 μm) isolated from the holotype specimen, but it is similar to the strain MFLU 17-0735 (6.5–10.7 × 1.6–2.7 μm) (Perera et al. 2020). Here, we use the ITS sequence similarity between the new collection and the type strain of *Allodiatrype thailandica* as basis for identification. *A. thailandica* has been reported in Thailand in 2016 as *Diatrype thailandica* and recognised as *A. thailandica* by Konta et al. (2020). This is the first report of *Allodiatrype thailandica* from China.

Neoeutypella M. Raza, Q.J. Shang, Phookamsak & L. Cai, Fungal Diversity 95: 167 (2019)

Note. The genus *Neoeutypella* was introduced by Phookamsak et al. (2019) and is characterised by carbonaceous stromata immersed or semi-immersed on the host, 8-spored asci and hyaline or pale reddish-brown to brown ascospores. In this study, we introduce a new collection of *N. baoshanensis*, isolated from Guizhou Province in China.

Neoeutypella baoshanensis M. Raza, Q.J. Shang, Phookamsak & L. Cai, Fungal Diversity 95: 168 (2019)

Mycobank No: 555372
Fig. 7

Description. see Phookamsak et al. (2019).

Specimens examined. China, Guizhou Province, Guiyang City, Gaopo Township (26°29'72.37"N, 106°29'59.33"E), on branches of unidentified plant, 30 November 2020. Altitude: 1589 m, S.H. Long, GP01 (GMB0052, KUN-HKAS 112696, living culture GMBC0052).

Additional sequences. GMB0052 (LSU: MW797050, RPB2: MW814896).

Note. The morphological characteristics of this specimen are consistent with those of *N. baoshanensis* a species described by Phookamsak et al. (2019). Based on phylogenetic and morphological analyses, we consider that this specimen is *Neoeutypella baoshanensis*.

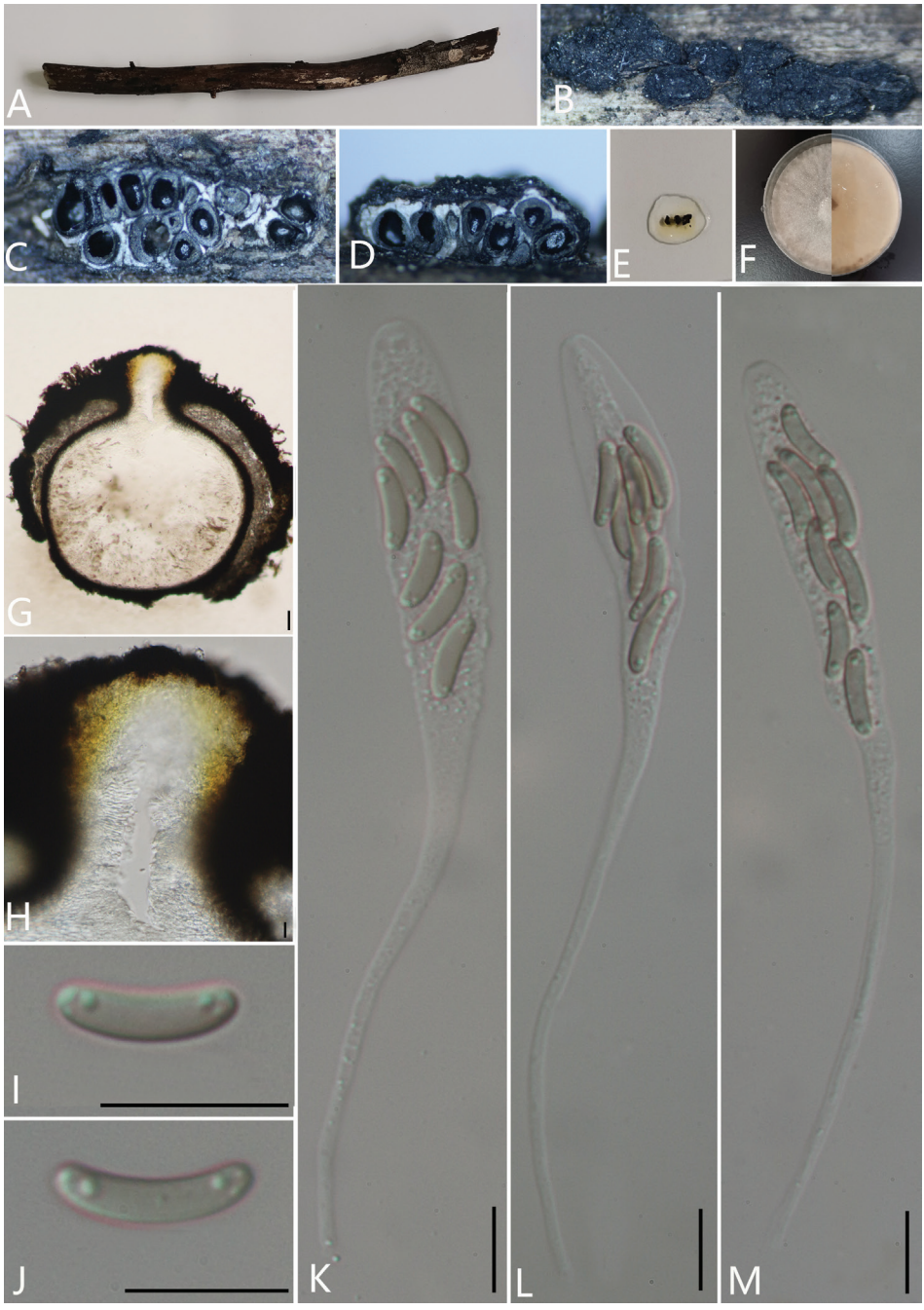

Figure 7. *Neoeutypella baoshanensis* (GMB0052) **A** stromata on host substrate **B** close-up of stromata **C** transverse section through ascostroma **D** vertical section through ascostroma **E** pigments in KOH **F** culture on PDA **G** section through the ascostroma **H** ostiolar canal **I, J** ascospores **K–M** asci. Scale bars: 20 μm (**G**); 10 μm (**H–M**).

Neoeutypella baoshanensis was described as the type species of *Neoeutypella* on dead wood of *Pinus armandii* Franch. from Yunnan Province in China (Phookamsak et al. 2019). This is the first record of *N. baoshanensis* from Guizhou Province, China.

Eutypa Tul. & C. Tul.

Notes. Tulasne & Tulasne (1863) introduced the genus *Eutypa* with *Eutypa lata* as the type species. This genus includes several phytopathogens, such as *E. lata* (Pers.) Tul. & C. Tul. and *E. leptoplaca* (Durieu & Mont.) Rappaz (Moyo et al. 2017). The morphological characteristics of this genus are black, rounded to irregular-shaped stromata on the host surface, erumpent through host epidermis, solitary to gregarious, entostromatic region, consisting of white pseudoparenchymatous cells and thin black pseudoparenchymatous tissue around the white entostroma, 8-spored, spindle-shaped asci and hyaline, oblong to allantoid ascospores (Rappaz 1987; Moyo et al. 2017). We introduce a new species of *Eutypa* collected from Guizhou Province in China.

Eutypa cerasi S.H. Long & Q.R. Li, sp. nov.

Mycobank No: 839657
Fig. 8

Holotype. GMB0048.

Etymology. Refers to its host, *Prunus cerasus*.

Description. *Saprobic* on decaying branches of *Prunus cerasus*. **Sexual morph:** *Stromata* immersed in bark, covering surface of host, irregular in shape, widely effused, flat, margin diffuse, surface dark brown to black, with punctiform ostioles scattered at surface. Endostroma consists of an outer layer of black, small, dense, thin parenchymal cells and an inner layer of white, large, loose parenchymal cells. *Perithecium* semi-immersed in stroma, globose to subglobose, glabrous, with cylindrical neck, brevicollous 203–304 µm high, 346–477 µm diam. (av. = 408 × 250 µm, n = 10), ovoid, obovoid to oblong. *Ostiole* opening separately, papillate or apapillate, central. *Peridium* 30–50 µm thick, dark brown to hyaline with *textura angularis* cell layers. *Asci* 83.2–120 × 5.1–8.2 µm (av. = 104.4 × 6.3 µm n = 30) 8–spored clavate, unitunicate, rounded to truncate apex, apical rings inamyloid. *Ascospores* 7.3–9.9 × 1.4–2 µm (av. = 8.5 × 1.7 µm, n = 30), overlapping, allantoid, slightly curved, subhyaline, smooth, aseptate, usually with oil droplets. **Asexual morph:** undetermined.

Culture characteristics. Ascospores germinating on PDA within 24 hours. Colonies on PDA, white when young, became pale yellow, irregular in shape, medium dense, flat or effuse, white from above, reverse white at margin, pale yellow at centre, no pigmentation produced on PDA medium, no conidia observed on PDA or on OA media.

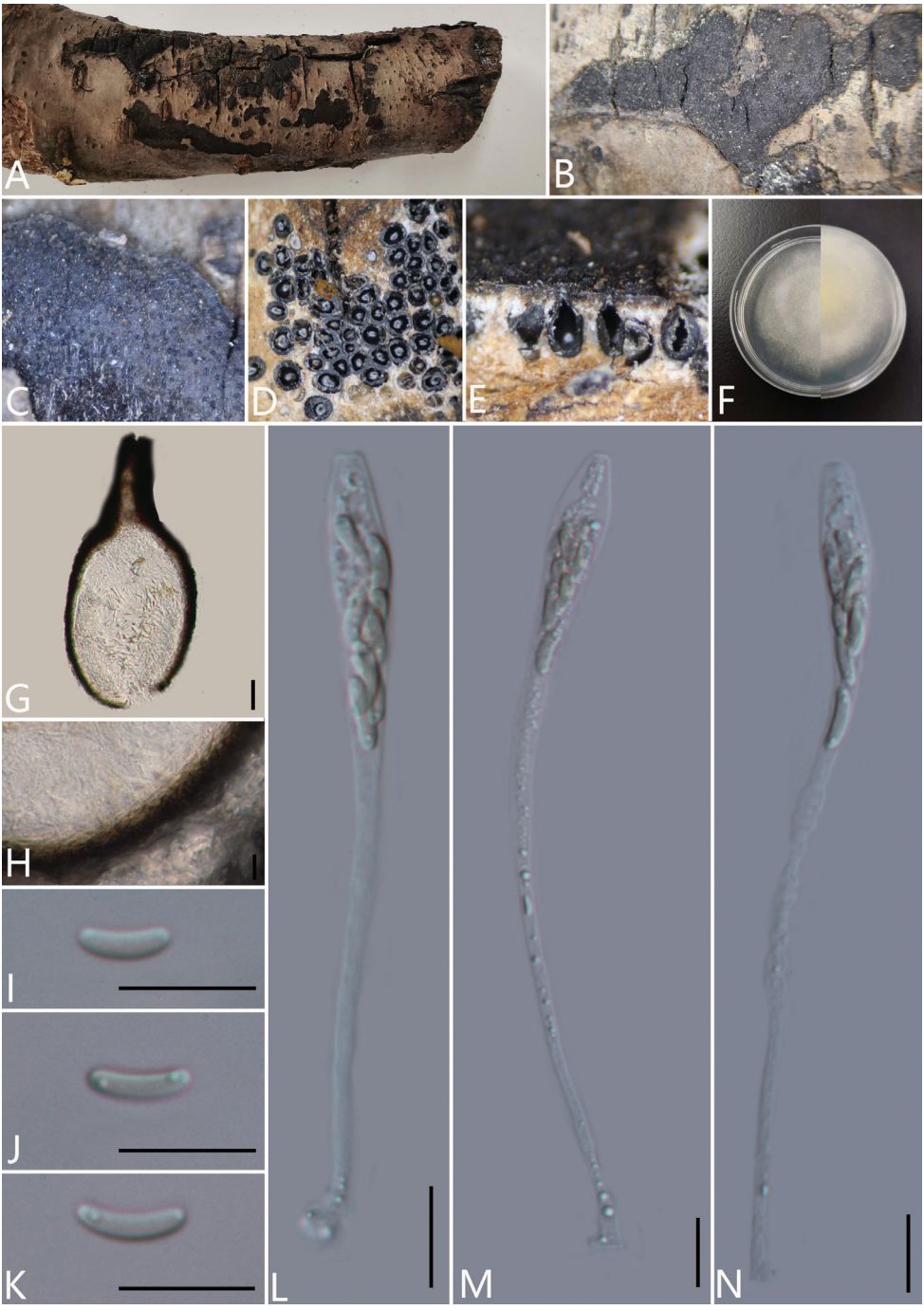

Figure 8. *Eutypa cerasi* (GMB0048, **holotype**) **A** stromata on host substrate **B, C** close-up of stroma **D** transverse section through ascostroma **E** vertical section through ascostroma **F** culture on PDA **G** section through the ascostroma **H** peridium **I–K** ascospores **L–N** asci. Scale bars: 20 μm (**G**); 10 μm (**H–N**).

Specimens examined. China, Guizhou Province, Guiyang City, Aha Lake National Wetland Park (26°32'50.21"N, 106°40'15.78"E), on branches of *Prunus cerasus*, 12 August 2020. Altitude: 1089 m, S.H. Long, AH4 (GMB0048, ***holotype***, KUNHKAS 112685, ***isotype***, ex-type living culture GMBC0048).

Additional specimens examined. China, Guizhou Province, Guiyang City, Aha Lake National Wetland Park (26°32'47.79"N, 106°40'21.09"E), on branches of *Cerasus* sp., 12 August 2020. Altitude: 1089 m, S.H. Long, AH40 (GMB0049, KUNHKAS 112683, living culture GMBC0049).

Additional sequences. GMB0048 (LSU: MW797048, RPB2: MW814894); GMB0049 (LSU: MW797049, RPB2: MW814895).

Notes. *Eutypa lata* is an important pathogen that has a wide range of hosts. However, the classification of *E. lata* is confusing because there are many variants in previous studies; now all are classified as *E. lata* (Index Fungorum 2020). Morphologically, the new collection GMB0048 has similar stromata with *Eutypa lata*, but the ascomata of the new collection are smaller than the ascomata (400 μm diam.) of the original description of *E. lata* (Tulasne & Tulasne, 1863). The ascomata and asci of the new collection are smaller than the ascomata (400–600 μm diam.) and asci (110–180 × 5–7 μm) of the description of *E. lata* (Rappaz 1987). Additionally, in the phylogenetic analyses, *E. cerasi* is located on a branch that forms a sister clade with EP18 and RGA01 and CBS 290.87 basal to *E. cerasi*. Therefore, combining phylogenetic and morphological analyses, we introduce *Eutypa cerasi* as a new species of *Eutypa*.

Paraeutypella **L.S. Dissan., J.C. Kang, Wijayaw. & K.D. Hyde.**

Notes. *Paraeutypella* was introduced by Dissanayake et al. (2021) to accommodate *Paraeutypella guizhouensis* and the genus currently comprises three species. The genus is characterised by poorly developed stromata erumpent through the bark, grouped and irregularly shaped, sometimes confluent, dark brown to black, spindle-shaped, 8-spored asci and allantoid, overlapping, subhyaline ascospores (Trouillas et al. 2011; de Almeida et al. 2016; Dissanayake et al. 2021). In this study, we illustrate *Paraeutypella citricola* collected from Guizhou Province in China.

Paraeutypella citricola **(Speg.). L.S. Dissan., Wijayaw., J.C. Kang & K.D. Hyde, in Dissanayake, Wijayawardene, Dayarathne, Samarakoon & Dai, Biodiversity Data Journal 9: e63864, 14 (2021)**

Mycobank No: 228646

Fig. 9

≡ *Eutypella citricola* Speg., Anal. Mus. nac. Hist. nat. B. Aires 6: 245 (1898)

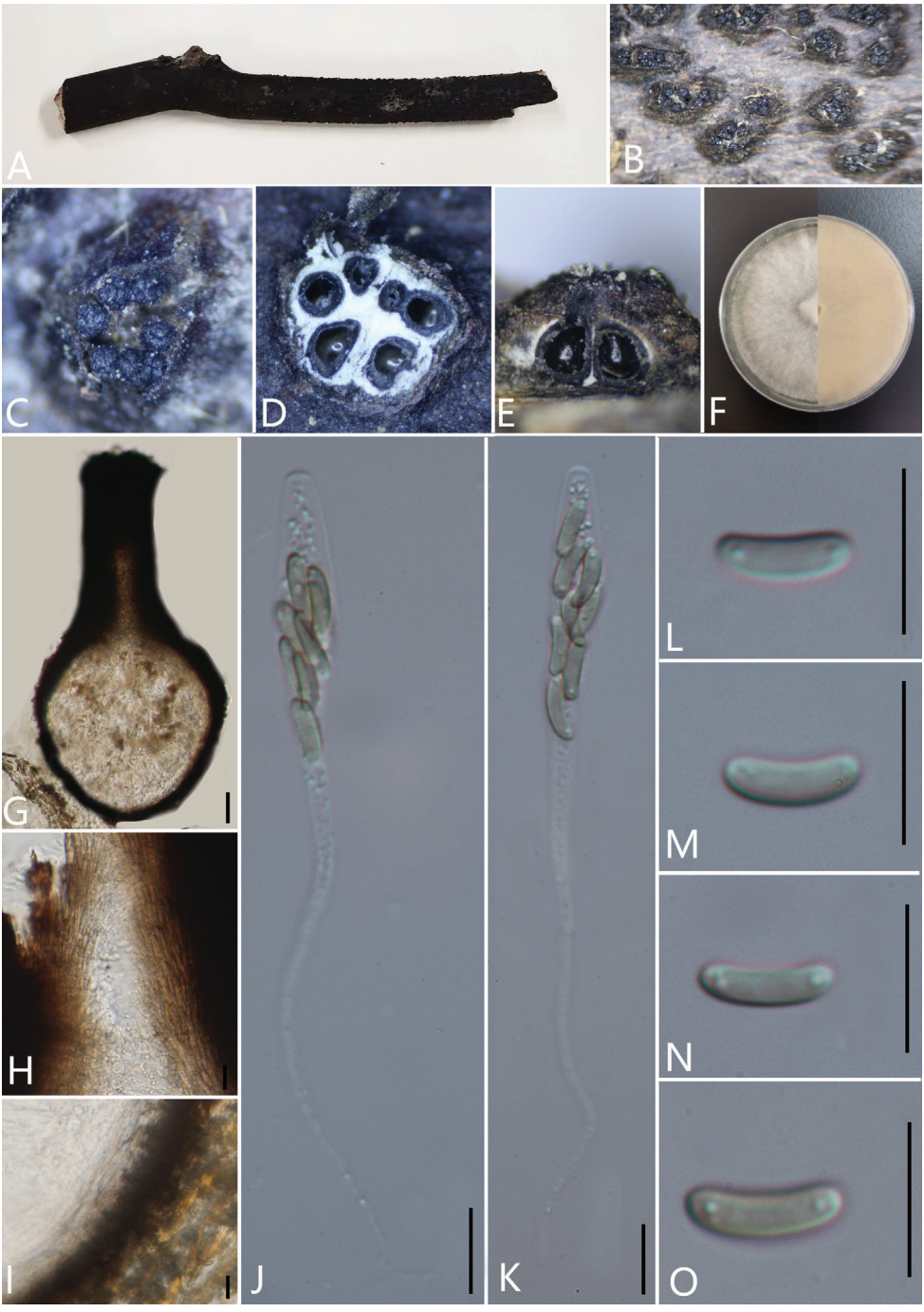

Figure 9. *Paraeutypella citricola* (GMB0053) **A** stromata on host substrate **B, C** stromata on host **D** transverse section through ascostroma **E** vertical section through ascostroma **F** culture on PDA **G** section through the ascostroma **H** ostiolar canal **I** peridium **J–K** ascospores **L–O** asci. Scale bars: 40 μm (**G**); 10 μm (**H–O**).

Table 2. The dimensions of the present species and some related species of *Diatrype* and *Allodiatrype*.

Species name	Stromata		Asci		Ascospores		Reference
	Length (mm)	Wide (mm)	Length (µm)	Wide (µm)	Length (µm)	Wide (µm)	
Allodiatrype arengae	0.69–0.94	0.37–0.93	54–109	6–10	7–10	2–3	Konta et al. (2020)
A. elaeidicola	1.2–2.8	0.9–1.66	60–91	4–7	8–10	1.5–3	Konta et al. (2020)
A. elaeidis	0.47–0.86	0.44–0.71	56–95	9–11	8–10	1.5–3	Konta et al. (2020)
A. thailandica	NA	1–2	55–80	5–7	3.8–6.9	1–1.4	Li et al. (2016)
Diatrype acericola	1–2	1–1.5	23–27	5–7	7.5–9	0.9–1.1	Vasilyeva and Ma (2014)
D. albopruinosa	0.5–1 diam.	0.5–1 diam	40–60	10–15	12–15	3.5–4	Vasilyeva and Ma (2014)
D. bullata	2–7 diam.	2–7 diam	25–30	5–7	7.5–9	Very thin	Vasilyeva and Ma (2014)
D. disciformis	NA	NA	75–115	NA	5–9	1.5–2	Senanayake et al. (2015)
D. enteroxantha	NA	1–3.5	18–28.5	5–9	7–10	1.5–2.5	de Almeida et al. (2016)
D. hypoxyloides	NA	NA	20–25	4–6	4–6	Very thin	Vasilyeva and Ma (2014)
D. lancangensis	**NA**	**NA**	**90.5–160.5**	**7–15**	**11–18.5**	**2–4**	**This study**
D. lijiangensis	1 diam.	1 diam	50–90	6–9	6–8	1–2	Thiyagaraja et al. (2019)
D. macounii	1–1.8 diam.	1–1.8 diam	25–30	4–6	4–6	0.7–1	Vasilyeva and Ma (2014)
D. stigma	NA	NA	25–30	5–7	6–8	1.5–2	Vasilyeva and Ma (2014)
D. subundulata	NA	NA	35–40	5–7	7–9	1.7–1.9	Vasilyeva and Ma (2014)
D. undulata	NA	NA	25–30	3.5–4.5	5–7	0.9–1.3	Vasilyeva and Ma (2014)
D. whitmanensis	NA	NA	50–82	8–15	7.5–10	1–1.5	Trouilla et al. 2010
Pseudodiatrype hainanensis	**2–3.6**	**1.6–3**	**110–155.5**	**6–10**	**8.5–13**	**1.5–2.5**	**This study**

Newly identified taxa are indicated in bold, NA: No description available.

Description. For description, see Dissanayake et al. (2021)

Specimens examined. China, Guizhou Province, Guiyang City: Aha Lake National Wetland Park (26°20'37.28"N, 108°21'4.34"E), on branches of unidentified plant, 30 August 2020. Altitude: 802 m, S.H. Long, LGS147 (GMB0053, KUNHKAS 112704, living culture GMBC0053).

Additional sequences. GMB0053 (LSU: 797053, RPB2: MW814898).

Notes. The ITS sequence data were compared by using NCBI and the result showed that it is 100% similar to the ex-type strain (HVVIT07) of *P. citricola*. The morphological features of the new collection are consistent with those described by Dissanayake et al. (2021). This collection is identified as a *P. citricolca*, based on morphological and molecular data.

Discussion

In this study, one new genus, three new species, two new records from China, a novel combination and two known species were reported from karst areas of China. We used molecular data to delimit the species of Diatrypaceae. The new genus *Pseudodiatrype* is morphologically similar to *Allodiatrype* and *Diatrype*, but distinct in the size of stromata, number of ascomata and colour of endostroma; it also formed a distinct branch in the phylogenetic analyses (Fig. 1). *Diatrype oregonensis* was transferred to *Diatrypella oregonensis* based on the phylogenetic analyses. Based on phylogenetic analyses, *Diatrypella pseudooregonensis* was introduced as an 8-spored species of *Diatrypella*.

Our phylogenetic analyses, based on ITS and β-tubulin, agree with the previous studies (Acero et al. 2004; Trouillas et al. 2011; Mehrabi et al. 2015, 2016; de Almeida et al. 2016; Shang et al. 2017; Dissanayake et al. 2021; Zhu et al. 2021). However, several genera are not monophyletic;for example, *Cryptosphaeria*, *Diatrype*, *Diatrypella*, and *Eutypa*. The identification of species of Diatrypaceae has been a problem due to the polyphyletic generic concepts based on the features of the stromata in early research (Fries 1823). Recently, new approaches have been proposed for classifying Diatrypaceae. Acero et al. (2004) proposed to classify them by ITS sequence-based phylogenetic analyses, while Carmarán et al. (2006) suggested that the identification should be based on the morphology of the asci. However, due to the lack of type specimens, the lack of β-tubulin sequence and polyphyletic origins have resulted in molecular data that correlate poorly with morphological criteria used to delineate genera and species within the Diatrypaceae (Acero et al. 2004). Moreover, Acero et al. (2004) has mentioned that *Diatrypella quercina* should be placed in the genus *Diatrype* despite its polysporous asci since the molecular data placed *Diatrypella quercina* in the branch of the genus *Diatrype*.

Diatrype and *Diatrypella* have morphologically similar verruculose stromata and allantoid ascospores and the polysporous or 8-spored ascus serve as a basis for distinguishing the two genera. However, in phylogenetic analyses, species of these two genera overlap. In this study, we used the phylogenetic analyses as the main basis for classification following Vasilyeva and Stephenson (2005) and Liu et al. (2015). Clade 1 contains *Diatrypella verruciformis* which is the type species of *Diatrypella*, of which *Diatrypella pseudooregonensis*, *Diatrypella oregonensis* have 8-spored, and other species in clade 1 have polyspored ascus. Clade 12 contains the *Diatrype* type species *Diatrype disciformis*, of which *Diatrype iranensis* and *Diatrype macrospora* have polyspored ascus, and other species in clade 12 have 8-spored ascus. Hence, we concluded that the number of ascospores in each ascus cannot be used as a criterion for distinguishing *Diatrypella* from *Diatrype*.

The phylogenetic tree shows that the classification of Diatrypaceae is confusing. Members of *Diatrypella* (*D. favacea*, *D. hubeiensis*, *D. pulvinata* and *D. yunnanensis*) cluster with *Diatrype palmicola* and *Diatrype lancangensis*.Maybe this clade should be identified as a new genus. We will discuss its classification status after more strains, more gene sequences and new taxonomic features are collected. Some species of *Diatrypella* (*D. iranensis* and *D. macrospora*) which have polysporous ascus are placed between species of *Diatrype*, and they are transferred to *Diatrype iranensis* and *Diatrype macrospora* by Zhu et al. (Zhu et al. 2021). *Diatrype enteroxantha* is often derived from the sister clade of *Allodiatrype* rather than the *Diatrype* clade. Additionally, *Eutypa microasca* (BAFC51550) clusters with *Peroneutypa* species (Clade 17). The above-mentioned confusion also showed in the original publication and other recent studies (Grassi et al. 2014; Mehrabi et al. 2016; Shang et al. 2018; Hyde et al. 2019; Phookamsak et al. 2019; Konta et al. 2020). Therefore, addressing the taxonomic confusion of this family requires a re-examination of older taxa, based on morphological studies, epitypification and multi-gene phylogenetic analyses (Ariyawansa et al. 2014).

Acknowledgements

This research was supported by the National Natural Science Foundation of China (32000009 and 31960005); the Fund of the Science and Technology Foundation of Guizhou Province ([2020]1Y059); Guiyang Science and Technology Planning Project No. (2017)30-19; Guizhou Province Ordinary Colleges and Universities Youth Science and Technology Talent Growth Project [2021]154. Nalin N. Wijayawardene would like to thank the National Natural Science Foundation of China (No. NSFC 31950410558), the State Key Laboratory of Functions and Applications of Medicinal Plants, Guizhou Medicial University (No. FAMP201906K) and High-Level Talent Recruitment Plan of Yunnan Provinces ("Young Talents" Program and "High-End Foreign Experts" Program); the Fund of High-Level Innovation Talents [No. 2015-4029], the Base of International Scientific and Technological Cooperation of Guizhou Province [No. [2017]5802].

Reference

Acero FJ, González V, Ballesteros JS, Rubio V, Checa J, Bills GF, Salazar O, Platas G, Peláez F (2004) Molecular phylogenetic studies on the Diatrypaceae based on rDNA-ITS sequences. Mycologia 96: 249–259. https://doi.org/10.1080/15572536.2005.11832975

Arhipova N, Gaitnieks T, Donis J, Stenlid J, Vasaitis R (2012) Heart-rot and associated fungi in Alnus glutinosa stands in Latvia. Scandinavian Journal of Forest Research 27: 327–336. https://doi.org/10.1080/02827581.2012.670727

Ariyawansa HA, Hawksworth DL, Hyde KD, Jones EGB, Maharachchikumbura SSN, Manamgoda DS, Thambugala KM, Udayanga D, Camporesi E, Daranagama A, Jayawardena R, Liu JK, Mckenzie EHC, Phookamsak R, Senanayake IC, Shivas RG, Tian Q, Xu JC (2014) Epitypification and neotypification: guidelines with appropriate and inappropriate examples. Fungal Diversity 69: 57–91. https://doi.org/10.1007/s13225-014-0315-4

Carmarán CC, Romero AI, Giussani LM (2006) An approach towards a new phylogenetic classification in Diatrypaceae. Fungal Diversity 23: 67–87.

Chomnunti P, Hongsanan S, Hudson BA, Tian Q, Peršoh D, Dhami MK, Alias AS, Xu JC, Liu XZ, Stadler M, Hyde KD (2014) The sooty moulds. Fungal Divers 66: 1–36. https://doi.org/10.1007/s13225-014-0278-5

Crous PW, Wingfield MJ, Guarro J, Cheewangkoon R, van der Bank M, Swart WJ, Stchigel AM, Cano-Lira JF, Roux J, Madrid H, Damm U, Wood AR, Shuttleworth LA, Hodges CS, Munster M, de Jesús Yáñez-Morales M, Zúñiga-Estrada L, Cruywagen EM, De Hoog GS, Silvera C, Najafzadeh J, Davison EM, Davison PJN, Barrett MD, Barrett RL, Manamgoda DS, Minnis AM, Kleczewski NM, Flory SL, Castlebury LA, Clay K, Hyde KD, Maússe-Sitoe SND, Chen S, Lechat C, Hairaud M, Lesage-Meessen L, Pawłowska J, Wilk M, Śliwińska-Wyrzychowska A, Mętrak M, Wrzosek M, Pavlic-Zupanc D, Maleme HM, Slippers B, Mac Cormack WP, Archuby DI, Grünwald NJ, Tellería MT, Dueñas M, Martín MP, Marincowitz S, de Beer ZW, Perez CA, Gené J, Marin-Felix Y, Groenewald JZ

(2013) Fungal Planet description sheets: 154–213. Persoonia: Molecular Phylogeny and Evolution of Fungi 31: 1–188. https://doi.org/10.3767/003158513X675925

Dayarathne MC, Phookamsak R, Hyde KD, Manawasinghe IS, Toanun C, Jones EBG (2016) *Halodiatrype*, a novel diatrypaceous genus from mangroves with *H. salinicola* and *H. avicenniae* spp. nov. Mycosphere 7: 612–627. https://doi.org/10.5943/mycosphere/7/5/7

Dayarathne MC, Wanasinghe DN, Devadatha B, Abeywickrama P, Jones EBG, Chomnunti P, Sarma VV, Hyde KD, Lumyong S, McKenzie EHC (2020) Modern taxonomic approaches to identifying diatrypaceous fungi from marine habitats, with a Novel Genus *Halocryptovalsa* Dayarathne & K.D.Hyde, Gen. Nov. Cryptogamie Mycologie, 41: 21–67. https://doi.org/10.5252/cryptogamie-mycologie2020v41a3

de Almeida DAC, Gusmão LFP, Miller AN (2016) Taxonomy and molecular phylogeny of Diatrypaceae (Ascomycota, Xylariales) species from the Brazilian semi-arid region, including four new species. Mycological Progress 15: 1–27.

Dissanayake LS, Wijayawardene NN, Dayarathne MC, Samarakoon MC, Dai DQ, Hyde KD, Kang JC (2021) *Paraeutypella guizhouensis* gen. et sp. nov. and *Diatrypella longiasca* sp. nov. (Diatrypaceae) from China. Biodiversity Data Journal 9: e63864. https://doi.org/10.3897/BDJ.9.e63864

Dong D, Fang C, Zhao W, Xie Z (2002) Evaluation of geochemical quality control in determination of Mn in soils using a sequential chemical extraction. Chinese Geographical Science 12: 166–170. https://doi.org/10.1007/s11769-002-0026-8

Fries EM (1823) Systema Mycologicum 3: 1–202.

Gao LL, Zhang Q, Sun XY, Jiang L, Zhang R, Sun GY, Zha YL, Biggs AR (2013) Etiology of moldy core, core browning, and core rot of fuji apple in China. Plant Disease 97: 510–516. https://doi.org/10.1094/PDIS-01-12-0024-RE

Glass NL, Donaldson GC (1995) Development of primer sets designed for use with the PCR to amplify conserved genes from filamentous ascomycetes. Applied & Environmental Microbiology 61: 1323–1330. https://doi.org/10.1128/aem.61.4.1323-1330.1995

Glawe DA, Rogers JD (1984) Diatrypaceae in the Pacific Northwest. Mycotaxon 20: 401–460.

Glez-Peña D, Gómez-Blanco D, Reboiro-Jato M, Fdez-Riverola F, David P (2010) ALTER: programoriented conversion of DNA and protein alignments. Nucleic Acids Research 38: 14–18. https://doi.org/10.1093/nar/gkq321

Grassi E, Belen Pildain M, Levin L, Carmaran C (2014) Studies in Diatrypaceae: the new species *Eutypa microasca* and investigation of ligninolytic enzyme production. Sydowia 66: 99–114.

Hall TA (1999) BioEdit: a user-friendly biological sequence alignment editor and analysis program for windows 95/98/NT. Nucleic Acids Symposium Series 41: 95–98.

Hyde KD, Norphanphoun C, Maharachchikumbura SSN, Bhat DJ, Jones EBG, Bundhun D, Chen YJ, Bao DF, Boonmee S, Calabon MS, Chaiwan N, Chethana KWT, Dai DQ, Dayarathne MC, Devadatha B, Dissanayake AJ, Dissanayake LS, Doilom M, Dong W, Fan XL, Goonasekara ID, Hongsanan S, Huang SK, Jayawardena RS, Jeewon R, Karunarathna A, Konta S, Kumar V, Lin CG, Liu JK, Liu NG, Luangsa-ard J, Lumyong S, Luo ZL, Marasinghe DS, McKenzie EHC, Niego AGT, Niranjan M, Perera RH, Phukhamsakda C, Rathnayaka AR, Samarakoon MC, Samarakoon SMBC, Sarma VV, Senanayake IC,

Shang QJ, Stadler M, Tibpromma S, Wanasinghe DN, Wei DP, Wijayawardene NN, Xiao YP, Yang J, Zeng XY, Zhang SN, Xiang MM (2020a) Refined families of Sordariomycetes. Mycosphere 11: 305–1059. https://doi.org/10.5943/mycosphere/11/1/7

Hyde KD, Dong Y, Phookamsak R, Jeewon R, Bhat DJ, Jones EBG, Liu NG, Abeywickrama PD, Mapook A, Wei D, Perera RH, Manawasinghe IS, Pem D, Bundhun D, Karunarathna A, Ekanayaka AH, Bao DF, Li JF, Samarakoon MC, Chaiwan N, Lin CG, Phutthacharoen K, Zhang SN, Senanayake IC, Goonasekara ID, Thambugala KM, Phukhamsakda C, Tennakoon DS, Jiang HB, Yang J, Zeng M, Huanraluek N, Liu JK, Wijesinghe SN, Tian Q, Tibpromma S, Brahmanage RS, Boonmee S, Huang SK, Thiyagaraja V, Lu YZ, Jayawardena RS, Dong W, Yang EF, Singh SK, Singh SM, Rana S, Lad SS, Anand G, Devadatha B, Niranjan M, Sarma VV, Liimatainen K, Hudson BA, Niskanen T, Overall A, Alvarenga RLM, Gibertoni TB, Pfliegler WP, Horváth E, Imre A, Alves AL, da Silva Santos AC, Tiago PV, Bulgakov TS, Wanasinghe DN, Bahkali AH, Doilom M, Elgorban AM, Maharachchikumbura SSN, Rajeshkumar KC, Haelewaters D, Mortimer PE, Zhao Q, Lumyong S, Xu JC, Sheng J (2020b) Fungal diversity notes 1151–1276: taxonomic and phylogenetic contributions on genera and species of fungal taxa. Fungal diversity 100: 5–277. https://doi.org/10.1007/s13225-020-00439-5

Hyde KD, Norphanphoun C, Abreu VP, Bazzicalupo A, Thilini Chethana KW, Clericuzio M, Dayarathne MC, Dissanayake AJ, Ekanayaka AH, He MQ, Hongsanan S, Huang SK, Jayasiri SC, Jayawardena RS, Karunarathna A, Konta S, Kušan I, Lee H, Li JF, Lin CG, Liu NG, Lu YZ, Luo ZL, Manawasinghe IS, Mapook A, Perera RH, Phookamsak R, Phukhamsakda C, Siedlecki I, Soares AM, Tennakoon DS, Tian Q, Tibpromma S, Wanasinghe DN, Xiao YP, Yang J, Zeng XY, Abdel-Aziz FA, Li WJ, Senanayake IC, Shang QJ, Daranagama DA, de Silva NI, Thambugala KM, Abdel-Wahab MA, Bahkali AH, Berbee ML, Boonmee S, Bhat DJ, Bulgakov TS, Buyck B, Camporesi E, Castañeda-Ruiz RF, Chomnunti P, Doilom M, Dovana F, Gibertoni TB, Jadan M, Jeewon R, Jones EBG, Kang JC, Karunarathna SC, Lim YW, Liu JK, Liu ZY, Plautz Jr HL, Lumyong S, Maharachchikumbura SSN, Matočec N, McKenzie EHC, Mešić A, Miller D, Pawłowska J, Pereira OL, Promputtha I, Romero AL, Ryvarden L, Su HY, Suetrong S, Tkalčec Z, Vizzini A, Wen TC, Wisitrassameewong K, Wrzosek M, Xu JC, Zhao Q, Zhao RL, Mortimer PE (2017) Fungal diversity notes 603–708: taxonomic and phylogenetic notes on genera and species. Fungal Diversity 87: 1–235. https://doi.org/10.1007/s13225-017-0391-3

Hyde KD, Tennakoon DS, Jeewon R, Bhat DJ, Maharachchikumbura SSN, Rossi W, Leonardi M, Lee HB, Mun HY, Houbraken J, Nguyen TTT, Jeon SJ, Frisvad JC, Dhanushka N, Wanasinghe DN, Luücking R, Aptroot A, Cáceres MES, Karunarathna SC, Hongsanan S, Phookamsak R, de Silva NI, Thambugala KM, Jayawardena RS, Senanayake IC, Boonmee S, Chen J, Luo ZL, Phukhamsakda C, Pereira OL, Abreu VP, Rosado AWC, Bart B, Randrianjohany E, Hofstetter V, Gibertoni TB, da Silva Soares AM, Plautz Jr HL, Sotão HMP, Xavier WKS, Bezerra JDP, de Oliveira TGL, de Souza-Motta CM, Magalhães OMC, Bundhun D, Harishchandra D, Manawasinghe IS, Dong W, Zhang SN, Bao DF, Samarakoon MC, Pem D, Karunarathna A, Lin CG, Yang J, Perera RH, Kumar V, Huang SK, Dayarathne MC, Ekanayaka AH, Jayasiri SC, Xiao YP, Konta S, Niskanen T, Liimatainen K, Dai YC, Ji XH, Tian XM, Mešić A, Singh SK, Phutthacharoen K, Cai L, Sorvongxay T,

Thiyagaraja V, Norphanphoun C, Chaiwan N, Lu YZ, Jiang HB, Zhang JF, Abeywickrama PD, Aluthmuhandiram JVS, Brahmanage RS, Zeng M, Chethana T, Wei DP, Réblová M, Fournier J, Nekvindová J, do Nascimento Barbosa R, dos Santos JEF, de Oliveira NT, Li GJ, Ertz D, Shang QJ, Phillips AJL, Kuo CH, Camporesi E, Bulgakov TS, Lumyong S, Jones EBG, Chomnunti P, Gentekaki E, Bungartz F, Zeng XY, Fryar S, Tkalčec Z, Liang J, Li GS, Wen TC, Singh PN, Gafforov Y, Promputtha I, Yasanthika E, Goonasekara ID, Zhao RL, Zhao Q, Kirk PM, Liu JK, Yan JY, Mortimer PE, Xu JC (2019) Fungal diversity notes 1036–1150: taxonomic and phylogenetic contributions on genera and species of fungal taxa. Fungal Diversity 96: 1–242. https://doi.org/10.1007/s13225-019-00429-2

Index Fungorum (2020) Index Fungorum http://www.indexfungorum.org/Names/Names.asp

Jurc D, Ogris N, Slippers B, Stenlid J (2006) First report of *Eutypella* canker of Acer pseudoplatanus in Europe. Plant Pathology 55: 577–577. https://doi.org/10.1111/j.1365-3059.2006.01426.x

Kauffman CH (1930) The fungous flora of Siskiyou Mountains in southern Oregon. Papers of the Michigan Academy of Science, Arts, and Letters 11: 151–210.

Klaysuban A, Sakayaroj J, Jones EG (2014) An additional marine fungal lineage in the Diatrypaceae, Xylariales: *Pedumispora rhizophorae*. Botanica marina 57: 413–420. https://doi.org/10.1515/bot-2014-0017

Konta S, Maharachchikumbura SSN, Senanayake IC, McKenzie EHC, Stadler M, Boonmee S, Phookamsak R, Jayawardena RS, Senwanna C, Hyde KD, Elgorban AM, Eungwanichayapant PD (2020) A new genus *Allodiatrype*, five new species and a new host record of diatrypaceous fungi from palms (Arecaceae). Mycosphere 11: 239–268. https://doi.org/10.5943/mycosphere/11/1/7

Li GJ, Hyde KD, Zhao RN, Hongsanan S, Abdel-Aziz FA, Abdel-Wahab MA, Alvarado P, Alves-Silva G, Ammirati JF, Ariyawansa HA, Baghela A, Bahkali AH, Beug M, Bhat DJ, Bojantchev D, Boonpratuang T, Bulgakov TS, Camporesi E, Boro MC, Ceska O, Chakraborty D, Chen JJ, Chethana KWT, Chomnunti P, Consiglio G, Cui BK, Dai DQ, Dai YC, Daranagama DA, Das K, Dayarathne MC, Crop ED, De Oliveira RJV, De Souza CAF, De Souza JI, Dentinger BTM, Dissanayake AJ, Doilom M, Drechsler-Santos ER, Ghobad-Nejhad M, Gilmore SP, Góes-Neto A, Gorczak M, Haitjema GH, Hapuarachchi KK, Hashimoto A, He MQ, Henske JK, Hirayama K, Iribarren MJ, Jayasiri SC, Jayawardena RS, Jeon SJ, Jerônimo GH, Jesus AL, Jones EBG, Kang JC, Karunarathna SC, Kirk PM, Konta S, Kuhnert E, Langer E, Lee HS, Lee HB, Li WJ, Li XH, Liimatainen K, Lima DX, Lin CG, Liu JK, Liu XZ, Liu ZY, Luangsa-Ard JJ, Lücking R, Lumbsch HT, Lumyong S, Leaño EM, Marano AV, Matsumura M, Mckenzie EHC, Mongkolsamrit S, Mortimer PE, Nguyen TTT, Niskanen T, Norphanphoun C, O'malleym MA, Parnmen S, Pawłowska J, Perera RH, Phookamsak R, Phukhamsakda C, PiresZottarelli CLA, Raspé O, Reck MA, Rocha SCO, De Santiago ALCMA, Senanayake IC, Setti L, Shang QJ, Singh SK, Sir EB, Solomon KV, Song J, Srikitikulchai P, Stadler M, Suetrong S, Takahashi H, Takahashi T, Tanaka K, Tang LP, Thambugala KM, Thanakitpipattana D, Theodorou MK, Thongbai B, Thummarukcharoen T, Tian Q, Tibpromma S, Verbeken A, Vizini A, Vlasák J, Voigt K, Wanasinghe DN, Wang Y, Weerakoon G, Wen HA, Wen TC, Wijayawardene NN, Wongkanoun S, Wrzosek M, Xiao YP, Xu JC, Yan JY, Yang J, Yang SD, Hu Y, Zhang

JF, Zhao J, Zhou LW, Peršoh D, Phillips AJL, Maharachchikumbura SSN (2016) Fungal Divers notes 253–366: taxonomic and phylogenetic contributions to fungal taxa. Fungal Diversity 78: 1–237. https://doi.org/10.1007/s13225-016-0366-9

Liu JK, Hyde KD, Gareth EBG, Ariyawansa HA, Bhat DJ, Boonmee S, Maharachchikumbura SS, Mckenzie EH, Phookamsak R, Phukhamsakda C, Shenoy BD, AbdelWahab MA, Buyck B, Chen J, Chethana KWT, Singtripop C, Dai DQ, Dai YC, Daranagama DA, Dissanayake AJ, Doilom M, D'souza MJ, Fan XL, Goonasekara ID, Hirayama K, Hongsanan S, Jayasiri SC, Jayawardena RS, Karunarathna SC, Li WJ, Mapook A, Norphanphoun C, Pang KL, Perera RH, Peršoh D, Pinruan U, Senanayake IC, Somrithipol S, Suetrong S, Tanaka K, Thambugala KM, Tian Q, Tibpromma S, Udayanga D, Wijayawardene NN, Wanasinghe D, Wisitrassameewong K, Zeng XY, Abdel-Aziz FA, Adamcík S, Bahkali AH, Boonyuen N, Bulgakov T, Callac P, Chomnunti P, Greiner K, Hashimoto A, Hofstetter V, Kang JC, Xing DL, Li H, Liu XZ, Liu ZY, Matsumura M, Mortimer PE, Rambold G, Randrianjohany E, Sato G, Sri-Indrasutdhi V, Tian CM, Verbeken A, Brackel W, Wang Y, Wen TC, Xu JC, Yan JY, Zhao RL, Camporesi, E (2015) Fungal diversity notes 1–110: taxonomic and phylogenetic contributions to fungal species. Fungal Diversity 72: 1–197. https://doi.org/10.1007/s13225-015-0324-y

Luque J, Garcia-Figueres F, Legorburu FJ, Muruamendiaraz A, Armengol J, Trouillas FP (2012) Species of Diatrypaceae associated with grapevine trunk diseases in Eastern Spain. Phytopathologia Mediterranea 51: 528–540. https://doi.org/10.14601/Phytopathol_Mediterr-9953

Lynch SC, Eskalen A, Zambino PJ, Mayorquin JS, Wang DH (2013) Identifcation and pathogenicity of Botryosphaeriaceae species associated with coast live oak (*Quercus agrifolia*) decline in southern California. Mycologia 105: 125–140. https://doi.org/10.3852/12-047

Maharachchikumbura SSN, Hyde KD, Jones EBG, McKenzie EHC, Bhat JD, Dayarathne MC, Huang SK, Norphanphoun C, Senanayake IC, Perera RH, Shang QJ, Xiao Y, D'souza MJ, Hongsanan S, Jayawardena RS, Daranagama DA, Konta S, Goonasekara ID, ZhuangWY, Jeewon R, Phillips AJL, Abdel-Wahab MA, Al-Sadi AM, Bahkali AH, Boonmee S, Boonyuen N, Cheewangkoon R, Dissanayake AJ, Kang J, Li QR, Liu JK, Liu XZ, Liu ZY, Luangsa-Ard JJ, Pang KL, Phookamsak R, Promputtha I, Suetrong S, Stadler M, Wen T, Wijayawardene NN (2016) Families of Sordariomycetes. Fungal Diversity 79: 1–317. https://doi.org/10.1007/s13225-016-0369-6

Mehrabi M, Asgari B, Hemmati R (2019) Two new species of *Eutypella* and a new combination in the genus *Peroneutypa* (Diatrypaceae). Mycological Progress 18: 1057–1069. https://doi.org/10.1007/s11557-019-01503-4

Mehrabi M, Hemmati R, Vasilyeva LN, Trouillas FP (2015) A new species and a new record of Diatrypaceae from Iran. Mycosphere 6: 60–68. https://doi.org/10.5943/mycosphere/6/1/7

Mehrabi M, Hemmati R, Vasilyeva LN, Trouillas FP (2016) *Diatrypella macrospora* sp. nov. and new records of diatrypaceous fungi from Iran. Phytotaxa 252: 43–55. https://doi.org/10.2307/3762061

Miao Q, Wang Y, Li J, Yuan S, Shi L, Gu X (2007) Study on the spring drought rule in the karst region of yunnan and guizhou plateau in china. International Society for Optics and Photonics 6790: 67903Z. https://doi.org/10.1117/12.746860

Miller MA, Pfeiffer W, Schwartz T (2010) Creating the CIPRES Science Gateway for inference of large phylogenetic trees. In: Gateway Computing Environments Workshop 2010 (GCE), New Orleans, Louisiana, November 2010: 1–8. https://doi.org/10.1109/GCE.2010.5676129

Moyo P, Damm U, Mostert L, Halleen F (2018a) *Eutypa*, *Eutypella*, and *Cryptovalsa* Species (Diatrypaceae) associated with Prunus species in South Africa. Plant Disease 102: 1402–1409. https://doi.org/10.1094/PDIS-11-17-1696-RE

Moyo P, Mostert L, Spies CF, Damm U, Hallen F (2018b) Diversity of Diatrypaceae species associated with dieback of grapevines in South Africa, with the description of *Eutypa cremea* sp. nov. Plant Disease 102: 220–230. https://doi.org/10.1094/PDIS-05-17-0738-RE

Nylander JAA (2004) MrModeltest v2.2. Program distributed by the author: 2. Evolutionary Biology Centre, Uppsala University 1–2.

O'Donnell K, Cigelnik E (1997) Two divergent intragenomic rDNA ITS2 types within amonophyletic lineage of the fungus Fusarium are nonorthologous. Molecular Phylogenetics and Evolution 7: 103–116. https://doi.org/10.1006/mpev.1996.0376

Paolinelli-Alfonso M, Serrrano-Gomez C, Hernandez-Martinez R (2015) Occurrence of *Eutypella microtheca* in grapevine cankers in Mexico. Phytopathologia Mediterranea 54: 86–93. https://doi.org/10.14601/Phytopathol_Mediterr-14998

Perera RH, Hyde KD, Maharachchikumbura S, Jones EBG, McKenzie EHC, Stadler M, Lee HB, Samarakoon MC, Ekanayaka AH, Camporesi E, Liu JK, Liu ZY (2020) Fungi on wild seeds and fruits. mycosphere 11: 2108–2480. https://doi.org/10.5943/mycosphere/11/1/14

Peršoh D, Melcher M, Graf K, Fournier J, Stadler M, Rmbold G (2009) Molecular and morphological evidence for the delimitation of *Xylaria hypoxylon*. Mycologia 101: 256–268. https://doi.org/10.3852/08-108

Phookamsak R, Hyde KD, Jeewon R, Bhat DJ, Jones EBG, Maharachchikumbura SSN, Raspé O, Karunarathna SC, Wanasinghe DN, Hongsanan S, Doilom M, Tennakoon DS, Machado AR, Firmino AL, Ghosh A, Karunarathna A, Mešić A, Dutta AK, Thongbai B, Devadatha B, Norphanphoun C, Senwanna C, Wei DP, Pem D, Ackah FK, Wang GN, Jiang HB, Madrid H, Lee HB, Goonasekara ID, Manawasinghe IS, Kušan I, Cano J, Gené J, Li JF, Das K, Acharya K, Anil Raj KN, Deepna Latha KP, Thilini Chethana KW, He MQ, Dueñas M, Jadan M, Martín MP, Samarakoon MC, Dayarathne MC, Raza M, Park MS, Teresa Telleria M, Chaiwan N, Matočec N, de Silva NO, Pereira OL, Singh PN, Manimohan P, Uniyal P, Shang QJ, Bhatt RP, Perera RH, Alvarenga RLM, Nogal-Prata S, Singh SK, Vadthanarat S, Oh SY, Huang SK, Rana S, Konta S, Paloi S, Jayasiri SC, Jeon JS, Mehmood T, Gibertoni TB, Nguyen TT, Singh U, Thiyagaraja V, Sarma VV, Dong W, Yu XD, Lu YZ, Lim YW, Chen Y, Tkalčec Z, Zhang ZF, Luo ZL, Daranagama DA, Thambugala KM, Tibpromma S, Camporesi E, Bulgakov TS, Dissanayake AJ, Senanayake IC, Dai DQ, Tang LZ, Khan S, Zhang H, Promputtha I, Cai L, Chomnunti P, Zhao RL, Lumyong S, Boonmee S, Wen TC, Mortimer PE, Xu JC (2019) Fungal diversity notes 929–1036: taxonomic and phylogenetic contributions on genera and species of fungal taxa. Fungal Diversity 95: 1–273. https://doi.org/10.1007/s13225-019-00421-w

Phukhamsakda C, McKenzie EHC, Phillips AJL, Gareth Jones EB, Jayarama Bhat D, Stadler M, Bhunjun CS, Wanasinghe DN, Thongbai B, Camporesi E, Ertz D, Jayawardena RS,

Perera RH, Ekanayake AH, Tibpromma S, Doilom M, Xu J, Hyde KD (2020) Microfungi associated with *Clematis* (Ranunculaceae) with an integrated approach to delimiting species boundaries. Fungal Diversity 102: 1–203. https://doi.org/10.1007/s13225-020-00448-4

Rambaut A (2012) FigTree: Tree Figure Drawing Tool Version 1.4.0 2006–2012, Institute of Evolutionary Biology, University of Edinburgh. http://tree.bio.ed.ac.uk/software/figtree/

Rappaz F (1987) Taxonomy and nomenclature of the octosporous Diatrypaceae. Mycologia Helvetica 2: 285–648.

Rolshausen PE, Mahoney NE, Molyneux RJ, Gubler WD (2006) A reassessment of the species concept in *Eutypa lata*, the causal agent of *Eutypa* dieback of grapevine. Phytopathology 96: 369–377. https://doi.org/10.1094/PHYTO-96-0369

Senanayake IC, Maharachchikumbura SN, Hyde KD, Bhat JD, Jones EG, Mckenzie EH, Dai DQ, Daranagama DA, Dayarathne MC, Goonasekara ID, Konta S, Li WJ, Shang QJ, Stadler M, Wijayawardene NN, Xiao YP, Norphanphoun C, Li Q, Liu XY, Bahkali AH, Kang JC, Wang Y, Wen TC, Wendt I, Xu JC, Camporesi E (2015) Towards unraveling relationships in Xylariomycetidae (Sordariomycetes). Fungal Diversity 73: 73–144. https://doi.org/10.1007/s13225-015-0340-y

Senwanna C, Phookamsak R, Doilom M, Hyde KD, Cheewangkoon R (2017) Novel taxa of Diatrypaceae from Para rubber (*Hevea brasiliensis*) in northern Thailand; introducing a novel genus *Allocryptovalsa*. Mycosphere 8: 1835–1855. https://doi.org/10.5943/mycosphere/8/10/9

Shang QJ, Hyde KD, Jeewon R, Khan S, Promputtha I, Phookamsak R (2018) Morpho-molecular characterization of *Peroneutypa* (Diatrypaceae, Xylariales) with two novel species from Thailand. Phytotaxa 356: 1–18. https://doi.org/10.1080/15572536.2005.11832975

Shang QJ, Hyde KD, Phookamsak R, Doilom M, Bhat DJ, Maharachchikumbura SS, Promputtha I (2017) *Diatrypella tectonae* and *Peroneutypa mackenziei* spp. nov. (Diatrypaceae) from northern Thailand. Mycological progress 16: 463–476. https://doi.org/10.1007/s11557-017-1294-0

Thiyagaraja V, Senanayake IC, Wanasinghe DN, Karunarathna SC, Worthy FR, To-Anun C (2019) Phylogenetic and morphological appraisal of *Diatrype lijiangensis* sp. nov. (Diatrypaceae, Xylariales) from China. Asian Journal of Mycology 2: 198–208. https://doi.org/10.5943/ajom/2/1/10

Trouillas FP, Gubler WD (2004) Identification and characterization of *Eutypa leptoplaca*, a new pathogen of grapevine in Northern California. Mycological Research 108: 1195–1204. https://doi.org/10.1017/S0953756204000863

Trouillas FP, Urbez-Torres JR, Gubler WD (2010) Diversity of diatrypaceous fungi associated with grapevine canker diseases in California. Mycologia 102: 319–336. https://doi.org/10.3852/08-185

Trouillas FP, Hand FP, Inderbitzin P, Gubler WD (2015) The genus *Cryptosphaeria* in the western United States: taxonomy, multilocus phylogeny and a new species, *C. multicontinentalis*. Mycologia 107: 1304–1313. https://doi.org/10.3852/15-115

Trouillas FP, Wayne MP, Sosnowski MR, Huang R, Peduto F, Loschiavo A, Savocchia S, Scott ES, Gubler WD (2011) Taxonomy and DNA phylogeny of Diatrypaceae associated with *Vitis vinifera* and other woody plants in Australia. Fungal Diversity 49: 203–223. https://doi.org/10.1007/s13225-011-0094-0

Tulasne L-R, Tulasne C (1863) Selecta Fungorum carpologia, Paris, 2, 56.

U'ren JM, Miadlikowska J, Zimmerman NB, Ltzoni F, Stajich JE, Arnold AE (2016) Contributions of North American endophytes to the phylogeny, ecology, and taxonomy of Xylariaceae (Sordariomycetes, Ascomycota). Molecular Phylogenetics and Evolution 98: 210–232. https://doi.org/10.1016/j.ympev.2016.02.010

Úrbez-Torres JR, Adams P, Kamas J, Gubler WD (2009) Identification, incidence, and pathogenicity of fungal species associated with grapevine dieback in Texas. American Journal of Enology and Viticulture 60: 497–507.

Úrbez-torres JR, Peduto F, Striegler RK, Urrearomero KE, Rupe JC, Cartwright RD, Gubler WD (2012) Characterization of fungal pathogens associated with grapevine trunk diseases in Arkansas and Missouri. Fungal Diversity 52: 169–189. https://doi.org/10.1007/s13225-011-0110-4

Vasilyeva LN, Ma HX (2014) Diatrypaceous fungi in north-eastern China. 1. *Cryptosphaeria* and *Diatrype*. Phytotaxa 186(5): 261–270. https://doi.org/10.11646/phytotaxa.186.5.3

Vasilyeva LN, Stephenson SL (2005) Pyrenomycetes of the Great Smoky Mountains National Park. II. *Cryptovalsa* Ces. et De Not. and *Diatrypella* (Ces. et De Not.) Nitschke (Diatrypaceae). Fungal Diversity 19: 189–200.

Vieira MLA, Hughes AFS, Gil VB, Vaz AB, Alves TM, Zani CL, Rosa CA, Rosa LH (2011) Diversity and antimicrobial activities of the fungal endophyte community associated with the traditional Brazilian medicinal plant Solanum cernuum Vell. (Solanaceae). Canadian Journal of Microbiology 58: 54–56. https://doi.org/10.1139/w11-105

Vilgalys R, Hester M (1990) Rapid genetic identification and mapping of enzymatically amplified ribosomal DNA from several *Cryptococcus* species. Journal of Bacteriology 172: 4238–4246. https://doi.org/10.1128/jb.172.8.4238-4246.1990

White TJ, Bruns T, Lee SJWT, Taylor JW (1990) Amplification and direct sequencing of fungal ribosomal RNA genes for phylogenetics. PCR protocols: a guide to methods and applications 18: 315–322. https://doi.org/10.1016/B978-0-12-372180-8.50042-1

Wijayawardene NN, Hyde KD, Al-Ani LKT, Tedersoo L, Haelewaters D, Rajeshkumar KC, Zhao RL, Aptroot A, Leontyev DV, Saxena RK, Tokarev YS, Dai DQ, Letcher PM, Stephenson SL, Ertz D, Lumbsch HT, Kukwa M, Issi IV, Madrid H, Phillips AJL, Selbmann L, Pfliegler WP, Horváth E, Bensch K, Kirk P, Kolaříková Z, Raja HA, Radek R, Papp V, Dima B, Ma J, Malosso E, Takamatsu S, Rambold G, Gannibal PB, Triebel D, Gautam AK, Avasthi S, Suetrong S, Timdal E, Fryar SC, Delgado G, Réblová M, Doilom M, Dolatabadi S, Pawłowska J, Humber RA, Kodsueb R, Sánchez-Castro I, Goto BT, Silva DKA, De Souza FA, Oehl F, Da Silva GA, Silva IR, Błaszkowski J, Jobim K, Maia LC, Barbosa FR, Fiuza PO, Divakar PK, Shenoy BD, Castañeda-Ruiz RF, Somrithipol S, Karunarathna SC, Tibpromma S, Mortimer PE, Wanasinghe DN, Phookamsak R, Xu J, Wang Y, Fenghua T, Alvarado P, Li DW, Kušan I, Matočec N, Maharachchikumbura SSN, Papizadeh M, Heredia G, Wartchow F, Bakhshi M, Boehm E, Youssef N, Hustad VP, Lawrey JD, Santiago ALCMA, Bezerra JDP, Souza-Motta CM, Firmino AL, Tian Q, Houbraken J, Hongsanan S, Tanaka K, Dissanayake AJ, Monteiro JS, Grossart HP, Suija A, Weerakoon G, Etayo J, Tsurykau A, Kuhnert E, Vázquez V, Mungai P, Damm U, Li QR, Zhang H, Boonmee S, Lu YZ, Becerra AG, Kendrick B, Brearley FQ, Motiejűnaitë J, Sharma B,

Khare R, Gaikwad S, Wijesundara DSA, Tang LZ, He MQ, Flakus A, Rodriguez-Flakus P, Zhurbenko MP, McKenzie EHC, Stadler M, Bhat DJ, Liu JK, Raza M, Jeewon R, Nassonova ES, Prieto M, Jayalal RGU, Yurkov A, Schnittler M, Shchepin ON, Novozhilov YK, Liu P, Cavender JC, Kang Y, Mohammad S, Zhang LF, Xu RF, Li YM, Dayarathne MC, Ekanayaka AH, Wen TC, Deng CY, Lateef AA, Pereira OL, Navathe S, Hawksworth DL, Fan XL, Dissanayake LS, Erdoðdu M (2020) Outline of Fungi and fungus-like taxa. Mycosphere 11: 1060–1456. https://doi.org/10.5943/mycosphere/11/1/8

Zhu H, Pan M, Wijayawardene NN, Jiang N, Ma R, Dai D, Tian C, Fan X (2021) The Hidden Diversity of Diatrypaceous Fungi in China. frontiers in Microbiology 12: 646262. https://doi.org/10.3389/fmicb.2021.646262

MycoKeys 83: 39–67 (2021)
doi: 10.3897/mycokeys.83.69906
https://mycokeys.pensoft.net

RESEARCH ARTICLE

A peer-reviewed open-access journal
MycoKeys
Launched to accelerate biodiversity research

A taxonomic study of *Nemania* from China, with six new species

Yin Hui Pi[1,2], Si Han Long[1], You Peng Wu[1], Li Li Liu[1], Yan Lin[1], Qing De Long[1], Ji Chuan Kang[3], Ying Qian Kang[4], Chu Rui Chang[1], Xiang Chun Shen[1,2], Nalin N. Wijayawardene[1,5,6], Xu Zhang[1], Qi Rui Li[1,2]

1 *State Key Laboratory of Functions and Applications of Medicinal Plants, Guizhou Medical University, Guiyang 550004, China* **2** *The High Efficacy Application of Natural Medicinal Resources Engineering Center of Guizhou Province (The Key Laboratory of Optimal Utilization of Natural Medicine Resources), School of Pharmaceutical Sciences, Guizhou Medical University, University Town, Guian New District, Guizhou, China* **3** *Engineering and Research Center for Southwest Bio-Pharmaceutical Resources of National Education Ministry of China, Guizhou University, Guiyang, Guizhou 550025, China* **4** *Key Laboratory of Environmental Pollution Monitoring and Disease Control, Ministry of Education of Guizhou and Guizhou Talent Base for Microbiology and Human Health, School of Basic Medical Sciences, Guizhou Medical University, Guiyang, China* **5** *Center for Yunnan Plateau Biological Resources Protection and Utilization, College of Biological Resource and Food Engineering, Qujing Normal University, Qujing, Yunnan 655011, China* **6** *Section of Genetics, Institute for Research and Development in Health and Social Care, No: 393/3, Lily Avenue, Off Robert Gunawardane Mawatha, Battaramulla 10120, Sri Lanka*

Corresponding author: Qi Rui Li (lqrnd2008@163.com)

Academic editor: Ekaphan Kraichak | Received 9 June 2021 | Accepted 29 July 2021 | Published 24 August 2021

Citation: Pi YH, Long SH, Wu YP, Liu LL, Lin Y, Long QD, Kang JC, Kang YQ, Chang CR, Shen XC, Wijayawardene NN, Zhang X, Li QR (2021) A taxonomic study of *Nemania* from China, with six new species. MycoKeys 83: 39–67. https://doi.org/10.3897/mycokeys.83.69906

Abstract

During an investigation of Xylariaceae from 2019 to 2020, isolates representing eight *Nemania* (Xylariacese) species were collected from Yunnan, Guizhou and Hainan Provinces in China. Morphological and multi-gene phylogenetic analyses, based on combined ITS, α-actin, *rpb2* and β-tubulin sequences, confirmed that six of them are new to science, viz. *Nemania camelliae*, *N. changningensis*, *N. cyclobalanopsina*, *N. feicuiensis*, *N. lishuicola* and *N. rubi*; one is a new record (*N. caries*) for China and one is a known species (*N. diffusa*). Morphological descriptions and illustrations of all species are detailed. In addition, the characteristics of *Nemania* are summarised and prevailing contradictions in generic concepts are discussed.

Keywords

phylogeny, six new species, taxonomy, Xylariaceae

Introduction

Nemania Gray was established by Gray (1821) for a heterogeneous assemblage of taxa and was affiliated with *Xylariaceae* Tul. & C. Tul. Since the early taxonomic description of this genus was ambiguous, taxonomists have often regarded some species of *Nemania* as synonyms of *Hypoxylon* Bull. For example, *Nemania angusta* (Petch) Y.M. Ju & J. D. Rogers was regarded as a synonym of *Hypoxylon angustum* Petch. (Miller 1961; Whalley et al. 1983; Ju and Rogers 2002). Subsequently, the generic concept of *Nemania* was modified by Pouzar (1985a, b) and Petrini and Rogers (1986). Granmo et al. (1999) and Ju and Rogers (2002) provided a comprehensive background to *Nemania* and accepted 37 species. Sánchez-Ballesteros et al. (2000) used the internal transcribed spacers (ITS) sequence to perform a phylogenetic study of *Nemania*, which supported the segregation of *Nemania* from *Hypoxylon*. However, their conclusion was based only on ITS sequences and *Xylaria* Hill & Schrank was not included in this study. Hence, the generic placement of *Nemania* in the *Xylariaceae* was unclear. Hsieh et al. (2005) used β-tubulin and α-actin to evaluate the phylogenetic relationship of several xylariaceous genera. It was found to be particularly useful in xylariaceous fungi as limited success in using ribosomal DNA genes to delineating genera and resolving generic relationships (Tang et al. 2007). Tang et al. (2007) re-established the phylogenetic relationships of *Nemania* with related genera, based on the combined dataset of ITS and *rpb2* which supported the separation of *Nemania* from *Hypoxylon*. However, Tang et al. (2007) stated that *Nemania* is closely related to *Xylaria* and phylogenetically distinct from *Annulohypoxylon* Y.M. Ju et al., *Daldinia* Ces. & De Not. and *Hypoxylon*. Ultimately, the boundaries of the genus became relatively clear and *Nemania* has been accepted as a distinct genus in *Xylariaceae* (Ju and Rogers 2002). The major morphological characteristics of *Nemania* include dark brown to black stromata, carbonaceous or at least brittle and not yielding pigments in 10% potassium hydroxide (KOH) (Ju and Rogers 2002), white soft tissue existing between or below the perithecia, ascospores usually pale brown and most of them have no obvious germ-slit and spore dehiscence in 10% KOH (Tang et al. 2007).

Nemania accepted 37 species by 2002, which occurs mainly distributed on the rotting wood of angiosperms (Ju and Rogers 2002; Tang et al. 2007). There are a few species introduced from China in recent years. Two new species (*N. flavitextura* Y.M. Ju, H.M. Hsieh & J.D. Rogers and *N. primolutea* Y.M. Ju, H.M. Hsieh & J.D. Rogers), collected from Taiwan, were reported by Ju et al. (2005). One new species and two new record species were discovered and described by Du et al. (2016) and Ariyawansa et al. (2015) in China. Recently, two new species (*N. yunnanensis* Tibpromma & Lu and *N. aquilariae* Tibpromma & Lu), collected from Yunnan Province, China, were discovered by Tibpromma et al. (2021). Ninety-three epithets of *Nemania* are listed on Index Fungorum (2021) (accession date: 06. 2021). Only 17 species of *Nemania* with gene sequences were retrieved from the NCBI database (https://www.ncbi.nlm.nih.gov) and morphological methods are the main distinguishing method for *Nemania*. Morphologically, it is mainly distinguished according to the germ slit, the size of the ascospores and the characteristics of the stromata.

In this study, eight species of *Nemania*, collected from Guizhou, Hainan and Yunnan Provinces in China, are introduced. Six new species are identified, based on morpho-molecular analyses, while *N. caries* is reported as a new record for China; *N. diffusa* has been previously reported from China (Du 2015). Detailed morphological descriptions, illustrations and phylogenetic information of all species are provided in this paper.

Materials and methods

Collection, isolation and morphology

Samples of rotting wood with fungi were collected from October 2019 to December 2020 in various nature reserves of Guizhou, Hainan and Yunnan Provinces, China. These samples were placed in sealed bags and the coordinates of sampling sites (such as latitude, longitude and altitude) were recorded. Specimens were taken to the laboratory for examination. Microscopic observations were made with fungi mounted in distilled water. A drop of Melzer's Reagent was added to determine whether or not the ascus apical ring blued (the amyloid iodine reaction) and the reaction and morphology of the ring could be observed. Fragments of stroma and perithecial wall were placed in 10% KOH on a microscope slide and the extractable pigment observed. Pure cultures were obtained with the single spore isolation method (Long et al. 2019) and the cultures were grown on oatmeal agar (OA) and potato dextrose agar (PDA).

Morphological examination of fungi on the rotting wood followed the methods of Xie et al. (2020). The characteristics of the stromata were observed with an Olympus SZ61 stereomicroscope and photographed using a fitted Canon 700D digital camera. The photomicrographs of asci and ascospores were taken with a Nikon digital camera (700D) fitted to a light microscope (Nikon Ni). Adobe Photoshop CS6 was used to arrange all the microphotographs. Measurements were performed using the Tarosoft image framework (v. 0.9.0.7). At least 30 ascospores, asci and ascus apical apparatus were measured for each specimen.

To prepare herbarium materials, the colonies grown on PDA were transferred to three 1.5 ml microcentrifuge tubes filled with sterile water and stored at 4 °C or with 10% glycerol at –20 °C. Herbarium materials were deposited in the Herbarium of Guizhou Medical University (**GMB**) and Herbarium of Kunming Institute of Botany, Chinese Academy of Sciences (**KUN**). Living cultures were deposited at Guizhou Medical University Culture Collection (**GMBC**).

DNA extraction, PCR amplification and sequencing

The BIOMIGA Fungal Genomic DNA Extraction Kit (GD2416, Biomiga, USA) was used to extract genomic DNA from fresh fungal mycelium, according to the manufacturer's instructions. The extracted DNA was stored at –20 °C.

Target regions of internal transcribed spacers (ITS) and RNA polymerase II second largest subunit (*rpb2*) regions were amplified symmetrically using primers of ITS4/

ITS5 (White et al. 1990; Gardes and Bruns 1993) and fRPB2-5F/fRPB2-7cR (Liu et al. 1999), respectively. ACT512F and ACT783R (Hsieh et al. 2005) and T11 and T22 (Tanaka et al. 2009; Hsieh et al. 2010) primers were used for the amplification of the α-actin gene (ACT) and β-tubulin (TUB2), respectively. The components of the polymerase chain reaction (PCR) mixture and thermal cycling programme were performed as described by Pi et al. (2020). The amplified PCR fragments were sent to Sangon Biotech (Shanghai) Co., China, for sequencing. All newly-generated sequences of ITS, α-actin, *rpb2* and β-tubulin regions were uploaded to the GenBank database and the accession numbers are shown in Table 1.

Sequence alignment and phylogenetic analyses

Except for newly-generated sequences, all sequences used for phylogenetic analysis were downloaded from GenBank, based on published literature and the highest hit rate of ITS in the GenBank database. Sequence data for the construction of the phylogenetic tree are listed in Table 1. Sequence alignments were generated using the MAFFT v.7.110 online programme (http://mafft.cbrc.jp/alignment/server/, Katoh and Standley 2013) under default settings. Multiple sequence alignments of ITS, α-actin, *rpb2* and β-tubulin were analysed individually and in combination, manually adjusted to achieve the maximum alignment and to minimise gaps using the BioEdit v.5 (Hall 1999). The file formats were converted in ALTER (Alignment Transformation EnviRonment) (http://www.sing-group.org/ALTER/). The Maximum Likelihood analysis was carried out with GTR+G+I model of site substitution by using RAxML 7.4.2 black box (https://www.phylo.org/, Stamatakis et al. 2008) and Bayesian Inference

Table 1. Taxa of *Nemania* and related genera used for phylogenetic analyses and their GenBank accession numbers.

Species	Strain number	GenBank Accession number				References
		ITS	*rpb2*	β-tubulin	α-actin	
Amphirosellinia fushanensis	HAST 91111209 (HT)	GU339496	GQ848339	GQ495950	GQ452360	Hsieh et al. (2010)
Am. nigrospora	HAST 91092308 (HT)	GU322457	GQ848340	GQ495951	GQ452361	Hsieh et al. (2010)
Astrocystis bambusae	HAST 89021904	GU322449	GQ844836	GQ495942	GQ449239	Hsieh et al. (2010)
As. bambusicola	MFLUCC 17-0127 (HT)	MF467942	MF467946	N/A	N/A	Hyde et al. (2017)
As. concavispora	MFLUCC 14-0174	KP297404	KP340532	KP406615	N/A	Daranagama et al. (2015)
As. mirabilis	HAST 94070803	GU322448	GQ844835	GQ495941	GQ449238	Hsieh et al. (2010)
Brunneiperidium gracilentum	MFLUCC 14-0011 (HT)	KP297400	KP340528	KP406611	N/A	Daranagama et al. (2015)
B. involucratum	MFLUCC 14-0009	KP297399	KP340527	KP406610	N/A	Daranagama et al. (2015)
Collodiscula bambusae	GZUH0102	KP054279	KP276675	KP276674	N/A	Li et al. (2015b)
C. fangjingshanensis	GZUH0109 (HT)	KR002590	KR002592	KR002589	N/A	Li et al. (2015a)
C. leigongshanensis	GZUH0107 (HT)	KP054281	KR002588	KR002587	N/A	Li et al. (2015a)
C. tubulosa	GACP QR0111 (HT)	MN017302	MN018403	MN018405	MN018402	Xie et al. (2020)
Daldinia bambusicola	CBS 122872 (HT)	KY610385	KY624241	AY951688	KU684037	Hsieh et al. (2005), Wendt et al. (2018)
Dematophora buxi	JDR 99	GU300070	GQ844780	GQ470228	GQ398228	Hsieh et al. (2010)
De. necatrix	CBS 349.36	AY909001	KY624275	KY624310	N/A	Pelaez et al. (2008), Wendt et al. (2018)

Species	Strain number	GenBank Accession number				References
		ITS	*rpb2*	β-tubulin	α-actin	
Discoxylaria myrmecophila	JDR 169	GU322433	GQ844819	GQ487710	GQ438747	Hsieh et al. (2010)
Entoleuca mammata	JDR 100	GU300072	GQ844782	GQ470230	GQ398230	Hsieh et al. (2010)
Hypoxylon pulicicidum	CBS 122622 (HT)	JX183075	KY624280	JX183072	JX183071	Bills et al. (2012), Wendt et al. (2018)
Kretzschmariella culmorum	JDR 88	KX430043	KX430045	KX430046	KX430044	Johnston et al. (2016)
Nemania abortiva	BISH 467 (HT)	GU292816	GQ844768	GQ470219	GQ374123	Hsieh et al. (2010)
N. aenea	CBS 680.86	AJ390427	N/A	N/A	N/A	Tang et al. (2007)
N. aenea var. *aureolutea*	ATCC 60819	AJ390428	N/A	N/A	N/A	Tang et al. (2007)
N. aquilariae	KUMCC 20-0268 (HT)	MW729422	MW717891	MW881142	MW717889	Tibpromma et al. (2021)
N. beaumontii	HAST 405	GU292819	GQ844772	GQ470222	GQ389694	Wendt et al. (2018)
N. bipapillata	HAST 90080610	GU292818	GQ844771	GQ470221	GQ389693	Hsieh et al. (2010)
N. camelliae	GMB0067	MW851888	MW836056	MW836030	MW836047	This study
	GMB0068 (HT)	MW851889	MW836055	MW836029	MW836046	This study
N. caries	GMB0069	MW851873	MW836069	MW836035	MW836051	This study
	GMB0070	MW851874	MW836071	MW836036	MW836050	This study
N. changningensis	GMB0056 (HT)	MW851875	MW836061	MW836027	MW836042	This study
	GMB0057	MW851876	MW836062	MW836028	MW836043	This study
N. chestersii	JF 04024	AJ390430	DQ631949	DQ840089	N/A	Tang et al. (2007, 2009)
N. cyclobalanopsina	GMB0061	MW851882	MW836058	MW836026	MW836039	This study
	GMB0062 (HT)	MW851883	MW836051	MW836025	MW836038	This study
N. diffusa	HAST 91020401	GU292817	GQ844769	GQ470220	GQ389692	Hsieh et al. (2010)
	GMB0071	MW851877	MW836067	MW836031	MW836053	This study
	GMB0072	MW851878	MW836068	MW836032	MW836052	This study
N. feicuiensis	GMB0058	MW851879	MW836064	MW836024	MW836045	This study
	GMB0059 (HT)	MW851880	MW836063	MW836023	MW836044	This study
N. fusoidispora	GZUH0098	MW851881	MW836070	MW836037	MW836054	Ariyawansa et al. (2015)
N. illita	YMJ 236	EF026122	GQ844770	EF025608	EF025593	Hsieh et al. (2010)
N. rubi	GMB0063	MW851884	MW836060	MW836022	MW836041	This study
	GMB0064 (HT)	MW851885	MW836059	MW836021	MW836040	This study
N. lishuicola	GMB0065 (HT)	MW851886	MW836065	MW836033	MW836048	This study
	GMB0066	MW851887	MW836066	MW836034	MW836049	This study
N. macrocarpa	WSP 265	GU292823	GQ844776	GQ470226	GQ389698	Hsieh et al. (2010)
N. maritima	HAST 89120401 (ET)	GU292822	GQ844775	GQ470225	GQ389697	Hsieh et al. (2010), Li et al. (2015a, b)
N. plumbea	JF TH-04-01	DQ641634	DQ631952	DQ840084	N/A	Tang et al. (2007, 2009)
N. primolutea	YMJ 91102001 (HT)	EF026121	GQ844767	EF025607	EF025592	Hsieh et al. (2010)
N. serpens	HAST 235	GU292820	GQ844773	GQ470223	GQ389695	Hsieh et al. (2010), Li et al. (2015a, b)
N. sphaeriostoma	JDR 261	GU292821	GQ844774	GQ470224	GQ389696	Hsieh et al. (2010)
N. yunnanensis	KUMCC 20-0267 (HT)	MW729423	MW717892	MW881141	MW717890	Tibpromma et al. (2021)
Podosordaria mexicana	WSP 176	GU324762	GQ853039	GQ844840	GQ455451	Hsieh et al. (2010)
Pod. muli	WSP 167 (HT)	GU324761	GQ853038	GQ844839	GQ455450	Hsieh et al. (2010)
Poronia pileiformis	WSP 88113001 (ET)	GU324760	GQ853037	GQ502720	GQ455449	Hsieh et al. (2010)
Por. punctata	CBS 656.78 (HT)	KT281904	KY624278	KX271281	N/A	Senanayake et al. (2015)
Rosellinia aquila	MUCL 51703	KY610392	KY624285	KX271253	N/A	Wendt et al. (2018)
R. merrillii	HAST 89112601	GU300071	GQ844781	GQ470229	GQ398229	Hsieh et al. (2010)
R. sanctae-cruciana	HAST 90072903	GU292824	GQ844777	GQ470227	GQ389699	Hsieh et al. (2010)
Stilbohypoxylon elaeicola	HAST 94082615	GU322440	GQ844827	GQ495933	GQ438754	Hsieh et al. (2010)
S. quisquiliarum	HAST 89091608	EF026120	GQ853021	EF025606	EF025591	Ju et al. (2007), Hsieh et al. (2010)
Xylaria allantoidea	HAST 94042903	GU324743	GQ848356	GQ502692	GQ452377	Hsieh et al. (2010)
X. apoda	HAST 90080804	GU322437	GQ844823	GQ495930	GQ438751	Hsieh et al. (2010)
X. compunctum	CBS 359.61	KT281903	KY624230	KX271255	N/A	Senanayake et al. (2015)
X. cubensis	JDR 860	GU991523	GQ848365	GQ502700	GQ455444	Hsieh et al. (2010)
X. digitata	HAST 919	GU322456	GQ848338	GQ495949	GQ449245	Hsieh et al. (2010)
X. juruensis	HAST 92042501	GU322439	GQ844825	GQ495932	GQ438753	Hsieh et al. (2010)

Notes: Type specimens are marked with HT (holotype), ET (epitype). N/A: sequences not available.

(BI) analysis was performed with MrBayes v.3.1.2 (Huelsenbeck and Ronquist 2001). The branch support was evaluated with a bootstrapping method of 1000 replicates (Hillis and Bull 1993). Posterior probabilities (PP) were determined by Markov Chain Monte Carlo sampling (MCMC) in MrBayes v. 3.2.2 (Ronquist et al. 2012). The nucleotide substitution model was estimated by MrModeltest v.2.3 (Posada and Crandall 1998). Six simultaneous Markov chains were run for 2000000 generations and the trees were sampled each 100th generation. The first 25% of trees were discarded during the burn-in phase of each analysis. The phylogenetic trees were viewed in Figtree v.1.4.0 and arranged by Photoshop CS6. The alignments and respective phylogenetic trees were uploaded in TreeBASE (submission number: 28371).

Results

Phylogenetic analyses

The multiple-genes sequence alignments of ITS, α-actin, *rpb2* and β-tubulin included 67 taxa, 2,041 positions including gaps (ITS: 1–486, α-actin: 487–677, *rpb2*: 678–1,715, β-tubulin: 1,716–2,041). *Daldinia bambusicola* Y.M. Ju et al. (CBS 122872) and *Hypoxylon pulicicidum* J. Fourn. et al. (CBS 122622) were selected as the outgroup taxa. A best-scoring ML tree is represented in Fig. 1. RAxML bootstrap support value ≥ 75% and Bayesian posterior probabilities (BYPP) value ≥ 0.90 are shown above the branches and indicated as thickened lines.

In the phylogenetic tree (Fig. 1), *Nemania* Gray is a sister taxon to the genera *Rosellinia* De Not., *Dematophora* R. Hartig and *Entoleuca* Syd. *Nemania* was divided into six sub-clades. In clade N1, *N. bipapillata* (Berk. & M.A. Curtis) Pouzar, *N. camelliae* sp. nov. and *N. lishuicola* sp. nov. grouped with high statistical values (100/1). In clade N2, *N. fusoidispora* Q.R. Li et al. and *N. illita* (Schwein.) Pouzar. grouped with high statistical values (100/1). Clade N3 contained the frequent species *N. diffusa* (Sowerby) S.F. Gray along with *N. cyclobalanopsina* sp. nov. grouping with high statistical values (100/1). In clade N4, *N. feicuiensis* sp. nov. with *N. abortiva* J.D. Rogers et al., *N. aquilariae* Tibpromma & Lu and *N. primolutea* Y.M. Ju et al. grouped with high statistical values (100/1). Within clade N5, *N. macrocarpa* Y.M. Ju & J.D. Rogers clustered in a well-supported sub-clade with *N. maritima* Y.M. Ju & J.D. Rogers with high statistical values (100/1). Clade N6 comprised *N. changningensis* sp. nov., *N. yunnanensis* Tibpromma & Lu, *N. caries* (Schwein.) Y.M. Ju & J.D. Rogers, *N. rubi* sp. nov., *N. plumbea* A.M.C. Tang et al., *N. chestersii* (J.D. Rogers & Whalley) Pouzar, *N. serpens* (Pers.) Gray with *N. aenea* (Nitschke) Pouzar, *N. aenea* var. *aureolutea* (L.E. Petrini & J.D. Rogers) Y.M. Ju & J.D. Rogers, *N. sphaeriostomum* (Schwein.) Lar.N. Vassiljeva & S.L. Stephenson and *N. beaumontii* (Berk. & M.A. Curtis) Y.M. Ju & J.D. Rogers grouping with high support values (100% ML, 1 BYPP).

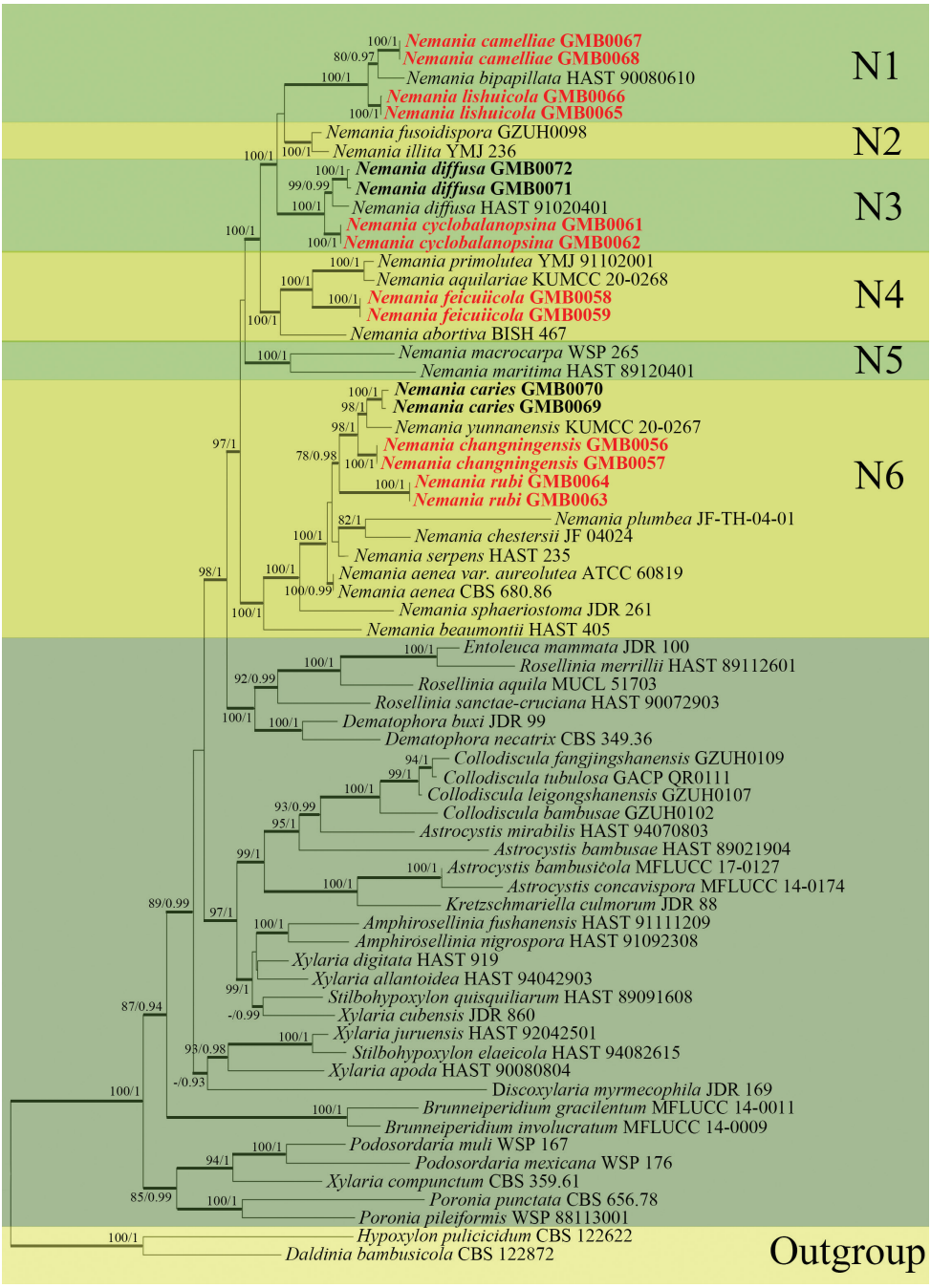

Figure 1. RAxML tree based on analysis of a combined dataset of ITS, α-actin, *rpb2* and β-tubulin sequences from taxa of *Nemania* and related genera. Bayesian posterior probability (PP) ≥ 0.90 is marked at the node and the maximum likelihood bootstrap support (BS) values greater than ≥ 75%; a dash ("-") indicates a value < 0.90 (PP) or < 75% (BS). The strain number is indicated after the species name. The here-studied strains are in **bold** and new species are indicated in red.

Taxonomy

***Nemania camelliae* Y.H. Pi & Q.R. Li, sp. nov.**
MycoBank No: 840086
Fig. 2

Etymology. Refers to the host genus name, *camellia*.

Material examined. China, Guizhou Province, Tongren City, Fanjingshan Nature Reserve (27°47'11.41"N, 108°43'43.90"E, altitude: 515 m), on dead wood of *Camellia* sp., 15 October 2020, Y.H. Pi, 2020FJS26 (GMB0068, ***holotype***; GMBC0068, ex-type living culture; KUN-HKAS 112689, ***isotype***).

Description. Saprobic on the surface of decaying wood of *Camellia* sp. ***Sexual morph*:** Stromata pulvinate to effused-pulvinate, rarely perithecioid, orbicular to irregularly elongated, often coalescent; single distribution or confluent into irregularly elongated compound stromata, 1.5–4 mm long × 1–2 mm wide × 0.5–1 mm high, surface dull black, hard-textured, with inconspicuous to moderately exposed perithecial contours and usually sloping margins, internally black between ascomata, carbonaceous; subperithecial tissue black, conspicuous; does not release a coloured pigment in 10% KOH. Perithecia 0.65–0.95 mm diam. × 0.65–0.7 mm high, subglobose to depressed-spherical. Ostioles finely papillate, black, conspicuously sunken in a shallow discoid depression; ostiolar area blackish, shiny, frequently flattened. Asci 180–290 × 6–11 μm (av. = 230 × 7.5 μm, n = 30), 8-spored, unitunicate, long-cylindrical, long-stipitate, the spore-bearing parts 80–95 μm long, apically rounded with a J+, apical apparatus, 2–3 × 2.5–4 μm (av. = 2.5 × 3 μm, n = 30), jar shape. Ascospores 10–14 × 4.5–7 μm (av. = 12 × 5.5 μm, n = 30), uniseriate, unicellular, ellipsoid to slightly fusoid, inequilateral, with slightly narrow rounded ends, smooth, brown to dark brown, with a fairly conspicuous, straight, almost spore-length germ slit on the least convex side; lacking a sheath and appendage; perispore indehiscent in 10% KOH. ***Asexual morph*:** Undetermined.

Culture characteristics. The colony grows on PDA medium with a diameter of 6 cm after one week at 25 °C; white, cottony, circular, flocculent or velvety, with light yellow to slightly yellow at the centre. Not sporulating on OA nor on PDA.

Other examined material. CHINA, Guizhou Province, Tongren City, Fanjingshan Nature Reserve (27°42'10.26"N, 108°31'35.34"E, altitude: 426 m), on dead wood of *Camellia* sp., 16 October 2020, Y.H. Pi, 2020FJS54-1 (GMB0067), living culture, GMBC0067.

Notes. Phylogenetic analyses showed that *Nemania camelliae* form a distinct clade with *N. bipapillata* (82% ML, 0.97 BYPP, Fig. 1). Morphologically, *N. camelliae* is similar to *N. immersidiscus* Van der Gucht et al. in having a small discoid depression around the ostiolar papilla. However, the stromata of *N. camelliae* are entirely carbonaceous, whereas those of *N. immersidiscus* contain white soft tissue between and beneath the perithecia (Ju and Rogers 2002). Moreover, *N. immersidiscus* has slightly thinner ascospores [(10–)11–14(–16) × (4–)4.5–5.5 μm)].

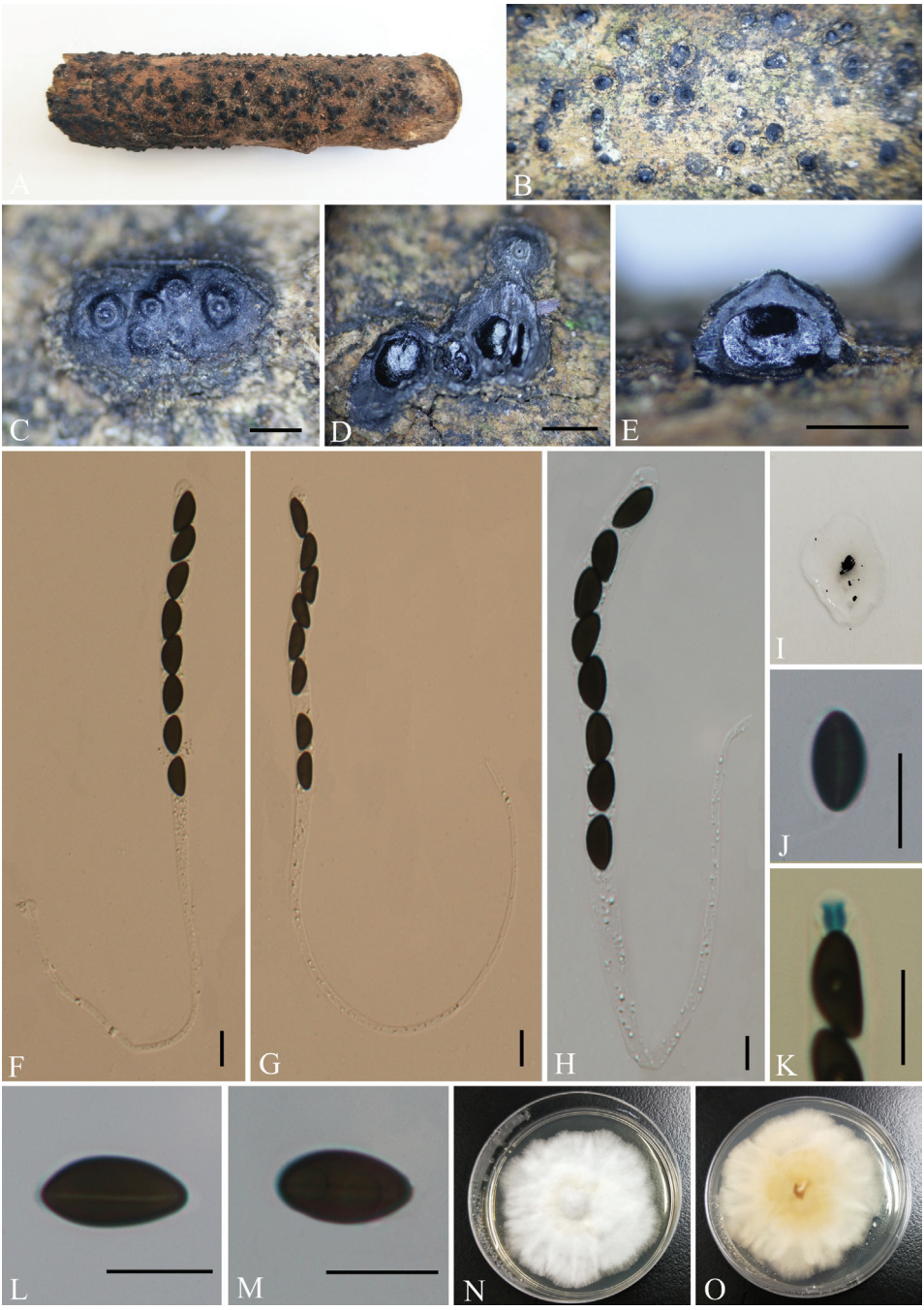

Figure 2. *Nemania camelliae* (GMB0068, **holotype**) **A** type material **B, C** stromata on the surface of host **D** transverse section of stroma **E** longitudinal section of stroma **F–H** asci with ascospores **I** pigments in 10% KOH **J** ascospore with indehiscent perispore in 10% KOH **K** ascus apical apparatus (stained in Melzer's Reagent) **L, M** ascospores **N, O** colonies on PDA (**N**-upper, **O**-lower). Scale bars: 0.5 mm (**C–E**); 10 μm (**F–H, J–M**).

Nemania caries **(Schwein.) Y.M. Ju & J.D. Rogers, Nova Hedwigia 74(1–2): 90 (2002)**
MycoBank No: 477305
Fig. 3

Synonyms. *Sphaeria caries* Schwein., Trans. Am. phil. Soc., New Series 4(2): 194 (1832).
Hypoxylon caries (Schwein.) Sacc., Syll. fung. (Abellini) 1: 393 (1882).
Hypoxylon balansae Speg., Anal. Soc. cient. argent. 26(1): 30 (1888).

Description. Saprobic on the surface of decaying wood. ***Sexual morph*****:** Stromata irregularly effused-pulvinate, 5.5–18 mm long × 3–9 mm wide × 0.4–0.6 mm thick, with conspicuous perithecial mounds, surface blackish-grey, carbonaceous, interior white, loosely fibrous to cottony; mature stromata lacking KOH extractable pigments. Perithecia 0.25–0.5 mm wide × 0.4–0.6 mm high, obovoid. Ostioles slightly higher than stromatal surface and with openings conic-papillate, black, inconspicuous, without encircling disc. Asci 130–200 × 7–13 μm (av. = 150 × 9.5 μm, n = 30), 8-spored, cylindrical, unitunicate, long-stipitate, the spore-bearing parts 65–95 μm long, apically rounded with a J+, short-cylindrical apical apparatus, 1.5–2.5 × 1–2.5 μm (av. = 2 × 1.5 μm, n = 30). Ascospores 9–13.5 × 3–7 μm (av. = 11.5 × 5 μm, n = 30), brown to light brown, smooth, with an inconspicuous, straight, germ slit 1/3 spore-length, nearly equilateral, with broadly rounded ends; perispore indehiscent in 10% KOH. ***Asexual morph*****:** Undetermined.

Culture characteristics. Colonies grow on PDA at 25 °C for two weeks, with a diameter of 4 cm. Colony on the surface is white or light orange, shallow, flat, zonnate, with irregular edges and orange on the reverse side. The colony reverse is orange. Not sporulating on OA nor on PDA.

Material examined. China, Yunnan Province, Changning County, Lancang River Nature Reserve (25°01'13.56"N, 99°35'25.12"E, altitude: 2626 m), on dead wood, 6 October 2019, Y.H. Pi, 2019LC369 (GMB0070, KUN-HKAS 112680), living culture, GMBC0070; CHINA, Yunnan Province, Changning County, Lancang River Nature Reserve (25°01'13.33"N, 99°35'26.55"E, altitude: 2641 m), on dead wood, 6 October 2019, Y.H. Pi, 2019LC401 (GMB0069, KUN-HKAS 112682), living culture, GMBC0069.

Known distribution. Hawaii (Rogers and Ju 2012), Martinique (Fournier et al. 2018), Paraguay, USA (Ju and Rogers 2002), Yunnan Province, China (this paper).

Notes. The phylogenetic analyses show *Nemania caries* groups with *N. changningensis* with high statistical support (100% ML, 1 BYPP, Fig. 1) and the comparison calculation within the alignment found that there is a 4% difference in ITS sequences between *N. changningensis* and *N. caries.* Morphologically, *N. caries* resembles *N. colubrina* J. Fourn. & Lechat which has medium brown ascospores and a similar size of ascospores. However, *N. colubrina* differs from *N. caries* by ellipsoid-inequilateral ascospores with narrowly-rounded ends (Ju and Rogers 2002; Fournier et al. 2018). *Nemania caries* is distinguished from *N. plumbea* by its dimension of ascospores, the

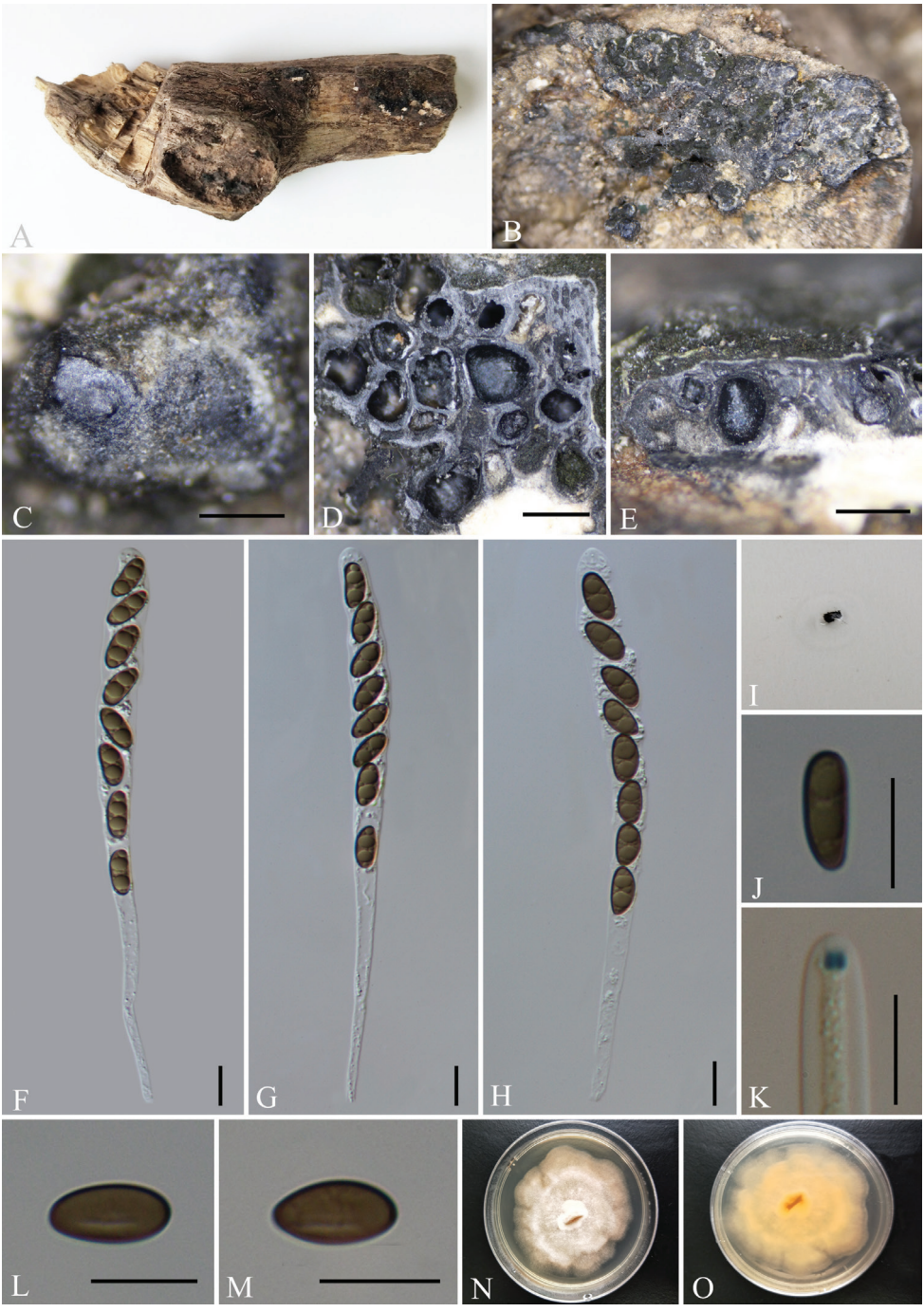

Figure 3. *Nemania caries* (GMB0070) **A** type material **B, C** stromata on the surface of host **D** transverse sections of stromata **E** longitudinal section of stroma **F–H** asci with ascospores **I** pigments in 10% KOH **J** ascospore with indehiscent perispore in 10% KOH **K** ascus apical apparatus (stained in Melzer's Reagent) **L, M** ascospores **N, O** Colonies on PDA (**N**-upper, **O**-lower). Scale bars: 0.5 mm (**C–E**); 10 μm (**F–H, J–M**).

latter has larger ascospores (13–16 × 5.4–6.6 μm) with narrowly-rounded ends (Tang et al. 2007). The specimens we collected from the Lancang River Nature Reserve in Yunnan fit the definition of *N. caries* well and represent the first record from China.

Nemania changningensis **Y.H. Pi & Q.R. Li, sp. nov.**
MycoBank No: 840087
Fig. 4

Etymology. Refers to the collection location, Changning County.

Material examined. China, Yunnan Province, Changning County, Lancang River Nature Reserve (25°01'35.02"N, 99°33'15.42"E, altitude: 2670 m), on dead wood, 3 October 2019, Y.H. Pi, 2019LC203 (GMB0056, ***holotype***; GMBC0056, ex-type living culture; KUN-HKAS 112668, ***isotype***).

Description. Saprobic on the surface of decaying wood. ***Sexual morph*****:** Stromata effused-pulvinate, confluent into irregularly elongated compound stromata, up to 18–35 mm long × 2–4 mm wide × 0.3–0.5 mm high, irregularly lobed, plane or with inconspicuous perithecial mounds and sloping margins; surface covered with white tissue, persistent layer, with blackish-grey carbonaceous sub-surface showing through in places; the tissue beneath the perithecial layer inconspicuous, greyish-white in places, the underlying wood blackened; mature stromata lacking KOH extractable pigments. Perithecia 0.45–0.6 mm diam. × 0.4–0.55 mm high, subglobose to depressed-spherical. Ostioles slightly higher than stromatal surface and with openings papillate, often surrounded by white tissue, inconspicuous, black, without encircling disc. Asci 100–140 × 7–10 μm (av. = 111 × 8.5 μm, n = 30), 8-spored, unitunicate, cylindrical, short-stipitate, the spore-bearing parts 70–90 μm long, the apical apparatus of immature asci blue in Melzer's Reagent, but not blue in mature asci. Ascospores 10–13 × 4–6.5 μm (av. = 11.5 × 5.5 μm, n = 30), uniseriate unicellular, smooth, light brown, slightly inequilateral, with broadly rounded ends, inconspicuous or lack a germ slit; perispore indehiscent in 10% KOH. ***Asexual morph*****:** Undetermined.

Culture characteristics. The colony grows slowly on the PDA with a diameter of 4.5 cm after 2 weeks at 25 °C. The colony on the surface is white, thick and flat in the middle, edges are shallow, irregular bands and rosettes. Colony reverse is orange and intermediate colour darker. Not sporulating on OA nor on PDA.

Other examined material. China, Yunnan Province, Changning County, Lancang River Nature Reserve (25°01'30.36"N, 99°35'30.53"E, altitude: 2586 m), on dead wood, 4 October 2019, Y.H. Pi, 2019LC342 (GMB0057), living culture, GMBC0057.

Notes. In the phylogenetic analyses, *N. changningensis* is on a separate branch and grouped with *N. caries* with high support values (100% ML, 1 BYPP, Fig. 1). In term of ascospores dimension, *N. changningensis* resembles *N. caries*, but differs in the perithecia of *N. caries* (obovoid, 0.3–0.6 mm diam. × 0.5–0.7 mm high), in the surface not covered with white tissue and in its apical apparatus of mature asci bluing in Melzer's Reagent (Miller 1961; Ju and Rogers 2002).

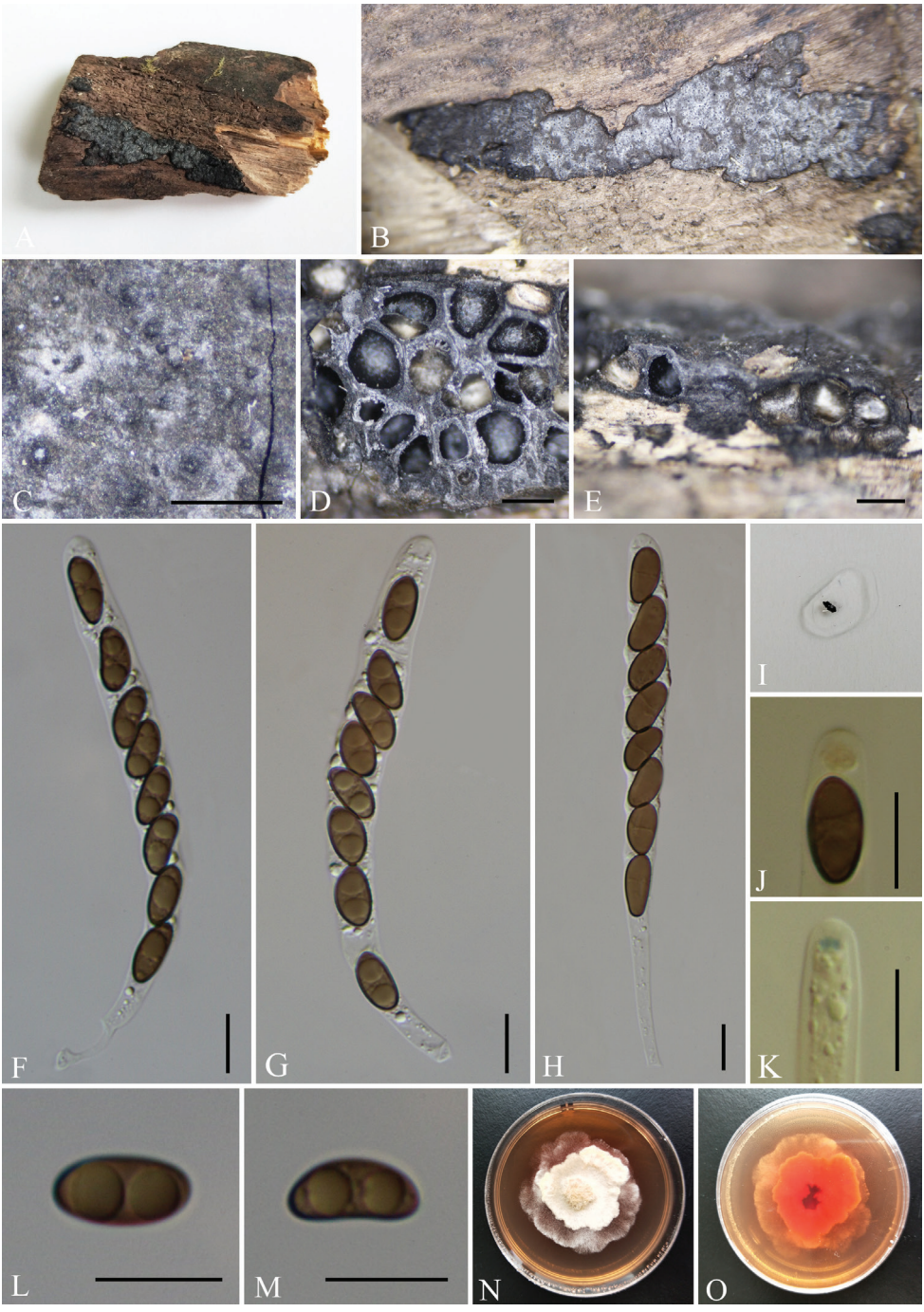

Figure 4. *Nemania changningensis* (GMB0056, **holotype**) **A** type material **B, C** stromata on the surface of host **D** transverse sections of stromata **E** longitudinal section of stroma **F–H** asci with ascospores **I** pigments in 10% KOH **J, K** asci apical apparatus (stained in Melzer's Reagent) **L, M** ascospores **N, O** colonies on PDA (**N**-upper, **O**-lower). Scale bars: 0.5 mm (**C–E**); 10 μm (**F–H, J–M**).

Nemania cyclobalanopsina **Y.H. Pi & Q.R. Li, sp. nov.**
MycoBank No: 840088
Fig. 5

Etymology. Refers to its host, *Cyclobalanopsis glauca*.

Material examined. China, Yunnan Province, Changning County, Lancang River Nature Reserve (25°01'9.46"N, 99°35'29.47"E, altitude: 2623 m), on dead wood of *C. glauca*, 6 October 2019, Y.H. Pi, 2019LC357 (GMB0062, holotype; GMBC0062, ex-type living culture; KUN-HKAS 112679, isotype).

Description. Saprobic on the surface of decaying branches of *C. glauca* (Thunb.) Oerst. ***Sexual morph*****:** Stromata effused-pulvinate, orbicular to ellipsoid or irregularly lobed, 6–26 mm long × 3.5–10 mm wide × 0.5–1 mm thick, occasionally confluent into larger compound stromata, with steep to sloping margins; surface light blackish, slightly blood colour; outer crust carbonaceous; interior black, entire tissue carbonaceous around the perithecia; mature stromata lacking KOH-extractable pigments. Perithecia 0.2–0.3 mm diam. × 0.38–0.46 mm high, subglobose obovoid or tubular. Ostioles higher than stromatal surface and with coarsely rounded-papillate, black, without encircling disc. Asci 90–160 × 7–11 μm (av. = 125 × 9 μm, n = 30), 8-spored, unitunicate, cylindrical, long-stipitate, the spore-bearing parts 65–85 μm long, apically rounded with a J+, short-cylindrical to slightly tubular apical apparatus stained in Melzer's Reagent, 1.5–2.5 × 2–3 μm (av. = 2 × 2.3 μm, n = 30). Ascospores 9–14 × 4.5–7.5 μm (av. = 11 × 6 μm, n = 30), uniseriate, unicellular, ellipsoid-inequilateral with broadly rounded ends, smooth, brown to dark brown, with a conspicuous, straight germ slit slightly less than spore-length to almost spore-length on the convex side; lacking a sheath and appendage; perispore indehiscent in 10% KOH. ***Asexual morph*****:** Undetermined.

Culture characteristics. Colonies on PDA medium in size with a diameter of 6 cm after two weeks at 25 °C; the surface is white, intermediate thick, cottony, dense, with undulate or ring edge, flat, low, whitish-yellow, reverse of the colony yellow at the centre. Not sporulating on OA nor on PDA.

Other examined material. China, Yunnan Province, Changning County, Lancang River Nature Reserve (25°52'17.40"N, 99°35'20.53"E, altitude: 1489 m), on dead wood of *C. glauca*, 4 October 2019, Y.H. Pi, 2019LC357-1 (GMB0061), living culture, GMBC0061.

Notes. In our phylogenetic analyses, *N. cyclobalanopsina* grouped with *N. diffusa* (100% ML, 1 BYPP, Fig. 1). Morphologically, *N. cyclobalanopsina* differs from *N. diffusa* by its blackish stromatal surfaces and coarsely rounded-papillate ostioles. Moreover, *N. diffusa* has larger perithecia (0.3–0.6 × 0.4–0.8 mm) (Granmo et al. 1999; Ju and Rogers 2002). In the multi-gene phylogenetic analysis, *N. cyclobalanopsina* appeared in a separate branch which is distinct from *N. diffusa* (Fig. 1). Moreover, there is a 3% difference in ITS sequences between *N. diffusa* and *N. cyclobalanopsina*. (Vu et al. 2019; Jeewon and Hyde 2016).

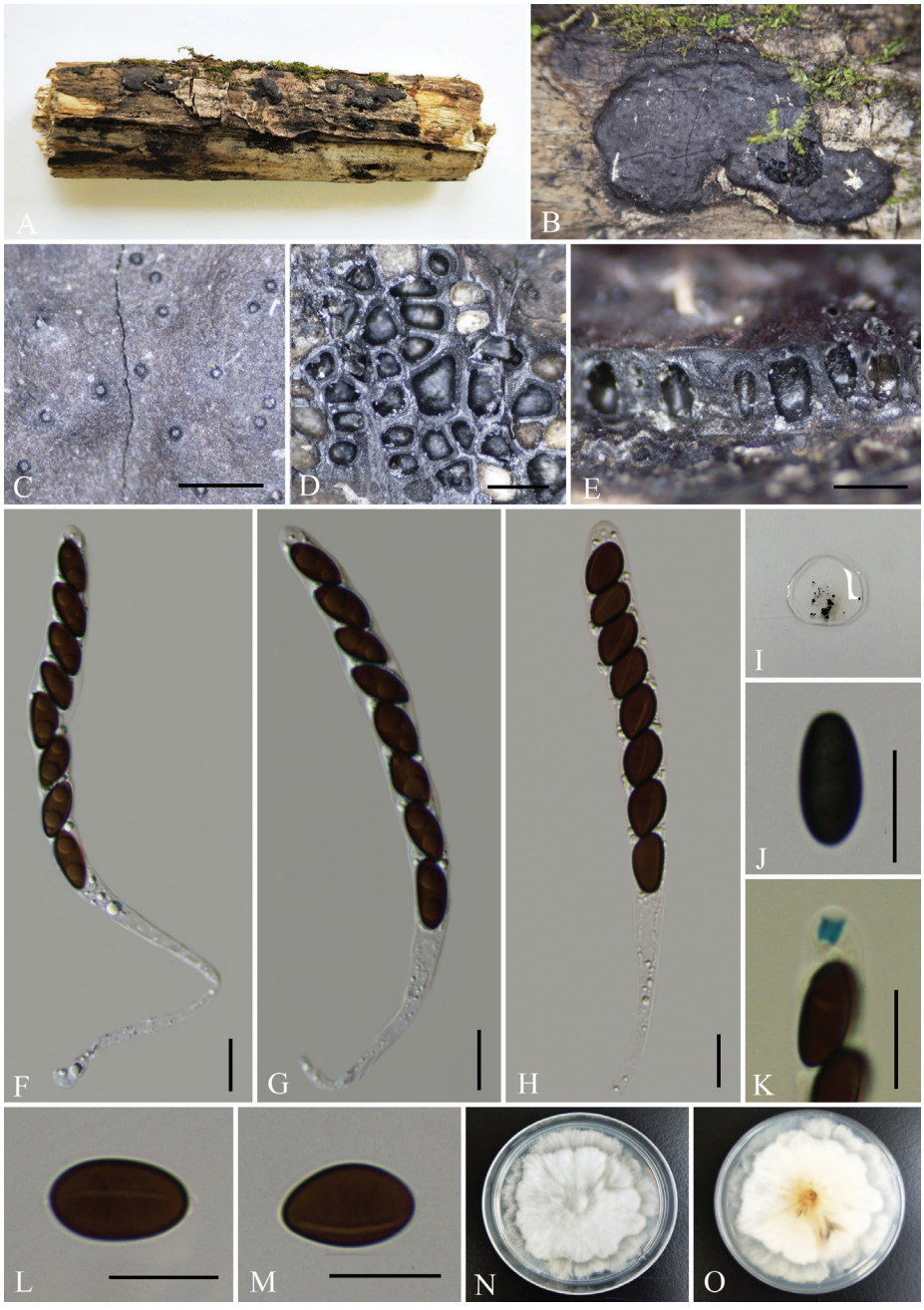

Figure 5. *Nemania cyclobalanopsina* (GMB0062, **holotype**) **A** type material **B, C** stromata on the surface of host **D** transverse sections of stromata **E** longitudinal sections of stromata **F–H** asci with ascospores **I** pigments in 10% KOH **J** ascospore with indehiscent perispore in 10% KOH **K** ascus apical apparatus (stained in Melzer's Reagent) **L, M** ascospores **N, O** colonies on PDA (**N**-upper, **O**-lower). Scale bars: 0.5 mm (**C–E**); 10 μm (**F–H, J–M**).

***Nemania diffusa* (Sowerby) S.F. Gray, Nat. Arr. Brit. Pl.: 517 (1821)**
MycoBank No: 477312
Fig. 6

Synonyms. *Sphaeria diffusa* Sowerby, Col. fig. Engl. Fung. Mushr. (London) 3(no. 25): tab. 373, fig. 10 (1802)
Sphaeria unita Fr., Elench. fung. (Greifswald) 2: 67 (1828)
Sphaeria exarata Schwein., Trans. Am. phil. Soc., New Series 4(2): 192 (1832)
Hypoxylon exaratum (Schwein.) Sacc., Syll. fung. (Abellini) 1: 392 (1882)
Ustulina linearis Rehm, Hedwigia 31(6): 310 (1892)
Hypoxylon lilacinofuscum Bres., Fl. Trident. Nov. 2: 43 (1892)
Hypoxylon cohaerens var. *brasiliense* Starbäck, Bih. K. svenska VetenskAkad. Handl., Afd. 3 27(no. 9): 8 (1901)
Hypoxylon vestitum Petch, Ann. R. bot. Gdns Peradeniya 8: 156 (1924)
Nemania unita (Fr.) Krieglst. & Enderle, Mitteilungsblatt der Arbeitsgemeinschaft Pilzkunde Niederrhein 1: 64 (1989)

Description. Saprobic on the surface of rotten wood. ***Sexual morph*:** Stromata effused-pulvinate, clear outline, ellipsoid or irregularly lobed, occasionally confluent into a larger compound stromata, 2–20 mm long × 2–9 mm wide × 0.5–1 mm thick, with conspicuous perithecial mounds, carbonaceous between the perithecia, surface dark brown or brown; the inter-perithecial tissue blackish, carbonaceous; does not release a coloured pigment in 10% KOH. Perithecia 0.3–0.55 diam. × 0.4–0.7 mm high, subglobose to obovoid. Ostioles finely conic-papillate, black, shiny. Asci 130–250 × 6–10 μm (av. = 170 × 8 μm, n = 30), 8-spored, unitunicate, cylindrical, long-stipitate, the spore-bearing parts 70–90 μm, apically rounded with a J+ apical apparatus, 1.5–2.5 × 2–3.5 μm (av. = 2 × 2.6 μm, n = 30), tubular with a faint upper rim, bluing in Melzer's Reagent. Ascospores 9.5–13 × 4.5–7 μm (av. = 11 × 5.5 μm, n = 30), unicellular, ellipsoid-inequilateral, with narrowly-rounded ends, smooth, brown to dark brown, with a conspicuous, straight germ slit spore-length to slightly less than spore-length on the ventral side; lacking a sheath and appendage; perispore indehiscent in 10% KOH. ***Asexual morph*:** Undetermined.

Culture characteristics. Colonies grow on PDA at 25 °C for a week reaching a diameter of 5 cm. Colonies are cotton white in colour, flocculent or velvety, dense, circular, radial. On the reverse, white edge, light yellow in the middle. Not sporulating on OA nor on PDA.

Material examined. China, Guizhou Province, Tongren City, Fanjingshan Nature Reserve (27°53'46.59"N, 108°431'16.29"E, altitude: 1058 m), on dead wood, 14 October 2020, Y.H. Pi, 2020FJS1 (GMB0072, KUN-HKAS 112686), living culture, GMBC0072; CHINA, Yunnan Province, Changning County: Lancang River Nature Reserve (21°54'17.44"N, 107°54'10.05"E, altitude: 1382 m), on dead wood, 1 October 2019, Y.H. Pi, 2019LC008 (GMB0071, KUN-HKAS 112658), living culture, GMBC0071.

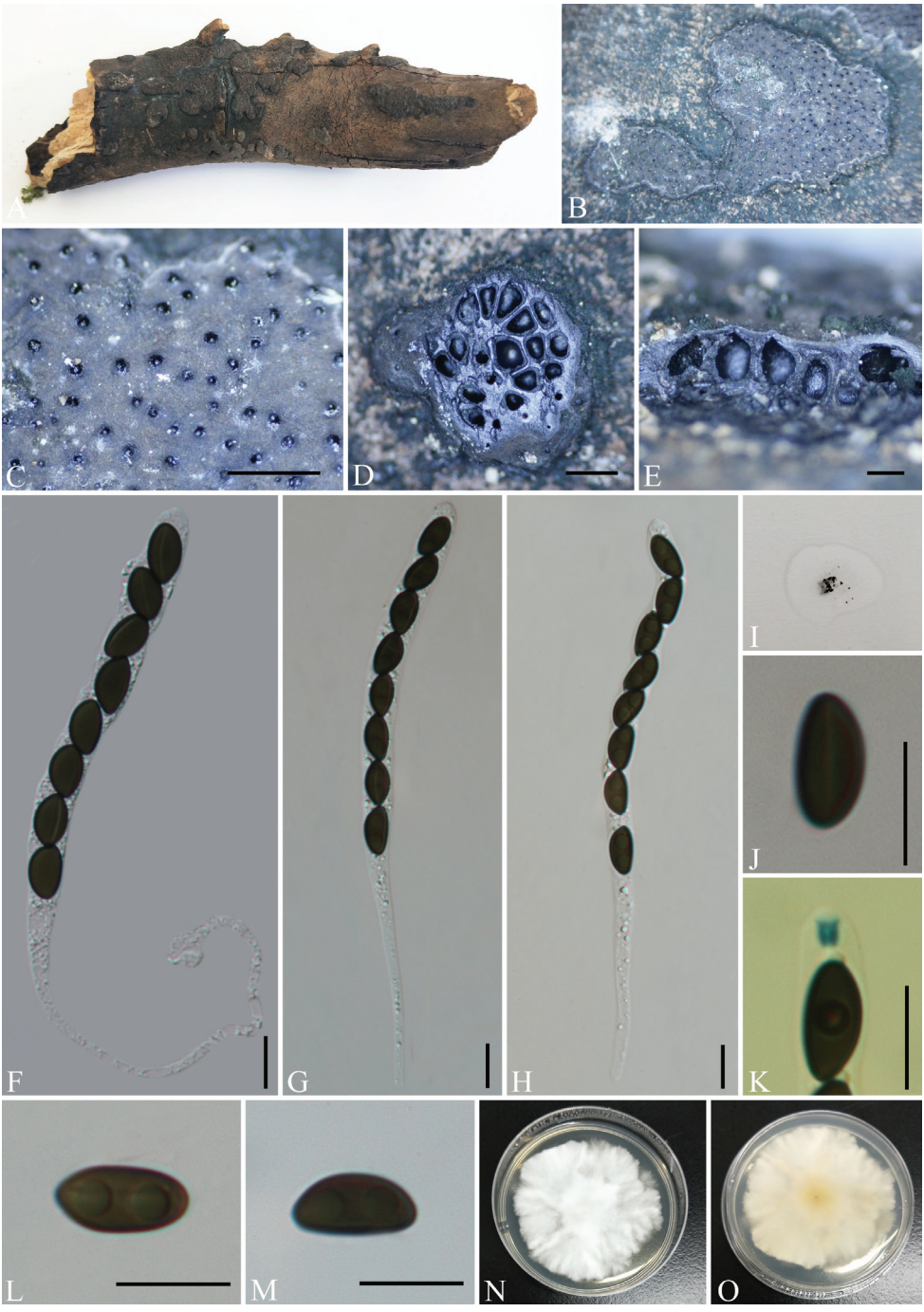

Figure 6. *Nemania diffusa* (GMB0072) **A** specimen **B, C** stromata on the surface of host **D** transverse sections of stromata **E** longitudinal sections of stromata **F–H** asci with ascospores **I** pigments in 10% KOH **J** ascospore with indehiscent perispore in 10% KOH **K** ascus apical apparatus (stained in Melzer's Reagent) **L, M** ascospores **N, O** colonies on PDA (**N**-upper, **O**-lower). Scale bars: 0.5 mm (**C–E**); 10 μm (**F–H, J–M**).

Notes. The new collection morphologically resembles *N. diffusa* (Gray 1821), having effused-pulvinate carbonaceous stromata with inconspicuous perithecial mounds, brown to dark brown ellipsoid-inequilateral ascospores (9.5–13.5 × 5–6 μm), with narrowly-rounded ends and a long germ slit on the ventral side (Granmo et al. 1999; Ju and Rogers 2002). Fournier et al. (2018) predicted that *N. diffusa* might be a species complex as it is difficult to identify, based solely on morphology, thus, it should be evaluated after extensive sampling and using DNA-based taxonomy. In phylogenetic analyses of combined ITS, *rpb2*, β-tubulin and α-actin genes (Fig. 1), new collections clearly showed its close kinship with *N. diffusa*. Only a 2% difference of ITS sequences existed between our strains and *N. diffusa* (HAST 91020401, authoritative strain). Therefore, we regard the new collection as *N. diffusa*. *Nemania carbonacea* Pouzar. can be confused with *N. diffusa* by having the same dark ascospores and nearly spore-length germ slits. However, *N. carbonacea* has white, soft stromatal tissue between the perithecia (Ju and Rogers 2002).

Nemania feicuiensis **Y.H. Pi & Q.R. Li, sp. nov.**
MycoBank No: 840089
Fig. 7

Etymology. Refers to the collection location, Emerald Park, Chinese name of jade, feicui.

Material examined. China, Hainan Province, Wuzhishan City, Emerald Park (18°48'9.64"N, 109°31'6.59"E, altitude: 352 m), on dead wood, 14 November 2020, Y.H. Pi, 2020FCGY12-2 (GMB0059, ***holotype***; GMBC0059, ex-type living culture; KUN-HKAS 112698, ***isotype***).

Description. Saprobic on the surface of decaying wood. ***Sexual morph*****:** Stromata effused-pulvinate, superficial, orbicular to ellipsoid or irregularly lobed, 5–27 mm long × 2.5–10 mm wide × 0.3–0.5 mm thick, surface blackish-grey, with inconspicuous perithecial outer mounds, crust weakly carbonaceous; interior black, stromatal tissue between the perithecia carbonaceous; mature stromata lacking KOH extractable pigments. Perithecia 0.3–0.55 mm diam. × 0.25–0.37 mm high, subglobose to depressed-spherical. Ostioles higher than stromatal surface and with openings slightly papillate, black, conspicuous, without encircling disc. Asci 130–180 × 7–11.5 μm (av. = 145 × 9 μm, n = 30), 8-spored, unitunicate, cylindrical, long-stipitate, the spore-bearing parts 65–85 μm long, apically rounded with a J+ apical apparatus, 1–2.5 × 2–3 μm (av. = 1.8 × 2.4 μm, n = 30), long-cylindrical. Ascospores 9.5–13 × 4–7.5 μm (av. = 11 × 6 μm, n = 30), uniseriate, unicellular, ellipsoid or slightly inequilateral, with broadly rounded ends, smooth, brown to dark brown, with a conspicuous, straight, almost spore-length germ slit on the flattened side; lacking a sheath and appendage; perispore indehiscent in 10% KOH. ***Asexual morph*****:** Undetermined.

Culture characteristics. Colonies grow slowly on PDA at 25 °C for 2 weeks, with a diameter of 5 cm. Colonies are cotton white in colour, flocculent or velvety, slightly convex, circular, shallow edges, radial, white to light yellow on the reverse, light brown in the middle. Not sporulating on OA nor on PDA.

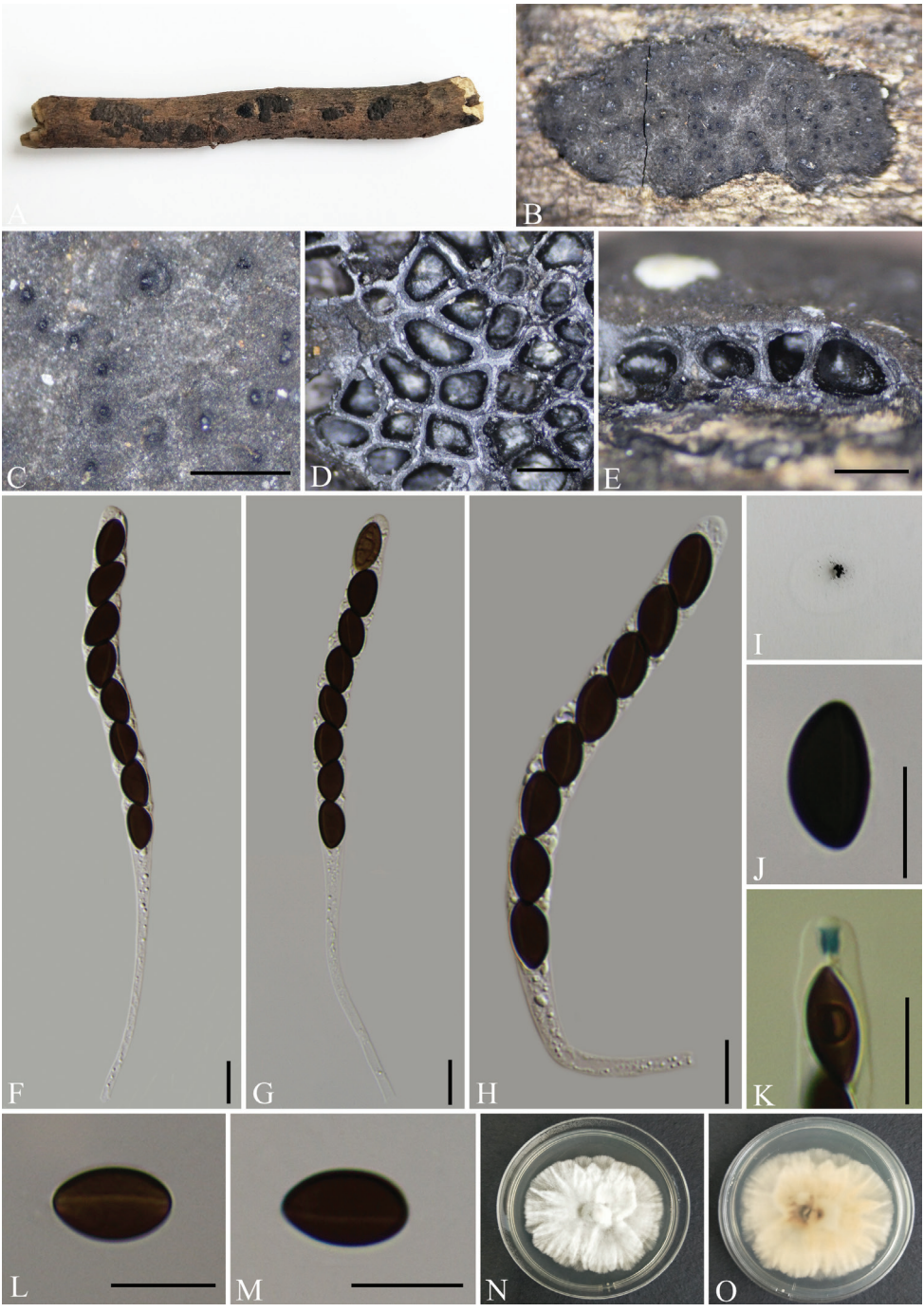

Figure 7. *Nemania feicuiensis* (GMB0059, **holotype**) **A** type material **B, C** stromata on the surface of host **D** transverse sections of stromata **E** longitudinal sections of stromata **F–H** asci with ascospores **I** pigments in 10% KOH **J** ascospore with indehiscent perispore in 10% KOH **K** ascus apical apparatus (stained in Melzer's Reagent) **L, M** ascospores **N, O** colonies on PDA (**N**-upper, **O**-lower). Scale bars: 0.5 mm (**C–E**); 10 μm (**F–H, J–M**).

Other examined material. China, Hainan Province, Wuzhishan City, Emerald Park (18°47'8.26"N, 109°31'5.34"E, altitude: 426 m), on dead wood, 16 November 2020, Y.H. Pi, 2020FCGY20 (GMB0058), living culture, GMBC0058.

Notes. The phylogenetic tree (Fig. 1) shows that *N. feicuiensis* and *N. primolutea* are closely related (100% ML, 1 BYPP). In morphology, *N. feicuiensis* differs from *N. primolutea* in that the latter has luteous stromatal surface and slightly smaller ascospores (10–13 × 4.5–5.5 μm) with narrowly-rounded ends (Ju et al. 2005). Furthermore, in the multi-gene phylogenetic analysis, *N. feicuiensis* appeared in a separate branch which is distinct from *N. primolutea* (Fig. 1). *Nemania feicuiensis* is similar to *N. diffusa* in stromatal anatomy and ascospores size, but differs by ascospores shape (broadly rounded ends vs. narrowly rounded ends) and the larger perithecia of *N. diffusa* (0.3–0.6 × 0.4–0.8 mm) (Ju and Rogers 2002).

Nemania lishuicola **Y .H. Pi & Q.R. Li, sp. nov.**
MycoBank No: 840090
Fig. 8

Etymology. Refer to the host, *quercus*.

Material examined. China, Yunnan Province, Changning County: Lancang River Nature Reserve (25°01'7.93"N, 99°35'30.74"E, altitude: 2629 m), on dead bark of *Quercus* sp., 4 October 2019, Y.H. Pi, 2019LC263 (GMB0065, ***holotype***; GMBC0065, ex-type living culture; KUN-HKAS 112673, ***isotype***).

Description. Saprobic on the surface of decaying wood of *Quercus* sp. ***Sexual morph*****:** Stromata pulvinate, attached to substrate along entire area of the base, containing one to several perithecia, frequently confluent, 1.5–4 mm long × 1–2 mm wide × 0.5–1 mm thick, with conspicuous perithecial mounds, carbonaceous between the perithecia, surface dull black and slightly shiny at maturity, the interperithecial tissue blackish, carbonaceous; not releasing a coloured pigment in 10% KOH. Perithecia 0.7–0.95 mm diam. × 0.65–0.85 mm high, subglobose to depressed-spherical. Ostioles coarsely papillate in discoid areas, ostiolar area blackish, shiny, frequently flattened, usually around a circle of white tissue. Asci 150–300 × 7–12 μm (av. = 200 × 9 μm, n = 30), 8-spored, unitunicate, cylindrical, long-stipitate, spore-bearing parts 95–130 μm long, apically rounded with a J+ apical apparatus, 2–3 × 2–3.5 μm (av. = 2.5 × 3 μm, n = 30), tubular with a faint upper rim. Ascospores 12.5–17 × 5–8.5 μm (av. = 15 × 6.5 μm, n = 30), uniseriate, unicellular, ellipsoid-inequilateral, with broadly rounded ends, smooth, brown to dark brown, with a conspicuous, straight germ slit spore-length to slightly less than spore-length on the flattened side; lacking a sheath and appendage; perispore indehiscent in 10% KOH. ***Asexual morph*****:** Undetermined.

Culture characteristics. Colonies grow on PDA, a diameter of 6 cm after one week at 25 °C, white, velvety to hairy, zonnate, rosette, high convex in centre, dense, white to cream from above, white irregular edge with light yellow to slightly yellow at centre from the below. Not sporulating on OA nor on PDA.

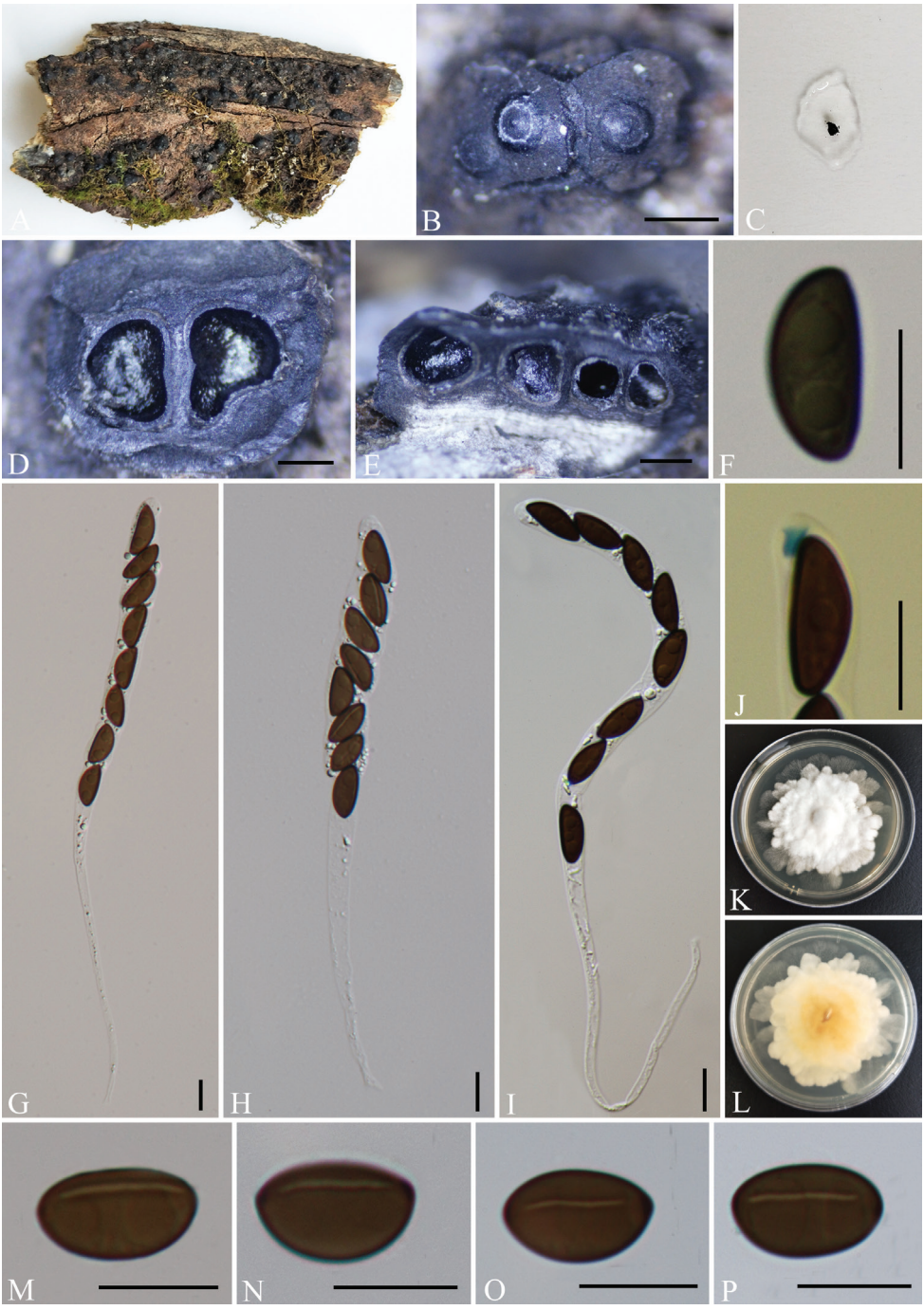

Figure 8. *Nemania lishuicola* (GMB0065, **holotype**) **A** type material **B** stromata on the surface of host **C** pigments in 10% KOH **D** transverse sections of stromata **E** longitudinal sections of stromata **F** ascospore with indehiscent perispore in 10% KOH **G–I** asci with ascospores **J** ascus apical apparatus (stained in Melzer's Reagent) **K, L** colonies on PDA (**K**-upper, **L**-lower) **M–P** ascospores. Scale bars: 0.5 mm (**B, D, E**); 10 μm (**F–J, M–P**).

Other examined material. China, Yunnan Province, Changning County: Lancang River Nature Reserve (25°01'30.75"N, 99°35'21.53"E, altitude: 2608 m), on dead bark of *Quercus* sp., 4 October 2019, Y.H. Pi, 2019LC253 (GMB0066), living culture, GMBC0066.

Notes. Phylogenetic analyses of combined ITS, *rpb2*, β-tubulin and α-actin genes (Fig. 1) show that *N. lishuicola* has a close relationship with *N. bipapillata* with high support values (100 MLBP, 1% BYPP). Morphologically, *N. lishuicola* differs from *N. bipapillata* by its larger ascospores (12.5–17 × 5–8.5 μm vs. 10.5–13.5 × 4.5–6 μm) (Miller 1961; Ju and Rogers 2002).

***Nemania rubi* Y.H. Pi & Q.R. Li, sp. nov.**

MycoBank No: 840091

Fig. 9

Etymology. Refers to the name of host genus, *rubus*.

Material examined. China, Guizhou Province, Pingba County (26°25'13.38"N, 106°24'25.23"E, altitude: 1255 m), on dead branches of *Rubus lambertianus* Ser., 5 September 2020, Y.H. Pi, 2020PB70 (GMB0064, ***holotype***; GMBC0064, ex-type living culture; KUN-HKAS 112695, ***isotype***).

Description. Saprobic on dead branches of *R. lambertianus*. ***Sexual morph*:** Stromata effused-pulvinate, irregular shape, multi-peritheciate, scattered, separate to confluent into larger compound stromata, 2.5–15 mm long × 2–9 mm wide × 0.4–0.6 mm thick; surface blackish, weakly carbonaceous, with unexposed perithecial contours, uneven and irregular, internally whitish between ascomata, tissue, soft-textured; not releasing a coloured pigment in 10% KOH. Perithecia 0.25–0.35 mm diam. × 0.2–0.3 mm high, subglobose. Ostioles papillate, black, obtusely conical to hemispherical, without encircling disc. Asci 85–160 × 7–11 μm (av. = 130 × 9 μm, n = 30), 8-spored, unitunicate, cylindrical, long-stipitate, spore-bearing parts 60–85 μm long, apically rounded with a J+, long-cylindrical apical apparatus, 1.5–2.5 × 2–3 μm (av. = 1.5 × 2.5 μm, n = 30). Ascospores 9–12 × 4–6 μm (av. = 10 × 4.8 μm, n = 30), uniseriate to irregularly-biseriate unicellular, smooth, olivaceous when fresh, turning brown to medium brown after a period of time, ellipsoid-inequilateral with often broadly-rounded ends, lacking a germ slit sheath and appendage; perispore indehiscent in 10% KOH. ***Asexual morph*:** Undetermined.

Culture characteristics. Colonies grow slowly on PDA medium with a diameter of 5 cm after 10 days at 25 °C. Colonies surface were white to pale orange, circular, cottony, low, dense, cottony mycelium, reverse with light orange mycelium. Not sporulating on OA nor on PDA.

Other examined material. China, Guizhou Province, Pingba County (26°25'10.24"N, 106°24'25.21"E, altitude: 1052 m), on dead wood, 5 September 2020, Y.H. Pi, 2020PB22 (GMB0063), living culture, GMBC0063.

Notes. In our phylogenetic analysis, *Nemania rubi* formed a distinct branch, which is sister to *N. changningensis* and *N. caries* (Fig. 1). In morphology, *N. rubi* is similar to

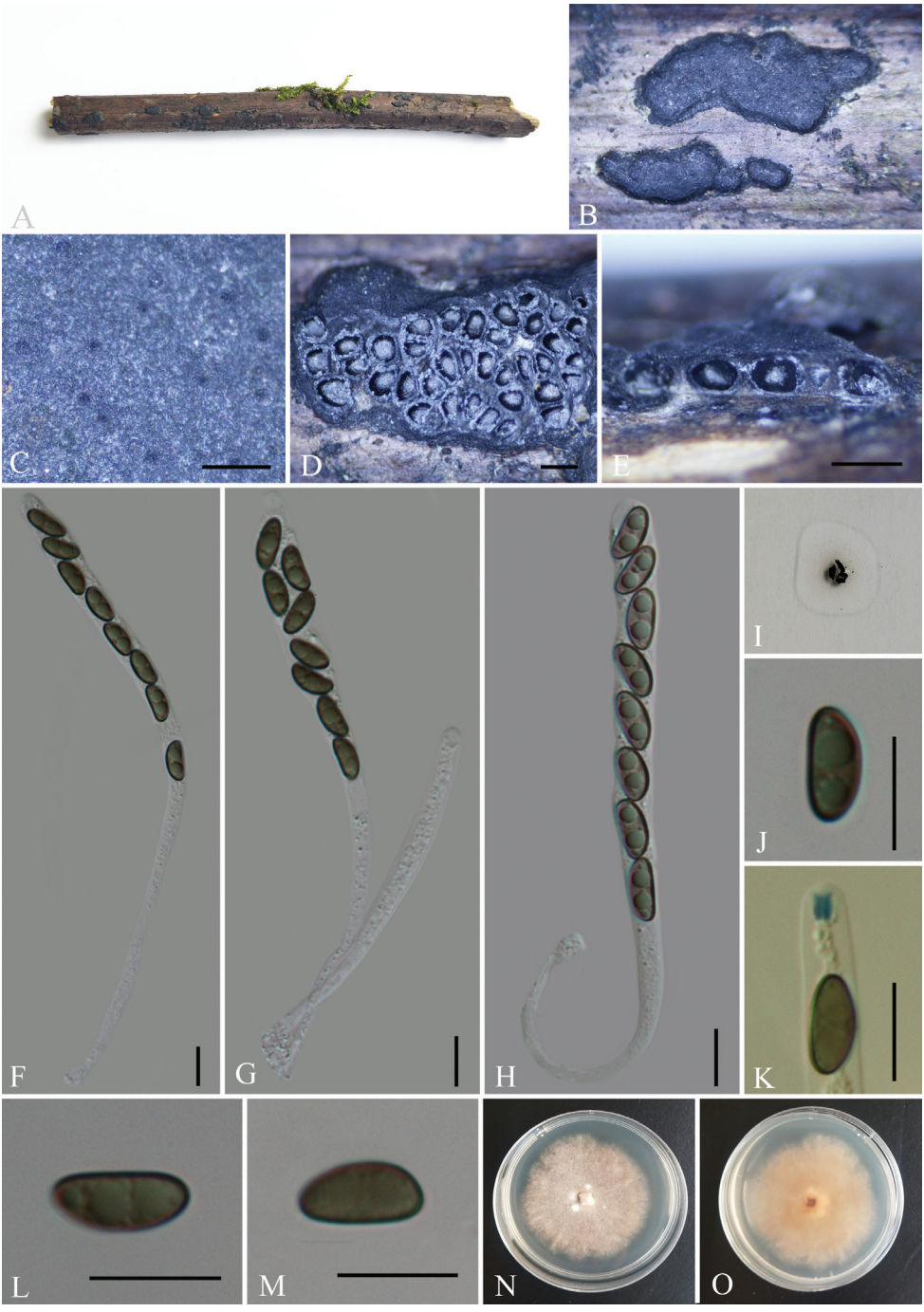

Figure 9. *Nemania rubi* (GMB0064, **holotype**) **A** type material **B, C** stromata on surface of host **D** transverse sections of stromata **E** longitudinal section of stromata **F–H** asci with ascospores **I** pigments in 10% KOH **J** ascospore with indehiscent perispore in 10% KOH **K** ascus apical apparatus (stained in Melzer's Reagent) **L, M** ascospores **N, O** colonies on PDA (**N**-upper, **O**-lower). Scale bars: 0.5 mm (**C–E**); 10 μm (**F–H, J–M**).

N. caries, but is distinct in having a long-cylindrical apical apparatus and the inequilateral ascospores lacking a germ slit (Miller 1961; Ju and Rogers 2002). In addition, the perithecia of *N. caries* are obovoid (0.3–0.6 × 0.5–0.7 mm) and its height is greater than the width (Tang et al. 2007). The ascomata surface of *N. rubi* ascomata is uneven with inconspicuous perithecial mounds, which is similar to those of *N. plumbea*, but the latter has larger ascospores (13–16 × 5.4–6.6 μm) with germ slits on the concave side (Tang et al. 2007).

Discussion

In this study, newly-collected *Nemania* species from Hainan, Yunnan and Guizhou Provinces were subjected to morpho-molecular analyses. Six new species were introduced while reporting one new record from China. *Nemania* showed a closer affinity to *Roselinia* than to *Kretzschmaria* Fr. and *Xylaria* (U'Ren et al. 2016), which is also supported in the phylogenetic analysis, based on ITS, *rpb2*, β-tubulin and α-actin sequences. Although no asexual morphs were observed in this study, *Nemania* has geniculisporium-like asexual morphs which are a common character in members of *Xylariaceae* (Fournier et al. 2018).

Nemania forms a single branch in the phylogenetic analysis, which supports that it is a monophyletic genus. However, *Nemania* genus is separated into six clades (N1–N6, Fig. 1), each of which have relatively-uniform morphological characteristics. N1 clade is represented by *N. bipapillata* and taxa in this clade have carbonaceous interior to the stromata, ostioles encircled with a disc and dark brown ascospores with a long germ slit. The species within clade N2 are distinguished from other *Nemania* species with fusoid-inequilateral and pale brown ascospores and by having white soft tissues between the perithecia. The species in clades N3, N4 and N5 have little difference in morphology and may be confused. Most taxa in clades N4 and N5 have usually brown, dark brown or blackish-brown ascospores with a germ slit longer than 2/3 spore length (Granmo et al. 1999; Ju and Rogers 2002; Fournier et al. 2018). The taxa in N6 clade have light brown or medium brown ascospores with a germ slit shorter than 2/3 spore length or seemingly lacking (Ju and Rogers 2002). Interestingly, the ascospores of most taxa in N6 clade are olivaceous brown when fresh, turning medium brown after desiccation.

Separation of members of *Nemania*, based on morphology, is relatively difficult and confusing (Fournier et al. 2018). In some early literature, the new species lacked the description of some key morphological characteristics (Du et al. 2016). Moreover, sequences are available for only a few species in GenBank, thus species identification, based on DNA sequences, is also problematic. Hence, it is essential to re-collect old species that lack ex-type cultures and DNA sequences and to epitypify them.

The similarity of morphological features between species is high, which makes it difficult for existing morphological taxonomic features to identify species. For example, species in clade N3, which includes *N. diffusa* and *N. cyclobalanopsina*, are difficult to identify, based solely on morphological characteristics, although their ITS sequence

differences can reach more than 3% (Jeewon and Hyde 2016; Vu et al. 2019). In this clade, we tentatively use multiple-genes sequence as the main classification basis for species. Molecular data should be the main identification basis for *Nemania* species, especially for clade N3. It is worth noting that we should compare sequences with that from type or authoritative strains.

Acknowledgements

This research was supported by the National Natural Science Foundation of China (32000009 and 31960005); the Fund of the Science and Technology Foundation of Guizhou Province ([2020]1Y059); the Fund of Special Project of Academic New Seedling Cultivation and Innovation Exploration in Guizhou Medical University [2018]5779-64; Guizhou Province Ordinary Colleges and Universities Youth Science and Technology Talent Growth Project [2021]154; National Natural Science Foundation of China [No. U1812403-4-4], the Fund of High-Level Innovation Talents [No. 2015-4029], the Base of International Scientific and Technological Cooperation of Guizhou Province [No. [2017]5802]; Yingqian Kang is grateful to the 111 Project (D20009) and Talent Base Project of Guizhou Province, China (FCJD2018-22).

References

Ariyawansa HA, Hyde KD, Jayasiri SC, Buyck B, Chethana KWT, Dai DQ, Dai YC, Daranagama DA, Jayawardena RS, Lücking R, Ghobad-Nejhad M, Niskanen T, Thambugala KM, Voigt K, Zhao RL, Li GJ, Doilom M, Boonmee S, Yang ZL, Cai Q, Cui YY, Bahkali AH, Chen J, Cui BK, Chen JJ, Dayarathne MC, Dissanayake AJ, Ekanayaka AH, Hashimoto A, Hongsanan S, Jones EBG, Larsson E, Li WJ, Li QR, Liu JK, Luo ZL, Maharachchikumbura SSN, Mapook A, McKenzie EHC, Norphanphoun C, Konta S, Pang KL, Perera RH, Phookamsak R, Phukhamsakda C, Pinruan U, Randrianjohany E, Singtripop C, Tanaka K, Tian CM, Tibpromma S, Abdel-Wahab MA, Wanasinghe DN, Wijayawardene NN, Zhang JF, Zhang H, Abdel-Aziz FA, Wedin M, Westberg M, Ammirati JF, Bulgakov TS, Lima DX, Callaghan TM, Callac P, Chang CH, Coca LF, Dal-Forno M, Dollhofer V, Fliegerová K, Greiner K, Griffith GW, Ho HM, Hofstetter V, Jeewon R, Kang JC, Wen TC, Kirk PM, Kytövuori I, Lawrey JD, Xing J, Li H, Liu ZY, Liu XZ, Liimatainen K, Lumbsch HT, Matsumura M, Moncada B, Nuankaew S, Parnmen S, Santiago ALCMA, Sommai S, Song Y, Souza CAF, Souza-Motta CM, Su HY, Suetrong S, Wang Y, Wei SF, Wen TC, Yuan HS, Zhou LW, Réblová M, Fournier J, Camporesi E, Luangsa-ard JJ, Tasanathai K, Khonsanit A, Thanakitpipattana D, Somrithipol S, Diederich P, Millanes AM, Common RS, Stadler M, Yan JY, Li XH, Lee HW, Nguyen TTT, Lee HB, Battistin E, Marsico O, Vizzini A, Vila J, Ercole E, Eberhardt U, Simonini G, Wen HA, Chen XH, Miettinen O, Spirin V, Hernawati (2015) Fungal diversity notes 111–252–taxonomic and phylogenetic contributions to fungal taxa. Fungal Diversity 75: 27–274. https://doi.org/10.1007/s13225-015-0346-5

Bills GF, González-Menéndez V, Martín J, Platas G, Fournier J, Peršoh D, Stadler M (2012) *Hypoxylon pulicicidum* sp. nov. (Ascomycota, Xylariales), a pantropical insecticide-producing endophyte. PLoS ONE 7: e46687. https://doi.org/10.1371/journal.pone.0046687

Daranagama DA, Camporesi E, Tian Q, Liu X, Liu X, Chamyuang S, Stadler M, Hyde KD (2015) *Anthostomella* is polyphyletic comprising several genera in *Xylariaceae*. Fungal Diversity 73: 203–238. https://doi.org/10.1007/s13225-015-0329-6

Du ZW, Ma HX, Li Y (2016) One new record and one new variety of *Nemania* from China. Journal of Fungal Research 14: 22–24. http://doi.org/10.13341/j.jfr.2014.1085

Du ZW (2015) Taxonomy and Molecular Phylogeny of *Kretzschmaria* and *Nemania* from China. Master Thesis, Jilin Agricultural University, Jilin Province, China.

Fournier J, Lechat C, Courtecuisse R (2018) The genera *Kretzschmariella* and *Nemania* (*Xylariaceae*) in Guadeloupe and Martinique (French West Indies). Ascomycete.org 10: 1–47. http://doi.org/10.25664/art-0226

Gardes M, Bruns TD (1993) ITS primers with enhanced specificity for basidiomycetes–application to the identification of mycorrhizae and rusts. Molecular Ecology 2: 113–118. https://doi.org/10.1111/j.1365-294X.1993.tb00005.x

Granmo A, Laessøe T, Schumacher T (1999) The genus *Nemania s.l.* (Xylariaceae) in Norden. Sommerfeltia 27: 1–96.

Gray SF (1821) A natural arrangement of British plants. Baldwin, Cradock, and Joy.

Hall TA (1999) BioEdit: a user-friendly biological sequence alignment editor and analysis program for Windows 95/98/NT. Nucleic Acids Symposium Series 41: 95–98. https://doi.org/10.1021/bk-1999-0734.ch008

Hillis DM, Bull JJ (1993) An empirical test of bootstrapping as a method for assessing confidence in phylogenetic analysis. Systematic Biology 42: 182–192. https://doi.org/10.1093/sysbio/42.2.182

Hsieh HM, Ju YM, Rogers JD (2005) Molecular phylogeny of *Hypoxylon* and closely related genera. Mycologia 97: 844–865. https://doi.org/10.1080/15572536.2006.11832776

Hsieh HM, Lin CR, Fang MJ, Rogers JD, Fournier J, Lechat C, Ju YM (2010) Phylogenetic status of *Xylaria* subgenus *Pseudoxylaria* among taxa of the subfamily Xylarioideae (*Xylariaceae*) and phylogeny of the taxa involved in the subfamily. Molecular Phylogenetics and Evolution 54: 957–969. https://doi.org/10.1016/j.ympev.2009.12.015

Huelsenbeck JP, Ronquist F (2001) MRBAYES: Bayesian inference of phylogenetic trees. Bioinformatics 17: 754–755. https://doi.org/10.1093/bioinformatics/17.8.754

Hyde KD, Norphanphoun C, Abreu VP, Bazzicalupo A, Thilini Chethana KW, Clericuzio M, Dayarathne MC, Dissanayake AJ, Ekanayaka AH, He MQ, Hongsanan S, Huang SK, Jayasiri SC, Jayawardena RS, Karunarathna A, Konta S, Kušan I, Lee H, Li JF, Lin CG, Liu NG, Lu YZ, Luo ZL, Manawasinghe IS, Mapook A, Perera RH, Phookamsak R, Phukhamsakda C, Siedlecki I, Soares AM, Tennakoon DS, Tian Q, Tibpromma S, Wanasinghe DN, Xiao YP, Yang J, Zeng XY, Abdel-Aziz FA, Li WJ, Senanayake IC, Shang QJ, Daranagama DA, de Silva NI, Thambugala KM, Abdel-Wahab MA, Bahkali AH, Berbee ML, Boonmee S, Bhat DJ, Bulgakov TS, Buyck B, Camporesi E, Castañeda-Ruiz RF, Chomnunti P, Doilom M, Dovana F, Gibertoni TB, Jadan M, Jeewon R, Jones EBG, Kang JC, Karunarathna SC, Lim YW, Liu JK, Liu ZY, Plautz Jr HL, Lumyong S, Maharachchi-

kumbura SSN, Matočec N, McKenzie EHC, Mešić A, Miller D, Pawłowska J, Pereira OL, Promputtha I, Romero AL, Ryvarden L, Su HY, Suetrong S, Tkalčec Z, Vizzini A, Wen TC, Wisitrassameewong K, Wrzosek M, Xu JC, Zhao Q, Zhao RL, Mortimer PE (2017) Fungal diversity notes 603–708: taxonomic and phylogenetic notes on genera and species. Fungal Diversity 87: 1–235. https://doi.org/10.1007/s13225-017-0391-3

Index Fungorum (2021) Index Fungorum. http://www.indexfungorum.org/names/Names.asp [Accessed on 6 June 2021]

Jeewon R, Hyde KD (2016) Establishing species boundaries and new taxa among fungi: recommendations to resolve taxonomic ambiguities. Mycosphere 7: 1669–1677. https://doi.org/10.5943/mycosphere/7/11/4

Johnston PR, Rogers JD, Park D, Martin NA (2016) *Entalbostroma erumpens* gen. et sp. nov. (*Xylariaceae*) from *Phormium* in New Zealand. Mycotaxon 131: 765–771. https://doi.org/10.5248/131.765

Ju YM, Rogers JD (2002) The genus *Nemania* (*Xylariaceae*). Nova Hedwigia 74: 75–120. https://doi.org/10.1127/0029-5035/2002/0074-0075

Ju YM, Rogers JD, Hsieh HM (2005) New *Hypoxylon* and *Nemania* species from Costa Rica and Taiwan. Mycologia 97: 562–567. https://doi.org/10.1080/15572536.2006.11832831

Ju YM, Hsieh HM, Ho MC, Szu DH, Fang MJ (2007) *Theissenia rogersii* sp. nov. and phylogenetic position of *Theissenia*. Mycologia 99: 612–621. https://doi.org/10.1080/15572536.2007.11832555

Katoh K, Standley DM (2013) MAFFT multiple sequence alignment software version 7: improvements in performance and usability. Molecular Biology and Evolution 30: 772–780. https://doi.org/10.1093/molbev/mst010

Li QR, Kang JC, Hyde KD (2015a) Two new species of the genus *Collodiscula* (Xylariaceae) from China. Mycological Progress 14: e52. https://doi.org/10.1007/s11557-015-1075-6

Li QR, Wen TC, Kang JC, Hyde KD (2015b) A new species of *Collodiscula* (*Xylariaceae*) from China. Phytotaxa 205: 187–196. https://doi.org/10.11646/phytotaxa.205.3.6

Liu YJ, Whelen S, Hall BD (1999) Phylogenetic relationships among ascomycetes: evidence from an RNA polymerase II subunit. Molecular Biology and Evolution 16: 1799–1808. https://doi.org/10.1093/oxfordjournals.molbev.a026092

Long QD, Liu LL, Zhang X, Wen TC, Kang JC, Hyde KD, Shen XC, Li QR (2019) Contributions to species of *Xylariales* in China-1. *Durotheca* species. Mycological Progress 18: e495. https://doi.org/10.1007/s11557-018-1458-6

Miller JH (1961) A Monograph of the World Species of *Hypoxylon*. University of Georgia Press, Athens, 158 pp.

Petrini LE, Rogers JD (1986) A summary of the *Hypoxylon serpens* complex. Mycotaxon 26: 401–436.

Pelaez F, González V, Platas G, Sánchez-Ballesteros J, Rubio V (2008) Molecular phylogenetic studies within the Xylariaceae based on ribosomal DNA sequences. Fungal Diversity 31: 111–134.

Pi YH, Zhang X, Liu LL, Long QD, Shen XC, Kang YQ, Hyde KD, Boonmee S, Kang JC, Li QR (2020) Contributions to species of *Xylariales* in China–4. *Hypoxylon wujiangensis* sp. nov. Phytotaxa 455: 21–30. https://doi.org/10.11646/phytotaxa.455.1.3

Posada D, Crandall KA (1998) Modeltest: testing the model of DNA substitution. Bioinformatics 14: 817–818. https://doi.org/10.1093/bioinformatics/14.9.817

Pourzar Z (1985a) Reassessment of *Hypoxylon serpens*-complex I. Ceska Mykologie 39: 15–25.

Pouzar Z (1985b) Reassessment of the *Hypoxylon serpens*-complex II. Ceska Mykologie 39: 129–134.

Rogers JD, Ju YM (2012) The Xylariaceae of the Hawaiian islands. North American Fungi 7: 1–35. https://doi.org/10.2509/naf2012.007.009

Ronquist F, Teslenko M, van der Mark P, Ayres DL, Darling A, Höhna S, Larget B, Liu L, Suchard MA, Huelsenbeck JP (2012) Mrbayes 3.2: efficient Bayesian phylogenetic inference and model choice across a large model space. Systematic Biology 61: 539–542. https://doi.org/10.1093/sysbio/sys029

Sánchez-Ballesteros J, González V, Salazar O, Acero J, Portal MA, Julian M, Rubio V, Bills GF, Polishook JD, Platas G, Mochales S, Pelaez F (2000) Phylogenetic study of *Hypoxylon* and related genera based on ribosomal ITS sequences. Mycologia 92: 964–977. https://doi.org/10.1080/00275514.2000.12061240

Senanayake IC, Maharachchikumbura SSN, Hyde KD, Bhat JD, Jones EBG, McKenzie EHC, Dai DQ, Daranagama DA, Dayarathne MC, Goonasekara ID, Konta S, Li WJ, Shang QJ, Stadler M, Wijayawardene NN, Xiao YP, Norphanphoun C, Li QR, Liu XZ, Bahkali AH, Kang JC, Wang Y, Wen TC, Wendt L, Xu JC, Camporesi E (2015) Towards unraveling relationships in Xylariomycetidae (Sordariomycetes). Fungal Diversity 73: 73–144. https://doi.org/10.1007/s13225-015-0340-y

Stamatakis A, Hoover P, Rougemont J (2008) A rapid bootstrap algorithm for the RAxML web servers. Systematic Biology 75: 758–771. https://doi.org/10.1080/10635150802429642

Tanaka K, Hirayama K, Yonezawa H, Hatakeyama S, Harada Y, Sano T, Shirouzu T, Hosoya T (2009) Molecular taxonomy of bambusicolous fungi: *Tetraplosphaeriaceae*, a new pleosporalean family with Tetraploa-like anamorphs. Studies in Mycology 64: 175–209. https://doi.org/10.3114/sim.2009.64.10

Tang A, Jeewon R, Hyde KD (2009) A re-evaluation of the evolutionary relationships within the *Xylariaceae* based on ribosomal and protein-coding gene sequences. Fungal Diversity 34: 127–155.

Tang A, Jeewon R, Hyde KD (2007) Phylogenetic relationships of *Nemania plumbea* sp. nov. and related taxa based on ribosomal ITS and RPB2 sequences. Mycological Research 111: 392–402. https://doi.org/10.1016/j.mycres.2007.01.009

Tibpromma S, Zhang L, Karunarathna SC, Du TY, Phukhamsakda C, Rachakunta M, Suwannarach N, Xu J, Mortimer PE, Wang YH (2021) Volatile constituents of endophytic Fungi isolated from *Aquilaria sinensis* with descriptions of two new species of *Nemania*. Life 11: e363. https://doi.org/10.3390/life11040363

U'Ren JM, Miadlikowska J, Zimmerman NB, Lutzoni F, Stajich JE, Arnold AE (2016) Contributions of North American endophytes to the phylogeny, ecology, and taxonomy of *Xylariaceae* (Sordariomycetes, Ascomycota). Molecular Phylogenetics and Evolution 98: 210–232. https://doi.org/10.1016/j.ympev.2016.02.010

Vu D, Groenewald M, de Vries M, Gehrmann T, Stielow B, Eberhardt U, Al-Hatmi A, Groenewald JZ, Cardinali G, Houbraken J, Boekhout T, Crous PW, Robert V, Verkley GJM

(2019) Large-scale generation and analysis of filamentous fungal DNA barcodes boosts coverage for kingdom fungi and reveals thresholds for fungal species and higher taxon delimitation. Studies in Mycology 92: 135–154. https://doi.org/10.1016/j.simyco.2018.05.001

Wendt L, Sir EB, Kuhnert E, Heitkämper S, Lambert C, Hladki AI, Romero AI, Luangsa-ard JJ, Srikitikulchai P, Peršoh D, Stadler M (2018) Resurrection and emendation of the Hypoxylaceae, recognised from a multigene phylogeny of the Xylariales. Mycological Progress 17: 115–154. https://doi.org/10.1007/s11557-017-1311-3

Whalley AJS, Edwards RL, Francis SM (1983) *Hypoxylon gwyneddii* sp. nov. from Wales. Transactions of the British Mycological Society 81: 389–446. https://doi.org/10.1016/S0007-1536(83)80091-6

White TJ, Bruns T, Lee SJWT, Taylor JW (1990) Amplification and direct sequencing of fungal ribosomal RNA genes for phylogenetics. PCR Protocols: A Guide to Methods and Applications 18: 315–322. https://doi.org/10.1016/B978-0-12-372180-8.50042-1

Xie X, Liu LL, Shen XC, Kang JC, Hyde KD, Kang JC, Li QR (2020) Contributions to species of Xylariales in China–3. *Collodiscula tubulosa*. Phytotaxa 428: 122–130. https://doi.org/10.11646/phytotaxa.428.2.6

MycoKeys 83: 69–84 (2021)
doi: 10.3897/mycokeys.83.71156
https://mycokeys.pensoft.net

RESEARCH ARTICLE

A peer-reviewed open-access journal
MycoKeys
Launched to accelerate biodiversity research

New species of *Yamadazyma* from rotting wood in China

Wan-Li Gao[1], Ying Li[1], Chun-Yue Chai[1], Zhen-Li Yan[2], Feng-Li Hui[1]

1 *School of Life Science and Technology, Nanyang Normal University, Nanyang 473061, China* **2** *State Key Laboratory of Motor Vehicle Biofuel Technology, Henan Tianguan Enterprise Group Co., Ltd., Nanyang 473000, China*

Corresponding author: Feng-Li Hui (fenglihui@yeah.net)

Academic editor: Thorsten Lumbsch | Received 6 July 2021 | Accepted 6 August 2021 | Published 26 August 2021

Citation: Gao W-L, Li Y, Chai C-Y, Yan Z-L, Hui F-L (2021) New species of *Yamadazyma* from rotting wood in China. MycoKeys 83: 69–84. https://doi.org/10.3897/mycokeys.83.71156

Abstract

Yamadazyma is one of the largest genera in the family Debaryomycetaceae (Saccharomycetales, Saccharomycetes) with species mainly found in rotting wood, insects and their resulting frass, but also recovered from flowers, leaves, fruits, tree bark, mushrooms, sea water, minerals, and the atmosphere. In the present study, several strains obtained from rotting wood in Henan and Yunnan Provinces of China were isolated. Based on morphology and a molecular phylogeny of the rDNA internal transcribed spacer region (ITS) and the D1/D2 domain of the large subunit (LSU) rDNA, these strains were identified as three new species: *Yamadazyma luoyangensis*, *Y. ovata* and *Y. paraaseri*; and three previously described species, *Y. insectorum*, *Y. akitaensis*, and *Y. olivae*. The three new species are illustrated and their morphology and phylogenetic relationships with other *Yamadazyma* species are discussed. Our results indicate a high undiscovered diversity of *Yamadazyma* spp. inhabiting rotting wood in China.

Keywords

Debaryomycetaceae, phylogeny, rotting wood-inhabiting yeast, taxonomy, *Yamadazyma*

Introduction

The genus *Yamadazyma* Billon-Grand (1989) was erected to accommodate 16 species previously assigned to the genus *Pichia* (Billon-Grand 1989). These species have coenzyme Q-9 as their main ubiquinone, form hat-shaped ascospores, produce

pseudohyphae, ferment sugars, and require an exogenous source of vitamins for growth (Billon-Grand 1989; Kurtzman 2011). However, *Yamadazyma* was not initially accepted as genus due to a phylogenetic analysis of D1/D2 LSU rDNA strongly suggesting its polyphyletic nature (Kurtzman and Robnett 1998). Kurtzman and Suzuki (2010) analyzed phylogenetic relationships among species of *Pichia* and related genera based on combined sequences of the D1/D2 LSU rDNA and SSU rDNA, and proposed a new circumscription for *Yamadazyma* with six sexual species and 11 asexual species assigned to the genus *Candida* (Kurtzman and Suzuki 2010). *Yamadazyma* was later resolved as a well-supported monophyletic clade and a generally accepted genus in the family Debaryomycetaceae, order Saccharomycetales (Kurtzman and Suzuki 2010; Kurtzman 2011). The monophyly of the *Yamadazyma* clade was also supported by combined analysis of the ITS and D1/D2 LSU rDNA (Groenewald et al. 2011; Haase et al. 2017). In the fifth edition of The Yeasts: A Taxonomic Study, *Yamadazyma philogaea*, the type species of the genus, as well as *Y. akitaensis*, *Y. mexicana*, *Y. nakazawae*, *Y. scolyti*, *Y. triangularis*, and 23 *Candida* species were placed in the *Yamadazyma* clade (Kurtzman 2011; Lachance et al. 2011). Since then, a few novel *Candida* species have been described from this clade, including *C. kanchanaburiensis* (Nakase et al. 2008), *C. khao-thaluensis*, *C. tallmaniae*, *C. oceani* (Burgaud et al. 2011), and *C. vaughaniae* (Groenewald et al. 2011). In addition, many new species, e.g., *Y. phyllophila*, *Y. paraphyllophila*, *Y. siamensis* (Kaewwichian et al. 2013), *Y. terventina* (Ciafardini et al. 2013), *Y. ubonensis* (Junyapate et al. 2014), *Y. dushanensis* (Wang et al. 2015), *Y. epiphylla*, *Y. insecticola* (Jindamorakot et al. 2015), *Y. riverae* (Lopes et al. 2015), *Y. barbieri* (Burgaud et al. 2016), *Y. endophytica* (Khunnamwong and Limtong 2016), *Y. kitorensis* (Nagatsuka et al. 2016), *Y. laniorum* (Haase et al. 2017), and *Y. cocois* (Maksimova et al. 2020), have been proposed as part of the genus, and three have already been transferred to *Yamadazyma* as new combinations: *Y. olivae*, *Y. tumulicola*, and *Y. takamatsuzukensis* (Nagatsuka et al. 2016). The *Yamadazyma* clade currently consists of 24 species of the genus *Yamadazyma* and 38 asexual species still assigned to the genus *Candida*, making it one of the largest genera tentatively assigned to the family Debaryomycetaceae (Groenewald et al. 2011; Kurtzman 2011; Maksimova et al. 2020). Among 24 species included in this genus, 7 were sexual morphs, viz. *Y. akitaensis*, *Y. mexicana*, *Y. nakazawae*, *Y. philogaea*, *Y. riverae*, *Y. scolyti*, and *Y. triangularis* (Kurtzman 2011; Lopes et al. 2015).

Yamadazyma species can be originally found in tropical, subtropical, and temperate regions of different continents, but most known species appear to exist in Asia and South America (Nakase et al. 2008; Groenewald et al. 2011; Kurtzman 2011; Lachance et al. 2011; Kaewwichian et al. 2013; Junyapate et al. 2014; Jindamorakot et al. 2015; Lopes et al. 2015; Wang et al. 2015; Burgaud et al. 2016; Khunnamwong and Limtong 2016; Nagatsuka et al. 2016). The genus has been heavily studied in Asia, and 17 species of *Yamadazyma* were previously reported in Japan and Thailand (Nakase et al. 2008; Groenewald et al. 2011; Kurtzman 2011; Lachance et al. 2011; Kaewwichian et al. 2013; Junyapate et al. 2014; Jindamorakot et al. 2015; Wang et al. 2015; Khunnamwong and Limtong 2016; Nagatsuka et al. 2016). By contrast, little is known about *Yamadazyma* spp. in China. To date, only three *Yamadazyma* species

have been described in China, namely *C. diospyri*, *Y. dushanensis*, and *Y. paraphyllophila* (Lachance et al. 2011; Kaewwichian et al. 2013; Wang et al. 2015). In this study, we collected rotting wood samples from Yunnan and Henan Provinces in China. After isolation and examination, three new species and three known species of *Yamadazyma* were identified based on phenotypic characteristics and phylogenetic analysis, increasing the species diversity of *Yamadazyma* in China.

Materials and methods

Sample collection and yeast isolation

Samples of rotting wood were collected in the Xishuangbanna Primeval Forest Park (Yunnan Province, China) and the Tianchi Mountain National Forest Park (Henan Province, China). The Xishuangbanna Primeval Forest Park (21°98'N, 100°88'E) is 500 m above sea level (MASL), with a hot and humid climate. The average annual temperature is between 16 °C and 28 °C, and the average annual rainfall is above 1,100 mm. The Tianchi Mountain National Forest Park (34°33'N, 112°28'E) is at 850 MASL, with a continental monsoon climate, average annual temperature of 14–16 °C, and average annual rainfall between 800 mm and 900 mm. Fifty decayed wood samples were collected during July and August in 2018–2020. The samples were stored in sterile plastic bags and transported under refrigeration to the laboratory over a period of no more than 24 h. The yeast strains were isolated from rotting wood samples in accordance with the methods described by Wang et al. (2015). Each sample (1 g) was added to 20 ml sterile yeast extract-malt extract (YM) broth (0.3% yeast extract, 0.3% malt extract, 0.5% peptone, 1% glucose, pH 5.0 ± 0.2) supplemented with 0.025% sodium propionate and 200 mg/L chloramphenicol in a 150 ml Erlenmeyer flask and then cultured for 3–10 days on a rotary shaker. Subsequently, 0.1 ml aliquots of the enrichment culture and appropriate decimal dilutions were spread on YM agar plates and then incubated at 25 °C for 3–4 days. Different yeast colony morphotypes were then isolated by repeated plating on YM agar and then stored on YM agar slants at 4 °C or in 15% glycerol at – 80 °C.

Phenotypic study

Morphological and physiological properties were determined according to those used by Kurtzman et al. (2011). The beginning of the sexual stage was determined by incubating single or mixed cultures of each of the two strains on cornmeal (CM) agar, 5% malt extract (ME) agar, dilute (1:9) V8 agar, or yeast carbon base plus 0.01% ammonium sulfate (YCBAS) agar at 15 and 25 °C for 6 weeks (Kurtzman 2011; Wang et al. 2015). The assimilation of carbon and nitrogen compounds and related growth requirements were tested at 25 °C. The effects of temperature from 25–40 °C were examined in liquid and agar plate cultures. Photomicrographs were taken using a Leica DM 2500 microscope (Leica Microsystems GmbH, Wetzlar, Germany) with a Leica

DFC295 digital microscope color camera, with bright field, phase contrast, and DIC optics. Novel taxonomic descriptions and proposed names were deposited in MycoBank (http://www.mycobank.org; 8 June 2021) (Crous et al. 2004).

DNA extraction, PCR amplification, and sequencing

Genomic DNA was extracted from the yeast using an Ezup Column Yeast Genomic DNA Purification Kit, according to the manufacturer's instructions (Sangon Biotech, Shanghai, China). The internal transcribed spacer (ITS) and the D1/D2 domain of the large subunit (LSU) rDNA were respectively amplified using ITS5/ITS4 (White et al. 1990) and NL1/NL4 (Kurtzman and Robnett 1998) primers with cycling conditions of 94 °C/30 s, 55 °C/50 s, 72 °C/60 s. All the PCR protocols had 35 cycles including 94 °C/5 min initial denaturation and 72 °C/10 min final extension.

The 25 μL total volume of PCR mixture contained 9.5 μL of ddH2O, 12.5 μL of 2X PCR Master Mix (TIANGEN Co., China), 1 μL of DNA template, and 1 μL of forward and reverse primers (10 μM each) in each reaction. PCR amplified products were checked on 1% agarose electrophoresis gels stained with GoldView I nuclear staining dye (1 μL/10 mL of agarose). Purification and sequencing of PCR products were done by Sangon Biotech (Shanghai) Co., Ltd., Shanghai, China. A consensus sequence for each gene region was assembled in SeqMan (DNAStar, Inc., Madison, WI, USA). The newly-generated sequences were deposited in GenBank (https://www.ncbi.nlm.nih.gov/genbank/ (accessed on 30 May 2021); Table 1).

Abbreviations:

CBS CBS-KNAW Collections, Westerdijk Fungal Biodiversity Institute, Utrecht, The Netherlands;
CECT the Spanish Type Culture Collection, Valencia, Spain;
VTCC Vietnam Type Culture Collection, Hanoi, Vietnam;
NYNU Microbiology Lab, Nanyang Normal University, Henan, China;
T type strain.

Phylogenetic analysis

The sequences obtained in this study and the reference sequences downloaded from GenBank (Table 1) were aligned using MAFFT v 7(https://mafft.cbrc.jp/alignment/server/large.html;) (Katoh et al. 2019) and manually edited using MEGA7 (Kumar et al. 2016). The best-fit nucleotide substitution models for individual and combined datasets were selected using jModelTest v2.1.7 (Darriba et al. 2012) according to the Akaike information criterion. Phylogenetic analyses of combined gene regions (ITS and D1/D2 LSU) were performed using MEGA7 for maximum parsimony (MP) analysis (Kumar et al. 2016) and PhyML v3.0 for maximum likelihood (ML) analysis (Guindon et al. 2010). *Scheffersomyces coipomoensis* (CBS 8178) and *Babjeviella inositovora* (CBS 8006) were used as the outgroup taxa based on Haase et al. (2017) and Nagatsuka et al. (2016).

Table 1. Sequences used in molecular phylogenetic analysis. Entries in bold are newly generated in this study.

Species	Strain no.	Locality	Sample	GenBank accession numbers	
				ITS	D1/D2
Candida aaseri	CBS 1913^T	Norway	Sputum	AY821838	U45802
C. amphixiae	CBS 9877^T	Panama	Beetle	EU491501	AY520327
C. andamanensis	CBS 10859^T	Thailand	Estuarine water	AB525239	AB334210
C. atlantica	CBS 5263^T	Portugal	Shrimp egg	AJ539368	U45799
C. atmosphaerica	CBS 4547^T	Spain	Atmosphere	AJ539369	U45779
C. blattariae	CBS 9876^T	Panama	Cockroach	FJ715435	AY640213
C. buinensis	CBS 6796^T	Papua New Guinea	Gelatinous exudate	HQ283376	U45778
C. cerambycidarum	CBS 9879^T	Panama	Beetle	AY964669	AY520299
C. conglobata	CBS 2018^T	–	Tubercular lung	AJ539370	U45789
C. dendronema	CBS 6270^T	South Africa	Frass	HQ283365	U45751
C. diddensiae	CBS 2214^T	USA	Shrimp	AY580315	U45750
C. diospyri	CBS 9769^T	China	Kaki fruit	AY450919	AY450918
C. endomychidarum	CBS 9881^T	Panama	Beetle	AY964672	AY520330
C. friedrichii	CBS 4114^T	Germany	D-glucitol solution	HQ283377	U45781
C. germanica	CBS 4105^T	Germany	Atmosphere	HQ283366	AF245401
C. gorgasii	CBS 9880^T	Panama	Beetle	AY964670	AY520300
C. insectorum	CBS 6213^T	South Africa	Frass	HQ283372	U45791
C. insectorum	**NYNU 1672**	**China**	**Rotten wood**	**MZ314279**	**MZ314278**
C. jaroonii	CBS 10790^T	Thailand	Frass	AB360437	DQ404493
C. kanchanaburiensis	CBS 11266^T	Thailand	Mushroom	NR_137581	KY106534
C. keroseneae	CECT 13058^T	UK	Aircraft fuel	FJ235128	FJ357698
C. khao-thaluensis	CBS 8535^T	Thailand	Leaf	HQ283374	HQ283383
C. koratica	CBS 10789^T	Thailand	Frass	AB360443	AB354232
C. lessepsii	CBS 9941^T	Panama	Beetle	AY964671	AY640214
C. membranifaciens	CBS 1952^T	India	Urine	AJ606465	U45792
C. michaelii	CBS 9878^T	Panama	Beetle	AY964673	AY520329
C. naeodendra	CBS 6032^T	South Africa	Frass	AY580316	U45759
C. oceani	CBS 11857^T	Atlantic Ocean	Deep-sea coral	NR_156008	GU002284
C. pseudoaaseri	CBS 11170^T	Germany	Blood culture	JN241686	JN241689
C. sinolaborantium	CBS 9940^T	Panama	Beetle	NR_111343	NG_055206
C. songkhlaensis	CBS 10791^T	Thailand	Frass	AB360438	DQ404499
C. spencermartinsiae	CBS 10894^T	Seawater	Florida	FJ008050	FJ008044
C. tallmaniae	CBS 8575^T	French Guiana	Flower	HQ283378	HQ283385
C. tammaniensis	CBS 8504^T	USA	Frass	HQ283375	AF017243
C. taylori	CBS 8508^T	Belize	Sea water	FJ008051	FJ008045
C. temnochilae	CBS 9938^T	Panama	Beetle	AY964678	AY242344
C. trypodendroni	CBS 8505^T	Canada	Beetle	FJ153212	AF017240
C. vaughaniae	CBS 8583^T	French Guiana	Flower	HQ283364	HQ283381
C. vrieseae	CBS 10829^T	Brazil	Bromeliad	FJ755905	EU200785
Yamadazyma akitaensis	CBS 6701^T	Japan	Exudate	DQ409164	U45766
Y. akitaensis	**NYNU 16719**	**China**	**Rotten wood**	**MZ314281**	**MZ314280**
Y. barbieri	CBS 14301^T	Brazil	Sea water	LT547714	LT547716
Y. cocois	VTCC 920004^T	Vietnam	Fruits of the coconut palm	MN764369	MN764369
Y. dushanensis	CBS 13914^T	China	Rotten wood	KM272249	KM272248
Y. endophytica	CBS 14163^T	Thailand	Corn leaf	KT307981	KT307981
Y. epiphylla	CBS 13384^T	Thailand	Rice leaf	LC006082	LC006026
Y. insecticola	CBS 13382^T	Thailand	Frass	LC006081	DQ400379
Y. kitorensis	CBS 14158^T	Japan	Red viscous gel	LC060995	LC060995
Y. laniorum	CBS 14780^T	USA	Bark	KY588337	KY588136
Y. luoyangensis	**NYNU 201023^T**	**China**	**Rotting wood**	**MW365549**	**MW365545**
Y. luoyangensis	**NYNU 201035**	**China**	**Rotting wood**	**MZ318445**	**MZ318422**
Y. mexicana	CBS 7066^T	Mexico	Agria cactus	AB054110	U45797
Y. nakazawae	CBS 6700^T	Japan	Exudate	EU343867	U45748

Species	Strain no.	Locality	Sample	GenBank accession numbers	
				ITS	D1/D2
Y. olivae	CBS 11171^{T}	Greece	Fermenting olive	FJ715432	FJ715430
Y. olivae	**NYNU 167106**	**China**	**Rotting wood**	**MZ314288**	**MZ314282**
Y. olivae	**NYNU 209116**	**China**	**Rotting wood**	**MZ318443**	**MZ318444**
Y. ovata	**NYUN 191125^{T}**	**China**	**Rotting wood**	**MT990560**	**MT990559**
Y. ovata	**NYUN 19130**	**China**	**Rotting wood**	**MZ318424**	**MZ318425**
Y. ovata	**NYUN 19116**	**China**	**Rotting wood**	**MZ318442**	**MZ318423**
Y. paraaseri	**NYNU 1811114^{T}**	**China**	**Rotting wood**	**MK682794**	**MK682805**
Y. paraaseri	**NYNU 181033**	**China**	**Rotting wood**	**MZ318421**	**MZ318460**
Y. paraphyllophila	CBS 9928^{T}	China, Taiwan	Pencil wood leaf	AY559447	AY562397
Y. philogaea	CBS 6696^{T}	South Africa	Soil	AB054107	U45765
Y. phyllophila	CBS 12572^{T}	Thailand	Corn leaf	AB734050	AB734047
Y. riverae	CBS 14121^{T}	Brazil	Rotting wood	KP900044	KP900043
Y. scolyti	CBS 4802^{T}	USA	Frass	EU343807	U45788
Y. siamensis	CBS 12573^{T}	Thailand	Sugarcane leaf	AB734049	AB734046
Y. takamatsuzukensis	CBS 10916^{T}	Japan	Air	AB365470	AB365470
Y. tenuis	CBS 615^{T}	Russia	Beetle	HQ283371	U45774
Y. terventina	CBS 12510^{T}	Italy	Olive oil	JQ247717	JQ247717
Y. triangularis	CBS 4094^{T}	Japan	Tamari soya	EU343869	U45796
Y. tumulicola	CBS 10917^{T}	Japan	Stone chamber	AB365463	AB365463
Y. ubonensis	CBS 12859^{T}	Thailand	Tree bark	NR_155998	AB759913
Scheffersomyces coipomoensis	CBS 8178^{T}	–	–	NR_111424	U45747
Babjeviella inositovora	CBS 8006^{T}	–	–	NR_111018	U45848

MP analysis was run using a heuristic search option of 1,000 search replicates with random-addition of sequences and tree bisection and reconnection (TBR) as the branch-swapping algorithm. Gaps were treated as missing data. Bootstrapping with 1,000 replicates was performed to determine branch support (Felsenstein 1985). Parsimony scores of tree length (TL), consistency index (CI), retention index (RI), and rescaled consistency (RC) were calculated for each generated tree. ML analysis was performed using a GTR site substitution model, including a gamma-distributed rate heterogeneity and a proportion of invariant sites (Guindon et al. 2010). Branch support was evaluated using a bootstrapping method of 1,000 bootstrap replicates (Hillis and Bull 1993). The phylogenies from MP and ML analyses were displayed using Mega7 and FigTree v1.4.3 (Rambaut 2016), respectively. ML and MP bootstrap support values above 50% are shown as first and second positionS above nodes, respectively.

Results

Molecular phylogeny

The alignment based on the combined nuclear dataset (ITS and D1/D2 LSU) included 65 taxa and two outgroup taxa (*Scheffersomyces coipomoensis* and *Babjeviella inositovora*), and was comprised of 1,103 characters including gaps (576 for ITS and 527 for D1/D2 LSU) in the aligned matrix. Of these characters, 351 were constant, 455 variable characters were parsimony-uninformative, and 297 characters were parsimony-

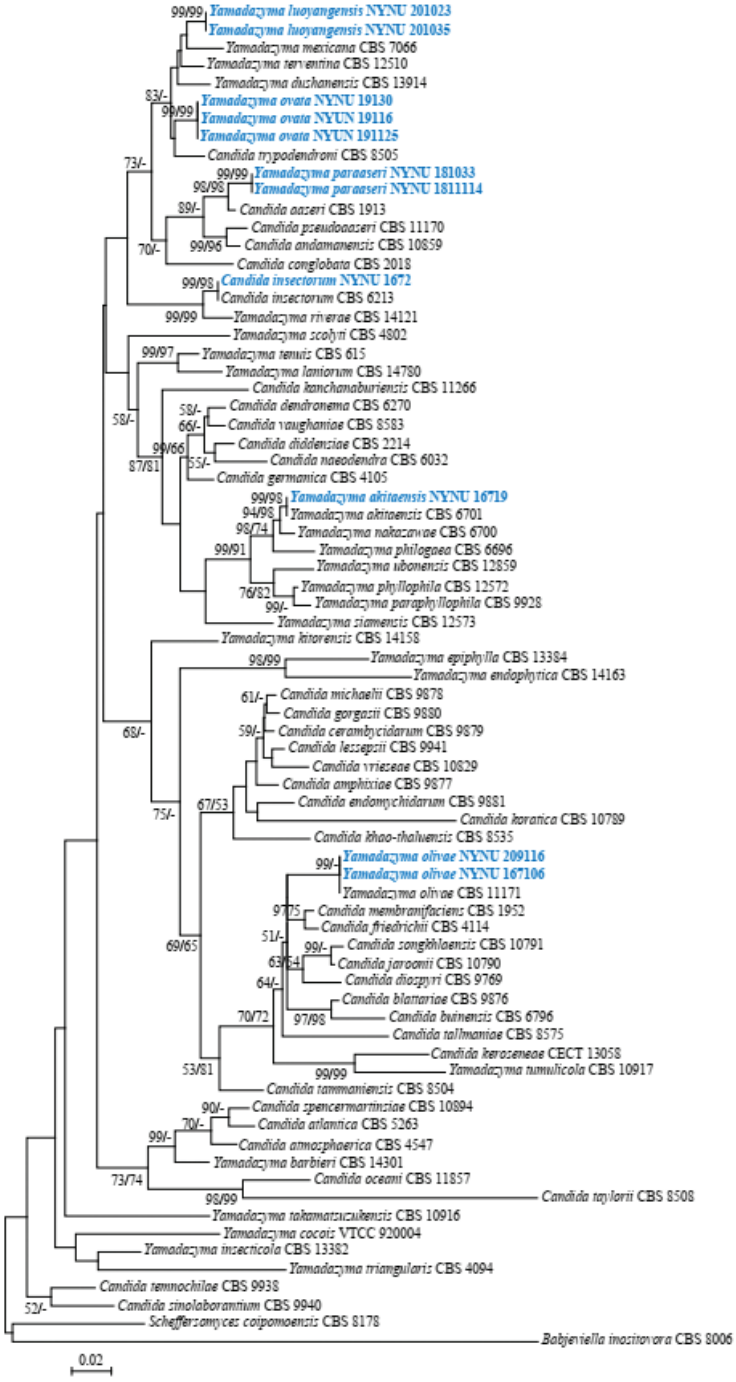

Figure 1. Maximum likelihood phylogenetic tree of *Yamadazyma* inferred from the combined ITS and D1/D2 LSU dataset and rooted with *Scheffersomyces coipomoensis* (CBS 8178) and *Babjeviella inositovora* (CBS 8006). ML and MP bootstrap support values above 50% are respectively shown at the first and second positions. Newly sequenced collections are in blue boldface.

informative. The heuristic search using MP analysis generated the most parsimonious tree (TL = 979, CI = 0.297, RI = 0.653, RC = 0.248). The best model applied in the ML analysis was GTR+I+G. The ML analysis yielded a best scoring tree with a final optimization likelihood value of –11,006.61. Both methods for phylogenetic tree inference resulted in a similar topology. Therefore, only the best scoring PhyML tree is shown with BS and BT values simultaneously in Figure 1.

According to the phylogenetic tree (Figure 1), three known species, *Y. insectorum*, *Y. akitaensis*, and *Y. olivae*, were part of *Yamadazyma*. *Yamadazyma luoyangensis*, *Y. ovata*, and *Y. paraaseri* are new to science based on the distinct and well-supported molecular phylogenetic placement and morphological differences with their closest described relatives (Table 2). Phylogenetically, *Y. luoyangensis* clustered together with *Y. ovata* and other species, including *Y. mexicana*, *Y. terventina*, *Y. dushanensis*, and *C. trypodendroni*, while *Y. paraaseri* was closely related to *C. aaseri* with high bootstrap support (98% ML/98% MP).

Taxonomy

***Yamadazyma luoyangensis* C.Y. Chai & F.L. Hui, sp. nov.**
MycoBank No: 840099
Figure 2

Type. China, Henan Province, Luoyang City, Song County, in rotting wood from a forest park, September 2020, J.Z. Li & Z.T Zhang (holotype NYNU 201023^{T}, culture ex-type CBS 16666, CICC 33509).

Etymology. The species name *luoyangensis* refers to the geographical origin of the type strain of this species.

Description. The cells are ovoid to ellipsoid (2–4 × 3.5–7 μm) and occur singly or in pairs after being placed in YM broth for three days at 25 °C (Figure 2A). Budding is multilateral. After three days of growth on YM agar at 25 °C, the colonies are white to cream-colored, buttery, and smooth, with entire margins. After seven days at 25 °C on a Dalmau plate culture with CM agar, pseudohyphae are formed, but true hyphae are not (Figure 2B). Asci or signs of conjugation are not observed on sporulation media. Glucose, galactose, trehalose, and cellobiose are fermented, but maltose, sucrose, melibiose, lactose, melezitose, raffinose, D-xylose, and inulin are not. Glucose, galactose, D-glucosamine, D-ribose, D-xylose, L-arabinose, D-arabinose, L-rhamnose, sucrose, maltose, trehalose, methyl α-D-glucoside, cellobiose, salicin, arbutin, melezitose, inulin, glycerol, erythritol, ribitol, D-glucitol, D-mannitol, galactitol, D-glucono-1, 5-lactone, 5-keto-D-gluconate, D-gluconate, succinate, citrate, and ethanol are assimilated. No growth is observed in L-sorbose, melibiose, lactose, raffinose, *myo*-inositol, 2-keto-D-gluconate, D-glucuronate, DL-lactate, or methanol. In nitrogen-assimilation tests, growth is present on ethylamine, L-lysine, glucosamine, and D-tryptophan, while growth is absent on nitrate, nitrite, cadaverine, creatine, creatinine, and imidazole. Growth is observed at 35 °C

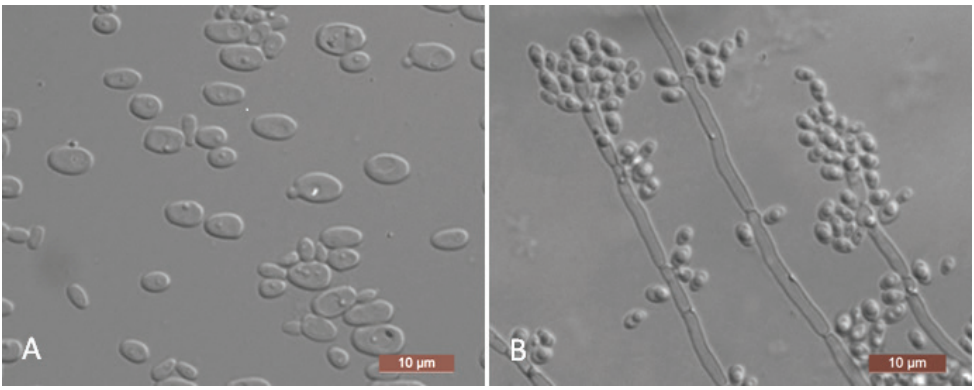

Figure 2. *Yamadazyma luoyangensis* (NYNU 201023, holotype) **A** budding cells after three days in YM broth at 25 °C **B** pseudohyphae on cornmeal agar after seven days at 25 °C. Scale bars: 10 µm.

Table 2. Physiological characteristics of the new *Yamadazyma* species and their closely related taxa.

Characteristics	*Y. luoyangensis*	*Y. mexicana*	*Y. ovata*	*C. trypodendroni*	*Y. paraaseri*	*C. aaseri*
Fermentation of						
D-Glucose	+	+	+	+	-	v
Assimilation of						
L-Sorbose	–	–	+	–	+	s
D-Glucosamine	+	+	+	–	+	–
L-Rhamnose	+	+	–	+	–	–
Melibiose	–	v	+	–	–	–
Lactose	–	+	–	–	+	v
Raffinose	–	+	–	–	–	–
Inulin	+	–	–	–	+	–
Xylitol	+		+	–	–	+
Galactitol	+	v	+	–	–	–
2-Keto-D-Gluconate	–	s	+	+	–	–
Cadaverine	–	n	–	+	–	+
Growth tests						
10%Nacl/5%glucose	+	+	+	v	–	+
Growth at 37 °C	–	+	+	–	+	+

+, positive reaction; –, negative reaction; s, slow positive reaction; v, variable reaction; n, data not available.

but not at 37 °C. Growth in the presence of 10% NaCl with 5% glucose is present, but growth in the presence of 0.01% cycloheximide and 1% acetic acid is absent. Starch-like compounds are not produced. Urease activity and diazonium blue B reactions are negative.

Additional isolate examined. China, Henan Province, Luoyang City, Song County, in rotting wood from a forest park, September 2020, J.Z. Li & Z.T Zhang, NYNU 201035.

GenBank accession numbers. Holotype NYNU 201023^{T} (ITS: MW365549; D1/D2 LSU: MW365545); additional isolate NYNU 201035 (ITS: MZ318445; D1/D2 LSU: MZ318422).

Notes. Two isolates representing *Y. luoyangensis* were resolved in a well-supported clade and are most closely related to *Y. mexicana* (Figure 1). *Yamadazyma luoyangensis* can be distinguished from *Y. mexicana* based on ITS and D1/D2 LSU loci (4/592 in ITS and 10/531 in D1/D2 LSU). Physiologically, *Y. luoyangensis* differs from *Y. mexicana* by its ability to assimilate inulin and 5-keto-D-gluconate and its inability to assimilate lactose, raffinose, and 2-keto-D-gluconate. Additionally, *Y. mexicana* grows at 37 °C, while *Y. luoyangensis* does not (Table 2) (Kurtzman 2011).

***Yamadazyma ovata* C.Y. Chai & F.L. Hui, sp. nov.**
MycoBank No: 840100
Figure 3

Type. China, Henan Province, Luoyang City, Song County, in rotting wood from a forest park, September 2019, J.Z. Li & Z.T Zhang (holotype NYNU 191125^{T}, culture ex-type CBS 16655, CICC 33500).

Etymology. The species name *ovata* refers to the ovoid cell morphology of the type strain.

Description. The cells are ovoid to ellipsoid (2–3 × 3–6.5 μm) and occur singly or in pairs after growth in a YM broth for three days at 25 °C (Figure 3A). Budding is multilateral. After three days of growth on YM agar at 25 °C, the colonies are white to cream-colored, buttery, and smooth with entire margins. After nine days at 25 °C, on a Dalmau plate culture with CM agar, pseudohyphae consisting of elongated cells with lateral buds are formed (Figure 3B). True hyphae are not observed. Asci or signs of conjugation are not observed on sporulation media. Glucose, galactose, and trehalose are fermented, but maltose, sucrose, melibiose, lactose, cellobiose, melezitose, raffinose, D-xylose, and inulin are not. Glucose, galactose, L-sorbose, D-glucosamine, D-ribose, D-xylose, L-arabinose, D-arabinose, sucrose, maltose, trehalose, methyl α-D-glucoside, cellobiose, salicin, melibiose, melezitose, glycerol, erythritol, ribitol, xylitol, D-glucitol, D-mannitol, D- galactitol, D-glucono-1, 5-lactone, 2-keto-D-gluconate, D-gluconate, succinate, citrate, and ethanol are assimilated. No growth is observed in L-rhamnose, lactose, raffinose, inulin, *myo*-inositol, D-glucuronate, DL-lactate, or methanol. In nitrogen-assimilation tests, growth is present on L-lysine, creatine, glucosamine, and D-tryptophan, while growth is absent on nitrate, nitrite, ethylamine, cadaverine, creatinine, or imidazole. Growth is observed at 37 °C, but not at 40 °C. Growth in the presence of 16% NaCl with 5% glucose is present, but growth in the presence of 0.01% cycloheximide and 1% acetic acid is absent. Starch-like compounds are not produced. Urease activity and diazonium blue B reactions are negative.

Additional isolates examined. China, Henan Province, Luoyang City, Song County, in rotting wood from a forest park, September 2019, J.Z. Li & Z.T Zhang, NYNU 19116, NYNU 19130.

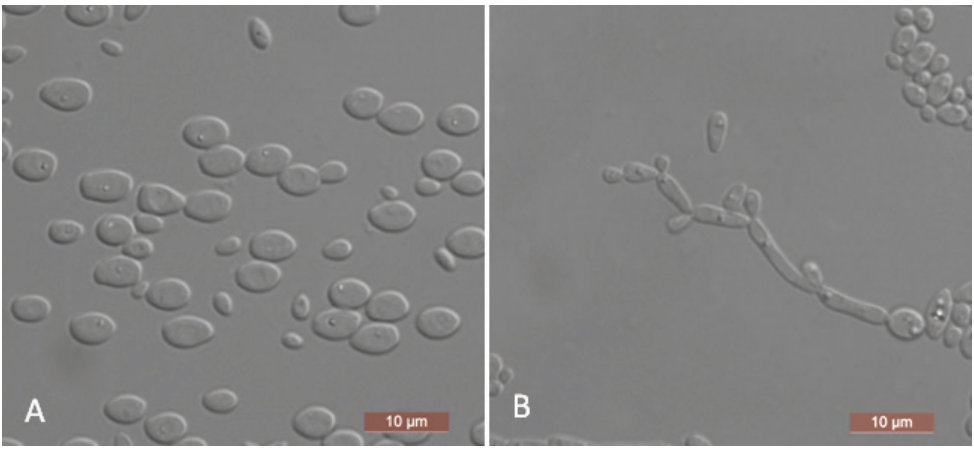

Figure 3. *Yamadazyma ovata* (NYNU 191125, holotype) **A** budding cells after three days in YM broth at 25 °C **B** pseudohyphae on cornmeal agar after nine days at 25 °C. Scale bars: 10 µm.

GenBank accession numbers. Holotype NYNU 191125^{T} (ITS: MT990560; D1/D2 LSU: MT990559); additional isolates NYNU 19116 (ITS: MZ318442; D1/D2 LSU: MZ318423), and NYNU 19130 (ITS: MZ318424; D1/D2 LSU: MZ318425).

Notes. We generated sequences for three isolates of *Y. ovata*, NYNU 191125, NYNU 19116, and NYNU 19130. This new species is phylogenetically most closely related to *C. trypodendroni* (Figure 1). *Yamadazyma ovata* can be distinguished from *C. trypodendroni* based on ITS and D1/D2 LSU loci (15/565 in ITS and 8/532 in D1/D2 LSU). Physiologically, *Y. ovata* can be differentiated from *C. trypodendroni* based on growth in L-sorbose, D-glucosamine, melibiose, and D-glucono-1, 5-lactone, all of which are positive for *Y. ovata* and negative for *C. trypodendroni* (Table 2) (Lachance et al. 2011).

Yamadazyma paraaseri C.Y. Chai & F.L. Hui, sp. nov.

MycoBank No: 840101
Figure 4

Type. China, Yunnan Province, Jinghong City, Mengyang Town, in rotting wood from a tropical rainforest, July 2018, K.F. Liu & Z.W. Xi (holotype NYNU 1811114^{T}, culture ex-type CBS 16010, CICC 33365).

Etymology. The species name *paraaseri* refers to its phylogenetic similarity to *C. aaseri*.

Description. The cells are ovoid to elongate (2–2.5 × 3–8.5 µm) and occur singly or in pairs after being placed in YM broth for three days at 25 °C (Figure 4A). Budding is multilateral. After three days of growth on YM agar at 25 °C, the colonies are white to cream-colored, buttery, and smooth, with entire margins. After two weeks at 25 °C on a Dalmau plate culture with CM agar, pseudohyphae consisting of elongated cells with lateral buds are formed (Figure 4B). True hyphae are not observed. Asci or signs of

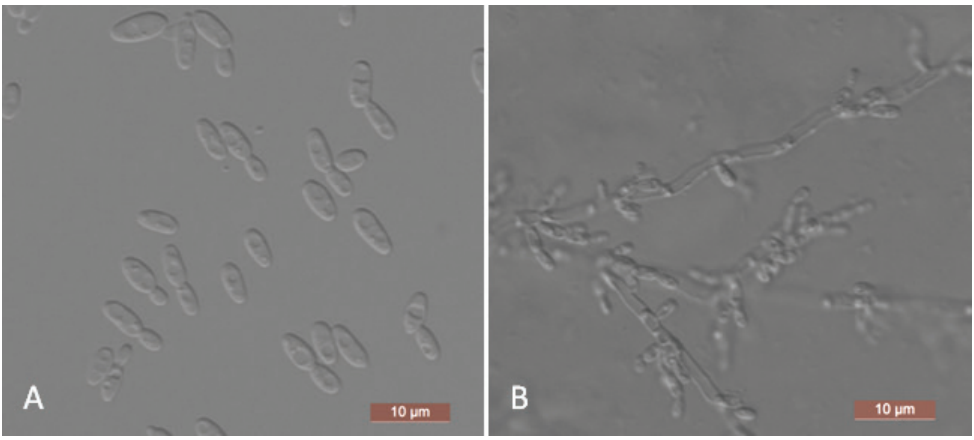

Figure 4. *Yamadazyma paraaseri* (NYNU 1811114, holotype) **A** budding cells after three days in YM broth at 25 °C **B** pseudohyphae on cornmeal agar after two weeks at 25 °C. Scale bars: 10 µm.

conjugation are not observed on sporulation media. Fermentation of sugars is absent. Glucose, galactose, L-sorbose, D-glucosamine, D-ribose, D-xylose, L-arabinose, D-arabinose, sucrose, maltose, trehalose, methyl α-D-glucoside, cellobiose, salicin, arbutin, lactose, melezitose, inulin, glycerol, erythritol, ribitol, D-glucitol, D-mannitol, D-gluconate, DL-lactate, succinate, citrate, and ethanol are assimilated. No growth is observed in L-rhamnose, melibiose, raffinose, xylitol, galactitol, *myo*-inositol, D-glucono-1, 5-lactone, 2-keto-D-gluconate, D-glucuronate, or methanol. In nitrogen-assimilation tests, growth is present on ethylamine, L-lysine, glucosamine, and D-tryptophan, while growth is absent on nitrate, nitrite, cadaverine, creatine, creatinine, and imidazole. Growth is observed at 37 °C but not at 40 °C. Growth in the presence of 0.01% cycloheximide, 10% NaCl with 5% glucose and 1% acetic acid is absent. Starch-like compounds are not produced. Urease activity and diazonium blue B reactions are negative.

Additional isolate examined. China, Yunnan Province, Jinghong City, Mengyang Town, in rotting wood from a tropical rainforest, July 2018, K.F. Liu & Z.W. Xi, NYNU 181033.

GenBank accession numbers. Holotype NYNU 1811114^{T} (ITS: MK682794; D1/D2 LSU: MK682805); additional isolate NYNU 181033 (ITS: MZ318421; D1/D2 LSU: MZ318460).

Notes. Two strains representing *Y. paraaseri* were clustered in a well-supported clade and were phylogenetically related to *C. aaseri* [7]. *Yamadazyma paraaseri* can be distinguished from *C. aaseri* based on ITS and D1/D2 LSU loci (8/573 in ITS and 8/531 in D1/D2 LSU). Physiologically, the ability to assimilate D-glucosamine and inulin and the inability to assimilate xylitol and D-glucono-1, 5-lactone are the primary differences between *Y. paraaseri* and its closest relative, *C. aaseri*. Additionally, *C. aaseri* can grow in 10% NaCl with 5% glucose, while *Y. paraaseri* cannot (Table 2) (Lachance et al. 2011).

Discussion

In this work, six *Yamadazyma* species were identified based on morphology and molecular phylogeny. All species were isolated from rotting wood collected in Henan and Yunnan Provinces, China. *Yamadazyma luoyangensis*, *Y. ovata*, and *Y. paraaseri* are proposed as new species in *Yamadazyma* due to their well-supported phylogenic positions and distinctive physiological traits. Also, three known species of *Yamadazyma*, *Y. insectorum*, *Y. akitaensis*, and *Y. olivae*, were clearly identified by both morphological and molecular approaches.

In the past, methods of species identification of *Yamadazyma* were based only on morphology and physiological characters such as the shape of ascospores and reactions in standard growth and fermentation tests (Billon-Grand 1989). Recent molecular phylogenetic analyses demonstrate that determining species boundaries using only morphology and physiological characters is not possible due to their variability under changing environmental conditions (Kurtzman 2011; Lachance et al. 2011). D1/D2 LSU sequence is an appropriate marker to identify species of *Yamadazyma* species through phylogenetic analysis, as revealed by Kurtzman and Robnett (1998). Many *Yamadazyma* species are described based on a polyphasic approach together with morphological and physiological characterization (Suh et al. 2005; Kurtzman 2007; Imanishi et al. 2008; Nagatsuka et al. 2009; Am-In et al. 2011). However, none to only two substitutions are present in D1/D2 LSU sequences of the ex-type strains of the closest related species within *Yamadazyma*, such as *C. diddensiae* and *C. naeodendra*, *Y. akitaensis* and *Y. nakazawae* as well as *C. jaroonii* and *C. songkhlaensis* (Groenewald et al. 2011; Wang et al. 2015). The ITS sequences show more variation between these closely related well-defined species in contrast to the low nucleotide differences in D1/D2 LSU sequences (Groenewald et al. 2011). Although D1/D2 LSU sequence is still an appropriate region to use for higher level taxon delimitations, it is clear that this sequence alone is not sufficient for species delimitation in the *Yamadazyma* clade. The ITS sequence is thus a good additional marker to obtain a better understanding of relatedness among *Yamadazyma* species.

Yamadazyma species have a worldwide distribution and are isolated from diverse substrates. They can be found in flowers, leaves, fruits, tree bark, mushrooms, sea water, mineral and atmosphere, but most known species appear to exist in rotting wood, insects and their resulting frass (Groenewald et al. 2011; Kurtzman 2011). This clade also includes the clinically significant species *C. aaseri*, *C. conglobata*, *C. pseudoaaseri*, and *Y. triangularis* (Kurtzman 2011; Lachance et al. 2011). These studies expanded our knowledge on the substrates where *Yamadazyma* species can occur, but on the other hand demonstrated the complicated ecological function of this genus. In this study, three known species and three new species were identified from rotting wood in China. Further research will focus on *Yamadazyma* diversity from a wide range of substrates.

Acknowledgements

We sincerely thank Dr. Jing-Zhao Li, Dr. Zheng-Tian Zhang, Dr. Kai-Fang Liu, and Dr. Zhi-Wen Xi for their help with collecting specimens. This project was supported by Grant No. 31570021 from the National Natural Science Foundation of China, China, No. 2018001 from the State Key Laboratory of Motor Vehicle Biofuel Technology, Henan Tianguan Enterprise Group Co., Ltd., China.

References

Am-In S, Limtong S, Yongmanitchai W, Jindamorakot S (2011) *Candida andamanensis* sp. nov., *Candida laemsonensis* sp. nov. and *Candida ranongensis* sp. nov., anamorphic yeast species isolated from estuarine waters in a Thai mangrove forest. International Journal of Systematic and Evolutionary Microbiology 61: 454–461. https://doi.org/10.1099/ijs.0.022038-0

Billon-Grand GA (1989) A new ascosporogenous yeast genus: *Yamadazyma* gen. nov. Mycotaxon 35: 201–204.

Burgaud G, Arzur D, Sampaio JP, Barbier G (2011) *Candida oceani* sp. nov., a novel yeast isolated from a mid-atlantic ridge hydrothermal vent (-2300 meters). Antonie van Leeuwenhoek 100: 75–82. https://doi.org/10.1007/s10482-011-9566-1

Burgaud G, Coton M, Jacques N, Debaets S, Maciel NOP, Rosa CA, Gadanho M, Sampaio JP, Casaregola S (2016) *Yamadazyma barbieri* f.a. sp. nov., an ascomycetous anamorphic yeast isolated from a Mid-Atlantic Ridge hydrothermal site (-2300 m) and marine coastal waters. International Journal of Systematic and Evolutionary Microbiology 66: 3600–3606. https://doi.org/10.1099/ijsem.0.001239

Ciafardini G, Zullo BA, Antonielli L, Corte L, Roscini L, Cardinali G (2013) *Yamadazyma terventina* sp. nov., a yeast species of the *Yamadazyma* clade from Italian olive oils. International Journal of Systematic and Evolutionary Microbiology 63: 372–376. https://doi.org/10.1099/ijs.0.045898-0

Crous PW, Gams W, Stalpers JA, Robert V, Stegehuis G (2004) MycoBank: An online initiative launch mycology into the 21st century. Studies in Mycology 50: 19–22.

Darriba D, Taboada GL, Doallo R, Posada D (2012) jModelTest 2: more models, new heuristics and parallel computing. Nature Methods 9: e772. https://doi.org/10.1038/nmeth.2109

Felsenstein J (1985) Confidence limits on phylogenies: an approach using the bootstrap. Evolution 39: 783–791. https://doi.org/10.1111/j.1558-5646.1985.tb00420.x

Groenewald M, Robert V, Smith MT (2011) The value of the D1/D2 and internal transcribed spacers (ITS) domains for the identification of yeast species belonging to the genus *Yamadazyma*. Persoonia 26: 40–46. https://doi.org/10.3767/003158511X559610

Guindon S, Dufayard JF, Lefort V, Anisimova M, Hordijk W, Gascuel O (2010) New algorithms and methods to estimate maximum-likelihood phylogenies: assessing the performance of PhyML 3.0. Systematic Biology 59: 307–321. https://doi.org/10.1093/sysbio/syq010

Haase MAB, Kominek J, Langdon QK, Kurtzman CP, Hittinger CT (2017) Genome sequence and physiological analysis of *Yamadazyma laniorum* f.a. sp. nov. and a reevaluation of the apocryphal xylose fermentation of its sister species, *Candida tenuis*. FEMS Yeast Research 17: fox019. https://doi.org/10.1093/femsyr/fox019

Hillis DM, Bull JJ (1993) An empirical test of bootstrapping as a method for assessing confidence in phylogenetic analysis. Systematic Biology 42: 182–192. https://doi.org/10.1093/sysbio/42.2.182

Imanishi Y, Jindamorakot, S, Mikata K, Nakagiri A, Limtong S, Potacharoen W, Tanticharoen M, Nakase T (2008) Two new ascomycetous anamorphic yeast species related to *Candida friedrichii-Candida jaroonii* sp. nov., and *Candida songkhlaensis* sp. nov. isolated in Thailand. Antonie van Leeuwenhoek 94: 267–276. https://doi.org/10.1007/s10482-008-9242-2

Jindamorakot S, Am-In S, Kaewwichian R, Limtong S (2015) *Yamadazyma insecticola* f.a., sp. nov. and *Yamadazyma epiphylla* f.a., sp. nov., two novel yeast species. International Journal of Systematic and Evolutionary Microbiology 65: 1290–1296. https://doi.org/10.1099/ijs.0.000100

Junyapate K, Jindamorakot, S, Limtong S (2014) *Yamadazyma ubonensis* f.a., sp. nov., a novel xylitol-producing yeast species isolated in Thailand. Antonie van Leeuwenhoek 105: 471–480. https://doi.org/10.1007/s10482-013-0098-8

Kaewwichian R, Yongmanitchai W, Kawasaki H, Wang PH, Yang SH, Limtong S (2013) *Yamadazyma siamensis* sp. nov., *Yamadazyma phyllophila* sp. nov. and *Yamadazyma paraphyllophila* sp. nov., three novel yeast species isolated from phylloplane in Thailand and Taiwan. Antonie van Leeuwenhoek 103: 777–788. https://doi.org/10.1007/s10482-012-9860-6

Katoh K, Rozewicki J, Yamada KD (2019) MAFFT online service: Multiple sequence alignment, interactive sequence choice and visualization. Briefings in Bioinformatics 20: 1160–1166. https://doi.org/10.1093/bib/bbx108

Khunnamwong P, Limtong S (2016) *Yamadazyma endophytica* f.a. sp. nov., an ascomycetous yeast species isolated from leaf tissue. International Journal of Systematic and Evolutionary Microbiology 66: 2717–2723. https://doi.org/10.1099/ijsem.0.001113

Kurtzman CP (2007) New anamorphic yeast species: *Candida infanticola* sp. nov., *Candida polysorbophila* sp. nov., *Candida transvaalensis* sp. nov. and *Trigonopsis californica* sp. nov. Antonie van Leeuwenhoek 92: 221–231. https://doi.org/10.1007/s10482-007-9150-x

Kurtzman CP (2011) *Yamadazyma* Billon-Grand (1989). In: Kurtzman CP, Fell JW, Boekhout T (Eds) The Yeasts – a Taxonomic Study, 5th edn, vol. 2. Elsevier, Amsterdam, 919–925. https://doi.org/10.1016/B978-0-444-52149-1.00081-1

Kurtzman CP, Robnett CJ (1989) Identification and phylogeny of ascomycetous yeasts from analysis of nuclear large subunit (26S) ribosomal DNA partial sequences. Antonie van Leeuwenhoek 73: 331–371. https://doi.org/10.1023/A:1001761008817

Kurtzman CP, Suzuki M (2010) Phylogenetic analysis of ascomycete yeasts that form coenzyme Q-9 and the proposal of the new genera *Babjeviella*, *Meyerozyma*, *Millerozyma*, *Priceomyces*, and *Scheffersomyces*. Mycoscience 51: 2–14. https://doi.org/10.1007/S10267-009-0011-5

Kurtzman CP, Fell JW, Boekhout T, Robert V (2011) Methods for isolation, phenotypic characterization and maintenance of yeasts. In: Kurtzman CP, Fell JW, Boekhout T (Eds) The

Yeasts – a Taxonomic Study, 5th edn, vol. 1. Elsevier, Amsterdam, 87–110. https://doi.org/10.1016/B978-0-444-52149-1.00007-0

Kumar S, Stecher G, Tamura K (2016) MEGA7: molecular evolutionary genetics analysis version 7.0 for bigger datasets. Molecular Biology and Evolution 33: 1870–1874. https://doi.org/10.1093/molbev/msw054

Lopes MR, Ferreira MC, Carvalho TFC, Pagnocca FC, Chagas RA, Morais PB, Rosa LH, Lachance MA, Rosa CA (2015) *Yamadazyma riverae* sp. nov., a yeast species isolated from plant materials. International Journal of Systematic and Evolutionary Microbiology 65: 4469–4473. https://doi.org/10.1099/ijsem.0.000597

Lachance MA, Boekhout T, Scorzetti G, Fell JW, Kurtzman CP (2011) *Candida* Berkhout (1923). In: Kurtzman CP, Fell JW, Boekhout T (Eds) The Yeasts – a Taxonomic Study, 5th edn, vol. 2. Elsevier, Amsterdam, 987–1279. https://doi.org/10.1016/B978-0-444-52149-1.00090-2

Maksimova IA, Glushakova AM, Thanh VN, Kachalkin AV (2020) *Yamadazyma cocois* f.a., sp. nov., an ascomycetous yeast isolated from coconuts. International Journal of Systematic and Evolutionary Microbiology 70: 3491–3496. https://doi.org/10.1099/ijsem.0.004203

Nagatsuka Y, Kiyuna T, Kigawa R, Sano C, Miura S, Sugiyama J (2009) *Candida tumulicola* sp. nov. and *Candida takamatsuzukensis* sp. nov., novel yeast species assignable to the *Candida membranifaciens* clade, isolated from the stone chamber of the Takamatsu-zuka tumulus. International Journal of Systematic and Evolutionary Microbiology 59: 186–194. https://doi.org/10.1099/ijs.0.65830-0

Nagatsuka Y, Ninomiya S, Kiyuna T, Kigawa R, Sano C, Sugiyama J (2016) *Yamadazyma kitorensis* f.a., sp. nov. and *Zygoascus biomembranicola* f.a., sp. nov., novel yeasts from the stone chamber interior of the Kitora tumulus, and five novel combinations in *Yamadazyma* and *Zygoascus* for species of *Candida*. International Journal of Systematic and Evolutionary Microbiology 66: 1692–16704. https://doi.org/10.1099/ijsem.0.000930

Nakase T, Jindamorakot S, Ninomiya S, Imanishi Y, Kawasaki H, Potacharoen W (2008) *Candida kanchanaburiensis* sp. nov., a new ascomycetous yeast species related to *Pichia nakazawae* isolated in Thailand. Journal of General and Applied Microbiology 54: 259–265. https://doi.org/10.2323/jgam.54.259

Rambaut A (2016) FigTree, version 1.4.3. University of Edinburgh, Edinburgh.

Suh SO, Nguyen NH, Blackwell M (2005) Nine new *Candida* species near *C. membranifaciens* isolated from insects. Mycology Research 109: 1045–1056. https://doi.org/10.1017/S0953756205003254

Wang Y, Ren YC, Li Y, Hui FL (2015) Molecular phylogeny and taxonomy of *Yamadazyma dushanensis* f.a., sp. nov., a cellobiose-fermenting yeast species from China. Current Microbiology 71: 268–273. https://doi.org/10.1007/s00284-015-0847-1

White TJ, Bruns TD, Lee S, Taylor J (1990) Amplification and direct sequencing of fungal ribosomal RNA genes for phylogenetics. In: Innis MA, Gelfand DH, Sninsky JJ, White TJ (Eds) PCR protocols, a guide to methods and applications. Academic, San Diego, 315–322. https://doi.org/10.1016/B978-0-12-372180-8.50042-1

MycoKeys 83: 85–103 (2021)
doi: 10.3897/mycokeys.83.71405
https://mycokeys.pensoft.net

RESEARCH ARTICLE

A peer-reviewed open-access journal
MycoKeys
Launched to accelerate biodiversity research

Two new psathyrelloid species of *Coprinopsis* (Agaricales, Psathyrellaceae) from China

Gu Rao[1], Dan Dai[1], Hui-Nan Zhao[1], Yi Liang[1], Yu Li[1], Bo Zhang[1]

1 *Engineering Research Center of Edible and Medicinal Fungi, Ministry of Education, Jilin Agricultural University, Changchun, Jilin 130118, Changchun, China*

Corresponding authors: Yu Li (yuli996@126.com), Bo Zhang (zhangbofungi@126.com)

Academic editor: María P. Martín | Received 10 July 2021 | Accepted 20 August 2021 | Published 8 September 2021

Citation: Rao G, Dai D, Zhao H-N, Liang Y, Li Y, Zhang B (2021) Two new psathyrelloid species of *Coprinopsis* (Agaricales, Psathyrellaceae) from China. MycoKeys 83: 85–103. https://doi.org/10.3897/mycokeys.83.71405

Abstract

In this study, *Coprinopsis jilinensis* and *Coprinopsis pusilla* were introduced, based on their morphological characteristics, the internal transcribed spacer (ITS) and large subunit ribosomal (LSU) region sequences of nrDNA. These new psathyrelloid species were found in Jilin Province, China. *Coprinopsis jilinensis* has brown pileus, utriform pleurocystidia, brown, smooth, dextrinoid basidiospores and tiny pore. It mainly grows on humus. *Coprinopsis pusilla* has small basidiomata, greyish-white pileus, thick and distinct veil at edges, subcolourless and verrucose basidiospores. It is poreless and it grows on the decaying wood of broad-leaved trees. Both of them belong to the *C.* sect. *Melanthinae*. A supplementary description of *C.* sect. *Melanthinae* was given in combination with the newly-discovered taxa and an identification key to the fourteen psathyrelloid species of *Coprinopsis* is provided. *Coprinopsis* sect. *Canocipes* and *C.* sect. *Quartoconatae* were evaluated and the phylogenetic position of the psathyrelloid species of *Coprinopsis* was discussed. *Psathyrella subagraria*, as a confusing species, was also discussed in this study.

Keywords

Asia, molecular systematics, morphology, new taxa, taxonomy

Introduction

Coprinoid mushrooms are fascinating fungal taxa with the characteristic of deliquescent lamellae. *Coprinus* sensu lato is not monophyletic (Johnson and Vilgalys 1998; Hopple and Vilgalys 1999; Park et al. 1999a, 1999b; Moncalvo et al. 2002). Based on molecular studies, Redhead et al. (2001) subdivided *Coprinus* s. l. into four genera,

Coprinus Pers. (Agaricaceae), *Corinopsis* P. Karst. (Psathyrellaceae), *Coprinellus* P. Karst. (Psathyrellaceae) and *Parasola* Redhead, Vilgalys & Hopple (Psathyrellaceae). Combined with anatomical characteristics, 100 species were divided from *Coprinus* s. l. into *Coprinopsis*, which were then widely accepted. The subdivision of the *Coprinus* s. l. was full of controversies at the time. Noordeloos et al. (2005) argued that there were many unresolved problems in the phylogeny and it was too early to subdivide it into four genera.

Schafer (2010) used the classification system of Redhead et al. (2001) to divide *Coprinopsis* into five sections, *Atramentarii*, *Lanatuli*, *Alachuani*, *Narcotici* and *Nivei*, corresponding to *Coprinus* sect. *Atramentarii* (Fries 1836), *C.* sect. *Lanatuli* (Fries 1836), *C. C.* subsect. *Alachuani* (Singer 1949), *C. C.* subsect. *Narcotici* (Uljé and Noordeloos 1993) and *C. C.* subsect. *Nivei* (Citerin 1992), but the traditional section *C.* sect. *Picacei* (Kauffman 1918) was not covered. Wächter and Melzer (2020) subdivided the genus *Coprinopsis* into 20 sections according to the subclades of the phylogenetic tree (*Cinereae*, *Filamentiferae*, *Melanthinae*, *Alopeciae*, *Xenobiae*, *Phlyctidosporae*, *Krieglsteinerorum*, *Erythrocephalae*, *Geesteranorum*, *Mitraesporae*, *Radiatae*, *Subniveae* and *Canocipes*).

Coprinopsis is a worldwide fungal taxon that includes some well-known species, such as *C. atramentaria*, characterised by hyphal pileus cuticle, abundant powdery to floccose veil covering the whole pileus, coprophilous, growing in a terrestrial or lignicolous habitat (Redhead et al. 2001). According to Kirk et al. (2008), 200 species of *Coprinopsis* were known so far the world over. At the time of submission, there are 228 records of *Coprinopsis* in Index Fungorum (www.indexfungorum.org), including synonyms, varieties, forms and names. There are few studies on *Coprinopsis* in China. According to the report of Huang (2019), there were only 16 species of *Coprinopsis* in China, amongst which eight species were newly recorded in China and reported in 2019. Based on traditional morphology, sequence data and phylogenetic analyses, two new species of *Coprinopsis* were found in Jilin Province, China. They both belong to the *C.* sect. *Melanthinae* and will be reported as follows.

Materials and methods

Collecting and morphological studies

The fresh basidiomata were collected from the Red Leaves Valley in Hanchongling (approximate 43°02'1.67"N, 127°59'36.55"E), Dunhua City, Yanbian Korean Autonomous Prefecture, Jilin Province, China. After dried at 45 °C for 1−2 days, they were stored in the Herbarium of Mycology of Jilin Agricultural University (HMJAU). Photos of fresh basidiomata were taken in the field. The macromorphology was observed from fresh basidiomata and the observation of microstructure was based on dry specimens under a light microscope (LEICA DM1000). The mainly used reagents are 5% potassium hydroxide (KOH) solution, 1% Congo Red and Melzer's Reagent.

The morphological description referred to Largent et al. (1977 and 1978). The surface of the basidiospores was observed and photographed under a scanning electron microscope (SEM) (Hitachi SU8000) at 2.0 kV, with a working distance of 8 mm. The following symbols were used in the description: [n/m/p] indicates that 'n' randomly selected basidiospores from 'm' basidiomata of 'p' collections were measured, 'avl' means the average length of basidiospores, except the extreme values, 'avw' means the average width of the basidiospores, except the extreme values, 'Q' represents the quotient of the length and width of a single basidiospores in side view, 'Q_m' refers to the average Q value of all basidiospores ± standard deviation. Dimensions for basidiospores are given as (a) b–c (d). The range of b–c contains a minimum of 90% of the measured values. Extreme values (i.e. a and b) are given in parentheses.

Research methods of molecular systematics

The total DNA of the specimens was extracted by the new plant genomic DNA extraction kit from Jiangsu Kangwei Century Biotechnology Company Limited. The amplification primers of LSU nrDNA (LSU) were LROR and LR5 (Vilgalys and Hester 1990), the ITS nrDNA (ITS) regions were ITS1 and ITS4 (White et al. 1990; Gardes and Bruns 1993). The amplification reactions were carried out in a 25 μl system and the total amount of the reactions was as follows: ddH_2O 13.5 μl, 10×Taq Buffer 5 μl, 10 mM dNTPs 1 μl, 10 mM upstream primer 1 μl, 10 mM downstream primer 1 μl, DNA sample 2 μl, 2 U/μm Taq Polymerase 1.5 μl. The cycle parameters were as follows: 4 min at 94 °C for 1 cycle; 40 s at 94 °C, 40 s at 54 °C, 1 min at 72 °C for 35 cycles; 10 min at 72 °C for 1 cycle; storage at 4 °C. The PCR product was subjected to 0.5% agarose gel electrophoresis to test strips. The sequencing work was entrusted to Shenggong Bioengineering (Shanghai) Company Limited and the sequencing results were clipped with Seqman 7.1.0 (Swindell and Plasterer 1997) and then submitted to GenBank (https://www.ncbi.nlm.nih.gov/genbank/). The newly-obtained sequences are shown in Table 1. The sequences of relevant taxa were downloaded from GenBank and from the related articles (Larsson and Örstadius 2008; Nagy et al. 2010; Nagy 2012; Örstadius et al. 2015; Crous 2017; Melzer et al. 2017).

The 'auto' strategy and normal alignment mode of MAFFT (Katoh et al. 2005) were used for Sequence alignment and Gblocks (Castresana et al. 2000; Talavera and Castresana 2007) was used to obtain the conservative segments of sequences with the following parameters: the minimum number of sequences for a conserved/flank

Table 1. Taxa, vouchers and sequence accession numbers of newly generated sequences.

Taxon	Voucher	ITS nrDNA	LSU nrDNA
Coprinopsis pusilla	HMJAU 58779	MZ398012	MZ398067
C. pusilla	HMJAU 58780	MZ398013	MZ398068
C. pusilla	HMJAU 58781	MZ398014	MZ398069
C. jilinensis	HMJAU 58782	MZ398015	MZ398070
C. jilinensis	HMJAU 58783	MZ398016	MZ398071

Table 2. The best models, based on ModelFinder and MegaX.

	BI	ML	NJ
ITS nrDNA	SYM+G4	TVMe+G4	T92+G5
LSU nrDNA	K2P+I	TIM2+F+I	K2+G5

position (12/12), the maximum number of contiguous non-conserved positions (8), minimum length of a block (10) and allowed gap positions (with half). ModelFinder (Kalyaanamoorthy et al. 2017) was used to select the best-fit models using the Bayesian Information Criterion (BIC). The Maximum Likelihood (ML) analyses were performed in IQTree 1.6.8 (Nguyen et al. 2015) and the Bayesian Inference phylogenies were performed in MrBayes 3.2.6 (Ronquist et al. 2012) (2 parallel runs, 2000000 generations), in which the initial 25% of sampled data were discarded as burn-in. The above software was integrated into PhyloSuite 1.2.2 (Zhang et al. 2020). The neighbour-joining (NJ) tree was carried out in Mega X (Kumar et al. 2018). The ML and NJ trees were evaluated by bootstrap analysis with 1000 replicates and the best models are shown in Table 2.

Results

BLASTn results

In the BLASTn alignment, based on ITS sequences, *Coprinopsis pusilla* and *C. melanthina* KC992961 (Örstadius et al. 2015) had the highest sequence identities (94.92%–95.26%), with 34–36 base differences. *Corpinopsis jilinensis* and *C. uliginicola* MG712323 (Zhang 2019) had the highest sequence identity (99.27%), with five base differences. The sequence identities between *C. jilinensis* and *C. uliginicola* KC992960 Type (Örstadius et al. 2015) were 93.98%–94.35%, with 39–42 base differences. In BLASTn alignment, based on LSU sequences, *C. pusilla* and *C. melanthina* KC992961 (Örstadius et al. 2015) had the highest sequence identities (99.14%–99.25%), with 7–8 base differences. *Corpinopsis jilinensis* and *C. uliginicola* KC992960 Type (Örstadius et al. 2015) had the highest sequence identity (99.13%), with eight base differences.

Phylogenetic analyses

After Gblocks clipping, the ITS data matrix included 31 sequences of 588 nucleotide sites from 16 taxa and the data matrix included 20 sequences of 921 nucleotide sites from 14 taxa (gaps included). In the ITS and LSU phylogenetic trees (Figs 1, 2), *Coprinopsis pusilla* and *C. jilinensis* both belong to *C.* sect. *Melanthinae*. *Coprinopsis pusilla* and *C. melanthina* formed a sister clade, *C. jilinensis* and *C. uliginicola* formed a sister clade, both of which were strongly supported. In the phylogenetic trees, based on

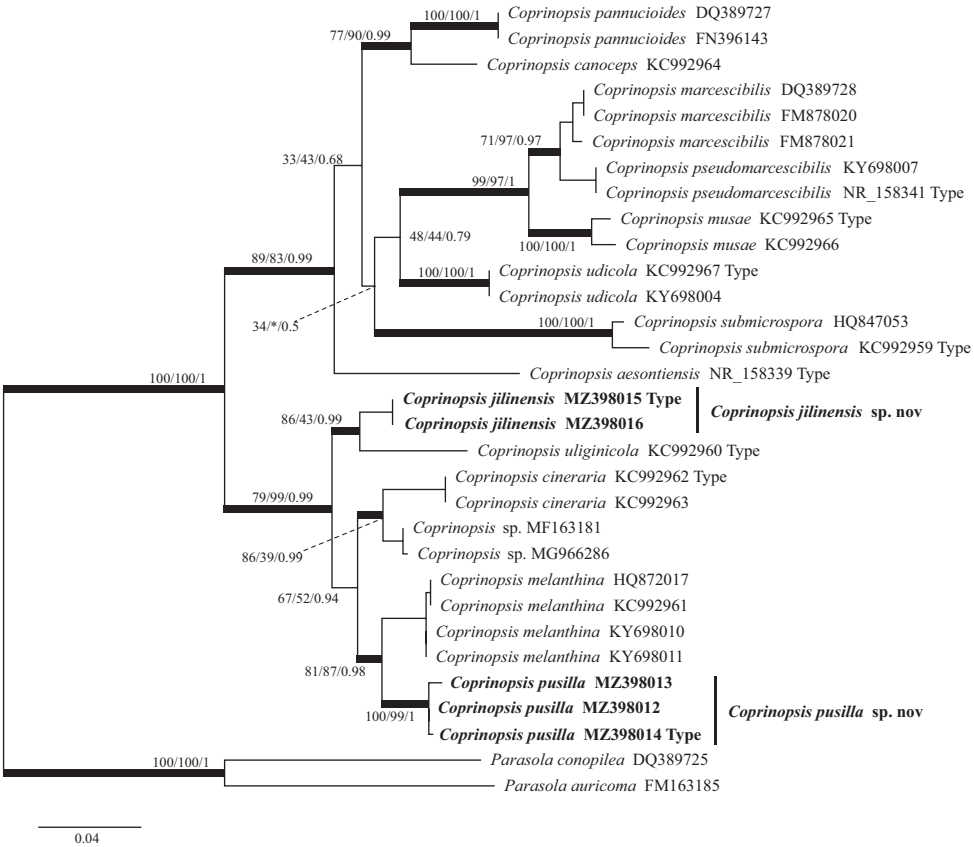

Figure 1. The phylogenetic tree of *Coprinopsis* by ITS nrDNA, based on the Maximum Likelihood method (ML). The three values of internal nodes respectively represent Maximum Likelihood bootstrap (MLBP)/neighbour-joining bootstrap (NJBP)/Bayesian posterior probability (BIPP). The thick node indicates the significantly-supported branch in at least two analyses (MLBP ≥ 70, NJBP ≥ 70, BIPP ≥ 95%). The GenBank accession number is marked after the species name. At the same time, the sequence from the type specimen is also marked at the end. Two new species from China are expressed in bold font and *Parasola conopilea* (Fr.) Örstadius & E. Larss and *P. auricoma* (Pat.) Redhead, Vilgalys & Hopple are selected as the outgroups.

ITS sequences (Fig. 1), *C. submicrospora* and *C. marcescibilis*/*C. pseudomarcescibilis*/*C. musae*/*C. udicola* formed a sister clade in the ML and BI trees (MLBP/BIPP: 34/0.5), but *C. submicrospora* and *C. canoceps*/*C. pannucioides* formed a sister clade in the NJ tree (NJBP: 39). In the phylogenetic trees, based on LSU nrDNA sequences (Fig. 2), *C. marcescibilis* and *C. pseudomarcescibilis* formed a sister clade with strong support in the NJ and BI trees (NJBP/BIPP: 99/0.8). However, in the ML tree, *C. marcescibilis* formed a sister clade with all taxa, except the outgroups (MLBP: 100) and *C. pseudomarcescibilis* formed a sister clade with all taxa, except the outgroups and *C. marcesci-*

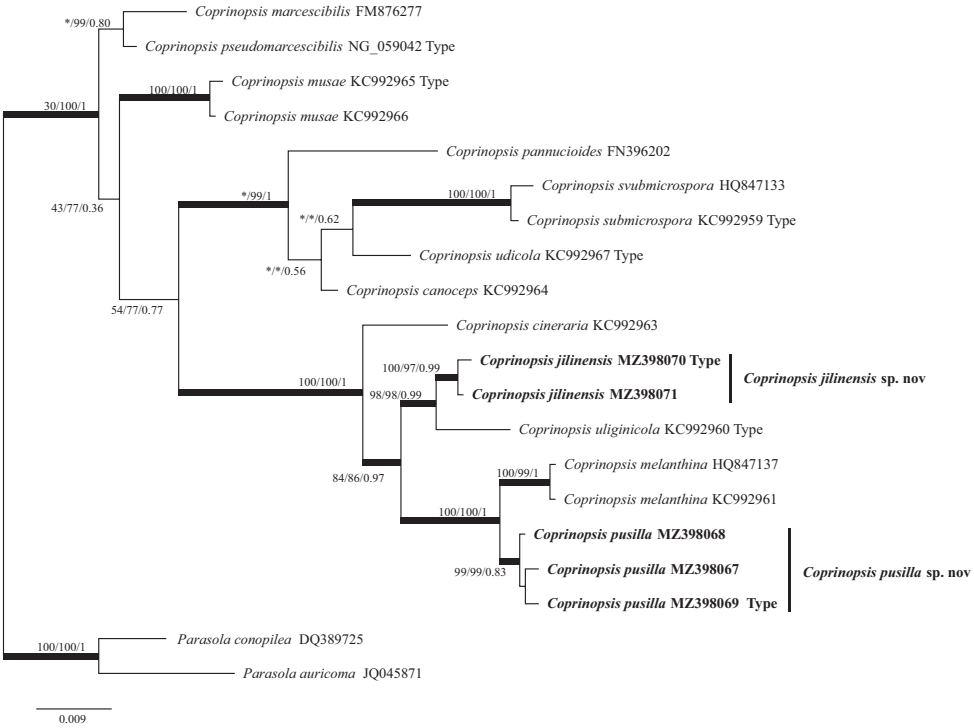

Figure 2. The phylogenetic tree of *Coprinopsis* by LSU nrDNA, based on Bayesian Inference (BI). The three values of internal nodes respectively represent Maximum Likelihood bootstrap (MLBP)/ neighbour-joining bootstrap (NJBP)/Bayesian posterior probability (BIPP). The thick node indicates the significantly-supported branch in at least two analyses (MLBP ≥ 70, NJBP ≥ 70, BIPP ≥ 95%). The GenBank accession number is marked after the species name. At the same time, the sequence from the type specimen is also marked at the end. Two new species from China are expressed in bold font and *Parasola conopilea* (Fr.) Örstadius & E. Larss and *P. auricoma* (Pat.) Redhead, Vilgalys & Hopple are selected as the outgroups.

bilis (MLBP: 30). In the analyses, based on different methods, the sister branch relationships of *C. pannucioides*, *C. submicrospora*, *C. uliginicola* and *C. canoceps* were different. In the BI tree, *C. pannucioides* and *C. submicrospora*/*C. udicola*/*C. canoceps* formed a sister clade with strong support (BIPP: 1), *C. canoceps* and *C. submicrospora*/*C. udicola* formed a sister clade (BIPP: 0.56), *C. submicrospora* and *C. udicola* formed a sister clade (BIPP: 0.62). In the ML tree, *C. submicrospora* and *C. udicola*/*C. canoceps*/*C. pannucioides* formed a sister clade with strong support (MLBP: 98), *C. udicola* formed a sister clade with *C. pannucioides*/*C. canoceps* (MLBP: 30) and *C. pannucioides* and *C. canoceps* formed a sister clade (MLBP: 50). In the NJ tree, *C. pannucioides* and *C. submicrospora*/*C. udicola*/*C. canoceps* formed a sister clade with strong support (NJBP: 99), *C. submicrospora* formed a sister clade with *C. udicola* /*C. canoceps* (NJBP: 38) and *C. udicola* and *C. canoceps* formed a sister clade (NJBP: 41).

Taxonomy

***Coprinopsis jilinensis* G. Rao, H.N. Zhao, B. Zhang & Y. Li, sp. nov.**
MycoBank No: 840297
Figures 3, 4, 7C, D

Typification. China. Red Leaves Valley in Hanchongling, Dunhua City, Yanbian Korean Autonomous Prefecture, Jilin Province, 22 August 2019, G. Rao & H.N Zhao (HMJAU 58782 Holotype!).

Sequences ex holotype. MZ398015 (ITS nrDNA), MZ398070 (LSU nrDNA).

Etymology. The epithet "*jilinensis*" refers to this species that was first discovered in Jilin Province, China.

Description. Basidiomata small to medium-sized. Pileus 33–52 mm broad, conical to convex, dark brown or clay brown, densely covered with white hairs, not sticky when dry or wet, not hygrophanous, veil remnants flocculent at edges. Lamellae close or crowded, grey-white to fleshy brown, brownish-black after drying, sinuate or adnexed, not the same length and width, edges slightly toothed, concolorous, not deliquescent. Stipe 80–95 × 5–9 mm, white to milky white, cylindrical, down slightly rough, fibrous, a little fragile, hollow, the base with white mycelium, dense or sparse, close to the stipe surface covered with brownish-yellow pubescent, no ring. Spore print without record.

Basidiospores [60, 2, 2] (8)8.5–10(10.2) × 4.5–5.9 (6) μm, avl = 9.1 μm, avw = 5.2 μm, Q = (1.62) 1.63–1.96 (2.02), Q_m = 1.77 ± 0.09, oval to long oval, brown, brownish-yellow or dark brown in 5% KOH solution, smooth, thick wall, dextrinoid, apical with small pores, 1–2 μm. Basidia 17–30 (39) × 8–10 (13) μm, clavate, 4-sterigmate up to 3–4 μm long, 2–3 sterigmate occasional. Pleurocystidia (30) 33–59 (60) × (11) 12–21 (23) μm, utriform and lageniform, sparse, smooth, hyaline. Cheilocystidia 27–56 × (10) 11–20 (22) μm, utriform and lageniform, smooth, hyaline, crowded in hymenium. Lamellar edge fertile. Pileipellis a cutis, up to 100 μm thick, hyphae (35) 42–111 (148) × (6) 7–34 (35) μm, ovoid, subcylindrical, with brownish-yellow to dark brown pigment, thick wall, encrusting pigment on the outer hyphae. Veil hyphae (5) 6–30 (33) μm wide, present dark encrusting pigment, thick wall, colourless to light yellow, cylindrical and subcylindrical. Stipitipellis a cutis, hyphae (5) 6–22 (32) μm diam., ovoid and subcylindrical, pale brown, with encrusting pigment, thick wall. Clamp connections present in all tissues.

Habitat and distribution. On humus of broad-leaved forest or coniferous and broad-leaved mixed forests in autumn.

Additional specimens examined. China. Red Leaves Valley in Hanchongling, Dunhua City, Yanbian Korean Autonomous Prefecture, Jilin Province, 14 September 2019, Gu Rao (HMJAU 58783).

Notes. *Coprinopsis jilinensis* is characterised by its small to medium-sized basidiomata, brown pileus with white hairs, smooth and dextrinoid basidiospores with small

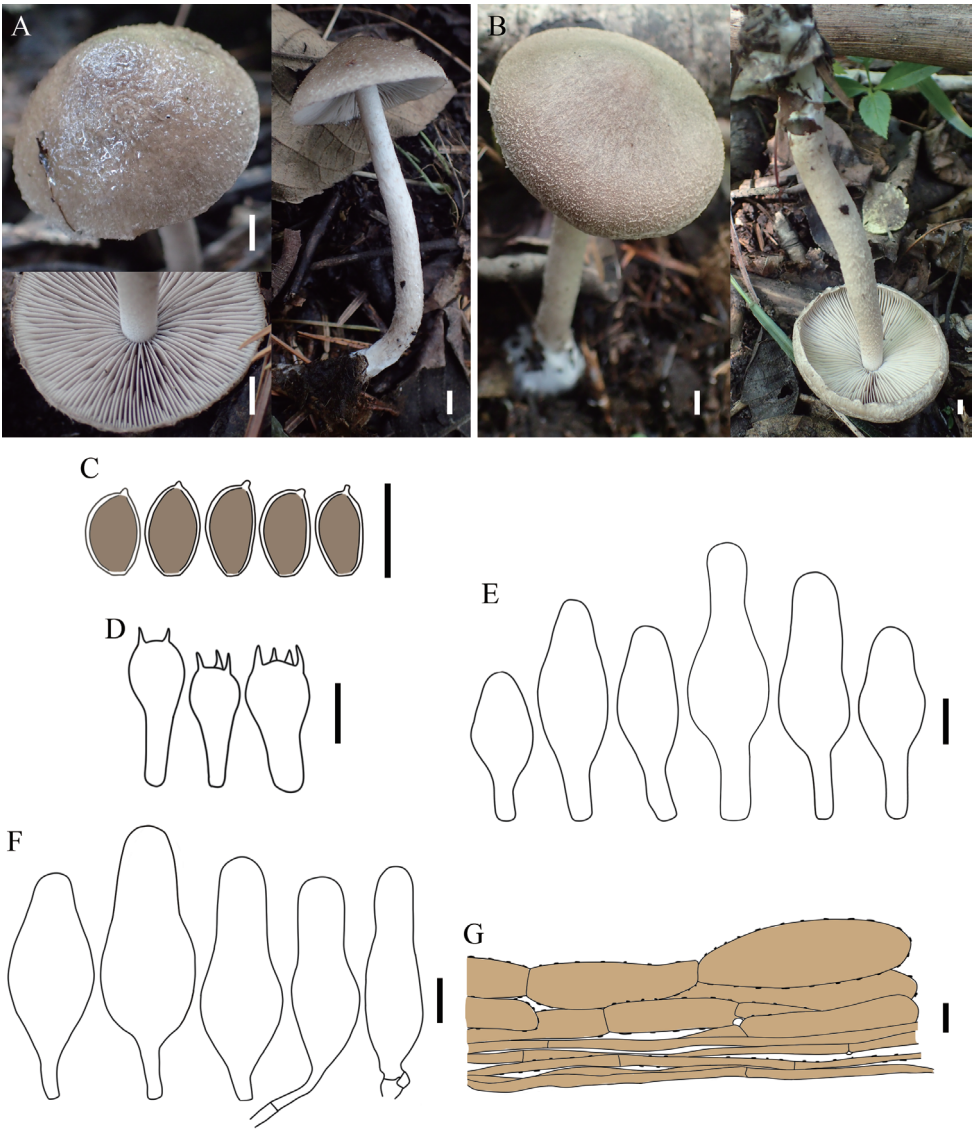

Figure 3. Basidiomata and microscopic features of *Coprinopsis jilinensis* **A** collection HMJAU 58783 **B** collection HMJAU 58782 **C** basidiospores **D** basidia **E** pleurocystidia **F** Cheilocystidia **G** pileipellis. Scale bars: 5 mm (**A, B**); 10 μm (**C–G**).

pores, pleurocystidia and cheilocystidia present. *C. jilinensis* forms a strongly-supported independent clade in ITS and LSU phylogeny trees (Figs 1, 2).

Morphologically and phylogenetic similar to *Coprinopsis jilinensis*, *C. uliginicola* is characterised by long basidiospores of 10–12(–15) μm, pleurocystidia absent and caulocystidia present, pileipellis no encrusting pigment (Smith 1972). Other similar species, *C. cineraria* is characterised by grey, hygrophanous and striate pileus, little short

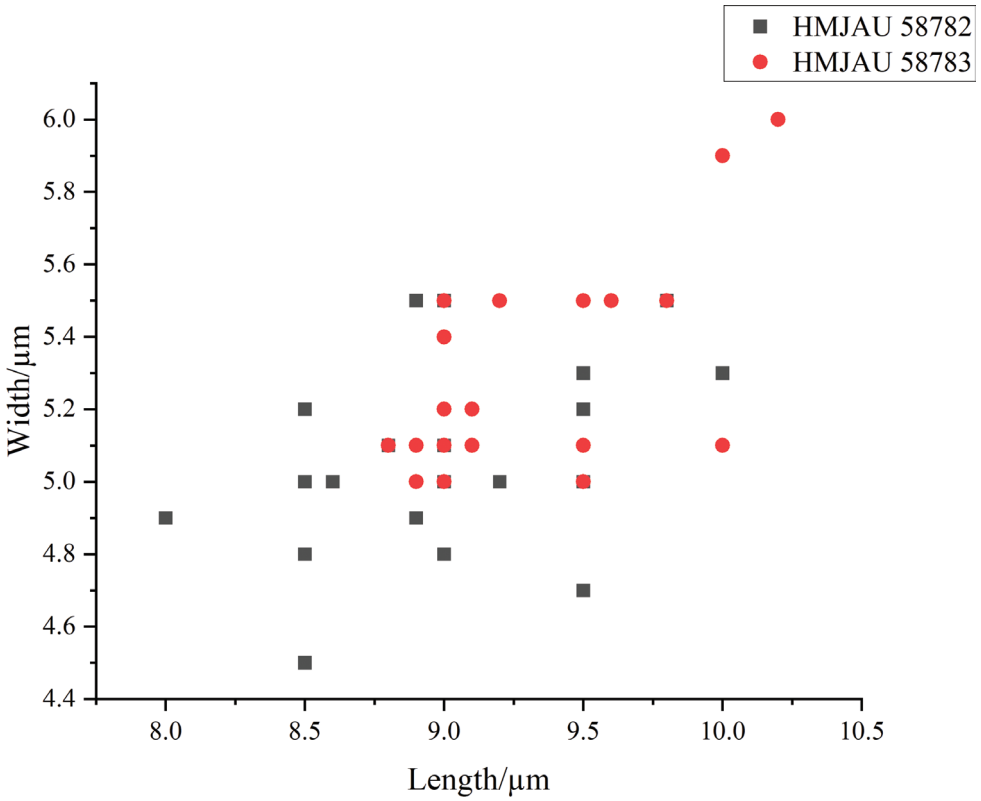

Figure 4. Scatter plot of basidiospores size in *Coprinopsis jilinensis*.

basidiospores (6.5–8.5 µm), pleurocystidia absent, pileipellis an epithelium (Takahashi 2000); *C. melanthina* is characterised by little long and subcolourless basidiospores (avl × avw = 10.5 × 5.8 µm), pleurocystidia absent (Kits van Waveren 1985); *C. pusilla* has small basidiomata, grey pileus, subcolourless and verrucose basidiospores (this study) and *Psathyrella subagraria* has hygrophanous pileus, thick flesh and caulocystidia present (Smith 1972), both of which could be clearly distinguished from *C. jilinensis* in terms of morphology.

***Coprinopsis pusilla* G. Rao, B. Zhang & Y. Li, sp. nov.**
MycoBank No: 840298
Figures 5, 6, 7A, B

Typification. China. Red Leaves Valley in Hanchongling, Dunhua City, Yanbian Korean Autonomous Prefecture, Jilin Province, 21 August 2019, Gu Rao (HMJAU 58781 Holotype!).

Sequences ex holotype. MZ398014 (ITS nrDNA), MZ398069 (LSU nrDNA).

Etymology. The epithet "*pusilla*" refers to this species having small basidiomata.

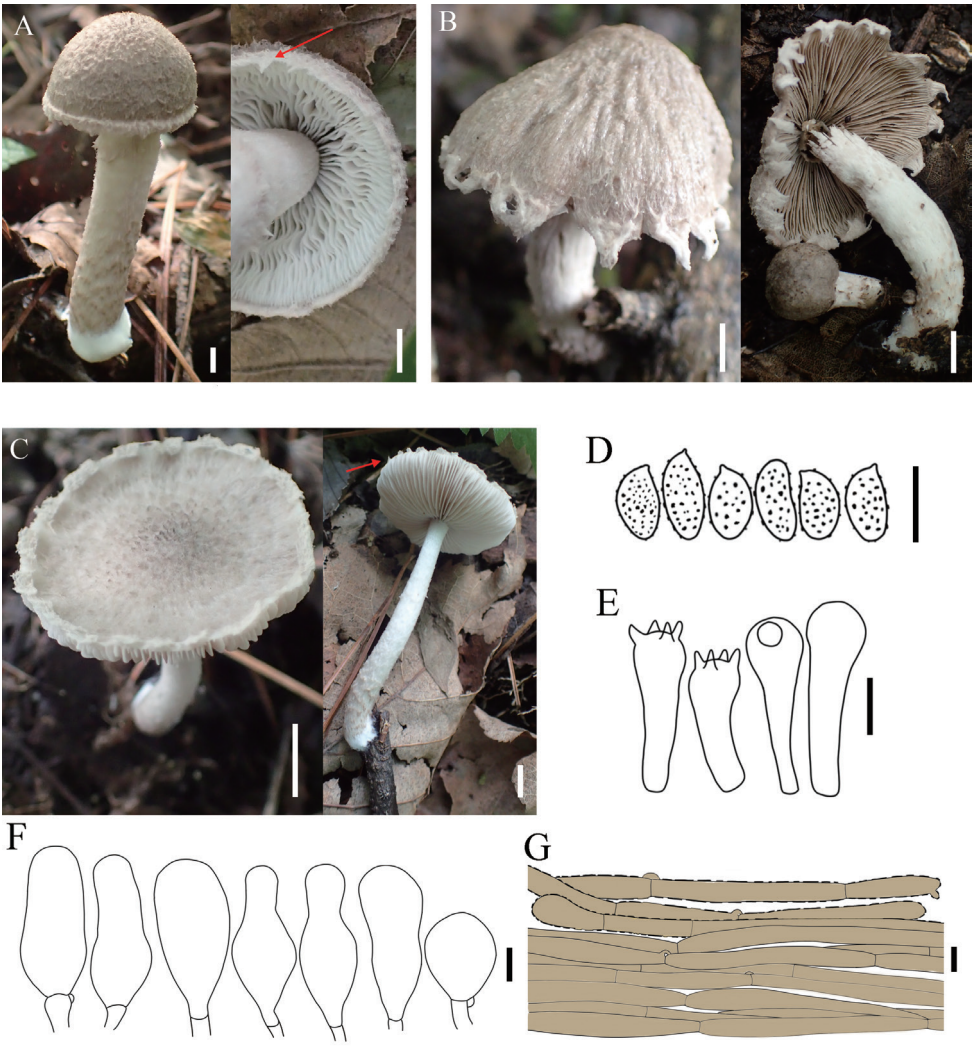

Figure 5. Basidiomata and microscopic features of *Coprinopsis pusilla* **A** collection HMJAU 58780 **B** collection HMJAU 58781 **C** collection HMJAU 58779 **D** basidiospores **E** basidia and basidioles **F** cheilocystidia **G** pileipellis. Scale bars: 5 mm (**A–C**); 10 μm (**D–G**).

Description. Basidiomata very small to small. Pileus 21–29 mm broad, bell-shaped to hemispherical when young, then convex, flat to slightly reflexed at edges, with inconspicuous bulge at the middle, grey or greyish-white when dry, no record when wet, densely covered with flocculent hairs, sometimes central with blackish-grey squamous tapering to the edges, not slime, sometimes the edges crack, hygrophanous no record, veil remnants dense at edges, triangular, subtriangular or massive, not easily disappearing. Lamellae close or crowded, subwhite, greyish-white or coffee brown,

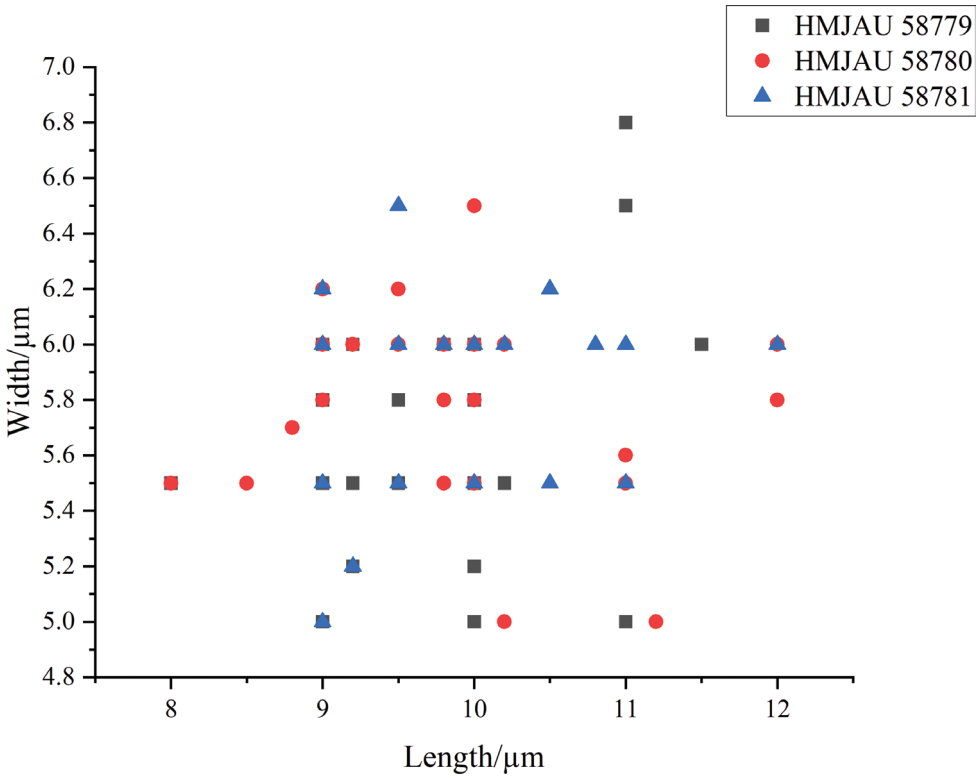

Figure 6. Scatter plot of basidiospores size in *Coprinopsis pusilla*.

flesh blond after drying, sinuate or adnexed, sometimes with vertical teeth, edges slightly toothed, concolorous, not deliquescent. Stipe 35–57 × 3–7 mm, cylindrical, subcylindrical, subequal or a little rough towards the base, white, cream white, hollow, a little fragile, not easy to detach from the cap, densely covered with white and flocculent hairs, brown, brownish-grey to brownish-yellow near the base, veil present at the stalk and cap joints, easily disappearing, no ring, the base with white mycelium. Spore print without record.

Basidiospores [90, 4, 3] 8–12 × 5–6.5 (6.8) µm, avl = 9.8 µm, avw = 5.8 µm, Q = 1.45–2.2 (2.24), Q_m = 1.70 ± 0.18 µm, oval, elliptic to long elliptic, subcolourless in 5% KOH and aqueous solution, surfaces verrucose, thin wall, no pores, not amyloid. Basidia (18) 19–32 (33) × 9–11 (12) µm, clavate, 4-sterigmate up to 3–4 µm long, 2-sterigmate occasional, without pseudoparaphyses. Pleurocystidia absent. Cheilocystidia (25) 27–53 (55) × (11) 13–21 µm, variable-shaped, subcylindrical, utriform, lageniform, reverse gourd-shaped and subcapitate, sphaeropedunculate elements present on gill edges, smooth, hyaline, thin wall to thick wall. Pileipellis a cutis, terminal hyphae (30) 31–84 (98) × (7) 8–17 (18) µm, with light brown pigment, mostly thick wall in the outer hyphae, present dark encrusting pigment, terminal hyphae present small cylindrical protrusions, about 3 × 3 µm. Veil hyphae (26) 27–100 (113) × (9)

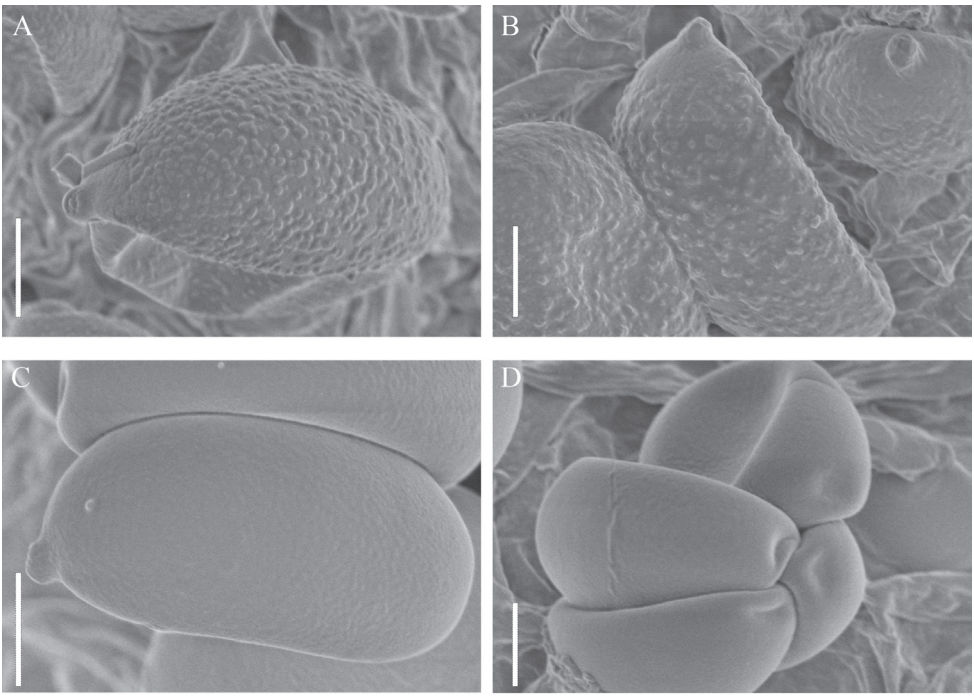

Figure 7. Scanning electron micrograph of basidiospores **A, B** *Coprinopsis pusilla* **C, D** *C. jilinensis*. Scale bars: 2 μm (**A–D**).

10–19 (20) μm, without encrusting pigment, thick wall, colourless to yellowish, cylindrical, subcylindrical, clavate or irregular. Stipitipellis a cutis, hyphae (21) 22–87 (88) × (9) 10–19 (20) μm, encrusting pigment not observed, colourless to light yellow, cylindrical, subcylindrical, clavate or irregular, terminal hyphae present small cylindrical protrusions. Clamp connections present in all tissues.

Habitat and distribution. On the dead and rotten wood of broad-leaved forest or coniferous and broad-leaved mixed forests in autumn.

Additional specimens examined. China. Red Leaves Valley in Hanchongling, Dunhua City, Yanbian Korean Autonomous Prefecture, Jilin Province, 6 August 2019, G. Rao (HMJAU 58779, HMJAU 58780).

Notes. *Coprinopsis pusilla* has a variable macromorphology, but stable micromorphology, which is characterised by small basidiomata, greyish-white pileus, thick and distinct veil remnants at edges, subcolourless and verrucose basidiospores, no pore, the habitat on the decaying wood of broad-leaved trees. *C. pusilla* forms a strongly-supported independent clade in both ITS and LSU phylogeny trees (Figs 1, 2).

Morphologically and phylogenetically similar to *Coprinopsis pusilla*, *C. melanthina* is characterised by larger brown pileus, fibrous veil at edges, longer basidiospores (avl = 10.5 μm) (Kits van Waveren 1985). *C. uliginicola* is characterised by large basidiomata, brown-black basidiospores, pore present (Smith 1972). *C. cineraria* is characterised by fibrous veil at the edges easily disappearing, smaller basidiospores (6.5–8.5 × 4–5 μm), pileipellis an epithelium (Takahashi 2000).

Discussion

Here we report two new psathyrelloid species of *Coprinopsis* from northern China. There is no unified definition of "psathyrelloid". Previously, "psathyrelloid" was mainly regarded as a species with the morphology of *Psathyrella*, including *Psathyrella* itself (Redhead et al. 2001). Örstadius et al. (2015) understood that "psathyrelloid" means that certain species of fungi with the morphology of *Psathyrella*, but belong to other genera in the phylogenetic analysis, so the species of *Psathyrella* were not included. These fungi were mainly distributed in *Coprinopsis* (Örstadius et al. 2015), *Typhrasa* (Örstadius et al. 2015; Wang et al. 2021), *Parasola* (Ganga and Manimohan 2019), *Homophron* (Örstadius et al. 2015), *Cystagaricus* (Örstadius et al. 2015), *Kauffmania* (Örstadius et al. 2015), *Lacrymaria* (Yan 2018) and so on. According to Redhead et al. (2001), coprinoid mushrooms were distributed in four genera: *Coprinus*, *Parasola*, *Coprinopsis* and *Coprinellus*. In Agaricaceae, Coprinoid mushrooms should also include *Montagnea*, *Podaxis* and *Xerocoprinus* (Moncalvo et al. 2002; Keirle et al. 2004). As there was no uniform standard, some fungi, such as *Parasola conopilea* (Ganga and Manimohan 2019), were intermediate between psathyrelloid and coprinoid species. With the introduction of molecular systematics, the species of coprinoid and psathyrelloid intersected with each other. Örstadius et al. (2015) studied the morphology of many psathyrelloid species of Psathyrellaceae and believed that the lack of the typical pattern of pseudoparaphyses was their main morphological characteristic. Since psathyrelloid species belong to different genera, their distributions were not indicated phylogenetically in their study. Worldwide, there were, currently, at least fourteen psathyrelloid species of *Coprinopsis* (Picón 2010; Portugalete 2011; Örstadius et al. 2015; Crous 2017; Larsson and Örstadius 2017; Melzer et al. 2017), which belong to *C.* sect. *Lanatulae* in Schafe's grouping system (Schafe 2010) and to three sections in Wächter's grouping system, *Melanthinae* (including *C. cineraria*, *C. melanthina*, *C. uliginicola*, *C. jilinensis* and *C. pusilla*), *Canocipes* (including *C. aesontiensis*, *C. canoceps*, *C. lotinae*, *C. pannucioides*, *C. submicrospora* and *C. udicola*) and *Quartoconatae* (including *C. marcescibilis*, *C. musae* and *C. pseudomarcescibilis*). Currently, the known sequences of these species in these three sections are all the psathyrelloid species of *Coprinopsis*.

According to the results of BLASTn analyses, ITS showed higher interspecific variability, so the ITS sequence was more advantageous in reflecting the interspecific relationship of *Coprinopsis* than the LSU sequence. The sequence identity between *C. jilinensis* from Jilin Province, China and *C. uliginicola* MG712323 from Hubei Province, China, was 99.27%. Based on the molecular sequence alone, *C. uliginicola* MG712323 and *C. jilinensis* could be the same species and subsequent re-examination of this specimen is recommended.

In this study, some sequences of *Coprinopsis* were selected, which belong to *C.* sect. *Melanthinae*, *C.* sect. *Canocipes* and *C.* sect. *Quartoconatae* in the grouping system proposed by Wächter and Melzer (2020). In the phylogenetic analyses (Figs 1, 2), whether in the phylogenetic trees, based on ITS or LSU, the tree shape of *C.* sect. *Melanthinae* obtained was consistent and the branches were stable. However, *C.* sect. *Canocipes* and *C.* sect. *Quartoconatae* were somewhat different from the grouping described by Wächter and Melzer (2020), based on different sequences and analyses. In the phylogenetic trees, based

on ITS, *C. udicola* and *C. submicrospora*, which originally belonged to *C.* sect. *canocipes*, formed a branch with three species belonging to *C.* sect. *Quartoconatae* in ML and BI trees. However, in the NJ tree, *C. udicola* formed a sister clade with three species belonging to *C.* sect. *Quartoconatae*. In the phylogenetic trees, based on LSU, *C.* sect. *Canocipes* and *C.* sect. *Quartoconatae* were well separated in the NJ tree, while in ML and BI trees, *C. musae* belonging to *C.* sect. *Quartoconatae* formed a sister clade with four species of *C.* sect. *Canocipes*. The branching relationships of phylogenetic trees, based on different molecular sequences and analyses may vary. Over-subdivision of sections would cause intersection. Subdivision of *C.* sect. *Canocipes* and *C.* sect. *Quartoconatae* may need to be reconsidered.

Coprinopsis sect. *Melanthinae* has a relatively clear systematic differentiation (Wächter and Melzer 2020), which is consistent with the results of this study. Currently, there are only six species in this section, including the *C. lignicola* nom. prov. (GenBank no.: MG966286 and MF163181). Combined with the two newly-discovered species, the expression of this section is modified as follows:

***Coprinopsis* sect. *Melanthinae* Wächter & A. Melzer**

Description. Basidiomata very small to large, on humus or lignicolous. Pileus not radially sulcate, lamellae not deliquescent. Veil strongly developed, consisting of chains of subcylindrical, sometimes encrusted cells. Basidiospores medium to large-sized, ellipsoid to ovoid in side view, strikingly pale or brown, thin or thick-walled, germ pore absent or very indistinct, surfaces verrucose or smooth. Pseudoparaphyses absent. Basidia 4-sterigmate, 2–3-sterigmate occasional, always clavate, never polymorphic. Marginal cells of the lamellar edge predominantly utriform. Pleurocystidia present or absent. Cheilocystidia and clamps present.

Coprinopsis pusilla has a variety of macroscopic morphology, including the shape and colour of the pileus, the shape of the veil and the thickness and length of the stipe and so on, which makes it difficult to determine whether it is the same species during the collection process, when the size of the basidiomata and ecological habits seem to be stable. The microscopic morphology of *C. pusilla* is relatively stable, including the size, shape, colour and decoration of basidiospores, the type of pileipellis and the presence or absence of cystidia. Interestingly, Coprinoid fungi are thought to be a taxon of dark-coloured basidiospores (Noordeloos et al. 2005), but *C. pusilla*, including *C. melanthina*, which is closely related to *C. pusilla*, have subcolourless basidiospores. Collection HMJAU 58779 and collection HMJAU 58780 were collected at approximately the same time in the same forest, which were not far apart from each other. However, due to the significant difference in macroscopic morphology, they were made into two collections. The macroscopic morphology of Collection HMJAU 58781, collected later, was also significantly different from the two specimens collected previously. Through the observation of the microscopic morphology of these collections and the phylogenetic analysis, combined with ITS and LSU molecular sequences, the results showed that the three collections were the same species.

Pleurocystidia is present in many species of *Coprinopsis*, such as *C. cinerea*, *C. jonesii* and *C. pseudoradiata* (Redhead et al. 2001), but in psathyrelloid species of *Coprinopsis*, spe-

cies with pleurocystidia are rare. The pleurocystidia are sparsely distributed in the hymenium of *C. jilinensis*, but not present in *C. uliginicola*, which is closely related to *C. jilinensis*. In psathyrelloid species of *Coprinopsis*, only *C. pannucioides* (Larsson and Örstadius 2008), *C. udicola* (existing but rare) (Örstadius et al. 2015) and *C. jilinensis* have pleurocystidia.

Psathyrella subagraria is a confusing species, described by Smith (1972) as it is very similar to *P. uliginicola* morphologically, with the main difference being that this species has pleurocystidia, which are mainly growing on humus. Since Smith (1972) introduced *P. subagraria*, no further reports have been made. Örstadius et al. (2015) moved *P. uliginicola* to *Coprinopsis*, based on molecular studies, the taxonomic status of *P. subagraria* being questionable. There are some differences between *P. subagraria* and *C. jilinensis* in macroscopic morphology, but they are similar in microscopic morphology. Smith (1972) described *P. subagraria* as having two basidiospores sizes [8–10 × 4–5 (10–12 × 4.5–5.5) μm], one of which was very close to the size of *C. jilinensis* [(8) 8.5–10 (10.2) × 4.5–5.9 (6) μm], requiring re-examination of the type specimens of *P. subagraria* in future studies.

Key to fourteen psathyrelloid species of *Coprinopsis*

1 Basidiospores no pore **2**
– Basidiospores with pore **6**
2 Basidiospores distinctly pigmented ..... ***C. submicrospora***
– Basidiospores hyaline to very pale brown **3**
3 Pileus < 20 mm, glabrous; pseudoparaphyses often present ..... ***C. musae***
– Pileus > 20 mm, hairy; pseudoparaphyses absent or unrecorded..... **4**
4 Pileus hygrophanous, striate; basidiospores avl < 9 μm; pileipellis an epithelium ..... ***C. cineraria***
– Pileus not or scarcely hygrophanous, not striate; basidiospores avl > 9 μm; pileipellis a cutis..... **5**
5 Pileus 25–80 mm, brown, fibrous veil at edges; basidiospores avl = 10.5 μm. ..... ***C. melanthina***
– Pileus 21–29 mm, grey or greyish-white, veil dense at edges; basidiospores avl = 9.8 μm..... ***C. pusilla***
6 Basidiospores avl > 11.5 μm..... **7**
– Basidiospores avl < 11.5 μm..... **10**
7 Pileus mostly brown, almost not striate, flocci at cap margin **8**
– Pileus mostly white or grey, striate, no flocci at cap margin..... **9**
8 Basidiospores 13.3–14.5 μm; irregular flocci on cap margin .... ***C. pseudomarcescibilis***
– Basidiospores 11.6–12.8 μm; denticulate flocci on cap margin ....***C. marcescibilis***
9 Pseudoparaphyses present, pleurocystidia absent; caulocystidia present..... ..... ***C. lotinae***
– Pseudoparaphyses absent; pleurocystidia rare, close to gill edge; caulocystidia absent ..... ***C. udicola***

10 Pleurocystidia present; cheilocystidia no long neck **11**
– Pleurocystidia absent; cheilocystidia part with long neck **12**
11 Pileus yellowish-white, papillate-umbonate; caulocystidia present; tufty ..... ***C. pannucioides***
– Pileus brown, not papillate-umbonate; caulocystidia absent; solitary or scattered ..... ***C. jilinensis***
12 Basidiomata medium-sized to large-sized (pileus > 50 mm); pileus pallid to greyish ..... ***C. uliginicola***
– Basidiomata very small to small (pileus < 50 mm); pileus not grey..... **13**
13 Stipe < 60 mm long; basidia 4-sterigmate; cheilocystidia not inflated fusiform ..... ***C. canoceps***
– Stipe > 60 mm long; basidia 1-, 2-, 4-sterigmate; cheilocystidia part inflated fusiform ..... ***C. aesontiensis***

Acknowledgements

We are grateful to the editors and reviewers for improving the manuscript. This study is funded by Key Project on R&D of Ministry of Science and Technology (No. 2018YFE0107800), Jilin Province Science and Technology Development Plan Project (No. 20190201026JC), Modern Agroindustry Technology Research System (No. CARS20) and Scientific and Technological Tackling Plan for the Key Fields of Xinjiang Production and Construction Corps (No. 2021AB004).

References

Castresana J (2000) Selection of conserved blocks from multiple alignments for their use in phylogenetic analysis. Molecular Biology and Evolution 17(4): 540–552. https://doi.org/10.1093/oxfordjournals.molbev.a026334

Citerin M (1992) Clé analytique du genre Coprinus. Documents Mycologiques 22(86): 1–28.

Crous PW, Wingfield MJ, Burgess TI, Hardy GEStJ, Barber PA, Alvarado P, Barnes CW, Buchanan PK, Heykoop M, Moreno G, Thangavel R, van der Spuy S, Barili A, Barrett S, Cacciola SO, Cano-Lira JF, Crane C, Decock C, Gibertoni TB, Guarro J, Guevara-Suarez M, Hubka V, Kolařík M, Lira CRS, Ordoñez ME, Padamsee M, Ryvarden L, Soares MA, Stchigel AM, Sutton DA, Vizzini A, Weir BS, Acharya K, Aloi F, Baseia IG, Blanchette RA, Bordallo JJ, Bratek Z, Butler T, Cano-Canals J, Carlavilla JR, Chander J, Cheewangkoon R, Cruz RHSF, da Silva M, Dutta AK, Ercole E, Escobio V, Esteve-Raventós F, Flores JA, Gené J, Góis JS, Haines L, Held BW, Horta Jung M, Hosaka K, Jung T, Jurjević Ž, Kautman V, Kautmanova I, Kiyashko AA, Kozanek M, Kubátová A, Lafourcade M, La Spada F, Latha KPD, Madrid H, Malysheva EF, Manimohan P, Manjón JL, Martín MP, Mata M, Merényi Z, Morte A, Nagy I, Normand AC, Paloi S, Pattison N, Pawłowska J, Pereira OL, Petterson ME, Picillo B, Raj KNA, Roberts A, Rodríguez A, Rodríguez-Campo FJ, Romański M, Ruszkiewicz-Michalska M, Scanu B, Schena L, Semelbauer M, Sharma R,

Shouche YS, Silva V, Staniaszek-Kik M, Stielow JB, Tapia C, Taylor PWJ, Toome-Heller M, Vabeikhokhei JMC, van Diepeningen AD, Van Hoa N, Van Tri M, Wiederhold NP, Wrzosek M, Zothanzama J, Groenewald JZ (2017) Fungal Planet description sheets: 558–624. Persoonia: Molecular Phylogeny and Evolution of Fungi 38: 240–384. https://doi.org/10.3767/003158517X698941

Fries EM (1836–1838) Epicrisis Systematis Mycologici seu Synopsis Hymenomycetum. Typographia Academica, Upsaliae, 610 pp.

Ganga KG, Manimohan P (2019) *Parasola psathyrelloides* (Psathyrellaceae), a new species from Kerala State, India. Phytotaxa 405(5): 255–262. https://doi.org/10.11646/phytotaxa.405.5.4

Gardes M, Bruns TD (1993) ITS primers with enhanced specificity for basidiomycetes – application to the identification of mycorrhizae and rusts. Molecular Ecology 2(2): 113–118. https://doi.org/10.1111/j.1365-294X.1993.tb00005.x

He MQ, Zhao RL, Hyde KD, Begerow D, Kemler M, Yurkov A, McKenzie EHC, Raspé O, Kakishima M, Sánchez-Ramírez S, Vellinga EC, Halling R, Papp V, Zmitrovich LV, Buyck B, Ertz D, Wijayawardene NN, Cui BK, Schoutteten N, Liu XZ, Li TH, Yao YJ, Zhu XY, Liu AQ, Li GJ, Zhang MZ, Ling ZL, Cao B, Antonín V, Boekhout T, Da Silva BDB, Crop ED, Decock C, Dima B, Dutta AK, Fell JW, Geml J, Ghobad-Nejhad M, Giachini AJ, Gibertoni TB, Gorjón SP, Haelewaters D, He SH, Hodkinson BP, Horak E, Hoshino T, Justo A, Lim YW, Menolli Jr N, Mešić A, Moncalvo JM, Mueller GM, Nagy LG, Nilsson RH, Noordeloos M, Nuytinck J, Orihara T, Ratchadawan C, Rajchenberg M, Silva-Filho AlGS, Sulzbacher MA, Tkalčec Z, Valenzuela R, Verbeken A, Vizzini A, Wartchow F, Wei TZ, Weiß M, Zhao CL, Kirk PM (2019) Notes, outline and divergence times of Basidiomycota. Fungal Diversity 99(1): 105–367. https://doi.org/10.1007/s13225-019-00435-4

Hopple Jr JS, Vilgalys R (1999) Phylogenetic relationships in the mushroom genus *Coprinus* and dark-spored allies based on sequence data from the nuclear gene coding for the large ribosomal subunit RNA: divergent domains, outgroups, and monophyly. Molecular Phylogenetics and Evolution 13(1): 1–19. https://doi.org/10.1006/mpev.1999.0634

Huang M (2019) Taxonomy and molecular phylogeny of coprinoid fungi from northeast China. Master Thesis, Jilin Agricultural University, Changchun, 117 pp.

Johnson J, Vilgalys R (1998) Phylogenetic systematics of *Lepiota* sensu lato based on nuclear large subunit rDNA evidence. Mycologia 90(6): 971–979. https://doi.org/10.1080/00275514.1998.12026994

Kalyaanamoorthy S, Minh BQ, Wong TK, Von Haeseler A, Jermiin LS (2017) ModelFinder: fast model selection for accurate phylogenetic estimates. Nature Methods 14(6): 587–589. https://doi.org/10.1038/nmeth.4285

Katoh K, Kuma KI, Toh H, Miyata T (2005) MAFFT version 5: improvement in accuracy of multiple sequence alignment. Nucleic Acids Research 33(2): 511–518. https://doi.org/10.1093/nar/gki198

Kauffman CH (1918) The Agaricaceae of Michigan. W. H. Crawford, state printers, Lansing, 924 pp. https://doi.org/10.5962/bhl.title.58545

Keirle MR, Hemmes DE, Desjardin DE (2004) Agaricales of the Hawaiian Islands. 8. Agaricaceae: *Coprinus* and *Podaxis*; Psathyrellaceae: *Coprinopsis*, *Coprinellus* and *Parasola*. Fungal Diversity 15(3): 33–124.

Kirk PM, Cannon PF, Minter DW, Stalpers JA (2008) Dictionary of the Fungi, 10th edn. CABI Publishing, UK, 771 pp.

Kumar S, Stecher G, Li M, Knyaz C, Tamura K (2018) MEGA X: molecular evolutionary genetics analysis across computing platforms. Molecular Biology and Evolution 35(6): 1547–1549. https://doi.org/10.1093/molbev/msy096

Largent DL (1986) How to identify mushrooms to genus I: macroscopic features. Mad River Press, Eureka, 166 pp.

Largent DL, Johnson D, Watling R (1977) How to identify mushrooms to genus : microscopic features. Mad River Press, Eureka, 148 pp.

Larsson E, Örstadius L (2008) Fourteen coprophilous species of *Psathyrella* identified in the Nordic countries using morphology and nuclear rDNA sequence data. Mycological Research 112(10): 1165–1185. https://doi.org/10.1016/j.mycres.2008.04.003

Melzer A, Ferisin G, Dovana F (2017) *Coprinopsis aesontiensis*, a new species found in Friuli Venezia Guilia, Italy. Micologia e Vegetazione Mediterrane 31(2): 123–132.

Moncalvo JM, Vilgalys R, Redhead SA, Johnson JE, James TY, Aime MC, Hofstetter V, Verduin SJW, Larsson E, Baroni TJ, Thorn RG, Jacobsson S, Clémençon H, Miller Jr OK (2002) One hundred and seventeen clades of euagarics. Molecular Phylogenetics and Evolution 23(3): 357–400. https://doi.org/10.1016/S1055-7903(02)00027-1

Nagy L (2012) An investigation of the phylogeny and evolutionary processes of deliquescent fruiting bodies in the mushroom family Psathyrellaceae (Agaricales). Szegedi Tudományegyetem, Szeged, 119 pp.

Nagy LG, Urban A, Örstadius L, Papp T, Larsson E, Vágvölgyi C (2010) The evolution of autodigestion in the mushroom family Psathyrellaceae (Agaricales) inferred from Maximum Likelihood and Bayesian methods. Molecular Phylogenetics and Evolution 57(3): 1037–1048. https://doi.org/10.1016/j.ympev.2010.08.022

Nguyen LT, Schmidt HA, Von Haeseler A, Minh BQ (2015) IQ-TREE: a fast and effective stochastic algorithm for estimating maximum-likelihood phylogenies. Molecular Biology and Evolution 32(1): 268–274. https://doi.org/10.1093/molbev/msu300

Örstadius L, Ryberg M, Larsson E (2015) Molecular phylogenetics and taxonomy in Psathyrellaceae (Agaricales) with focus on psathyrelloid species: introduction of three new genera and 18 new species. Mycological Progress 14(5): 1–42. https://doi.org/10.1007/s11557-015-1047-x

Park DS, Go SJ, Kim YS, Seok SJ, Ryu JC, Sung JM (1999) Phylogenetic relationships of genera *Coprinus* and *Psathyrella* on the basis of ITS region sequences. The Korean Journal of Mycology 27(4): 274–279.

Park DS, Go SJ, Ryu JC (1999) Phylogenetic relationships of coprinoid taxa and an agaric-like gastroid taxon based on the sequences of internal transcribed spacer (ITS) regions. The Korean Journal of Mycology 27(6): 406–411.

Picón GRM (2010) *Coprinopsis lotinae* (Picón) Picón, comb. nov. (Psathyrellaceae). Zizak 7: 43–45.

Redhead SA, Vilgalys R, Moncalvo JM, Johnson J, Hopple Jr JS (2001) *Coprinus* Pers. and the disposition of *Coprinus* species sensu lato. Taxon 50(1): 203–241. https://doi.org/10.2307/1224525

Ronquist F, Teslenko M, Van Der Mark P, Ayres DL, Darling A, Höhna S, Larget B, Liu L, Suchard MA, Huelsenbeck JP (2012) MrBayes 3.2: efficient Bayesian phylogenetic inference and model choice across a large model space. Systematic Biology 61(3): 539–542. https://doi.org/10.1093/sysbio/sys029

Schafer DJ (2010) Keys to sections of *Parasola*, *Coprinellus*, *Coprinopsis* and *Coprinus* in Britain. Field Mycology 11(2): 44–51. https://doi.org/10.1016/j.fldmyc.2010.04.006

Singer R (1949) The Agaricales (mushrooms) in modern taxonomy. Chronica Botanica, New York, 832 pp.

Smith AH (1972) The North American species of *Psathyrella*. Memoirs of the New York Botanical Garden 24: 1–633.

Swindell SR, Plasterer TN (1997) Sequence data analysis guidebook. Humana Press, Totowa, 352 pp. https://doi.org/10.1385/0896033589

Takahashi H (2000) Two new species and one new variety of Agaricales from central Honshu, Japan. Mycoscience 41(1): 15–23. https://doi.org/10.1007/BF02464381

Talavera G, Castresana J (2007) Improvement of phylogenies after removing divergent and ambiguously aligned blocks from protein sequence alignments. Systematic Biology 56(4): 564–577. https://doi.org/10.1080/10635150701472164

Uljé CB (2005) Flora Agaricina Neerlandica Volume 6, CRC Press, Boca Raton, 226 pp.

Uljé CB, Noordeloos ME (1993) Studies in *Coprinus* III—*Coprinus* section *Veliformes*. Subdivision and revision of subsection *Nivei* emend. Persoonia-Molecular Phylogeny and Evolution of Fungi 15(3): 257–301.

Van Waveren EK (1985) The Dutch, French and British species of *Psathyrella*. Persoonia-Supplement 2(1): 3–300.

Vilgalys R, Hester M (1990) Rapid genetic identification and mapping of enzymatically amplified ribosomal DNA from several Cryptococcus species. Journal of Bacteriology 172(8): 4238–4246. https://doi.org/10.1128/jb.172.8.4238-4246.1990

Wächter D, Melzer A (2020) Proposal for a subdivision of the family Psathyrellaceae based on a taxon-rich phylogenetic analysis with iterative multigene guide tree. Mycological Progress 19(11): 1151–1265. https://doi.org/10.1007/s11557-020-01606-3

Wang SN, Hu YP, Chen JL, Qi LL, Zeng H, Ding H, Huo GH, Zhang LP, Chen FS, Yan JQ (2021) First record of the rare genus Typhrasa (Psathyrellaceae, Agaricales) from China with description of two new species. MycoKeys 79: 119–128. https://doi.org/10.3897/mycokeys.79.63700

Yan JQ (2018) Taxonomy and Molecular Phylogeny of *Psathyrella* and related genera in China. PhD Thesis, Jilin Agricultural University, Changchun, 193 pp.

Zhang D, Gao F, Jakovlić I, Zou H, Zhang J, Li WX, Wang GT (2020) PhyloSuite: an integrated and scalable desktop platform for streamlined molecular sequence data management and evolutionary phylogenetics studies. Molecular Ecology Resources 20(1): 348–355. https://doi.org/10.1111/1755-0998.13096

Zhang X (2019) Diversity of macro-basidiomycetes in Xingshan County, Hubei province. Master Thesis, Nanjing Normal University, Nanjing, 98 pp.

MycoKeys 83: 105–121 (2021)
doi: 10.3897/mycokeys.83.71140
https://mycokeys.pensoft.net

RESEARCH ARTICLE

A peer-reviewed open-access journal
MycoKeys
Launched to accelerate biodiversity research

Phylogenetic and morphological analyses of *Coniochaeta* isolates recovered from Inner Mongolia and Yunnan revealed three new endolichenic fungal species

Hong-Li Si[1*], Yue-Min Su[1*], Xiao-Xiao Zheng[1], Meng-Yao Ding[1], Tanay Bose[2], Run-Lei Chang[1]

1 *College of Life Science, Shandong Normal University, Jinan 250014, Shandong, China* **2** *Department of Biochemistry, Genetics & Microbiology, Forestry and Agricultural Biotechnology Institute (FABI), University of Pretoria, Pretoria 0002, South Africa*

Corresponding author: Run-Lei Chang (runlei.chang@163.com)

Academic editor: Cecile Gueidan | Received 6 July 2021 | Accepted 12 August 2021 | Published 9 September 2021

Citation: Si H-L, Su Y-M, Zheng X-X, Ding M-Y, Bose T, Chang R-L (2021) Phylogenetic and morphological analyses of *Coniochaeta* isolates recovered from Inner Mongolia and Yunnan revealed three new endolichenic fungal species. MycoKeys 83: 105–121. https://doi.org/10.3897/mycokeys.83.71140

Abstract

Lichens are the result of a symbiotic interaction between fungi (mycobionts) and algae (phycobionts). Aside from mycobionts, lichen thalli can also contain non-lichenised fungal species, such as lichenicolous and endolichenic fungi. For this study, three surveys were conducted in China's Yunnan Province and Inner Mongolia Autonomous Region between 2017 and 2020. Several samples of four lichen species were collected during these surveys: *Candelaria fibrosa*, *Flavoparmelia caperata*, *Flavopunctelia flaventior* and *Ramalina sinensis*. Six isolates of *Coniochaeta* were recovered from these four lichen species. The phylogenetic and morphological analyses revealed that two of these isolates were previously identified species, *Coniochaeta velutinosa* and *C. acaciae*. Those remaining were from potentially unknown species. We used molecular and morphological data to describe these previously-unknown species as *Coniochaeta fibrosae* **sp. nov.**, *C. mongoliae* **sp. nov.** and *C. sinensis* **sp. nov.** The findings of this study significantly improve our understanding of the variety and habitat preferences of *Coniochaeta* in China and globally.

Keywords

Coniochaetaceae, lichens, molecular phylogeny, Mongolia, Yunnan Province

* These two authors contributed equally.

Introduction

Lichens are a symbiotic relationship between heterotrophic fungi and algae (including cyanobacteria) that are usually referred to as mycobiont and phycobiont, respectively (Nash and Thomas 2008; Tripathi and Joshi 2019). Lichens exhibit a diversity of colours, thallus morphology and fruiting bodies (Ahmadjian 1993). Lichens have a limited fossil record, yet recent molecular-clock analyses suggested their being at least 250 million years old (Nelsen et al. 2020). Apart from the mycobionts, a lichen thallus can also house non-lichenised fungal species, such as lichenicolous and endolichenic fungi. The former utilise lichens as their hosts (Lawrey and Diederich 2003), whereas the latter behave similar to 'endophytes' (Arnold et al. 2009; Suryanarayanan and Thirunavukkarasu 2017). Various species of *Coniochaeta* are examples of endolichenic fungi (Zhang et al. 2016; Harrington et al. 2019).

Coniochaeta is a genus of pleomorphic yeasts belonging to the Coniochaetales (Ascomycota) with global distribution (García et al. 2006; Damm et al. 2010; Raja et al. 2012; Vazquez-Campos et al. 2014; Nasr et al. 2018; Harrington et al. 2019). This genus has distinct asexual and sexual states in its life cycle. Previously, the genus *Lecythophora* was erected to include asexual states of *Coniochaeta* (Weber 2002). After the dual nomenclature of pleomorphic fungi was discontinued (Hawksworth 2011), following the principle of priority, these genera were reclassified under *Coniochaeta* (Khan et al. 2013; Réblová et al. 2016).

The sexual state of *Coniochaeta* is characterised by dark brown to black ascomata with setae. These ascomata can either be pyriform ostiolate or globose non-ostiolate. Asci are thin-walled, producing single-celled, smooth ascospores with an elongated embryo crack (García et al. 2006; Asgari et al. 2007). In contrast, the asexual state of *Coniochaeta* has distinctive pink salmon to dark brown colonies producing phialidic conidiogenous cells (Checa 1988; Damm et al. 2010; Khan et al. 2013). *Coniochaeta* has been isolated from various substrates, such as butter, faeces, wood, soil, uranium wastewater, plants and lichens (Weber 2002; García et al. 2006; Vazquez-Campos et al. 2014; Harrington et al. 2019). Some *Coniochaeta* species are also known to be human and animal pathogens (Hoog et al. 2000; Perdomo et al. 2013; Troy et al. 2013).

Several *Coniochaeta* species have been isolated from Asia (Kamiya et al. 1995; García et al. 2006; Asgari et al. 2007). Previously, three undescribed *Coniochaeta* species were identified from China growing on plant litters and herbivore faeces, but none associated with liches (Chang and Wang 2011; Hyde et al. 2020). In this study, six isolates of *Coniochaeta* species were recovered from four lichen species collected from the Yunnan Province and the Inner Mongolia Autonomous Region of China. Analyses of molecular and morphological data indicated these six isolates represented five species of *Coniochaeta*. Amongst these were two previously-described taxa, *C. velutinosa* and *C. acaciae*, whereas the remaining three were undescribed. Here, we describe these species as *Coniochaeta mongoliae* sp. nov., *C. sinensis* sp. nov. and *C. fibrosae* sp. nov. This study substantially augments our current knowledge on the diversity and host range of *Coniochaeta* and endolichenic fungi from China.

Materials and methods

Collection of lichen samples

Between 2017 and 2020, three surveys were conducted in the Yunnan Province and Inner Mongolia Autonomous Region of China. During these surveys, multiple samples of four lichens species were collected. Samples of *Flavoparmelia caperata* (2017), *Flavopunctelia flaventior* (2017) and *Candelaria fibrosa* (2020) were collected from the Yunnan Province, whereas *Ramalina sinensis* was collected from the Inner Mongolia Autonomous Region in 2019. During their transit, all lichen samples were stored separately in paper bags.

Isolation of fungi from lichen thalli

All lichen samples were repeatedly rinsed with tap water followed by deionised water. Using a Leica Zoom 2000 stereomicroscope, the upper cortex was scraped off with a sterile blade. The medullary layer was carefully dissected and rinsed using sterile deionised water. Thereafter, these medullary tissues were placed on to 2% potato dextrose agar (PDA) plates, amended with 0.05% streptomycin. All Petri plates were incubated for 14 days at 25 °C. Hyphal tips of mycelia emerging from the medullary tissues were sub-cultured on to fresh PDA plates.

Ex-holotype cultures of undescribed fungal species, described in this study, were deposited in the China General Microbiological Culture Collection Center (CGMCC), Beijing, China. The holotype specimens were deposited in the culture collection of the Institute of Microbiology (HMAS), Beijing, China (Accession numbers are listed in Table. 1).

Morphology and growth studies

Colony morphologies of ex-holotypes, representing four potentially new fungal species, were described from eight-day-old cultures growing at 25 °C. A Leica DM6 compound microscope attached to a Zeiss Axio Imager Z2 camera was used for measuring and photographing microscopic morphological characters. A minimum of 50 conidia and conidiogenous cells per isolate were measured using the software ImageJ (Rasband 1997; Schneider et al. 2012).

For the growth study, ex-holotype isolates were sub-cultured on to PDA and incubated for five days at 25 °C. Thereafter, 5 mm diam. agar plugs were placed at the centre of 90 mm Petri dishes. Three replicates per ex-type isolate were incubated at 5, 10, 15, 20, 25, 30 and 35 °C (± 0.5 °C). The colony diameter of each isolate was measured daily up to the eighth day.

DNA extraction, PCR amplification and sequencing

For all undescribed fungal species, eight-day-old cultures growing at 25 °C were used for the extraction of total genomic DNA using PrepMan™ Ultra Sample Preparation Reagent

(Applied Biosystems, California, USA), following the manufacturer's instructions. The complete internal transcribed spacers (ITS) and the partial 28S nuclear ribosomal large subunit rRNA gene (LSU) were amplified using the primer pairs ITS1/ITS4 (White et al. 1990) and LR0R/LR5 (Vilgalys and Hester 1990; White et al. 1990), respectively.

Each 25 µl of PCR reaction included 10.5 µl of PCR grade water, 12.5 µl of 1–5™ 2× High-Fidelity Master Mix (buffer, $MgCl_2$, dNTPs and Taq; Tsingke Co., China), 0.5 µl each of forward and reverse primers and 1 µl DNA template. For both gene regions, PCR amplifications were conducted with an initial denaturation at 94 °C for 3 min, followed by 30 cycles of 94 °C for 30 sec, 56 °C for 1 min, 72 °C for 1 min; final extension at 72 °C for 10 min. Positive amplifications were verified using agarose gel electrophoresis.

All the PCR products were sequenced by QingDao MDBio Biotech Co., Ltd., China. The resulting sequences were assembled using Geneious v.10.2.2 (Biomatters, Auckland, New Zealand). Preliminary identification of the sequences was undertaken using the BLAST algorithm (Altschul et al. 1990) available through the NCBI GenBank. All the sequences, generated in this study, were deposited at GenBank (Table1).

Phylogenetic analyses

For the purpose of phylogenetic analyses, we constructed three separate datasets. These are as follows: a) ITS, b) LSU and c) ITS + LSU. Each dataset included sequences generated in this study and those retrieved from the NCBI GenBank. Where available, ex-type sequences of previously-known *Coniochaeta* species were added to the datasets. For all three datasets, *Paragaeumannomyces garethjonesii* and *Zanclospora jonesii* were selected as the outgroup taxa (Table 1). All datasets were aligned using MAFFT v. 7 (Katoh and Standley 2013); thereafter, manually adjusted if needed using MEGA v.7 (Kumar et al. 2016). All aligned sequence datasets were deposited to TreeBase (Acc. No 28404).

Software for Maximum Likelihood (ML) and Bayesian Inference (BI) phylogenetic analysis was accessed through the CIPRES Science Gateway platform (Miller et al. 2010). jModeltest 2.2 (Nylander et al. 2008) was used for selecting appropriate substitution models. ML analyses were done using RAxML v. 8.2.4 (Stamatakis 2006; Stamatakis et al. 2008) using the GTR substitution model and 1000 bootstrap replicates. BI analyses were undertaken using MrBayes v.3.2 (Ronquist et al. 2012). Four MCMC chains were run from a random starting tree for five million generations and trees were sampled every 100th generation. A quarter of the sampled trees were discarded during burn-in. The remaining trees were used for constructing consensus trees. The resulting ML and BI trees were viewed with FigTree v.1.4 (Rambaut 2009).

Results

Isolation

In this study, four lichen species were collected from Yunnan Province and the Inner Mongolia Autonomous Region in 2017, 2019 and 2020. A total of six isolates of

Table 1. GenBank accession numbers *Coniochaeta* species used for the phylogenetic analyses. T = ex-type isolates.

Taxa	Strain	HMAS	GenBank accession number	
			LSU	ITS
Coniochaeta acaciae	MFLUCC 17-2298^T		MG062737	MG062735
C. acaciae	**CX37**		**MW750757**	**MW750761**
C. africana	CBS:120868^T		NG_066150	NR_137725
C. angustispora	CBS:144.70		MH871308	MH859528
C. arenariae	MFLUCC 18-0405^T		MN017893	-
C. baysunika	MFLUCC 17-0830^T		MG828996	MG828880
C. boothii	CBS:381.74^T		AJ875226	NR_159776
C. cateniformis	UTHSC 01-1644^T		HE610329	NR_111517
C. cephalothecoides	L821		KY064030	KY064029
C. coluteae	MFLUCC 17-2299^T		MG137252	MG137251
C. cruciata	FMR 7409		AJ875222	-
C. cymbiformispora	NBRC 32199		LC146726	LC146726
C. cipronana	CBS:144016^T		-	NR_157478
C. decumbens	CBS:153.42^T		NG_067257	NR_144912
C. dendrobiicola	DLCCR7		MK225603	MK225602
C. discoidea	CBS:158.80^T		NG_064120	NR_159779
C. discospora	CBS:168.58		MH869278	MH857740
C. ellipsoidea	CBS:137.68^T		MH870804	MH859091
C. endophytica	AEA 9094^T		EF420069	EF420005
C. euphorbiae	CBS:139768 = 1001^T		-	KP941076
C. extramundana	CBS:247.77^T		MH872828	MH861057
C. fasciculata	CBS:205.38^T		FR691988	NR_154770
C. fibrosae	**CGMCC3.20304^T**	**350271**	**MW750758**	**MW750760**
C. fibrosae	**CX04D1**		**MW750755**	**MW750756**
C. fodinicola	FRL = CBS:136963^T		KF857172	JQ904603
C. gigantospora	ILLS:60816^T		JN684909	JN684909
C. hansenii	CBS:885.68		AJ875223	-
C. hoffmannii	CBS:245.38^T		AF353599	NR_167688
C. iranica	CBS:139767 = 0806^T		-	KP941078
C. krabiensis	MFLU 16-1230^T		MN017892	-
C. leucoplaca	CBS:486.73		MH872465	-
C. ligniaria	98.1105		AF353585	-
C. lignicola	CBS:267.33^T		NG_067344	NR_111520
C. luteorubra	UTHSC 01-20^T		HE610328	HE610330
C. luteoviridis	CBS:206.38^T		NG_067348	NR_154769
C. malacotricha	F2106		AF353589	-
C. marina	MFLUCC 18-0408^T		MK458765	MK458764
C. mutabilis	CBS:157.44^T		NG_042382	NR_111519
C. navarrae	LTA3 = CBS:141016^T		KU762326	KU762326
C. nepalica	NBRC 30584^T		LC146727	LC146727
C. ornata	FMR7415^T		AJ875228	-
C. ostrea	CBS:507.70^T		NG_064080	NR_159772
C. polymorpha	CBS:132722^T		HE863327	NR_121473
C. polysperma	CBS:669.77^T		MH872868	MH861109
C. prunicola	CBS:120875^T		GQ154602	GQ154540
C. pulveracea	CAB683		GQ351559	-
C. punctulata	CBS:159.80		MH873024	MH861254
C. mongoliae	**CGMCC3.20250^T**	**350270**	**MW077646**	**MW077645**
C. rhopalochaeta	CBS:109872^T		GQ351561	-
C. rosae	TASM:6127^T		NG_066204	NR_157509
C. savoryi	CBS:725.74^T		MH872627	MH860890
C. simbalensis	NFCCI:4236^T		MG917738	NR_164024
C. sinensis	**CGMCC3.20306^T**	**350269**	**MW422265**	**MW422269**
C. sordaria	CBS:492.73		MH878380	-
C. subcorticalis	CBS:551.75		AF353593	-

Taxa	Strain	HMAS	GenBank accession number	
			LSU	ITS
C. taeniospora	LTA = CBS:141014[T]		KU762324	KU762324
C. tetraspora	CBS:139.68		MH870806	MH859093
C. velutina	CBS:981.68		MH870991	MH859264
C. velutinosa	Co29		GU553330	GU553327
C. velutinosa	**CGMCC3.20249**		**MW346687**	**MW298866**
C. verticillata	CBS:816.71[T]		AJ875232	NR_159774
C. vineae	KUMCC 17-0322[T]		-	NR_168225
C. canina	UTHSC 11-2460		NG_042720	NR_120211
Zanclospora jonesii	MFLUCC15-1015[T]		NG_067549	KY212753
Paragaeumannomyces garethjonesii	MFLUCC 15-1012[T]		NG_059017	KY212751

Coniochaeta were recovered from these four lichen species. These are CX03C1 and CX04D1 from *Candelaria fibrosa*, 8004b from *Flavoparmelia caperata*, CS-04 and CS-09 from *Ramalina sinensis* and CX37 from *Flavopunctelia flaventior*.

Preliminary identification of these isolates, using the BLAST algorithm, indicated isolates 8004b and CX37 were known *Coniochaeta* species, *C. velutinosa* and *C. acaciae*, respectively, whereas, CX03C1, CX04D1, CS-04 and CS-09 were potentially undescribed species.

Phylogenetic analyses

Both single gene and concatenated datasets were used for phylogenetic analyses using ML and BI approaches. The single gene dataset for ITS included 53 taxa, whereas the LSU had 61 taxa. The concatenated dataset included 65 taxa and 1489 characters including gaps (ITS: 1–655; LSU: 656–1489). Individual gene trees for *Coniochaeta* species had similar topologies and were congruent with the tree generated using the concatenated dataset when taxon sampling overlapped. Bootstrap values < 75% and posterior probability < 0.95 were considered unreliable (Fig. 1, Suppl. material 1 and Suppl. material 2).

In the phylogenetic trees, constructed using the concatenated dataset, isolates CX03C1 and CX04D1 formed a monophyletic clade (Taxon 1) and sister to *C. pulveracea* (Fig. 1). Even though, in the phylogenetic trees using a single gene, isolates of Taxon 1 emerged as a monophyletic clade, yet the sister taxon varied. For ITS, *C. boothii* was found sister to Taxon 1, whereas for LSU, it was *C. pulveracea* (Suppl. material 1: Fig S1 and Suppl. material 2: S2).

In the tree constructed using the concatenated dataset, isolate CX37 (Taxon 2) formed a monophyletic clade with *C. acaciae* with high statistical support. Similar topologies were also observed in the ITS and LSU trees.

The phylogenetic position of isolates CS-04 (Taxon 3) and CS-09 (Taxon 4) substantially varied across the phylogenetic trees. In the trees using the concatenated dataset, isolates CS-04 (Taxon 3) and CS-09 (Taxon 4) nested within a clade that included *C. fasciculata* and *C. vineae* (Fig. 1). In ITS gene trees, isolates CS-04 and CS-09 nested within a clade that included *C. coluteae*, *C. fasciculata* and *C. vineae* (Suppl. material 1). In the LSU trees, isolate CS-04 (Taxon 3) grouped with a clade that included *C. leucoplaca*, *C. cephalothecoides*, *C. endophytica*, *C. prunicola*

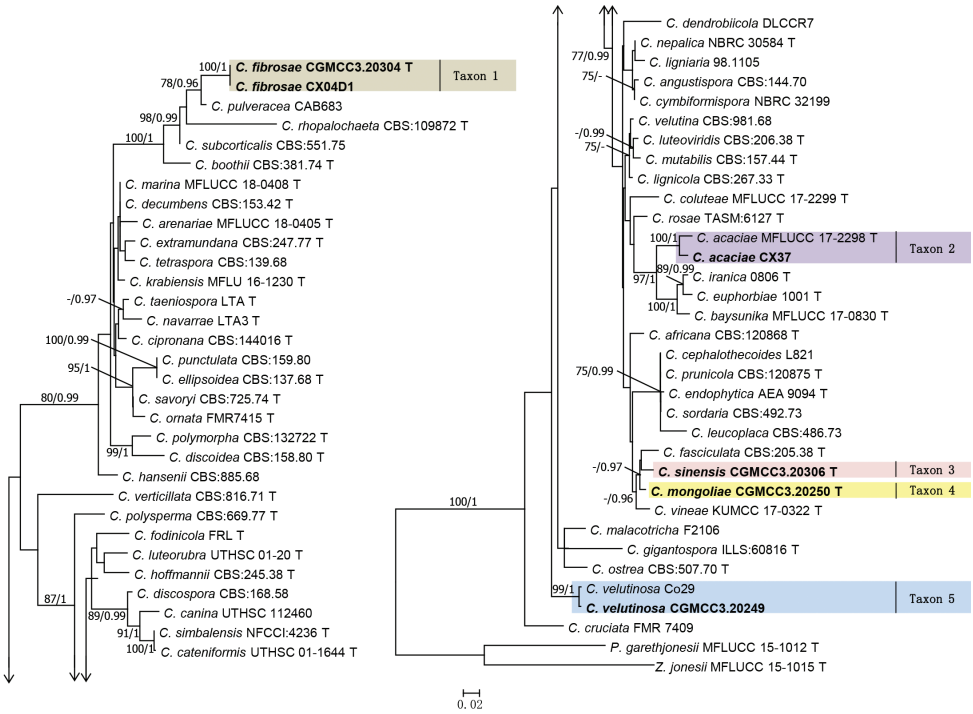

Figure 1. Maximum Likelihood tree constructed using ITS+LSU dataset. Bootstrap support values ≥ 75% and posterior probabilities ≥ 0.95 are indicated above the nodes as ML / PP. The isolates obtained in this study are shown in bold. T = ex-type isolates.

and *C. sordaria* (Suppl. material 2), whereas, isolate CS-09 formed a monophyletic clade with *C. mutabilis* (Suppl. material 2). Irrespective of the trees, the statistical support for all the groups was unreliable.

Irrespective of the datasets and phylogenetic approaches, isolate 8004b (Taxon 5) was grouped with *C. velutinosa* (Asgari and Zare 2006) with high statistical support (Fig. 1, Suppl. material 1 and Suppl. material 2).

Taxonomy

Coniochaeta fibrosae **H. L. Si & Y. M. Su, sp. nov.**
MycoBank No: 839390
Figure 2

Holotype. China, Yunnan Province: Tiesuo township, 26°32'71"N, 100°57'3"E, ca. 2120 m elev., isolated from *Candelaria fibrosa*, 13 Nov 2020, H. L. Si, CX03C1 (HMAS 350271, holotype), ex-type culture CGMCC3.20304.

Etymology. The name relates to the lichen *Candelaria fibrosa* and both isolates of this fungus were isolated from its medulla.

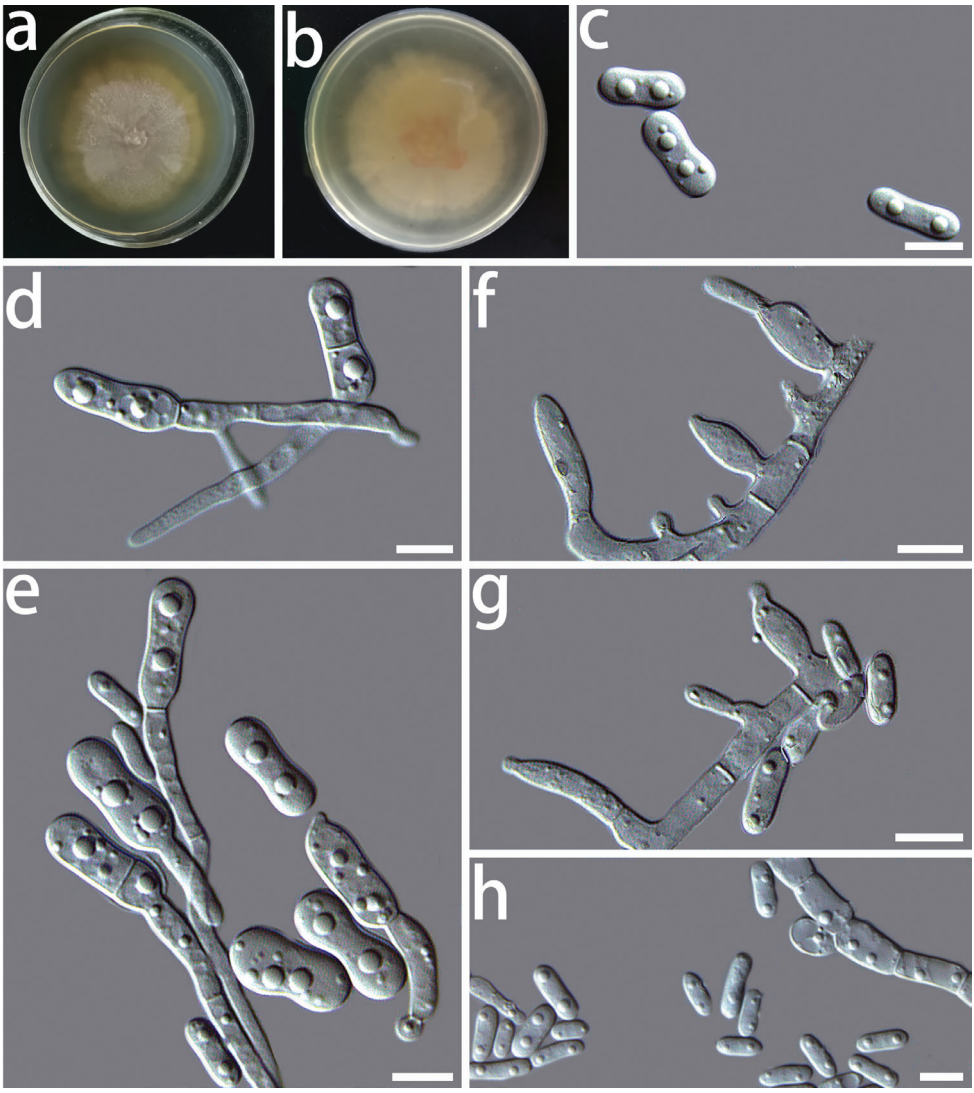

Figure 2. Morphological characters of *Coniochaeta fibrosae* sp. nov. (HMAS 350271) **a, b** cultures on PDA from the surface and reverse **c** swollen conidia **d, e** swollen conidia germinate hyphae **f, g** conidiogenous cells **h** conidia. Scale bars: 10 μm.

Description. Colony on PDA after 8 d, hyphae hyaline, multi-guttulate, septate, smooth-walled; conidiophores short; conidiogenous cells hyaline, phialidic or oval in shape, single or in clusters on short lateral branches, measuring 2.9–7.2 × 1.8–3.7 μm ($\overline{x}$= 4.7 × 2.6 μm, n = 50) (Fig. 2f, g); two types of conidia were observed, swollen conidia were hyaline, one-celled, dumb-bell-shaped, with hyphae emerging from both ends (Fig. 2d, e), measuring 7.6–16.5 × 2.3–4.1 μm ($\overline{x}$ = 9.7 × 3.1 μm, n = 50) (Fig. 2c), oblong conidia were hyaline, one-celled, often oblong to ellipsoidal in shape, measuring 3.4–6.8 × 1.4–2.7 μm ($\overline{x}$ = 4.7 × 1.8 μm, n = 50) (Fig. 2h). Chlamydospores absent. Sexual morph unknown.

Culture characteristics. The optimal temperature for growth was 25 °C on PDA. No growth was detected at 5 and 35 °C. Colonies on PDA after 8 d at 25 °C were white, circular, margin entire, flat, dense, partially immersed in the medium and sticky protuberance at the centre of the colony.

Additional specimen examined. China, Yunnan Province: Tiesuo township, 26°32'71"N, 100°57'3"E, ca. 2120 m elev., isolated from on *Candelaria fibrosa*, 13 Nov 2020, H. L. Si, CX04D1**.**

Notes. In the phylogenetic analyses, both isolates of *C. fibrosae* sp. nov. formed a monophyletic clade, but the sister taxon differed between datasets. These sibling species were either *C. boothii* (ITS) or *C. pulveracea* (LSU and concatenated). Both of these sibling species were described, based on their sexual state and chlamydospores (Manoharachary and Ramarao 1973; Romero et al. 1999; García et al. 2006). However, we did not find sexual reproductive structures in our species. As a result, we were unable to compare the morphology of these species.

***Coniochaeta sinensis* H. L. Si & Y. M. Su, sp. nov.**
MycoBank: 839388
Figure 3

Holotype. China, the Inner Mongolia Autonomous Region: Chifeng City, 44°13'46"N, 118°44'57"E, ca. 1500 m elev., isolated from the medulla of *Ramalina sinensis*, 11 Oct 2019, H. L. Si, CS-04 (HMAS 350269, holotype), ex-type culture CGMCC3.20306.

Etymology. The name relates to the lichen *Ramalina sinensis*, as a single isolate of this fungus was obtained from the medulla of this lichen.

Description. Colony on PDA after 8 d, hyphae hyaline, multi-guttulate, septate, smooth-walled, often hyphal strands consolidating to form bundles, conidiophores short or absent; conidiogenous cells hyaline, phialidic or oval in shape, single or in clusters on short lateral branches, measuring 2.8–7.1 × 1.1–3.7 µm ($\overline{x}$ = 4.2 × 2.3 µm, n = 50) (Fig. 3c–e); conidia hyaline, one-celled, often oblong to ellipsoidal in shape, measuring 2.5–4.6 × 0.7–2.1 µm ($\overline{x}$ = 3.3 × 1.2 µm, n = 50) (Fig. 3g, h); chlamydospore solitary or in short chains, hyaline, thick-walled, elongate ellipsoidal or almost globose in shape, measuring 3.7–6.6 × 2.5–5.4 µm ($\overline{x}$ = 4.8 × 3.7 µm, n = 50) (Fig. 3f). Sexual morph unknown.

Culture characteristics. The optimal temperature for growth is 30 °C. No growth was detected at 5 and 35 °C. Colonies on PDA after 8 d at 30 °C were yellow in the centre and white around the edges, circular, margin entire, flat, dense, partially immersed in the medium, the centre of the colony slightly bulging.

Notes. *Coniochaeta sinensis* sp. nov. clusters with *C. vineae*, *C. fasciculata* and *C. mongoliae* sp. nov. in our phylogenetic tree, constructed using the concatenated dataset, but the statistical support was insignificant. Amongst these species, *C. vineae* is only known in its sexual morph (Hyde et al. 2020). There are, however, significant morphological differences amongst *C. sinensis* sp. nov., *C. fasciculata* and *C. mongoliae* sp. nov. These are (1) the shapes and sizes of conidiogenous cells, (2) the shapes and sizes of conidia and (3) the

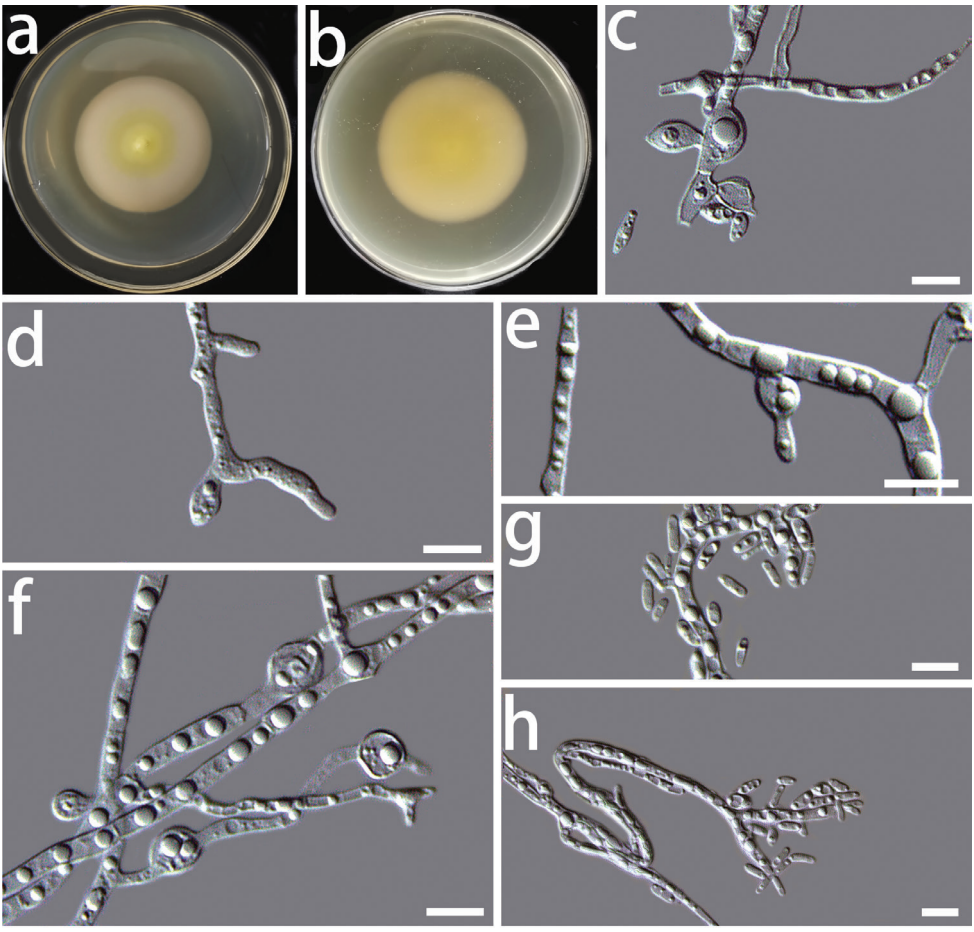

Figure 3. Morphological characters of *Coniochaeta sinensis* sp. nov. (HMAS 350269) **a, b** cultures on PDA from the surface and reverse **c, d** conidiogenous cells **e** conidiogenous cell that is producing conidia **f** chlamydospores **g, h** conidia. Scale bars: 10 μm.

shapes and sizes of chlamydospores. When compared to *C. mongoliae* sp. nov., *C. sinensis* sp. nov. has smaller conidiogenous cells and conidia. The conidia of *C. sinensis* sp. nov. are significantly smaller than those of *C. fasciculata* (Beyma 1939). Aside from that, the chlamydospores of *C. sinensis* sp. nov. are longer than those of *C. mongoliae* sp. nov.

***Coniochaeta mongoliae* H. L. Si & Y. M. Su, sp. nov.**
MycoBank: 839389
Figure 4

Holotype. China, the Inner Mongolia Autonomous Region, Chifeng City, 44°13'46"N, 118°44'57"E, ca. 1500 m elev., isolated from the medulla of *Ramalina*

sinensis, 11 Oct 2019, H. L. Si, CS-09 (HMAS 350270, holotype), ex-type living culture, CGMCC 3.20250.

Etymology. The lichen was collected in the Inner Mongolia Autonomous Region, thus the name.

Description. Colony on PDA after 8 d, hyphae hyaline, multi-guttulate, septate, smooth-walled, often with hyphal strands consolidating to form bundles; conidiophores short or absent; conidiogenous cells hyaline, flask or acicular in shape, measuring 3.3–12.5 × 1.6–5.1 µm ($\bar{x}$ = 6.6 × 2.9 µm, n = 50) (Fig. 4c, d); conidia hyaline, smooth-walled, ellipsoidal, 3.3–8.4 × 0.6–1.9 µm ($\bar{x}$ = 4.8 × 1.3 µm, n = 50) (Fig. 4g

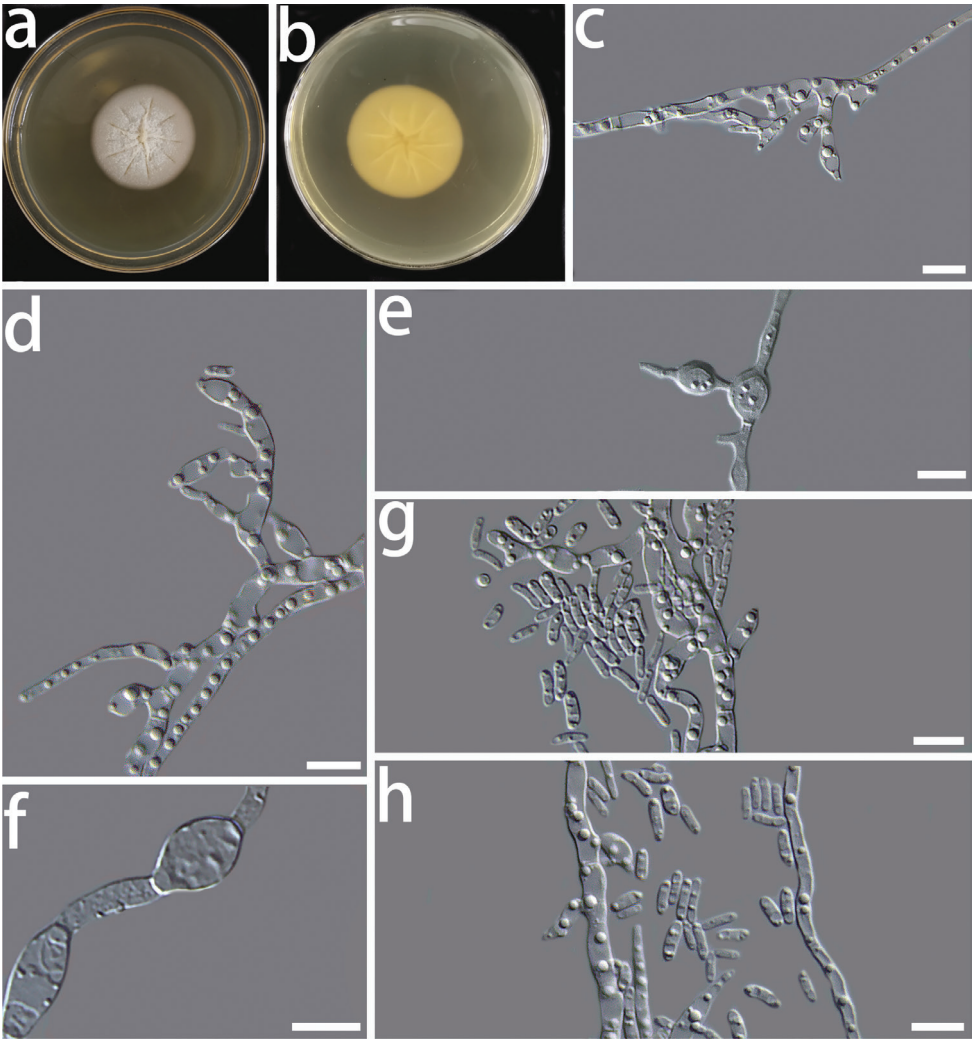

Figure 4. Morphological characters of *Coniochaeta mongoliae* sp. nov. (HMAS 350270) **a, b** cultures on PDA from the surface and reverse, **c, d** conidiogenous cells **e, f** chlamydospores **g, h** conidia. Scale bars: 10 µm.

and h); chlamydospore solitary or in short chains, hyaline, thick-walled, elongate ellipsoidal or almost globose in shape, measuring 2.7–6.7 × 2.6–5.4 μm ($\overline{x}$ = 4.6 × 3.8 μm, n = 50) (Fig. 4e, f). Sexual morph unknown.

Culture characteristics. The optimal temperature for growth is 25 °C. No growth was detected at 5 °C and 35 °C. Colonies on PDA after 8 d at 25 °C were white to light pink in colour, circular, flat, dense, partially immersed in the medium, the centre of the colony is rough, forming radial grooves.

Notes. In the phylogenetic tree using the concatenated dataset, *Coniochaeta mongoliae* sp. nov. clustered in a clade that included *C. sinensis* sp. nov., *C. vineae* and *C. fasciculata*, but with low statistical support. Moreover, these four species have substantial morphological differences (for details, see the notes for *C. sinensis* sp. nov.).

Discussion

In the present study, *Candelaria fibrosa*, *Flavoparmelia caperata*, *Flavopunctelia flaventior* and *Ramalina sinensis* were collected from the Yunnan and Inner Mongolia Regions of China between 2017 and 2020. We isolated six *Coniochaeta* isolates from these lichens, which we classified into five species. Two of these were previously-described species, while the other three were unknown. Here, we describe these three previously-unknown species as *C. fibrosae* sp. nov., *C. sinensis* sp. nov. and *C. mongoliae* sp. nov.

The majority of species in the genus *Coniochaeta* are saprophytes or pathogens of plants and humans, while many others have an unknown ecological function (Harrington et al. 2019). Species of *Coniochaeta* are frequently isolated from asymptomatic tissues of woody plants and lichens throughout temperate and northern North America (Del Olmo-Ruiz 2012). Some of these species were found exclusively on plants or lichens, such as *C. endophytica* and *C. hoffmannii*, respectively (Zhang et al. 2016; Harrington et al. 2019) or on both, such as *Coniochaeta* sp. Clade 9 (Del Olmo-Ruiz 2012). The two previously-described species recovered in this study (*C. acaciae* and *C. velutinosa*) were also isolated from barley leaves in Iran (Asgari and Zare 2006) and dead *Acacia* species branches in Uzbekistan (Samarakoon et al. 2018). This demonstrates *Coniochaeta*'s ability to thrive in a variety of habitats, yet their ecological role in all these environments is still largely unknown.

The lack of sequences for protein-coding gene regions is one of the pitfalls in identifying taxa in the genus *Coniochaeta*. For the majority of species, only ITS and LSU sequences are currently available. Sequences for the largest subunit of RNA polymerase II (rpb1), the second-largest subunit of RNA polymerase II (rpb2), translation elongation factor 1-alpha (tef1) or β-tubulin gene (tub2) were only used in a few studies involving a limited number of species (Spatafora et al. 2006; Voglmayr et al. 2016; Samarakoon et al. 2018; Harrington et al. 2019). Due to the paucity of sequences, we could not include those gene regions in this study. Moreover, even after repeated attempts, we could not amplify the rpb1, rpb2 and tub2 gene regions for the species isolated in this study. Con-

sequently, there is an urgent need for primers that can successfully amplify protein-coding genes from a wide variety of taxa in order to demystify the taxonomy for this genus.

In this study, we identified the isolate CX37 as *Coniochaeta acaciae*. This is because, in the phylogenies using both concatenated and single-gene datasets, isolate CX37 and ex-type sequences of *C. acaciae* grouped into a monophyletic clade. However, pair-wise comparison of gene regions showed there were at least 15 bps (ITS) and 6 bps (LSU) differences between CX37 and ex-type sequences of *C. acaciae* (Samarakoon et al. 2018). Moreover, following the protocol suggested by Damm et al. (2010) and Harrington et al. (2019), we could not induce ascomata formation in the isolate CX37. This hindered us from comparing the sexual structures of this species. In the future, the discovery of more isolates of *C. acaciae* will allow us to clarify the taxonomy of this species.

In the present study, through repeated sampling, we isolated five *Coniochaeta* species associated with four lichen species in China. Amongst these, three were previously-undescribed species. Data emerging from this study substantially augmented our current knowledge on the diversity and host range of this genus in China and globally. However, our surveys were exclusively conducted in two Provinces in China. Currently, more surveys should be conducted in various ecoregions of China to catalogue the diversity of *Coniochaeta* and various other endolichenic fungi.

Acknowledgements

This study was funded by The National Natural Science Foundation of China (Grant# 31600100). Thanks to Prof. Li-Song Wang from Kunming Institute of Botany, Chinese Academy of Sciences and Prof. Zun-Tian Zhao from Shandong Normal University for their assistance with the identification of lichens.

References

Ahmadjian V (1993) The lichen symbiosis. John Wiley & Sons Inc, 250 pp.

Altschul SF, Gish W, Miller W, Myers EW, Lipman DJ (1990) Basic local alignment search tool. Jorunal of Molecular Biology 215: 403–410. http://dx.doi.org/10.1006/jmbi.1990.9999

Arnold AE, Jolanta Miadlikowska, K. Lindsay Higgins, Snehal D. Sarvate, Paul Gugger, Amanda Way, Valérie Hofstetter, Frank Kauff, Lutzoni F (2009) A phylogenetic estimation of trophic transition networks for Ascomycetous fungi: are lichens cradles of symbiotrophic fungal diversification? Systematic Biology 58: 283–297. https://doi.org/10.1093/sysbio/syp001

Asgari B, Zare R (2006) Two new *Coniochaeta* species from Iran. Nova Hedwigia Band 82: 227–236. http://dx.doi.org/10.1127/0029-5035/2006/0082-0227

Asgari B, Zare R, Gams W (2007) *Coniochaeta ershadii*, a new species from Iran, and a key to well-documented *Coniochaeta* species. Nova Hedwigia 84: 175–187. http://dx.doi.org/10.1127/0029-5035/2007/0084-0175

Beyma FH van (1939) Beschreibung einiger neuer Pilzarten aus dem Centraalbureau voor Schimmelcultures Baarn (Holland). V. Mitteilung. Zentralblatt für Bakteriologie und Parasitenkunde, Abteilung 2. 99: 381–394.

Chang Jong-How, Wang Yei-Zeng (2011) Taxonomy of *Coniochaeta leucoplaca* and *C. velutina*: morphological and molecular studies based on LSU rDNA of isolates from Taiwan. Nova Hedwigia 92: 57–67. https://doi.org/10.1127/0029-5035/2011/0092-0057

Checa J (1988) The genus *Coniochaeta* (Sacc.) Cooke (Coniochaetaceae, Ascomycotina) in Spain. Crypt Mycol 9(1): 1–34.

Damm U, Fourie PH, Crous PW (2010) *Coniochaeta* (*Lecythophora*), *Collophora* gen. nov. and *Phaeomoniella* species associated with wood necroses of Prunus trees. Persoonia - Molecular Phylogeny and Evolution of Fungi 24: 60–80. https://doi.org/10.3767/003158510X500705

Del Olmo-Ruiz M (2012) Diversity, distributions, and host affiliations of fungal endophytes associated with seedless vascular plants. PhD Thesis, University of Arizona, Arizona.

García D, Stchigel AM, Cano J, Calduch M, Hawksworth DL, Guarro J (2006) Molecular phylogeny of Coniochaetales. Mycological Research 110: 1271–1289. https://doi.org/10.1016/j.mycres.2006.07.007

Harrington AH, Olmo-Ruiz M, U'Ren JM, Garcia K, Arnold AE (2019) *Coniochaeta endophytica* sp. nov., a foliar endophyte associated with healthy photosynthetic tissue of Platycladus orientalis (Cupressaceae). Plant and Fungal Systematics 64: 65–79. https://doi.org/10.2478/pfs-2019-0008

Hawksworth DL (2011) A new dawn for the naming of fungi: impacts of decisions made in Melbourne in July 2011 on the future publication and regulation of fungal names. IMA Fungus 2: 155–162. https://doi.org/10.3897/mycokeys.1.2062

Hoog Gd, Guarro J, Gene J, Figueras M (2000) Atlas of clinical fungi 2nd ed. Baard-Delft: Centraalbureau vor Schimmelcultures/Universitat Rovira Virgili.

Hyde KD, Dong Y, Phookamsak R, Jeewon R, Bhat DJ, Jones EBG, Liu N-G, Abeywickrama PD, Mapook A, Wei D, Perera RH, Manawasinghe IS, Pem D, Bundhun D, Karunarathna A, Ekanayaka AH, Bao D-F, Li J, Samarakoon MC, Chaiwan N, Lin C-G, Phutthacharoen K, Zhang S-N, Senanayake IC, Goonasekara ID, Thambugala KM, Phukhamsakda C, Tennakoon DS, Jiang H-B, Yang J, Zeng M, Huanraluek N, Liu J-K, Wijesinghe SN, Tian Q, Tibpromma S, Brahmanage RS, Boonmee S, Huang S-K, Thiyagaraja V, Lu Y-Z, Jayawardena RS, Dong W, Yang E-F, Singh SK, Singh SM, Rana S, Lad SS, Anand G, Devadatha B, Niranjan M, Sarma VV, Liimatainen K, Aguirre-Hudson B, Niskanen T, Overall A, Alvarenga RLM, Gibertoni TB, Pfliegler WP, Horváth E, Imre A, Alves AL, da Silva Santos AC, Tiago PV, Bulgakov TS, Wanasinghe DN, Bahkali AH, Doilom M, Elgorban AM, Maharachchikumbura SSN, Rajeshkumar KC, Haelewaters D, Mortimer PE, Zhao Q, Lumyong S, Xu J, Sheng J (2020) Fungal diversity notes 1151–1276: taxonomic and phylogenetic contributions on genera and species of fungal taxa. Fungal Diversity 100: 5–277. https://doi.org/10.1007/s13225-020-00439-5

Kamiya S, Uchiyama S, Udagawa SI (1995) Two new species of *Coniochaeta* with a cephalothecoid peridium wall. Mycoscience 36: 377–383. https://doi.org/10.1007/BF02268619

Katoh K, Standley DM (2013) MAFFT multiple sequence alignment software version 7: improvements in performance and usability. Molecular Biology and Evolution 30: 772–780. https://doi.org/10.1093/molbev/mst010

Khan Z, Gené J, Ahmad S, Cano J, Al-Sweih N, Joseph L, Chandy R, Guarro J (2013) *Coniochaeta polymorpha*, a new species from endotracheal aspirate of a preterm neonate, and transfer of *Lecythophora* species to *Coniochaeta*. Antonie van Leeuwenhoek 104: 243–252. https://doi.org/10.1007/s10482-013-9943-z

Kumar S, Stecher G, Tamura K (2016) MEGA7: Molecular evolutionary genetics analysis version 7.0 for bigger datasets. Molecular Biology and Evolutionl 33: 1870–1874. https://doi.org/10.1093/molbev/msw054

Lawrey JD, Diederich P (2003) Lichenicolous fungi: interactions, evolution, and biodiversity. Bryologist 106: 80–120. https://doi.org/10.1093/molbev/msw054

Manoharachary C, Ramarao P (1973) *Thielavia boothii* sp. nov. from pond mud. Transactions of the British Mycological Society 61: 196–198. https://doi.org/10.1016/S0007-1536(73)80105-6

Miller MA, Pfeiffer WT, Schwartz T (2010) Creating the CIPRES science gateway for inference of large phylogenetic trees. In: 2010 Gateway Computing Environments Workshop (GCE), 2010, 1–8. https://doi.org/10.1109/GCE.2010.5676129

Nash, Thomas H (2008) Lichen biology. University Press, Cambridge, 498 pp. https://doi.org/10.1017/CBO9780511790478

Nasr S, Bien S, Soudi MR, Alimadadi N, Fazeli SS, Damm U (2018) Novel *Collophorina* and *Coniochaeta* species from *Euphorbia polycaulis* , an endemic plant in Iran. Mycological Progress 17: 755–771. https://doi.org/10.1007/s11557-018-1382-9

Nelsen MP, Lücking R, Boyce CK, Lumbsch HT, Ree RH (2020) No support for the emergence of lichens prior to the evolution of vascular plants. Geobiology 18: 3–13. https://doi.org/10.1111/gbi.12369

Nylander J, Wilgenbusch JC, Dan LW, Swofford DL (2008) AWTY (Are We There Yet?): A system for graphical exploration of MCMC convergence in Bayesian phylogenetics. Bioinformatics 24: 581–583. https://doi.org/10.1093/bioinformatics/btm388

Perdomo H, Garcia D, Gene J, Cano J, Sutton DA, Summerbell R, Guarro J (2013) *Phialemoniopsis*, a new genus of Sordariomycetes, and new species of *Phialemonium* and *Lecythophora*. Mycologia 105: 398–421. https://doi.org/10.3852/12-137

Raja HA, Fournier J, Shearer CA, Miller AN (2012) Freshwater ascomycetes: *Coniochaeta gigantospora* sp. nov. based on morphological and molecular data. Mycoscience 53: 373–380. https://doi.org/10.1007/s10267-012-0181-4

Rambaut A (2009) FigTree v1. 3.1. http://tree bio ed ac uk/software/figtree/

Rasband W (1997) ImageJ, US National Institutes of Health, Bethesda, Maryland, USA. http://imagej.nih.gov/ij

Réblová M, Miller AN, Rossman AY, Seifert KA, Crous PW, Hawksworth DL, Abdel-Wahab MA, Cannon PF, Daranagama DA, De Beer ZW, Huang S-K, Hyde KD, Jayawardena R, Jaklitsch W, Jones EBG, Ju Y-M, Judith C, Maharachchikumbura SSN, Pang K-L, Petrini LE, Raja HA, Romero AI, Shearer C, Senanayake IC, Voglmayr H, Weir BS, Wijayawarden NN (2016) Recommendations for competing sexual-asexually typified generic names in Sordariomycetes (except Diaporthales, Hypocreales, and Magnaporthales). IMA Fungus 7: 131–153. https://doi.org/10.5598/imafungus.2016.07.01.08

Romero AI, Carmaran CC, Lorenzo LE (1999) A new species of *Coniochaeta* with a key to the species known in Argentina. Mycological Research 103: 689–695. https://doi.org/10.1017/S0953756298007564

Ronquist F, Teslenko M, van der Mark P, Ayres DL, Darling A, Höhna S, Larget B, Liu L, Suchard MA, Huelsenbeck JP (2012) MrBayes 3.2: efficient Bayesian phylogenetic inference and model choice across a large model space. Systematic Biology 61: 539–542. https://doi.org/10.1093/sysbio/sys029

Samarakoon MC, Gafforov Y, Liu N, Maharachchikumbura S, Bhat JD, Liu JK, Promputtha I, Hyde KD (2018) Combined multi-gene backbone tree for the genus *Coniochaeta* with two new species from Uzbekistan. Phytotaxa 336: 43–58. https://doi.org/10.11646/phytotaxa.336.1.3

Schneider CA, Rasband WS, Eliceiri KW (2012) NIH Image to ImageJ: 25 years of image analysis. Nature Methods 9: 671–675. https://doi.org/10.1038/nmeth.2089

Spatafora JW, Sung GH, Johnson D, Hesse C, O'Rourke B, Serdani M, Spotts R, Lutzoni F, Hofstetter V, Miadlikowska J (2006) A five-gene phylogeny of Pezizomycotina. Mycologia 98: 1018–1028. https://doi.org/10.1080/15572536.2006.11832630

Stamatakis A (2006) RAxML-VI-HPC: maximum likelihood-based phylogenetic analyses with thousands of taxa and mixed models. Bioinformatics 22: 2688–2690. https://doi.org/10.1093/bioinformatics/btl446

Stamatakis A, Hoover P, Rougemont J (2008) A rapid bootstrap algorithm for the RAxML web servers. Systematic Biology 57: 758–771. https://doi.org/10.1080/10635150802429642

Suryanarayanan TS, Thirunavukkarasu N (2017) Endolichenic fungi: the lesser known fungal associates of lichens. Mycology 8: 189–196. https://doi.org/10.1080/21501203.2017.1352048

Tripathi M, Joshi Y (2019) What are lichenized fungi? In: Endolichenic Fungi: Present and Future Trends. Springer, Singapore, 1–26. https://doi.org/10.1007/978-981-13-7268-1_1

Troy GC, Panciera DL, Phillip PJ, Sutton DA, Josepa G, Cano JF, Josep G, Thompson EH, Wickes BL (2013) Mixed infection caused by *Lecythophora canina* sp. nov. and *Plectosphaerella cucumerina* in a German shepherd dog. Medical mycology: official publication of the International Society for Human and Animal Mycology 51 (5): 455–460. https://doi.org/10.3109/13693786.2012.754998

Vazquez-Campos X, Kinsela A, Waite T, Collins R, Neilan B (2014) *Fodinomyces uranophilus* gen. nov. sp. nov. and *Coniochaeta fodinicola* sp. nov., two uranium mine-inhabiting Ascomycota fungi from northern Australia. Mycologia 106: 1073–1089. https://doi.org/10.3852/14-013

Vilgalys R, Hester M (1990) Rapid genetic identification and mapping of enzymatically amplified ribosomal DNA from several *Cryptococcus* species. Journal of Bacteriology 172: 4238–4246. https://doi.org/10.1128/jb.172.8.4238-4246.1990

Voglmayr, Hermann, Friebes, Gernot, Jaklitsch, Walter M, Garcia, Susana (2016) *Lopadostoma taeniosporum* revisited and a new species of *Coniochaeta*. Sydowia 68: 87–97. https://doi.org/10.1016/j.simyco.2017.05.001

Weber E (2002) The *Lecythophora-Coniochaeta* complex: I. Morphological studies on *Lecythophora* species isolated from *Picea abies*. Nova Hedwigia 74: 159–185. https://doi.org/10.1127/0029-5035/2002/0074-0159

White TJ, Bruns T, Lee S, Taylor J (1990) Amplification and direct sequencing of fungal ribosomal RNA genes for phylogenetics. In: Innis MA, Gelfand DH, Sninsky JJ, White TJ (Eds) PCR Protocols. Academic Press, San Diego, 315–322. https://doi.org/10.1016/B978-0-12-372180-8.50042-1

Zhang T, Wei X-L, Wei Y-Z, Liu H-Y, Yu L-Y (2016) Diversity and distribution of cultured endolichenic fungi in the Ny-Ålesund Region, Svalbard (High Arctic). Extremophiles 20: 461–470. https://doi.org/10.1007/s00792-016-0836-8

Supplementary material 1

Figure S1. ML tree generated from ITS sequence data

Authors: Hong-Li Si, Yue-Min Su, Xiao-Xiao Zheng, Meng-Yao Ding, Tanay Bose, Run-Lei Chang

Data type: Pdf. file

Explanation note: Maximum Likelihood tree constructed using ITS dataset. Bootstrap support values ≥ 75% and posterior probabilities ≥ 0.95 are indicated above the nodes as ML / PP. The isolates obtained in this study are shown in bold. T = ex-type isolates.

Link: https://doi.org/10.3897/mycokeys.83.71140.suppl1

Supplementary material 2

Figure S2. ML tree generated from LSU sequence data

Authors: Hong-Li Si, Yue-Min Su, Xiao-Xiao Zheng, Meng-Yao Ding, Tanay Bose, Run-Lei Chang

Data type: Pdf. file

Explanation note: Maximum Likelihood tree constructed using LSU dataset. Bootstrap support values ≥ 75% and posterior probabilities ≥ 0.95 are indicated above the nodes as ML / PP. The isolates obtained in this study are shown in bold. T = ex-type isolates.

Link: https://doi.org/10.3897/mycokeys.83.71140.suppl2

MycoKeys 83: 123–144 (2021)
doi: 10.3897/mycokeys.83.68582
https://mycokeys.pensoft.net

RESEARCH ARTICLE

A peer-reviewed open-access journal
MycoKeys
Launched to accelerate biodiversity research

Three new species of *Rhytidhysteron* (Dothideomycetes, Ascomycota) from Mexico

Aurora Cobos-Villagrán[1], Ricardo Valenzuela[1], César Hernández-Rodríguez[2], Rosa Paulina Calvillo-Medina[5], Lourdes Villa-Tanaca[2], Luz Elena Mateo-Cid[3], Abigail Pérez-Valdespino[4], César Ramiro Martínez-González[6], Tania Raymundo[1]

1 *Instituto Politécnico Nacional, Escuela Nacional de Ciencias Biológicas, Laboratorio de Micología, Prolongación de Carpio y Plan de Ayala s/n, Mexico City 11340, Mexico* **2** *Instituto Politécnico Nacional, Escuela Nacional de Ciencias Biológicas, Laboratorio Experimental de Bacterias y Levaduras, Prolongación de Carpio y Plan de Ayala s/n, Mexico City 11340, Mexico* **3** *Instituto Politécnico Nacional, Escuela Nacional de Ciencias Biológicas, Laboratorio de Ficología, Prolongación de Carpio y Plan de Ayala s/n, Mexico City 11340, Mexico* **4** *Instituto Politécnico Nacional, Escuela Nacional de Ciencias Biológicas, Laboratorio de Ingeniería Genética, Prolongación de Carpio y Plan de Ayala s/n, Mexico City 11340, Mexico* **5** *Facultad de Química, Universidad Autónoma de Querétaro, Cerro de las Campanas s/n, Querétaro 76010, Mexico* **6** *Universidad Autónoma Chapingo, Departamento de Fitotecnia, Instituto de Horticultura, Km 38.5 Carretera Federal México-Texcoco, Texcoco, Estado de México 56230, Mexico*

Corresponding author: Tania Raymundo (traymundoo@ipn.mx)

Academic editor: Cecile Gueidan | Received 12 May 2021 | Accepted 9 August 2021 | Published 14 September 2021

Citation: Cobos-Villagrán A, Valenzuela R, Hernández-Rodríguez C, Calvillo-Medina RP, Villa-Tanaca L, Mateo-Cid LE, Pérez-Valdespino A, Martínez-González CR, Raymundo T (2021) Three new species of *Rhytidhysteron* (Dothideomycetes, Ascomycota) from Mexico. MycoKeys 83: 123–144. https://doi.org/10.3897/mycokeys.83.68582

Abstract

The genus *Rhytidhysteron* is characterised by forming navicular to apothecial hysterothecia, exposing the green, yellow, orange, red, vinaceous or black colours of the hymenium which generally releases pigments in the presence of KOH. The exciple is smooth or striated, the asci bitunicate and ascospores have 1–5 transverse septa. To date, twenty-six *Rhytidhysteron* species have been described from the Tropics. The present study aims to describe three new species in the Neotropics of Mexico based on molecular methods and morphological features. Illustrations and a taxonomic key are provided for all known species of this genus. *Rhytidhysteron cozumelense* from the Isla Cozumel Biosphere Reserve, *R. esperanzae* from the Sierra Juárez, Oaxaca and *R. mesophilum* from the Sierra Madre Oriental, Hidalgo are described as new species. With the present study, the number of species of *Rhytidhysteron* known from Mexico is now increased to eight.

Keywords

Hysteriaceae, Hysteriales, Neotropic, phylogeny, taxonomy

Introduction

The genus *Rhytidhysteron* was described by Spegazzini (1881) and has been shown to belong to the Hysteriaceae (Boehm et al. 2009a, 2009b; Wijayawardene et al. 2020). The genus is characterised by forming hysterothecia, with lenticular or irregular, striated, or smooth openings; epithecium of various colours; excipulum composed of 1–2 layers of cells of angularis texture or globose texture. *Rhytidhysteron* presents dense hamathecium, composed of branched pseudo-paraphyses, enclosed in a gelatinous matrix; octosporic, bitunicate, cylindrical asci; 1–3 septa ascospores, constricted in the central septum, reddish-brown to brown (Spegazzini 1881; Samuels and Müller 1979; Kutorga and Hawksworth 1997; Boehm et al. 2009b; Thambugala et al. 2016).

The distribution of the genus is Pantropical. It has been reported as an endophytic fungus (Rashmi et al. 2019) and causes mycosis in humans (Chowdhary et al. 2008; Mishra et al. 2014; Mahajan et al. 2014; Chander et al. 2016).

The species with the largest distribution is *Rhytidhysteron rufulum*. It has been described from various places, with slight morphological differences depending on where it was found. *R. rufulum* have hysterothecia 1500–2000 µm long, ascospores of (19–)26–36(–43) µm and the colour of the red epithecium in Melzer's Reagent changes to bright orange (Samuels and Müller 1979). According to Kutorga and Hawksworth (1997), the length of the hysterothecia ranges from 2500–4000 µm, ascospores from (22–)25–35(–39) µm and has dark brown to reddish epithecium in potassium hydroxide (KOH) which changes to pale greenish-brown or from red wine to intense pink. On the other hand, in the description made by Almeida et al. (2014), the size of the ascomata ranges from 800–2500 µm, ascospores from 21–32 µm and has black or red epithecium without extractable KOH pigment. The specimens from Thailand have ascomata from 900–2350 µm, ascospores from 28–36 µm and black or red epithecium are not reported to have a reaction with any reagent (Thambugala et al. 2016). Finally, Cobos-Villagrán et al. (2020), for the Mexican specimens, report ascomata of 1000–3000 µm, ascospores of 22.4–30.4 µm and orange-reddish, yellow or black epithecia changing to magenta in reaction with KOH. These morphological variations within *R. rufulum* have caused confusion in various fungal collections around the world and, as a result, they have been grouped into a complex of species (Boehm et al. 2009b; Murillo et al. 2009; Yacharoen et al. 2015; Doilom et al. 2016; Thambugala et al. 2016; Soto-Medina and Lücking 2017).

Twenty-six species are known worldwide according to the Fungorum Index (2021) and, in the last two years, it has had greater relevance, since at least seven species have been described. In the present work, morphological and molecular analyses of distinct specimens of *Rhytidhysteron* obtained from different locations in Mexico were performed. Phylogenetic relationships were inferred based on internal transcribed spacer (ITS), nuclear large subunit ribosomal DNA (LSU) and elongation factor 1-alpha (tef1). Additionally, a dichotomous key is provided with all the species described so far.

Materials and methods

Study zone

The specimens have been found from three different sites: one from Cozumel Island Biosphere Reserve, Quintana Roo, which is located between coordinates 20°35'20" and 20°17'16" north latitude (N) and –86°43'55" and –87°00'07" west longitude (W). The climate, according to the Köppen system, modified by García (1981), is of the AmW (I) type, warm humid with abundant rain in summer. The average annual temperature is 25.5 °C. Average annual rainfall is 1570 mm (INEGI 2013; García-Martínez et al. 2021). The type of vegetation present in the town of San Gervasio is tropical dry forest, at 0 m above sea level.

The second specimen from La Esperanza, Santiago Comaltepec, Chinantla was collected from the Sierra de Juárez in the State of Oaxaca, between coordinates 17°32' and 17°44' north latitude (N) and –96°16' and –96°36' west longitude (W); altitude between 100 and 3200 m a.s.l. La Esperanza presents different types of climates, the main ones, according to the Köppen system, modified by García (1981), are temperate humid with abundant rain in summer, C (m) and semi-warm humid with rain all year round. The temperature range is 10–26 °C. The range of precipitation is 800–4000 mm (INEGI 2008). The type of vegetation present in the town of La Esperanza is tropical cloud forest, at 1600 m a.s.l.

The last of the specimens is from Laguna de Atezca, Molango de Escamilla, which is located in the Sierra Madre Oriental in the State of Hidalgo, between the coordinates 20°42' and 20°59' of north latitude (N) and –98°41' and –98°53' of West longitude (W), altitude between 300 and 2200 m a.s.l. The Laguna de Atezca presents different types of climates, the main ones, according to the Köppen system, modified by García (1981), are semi-warm humid with rain throughout the year, ACf and temperate humid with abundant rain in summer, C (m). The average annual temperature is 17 °C. Average annual rainfall is 1438 mm (INEGI 2009). The type of vegetation present in the town of Laguna de Atezca is tropical cloud forest, at 1281 m a.s.l.

Morphological study

The specimens were obtained by searching for dry or fallen branches in each of the localities. The material was examined following traditional techniques in mycology (Cifuentes et al. 1986). Photographs were taken using a digital camera (Nikon, D7000, Tokyo, Japan) with an 85 mm macro lens (Nikon, Tokyo, Japan). The fresh collected specimens were used to obtain morphological data such as the colour of the epithecium, growth habit and habitat. Ascomata were measured by a stereomicroscope (Zeiss 475002, Jena, Germany). Cross sections were made in the middle part of the ascomata and mounted on temporary slides in 70% alcohol and 10% KOH. Sections were observed under an optical microscope (Zeiss K-7, Jena, Germany) for the measurement of the characters of taxonomic importance.

DNA extraction, amplification and sequencing

The DNA of each specimen of *Rhytidhysteron* spp. was obtained using the cetyltrimethylammonium bromide (CTAB) method, according to Doyle and Doyle (1987). Three molecular markers were used, the ribosomal large subunit (LSU), the internal transcribed spacer rDNA-ITS1 5.8S rDNA-ITS2 (ITS) and translation elongation translation factor 1-α (*tef1*). The primers used for LSU were LOR0f and LR5r (Vilgalys and Hester 1990), for ITS, these were ITS1f and ITS4r (White et al. 1990; Schoch et al. 2012) and *tef1* EF1-B-F1 and EF1-B-R (Wu et al. 2014). DNA amplifications were performed in a GeneAmp PCR System 9700 thermal cycler (Thermo Fisher Scientific), following recommendations by White et al. (1990) for ITS, Vilgalys and Hester (1990) for LSU and Wu et al. (2014) for *tef1*. The PCR products were verified by agarose gel electrophoresis. The gels were run for 1 h at 95 V cm^{-3} in 1.5% agarose and 1× TAE buffer (Tris Acetate-EDTA). The products were then dyed with GelRed (Biotium, USA) and viewed in a transilluminator (Infinity 300 Vilber, Loumat, Germany). Finally, the products were purified using the ExoSap Kit (Affymetrix, USA) according to the manufacturer´s instructions and were prepared for the sequencing reaction using the BigDye Terminator Cycle Sequencing Kit v. 3. 1 (Applied BioSystems). Sequencing was carried out in a genetic analyser (Sanger sequencing) by Macrogen Inc. (Seoul, Korea). The sequences of both strains of each sample were analysed, edited and assembled using BioEdit v. 1.0.5 (Hall 1999) to create consensus sequences. The consensus sequences were compared with those in the GenBank database of the National Center for Biotechnology Information (NCBI) using the BLASTN 2.2.19 tool (Zhang et al. 2000).

Phylogenetic analyses

In order to study phylogenetic relationships, our newly produced sequences of six individuals of *Rhytidhysteron* were added to reference sequences of ITS, LSU and *tef1* (Table 1) deposited in the NCBI database (http://www.ncbi.nlm.nih.gov/genbank/). Each gene region was independently aligned using the online version of MAFFT v7 (Katoh et al. 2002, 2017; Katoh and Standley 2013). Alignments were reviewed in PhyDE (Müller et al. 2005), followed by minor manual adjustments to ensure character homology between taxa. The matrices were formed for ITS by 28 taxa (667 characters), for LSU by 31 taxa (875 characters); while the *tef1* consisted of 24 taxa (896 characters). *Gloniopsis calami* was used as the outgroup. The aligned matrices were concatenated into a single matrix (31 taxa, 2438 characters). Five partitioning schemes were established: one for the ITS, one for the LSU, and three to represent the three codon positions of the *tef1* gene region, which were established using the option to minimize the stop codons with Mesquite v3.2 (Maddison and Maddison 2017). The best evolutionary model for alignment was sought using PartitionFinder (Lanfear et al. 2014, 2017; Frandsen et al. 2015). Phylogeny

Table 1. Species names, strain numbers, isolation source, locality and GenBank accession numbers for the taxa used in this phylogenetic analysis. Sequences generated for this study are in bold.

Species	Isolate No.	LSU	ITS	*tef1*	Source and Locality
Rhytidhysteron bruguierae	MFLUCC 17–1502	MN632453.1	MN632458.1	MN635662.1	Dead stems of *Chromolaena odorata*, Thailand
R. bruguierae	MFLUCC 17–1509	MN632455.1	MN632460.1	-	Dead stems of *Chromolaena odorata*, Thailand
R. bruguierae	MFLUCC 17–1511	MN632454.1	MN632459.1	-	Dead stems of *Chromolaena odorata*, Thailand
R. bruguierae	MFLUCC 17–1515	MN632452.1	MN632457.1	MN635661.1	Dead stems of *Chromolaena odorata*, Thailand
*R. bruguierae**	MFLU 18–0571	NG_068292.1	-	MN077056.1	Submerged branches of *Bruguiera* sp. Thailand
R. camporesii	KUN-HKAS 104277	MN429072.1	MN429069.1	MN442087.1	Dead stems, China
R. chromolanae	MFLUCC 17–1516	MN632456.1	MN632461.1	MN635663.1	Dead stems of *Chromolaena odorata*, Thailand
R. cozumelense	**A. Cobos-Villagrán 951**	**MW9394459**	**MZ056797**	**MZ457338**	**Dead twigs of *Tabebuia rosea*, Mexico**
R. cozumelense	**T. Raymundo 7321**	**MW9394460**	**MZ056798**	**MZ457339**	**Dead twigs of *Tabebuia rosea*, Mexico**
R. erioi	MFLU 16–0584	MN429071.1	MN429068.1	MN442086.1	Dead stems, Thailand
R. esperanzae	**T. Raymundo 6579**	**MW9394457**	**MZ477203**	**MZ457336**	**Dead stems Mexico**
R. esperanzae	**R. Valenzuela 17206**	**MW9394458**	**MZ477204**	**MZ457337**	**Dead stems Mexico**
R. hysterinum	EB 0351	GU397350.1	-	GU397340.1	Dead branches, France
R. hongheense	KUMCC 20–0222	MW264193.1	MW264214.1	MW256815.1	Dead twigs of *Dodonaea*, China
R. hongheense	HKAS112348	MW541820.1	MW541824.1	MW556132.1	Dead twigs of *Dodonaea*, China
*R. magnoliae**	MFLUCC 18–0719	MN989384.1	NR_170019.1	MN997309.1	Dead twigs of *Magnolia grandiflora*, China
*R. mangrovei**	MFLU 18–1894	NG_067868.1	NR_165548.1	MK450030.1	Dead twigs of mangrove, Thailand
R. mesophilum	**A. Trejo 74**	**MW9394461**	**MZ056799**	**MZ457340**	**Dead stems, México**
R. mesophilum	**A. Cobos-Villagrán 1800**	**MW939462**	**MZ056800**	**MZ457341**	**Dead stems, México**
*R. mexicanum**	RV17107.1	MT626026	MT626028	-	Dead wood, Mexico
R. mexicanum	RV17107.2	MT626027	MT626029	-	Dead wood, Mexico
*R. neorufulum**	MFLUCC 13–0216	NG_059649.1	NR_164242.1	KU510400.1	Dead wood, Thailand
R. neorufulum	MFLUCC 13–0221	KU377567.1	KU377562.1	-	Dead wood, Thailand
R. neorufulum	MFLUCC 17–2236	MH063266.1	MH062956.1	-	Dead wood, Thailand
R. opuntiae	GKM 1190	GQ221892.1	-	GU397341.1	Kenya
R. rufulum	MFLUCC 14–0577	KU377565.1	KU377560.1	KU510399.1	Woody litter, Thailand
R. tectonae	MFLUCC 13–0710	KU764698.1	KU144936.1	-	Dead branches, India
*R. thailandicum**	MFLUCC 14–0503	NG_059648.1	NR_164241.1	KU497490.1	Dead wood, Thailand
R. thailandicum	MFLU 19–2373	MN989429.1	MN989428.1	MN989431.1	Dead wood, Thailand
R. thailandicum	MFLUCC 13–0051	MN509434.1	MN509433.1	MN509435.1	Dead wood, Thailand
*Gloniopsis calami**	MFLUCC 15–0739	NG_059715.1	KX669036.1	KX671965.1	Unknown

*Ex-type strains.

was performed with Bayesian inference using MrBayes v3.2.6 x64 (Huelsenbeck and Ronquist 2001). The information block for the matrix includes two independent runs of the MC3 chains using 10 million generations (standard deviation ≤0.1). The convergence of the chains was displayed in Tracer v1 (Rambaut et al. 2014). The highest credibility phylogram of the clades recovered with TreeAnnotator v. 1.8 (Bouckaert et al. 2014) was chosen with a 25% burn-in.

Results

Phylogenetic analysis

The ITS, LSU and *tef1* sequences obtained from *Rhytidhysteron cozumelense*, *Rhytidhysteron esperanzae* and *Rhytidhysteron mesophilum* were deposited in GenBank (Table 1). In the Bayesian analysis, the standard deviation between the chains stabilized at 0.001 after 10 million generations, indicating that MC3 reached a stationary phase. To confirm that the sample size was sufficient, the parameter file was examined in Tracer 1.6 (Rambaut et al. 2014): all parameters had an estimated sample size of over 1,500. The posterior probabilities (PP) obtained were estimated by generating a strict consensus tree in MrBayes. Bayesian inference analysis recovered well-supported clades (PP = 1) of the three species *Rhytidhysteron cozumelense*, *Rhytidhysteron esperanzae* and *Rhytidhysteron mesophilum* (Figure 1).

Taxonomy

Rhytidhysteron cozumelense **Cobos-Villagrán, R. Valenz., Hdz-Rdz., Calvillo-Medina & Raymundo sp. nov**
MycoBank No: 839084
Fig. 2

Diagnosis. Differs from *Rhytidhysteron rufulum* in its host (Bignoniaceae), size of ascomata (2.5–3.5 × 1.1–1.5 × 1.0–1.9 mm), asci (182–191 × 12–13 µm) and its reaction with KOH being faster (one to five seconds).

Type. ***Holotype*****:** Mexico. Quintana Roo, Cozumel Municipality, San Gervasio Chen-tuk archaeological zone, 20°29'50"N, –86°50'39"W, 0 m a.s.l., 21 January 2018, A. Cobos-Villagrán 951 (ENCB), on *Tabebuia rosea* DC. (Bignoniaceae), GenBank: LSU MW9394459, ITS MZ056797, tef1 MZ457338**.**

Description. *Ascomata* hysterothecial to apothecial 2.5–3.5 mm long, 1.1–1.5 mm wide, (0.8)1.0–1.9 mm high, erumpent, solitary, boat-shaped hysterothecia, subglobose, elongated, compressed in the apex, with conspicuous longitudinal groove or cleft and becoming lenticular when mature or exposed to moisture, black, carbonaceous when dry. *Margin* involute, smooth to perpendicularly slightly striated, black. *Exciple* integrated in two layers, the first carbonaceous, glabrous, 45–100 µm thick, wide at the base, composed of pseudoparenchymal cells of *textura prismatica* (iso-radiating cells), thick-walled, the second composed of cells hyaline, thin-walled. *Pseudoparaphyses* up to 2.5 µm wide, filamentous, capitate, hyaline, septate, enclosed in a gelatinous matrix, strongly anastomosed above the asci. *Epithecium* reddish brown (8F7) when fresh, black in old specimens or when dry, becoming greyish magenta (13B5) in the presence of 10% KOH. *Asci* 182–191 × 12–13 µm, bitunicate, cylindrical, hyaline, uniseriate, octosporic, thick-walled, with a sinuous base. *Ascospores* 26–29(–31) × 9–11 (–13) µm, ($\bar{x}$= 28 × 10.2 µm, n = 30), ellipsoidal to fusiform, rounded at both ends, dark brown in colour with three transverse septa, with a thick and smooth wall.

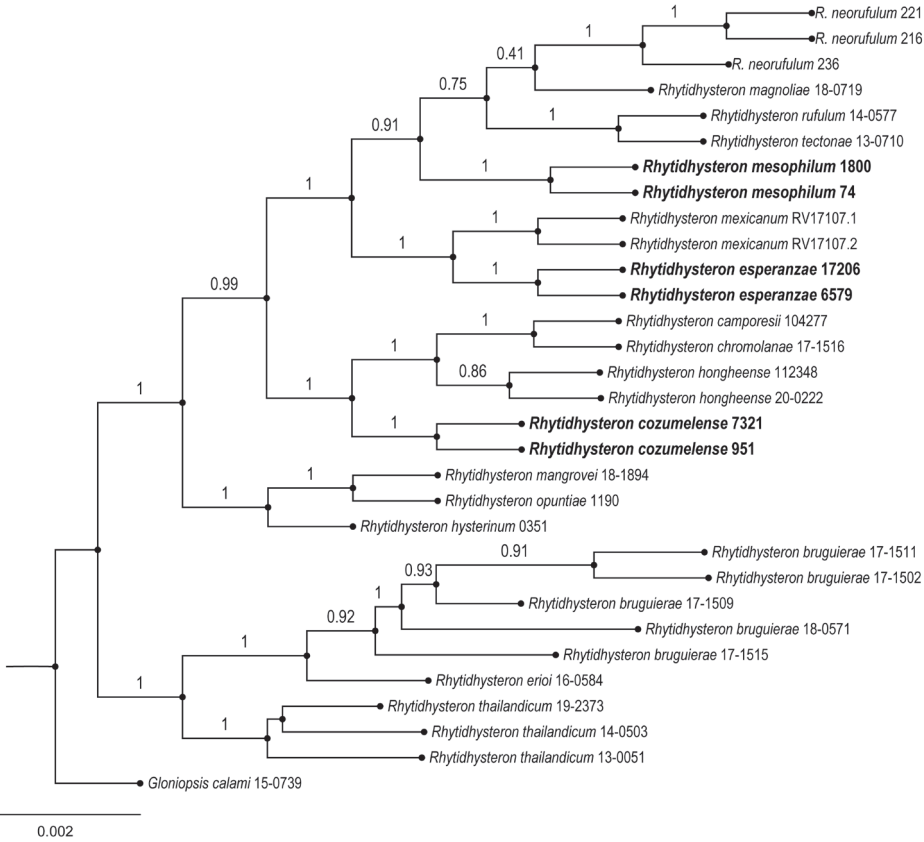

Figure 1. Phylogenetic relationships within the genus *Rhytidhysteron* based on a Bayesian analysis of a combined dataset of ITS, LSU and *tef1* sequence data. *Gloniopsis calami* 150739 was used as the outgroup. The posterior probabilities for each clade are shown above the branches. The new species *Rhytidhysteron cozumelense*, *Rhytidhysteron esperanzae* and *Rhytidhysteron mesophilum* are shown in bold.

Distribution. Known from a single local Island in the Cozumel Biosphere Reserve, Mexico.

Ecology. Dead twigs of *Tabebuia rosea* DC. (Bignoniaceae).

Etymology. The epithet refers to the Island in the Cozumel Biosphere Reserve where the species was found.

Specimens examined. Mexico, Quintana Roo, Cozumel Municipality, San Gervasio Chen-tuk archaeological zone, 20°29'54"N, –86°50'43"W, 13 m a.s.l., 21 January 2018, T. Raymundo 7321, R. Valenzuela 17985 (ENCB); 17 June 2018, A. Cobos-Villagrán 1838 (ENCB).

Notes. *Rhytidhysteron cozumelense* is characterised by black ascomata with a reddish brown epithecium and a smooth to slightly striated margin that, in reaction with 10% KOH, changes to greyish magenta. *R. mesophilum* has a similar reaction in KOH, but with several tones of green in the hysterothecia, a reddish orange to orange red

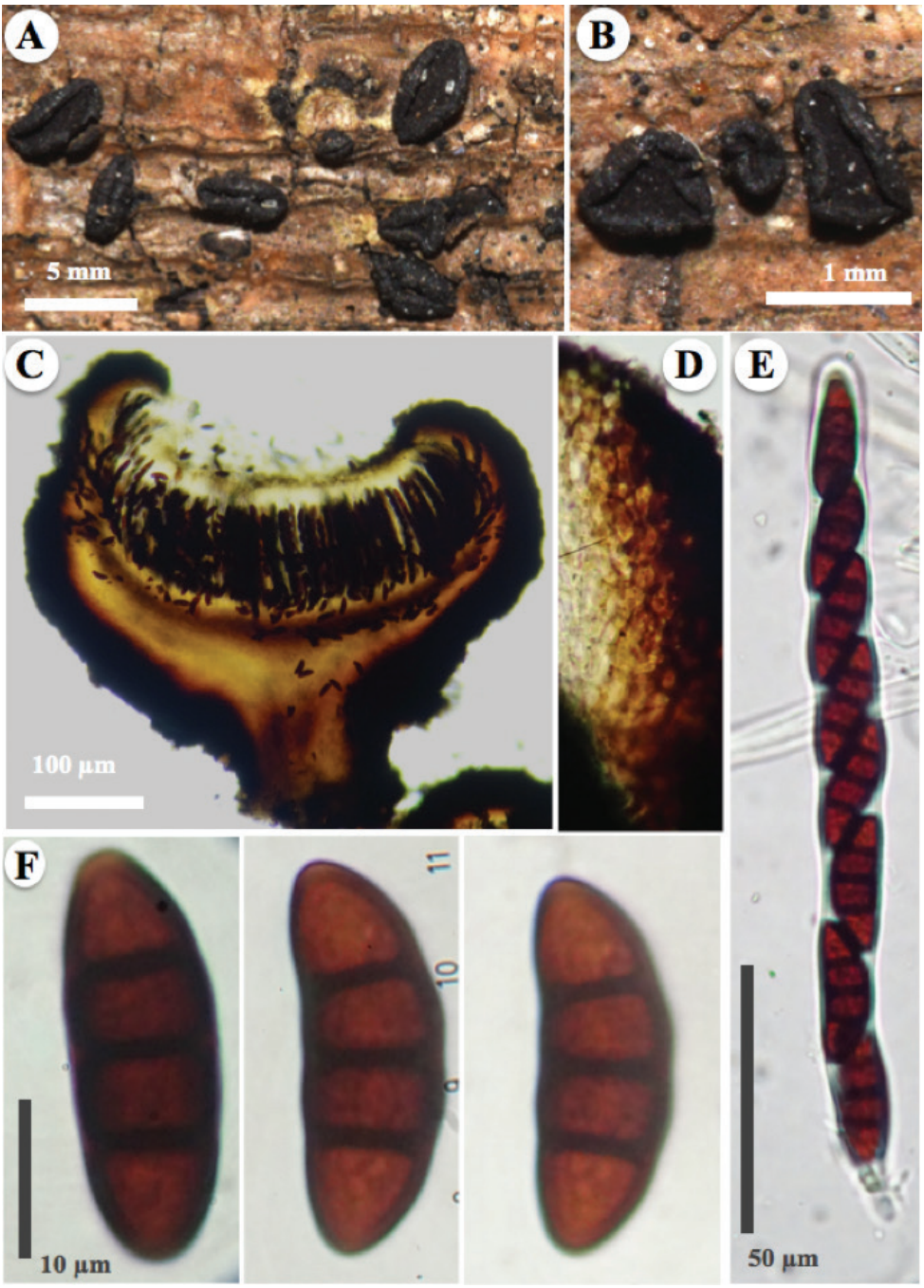

Figure 2. *Rhytidhysteron cozumelense* (Holotype, A. Cobos-Villagrán 951) **A** appearance of ascomata hysterothecial and apothecial on host **B** ascomata apothecial close-up, striated margin and black epithecium **C–F** microscopical features stained with alcohol (70%) and KOH (10%) reagent **C** ascomata apothecial cross-section with alcohol (70%) **D** exciple of iso-radiating cells (*textura prismatica*), close-up **E** asci **F** ascospores.

epithecium and a perpendicularly striate with irregular slits and yellowish green pruina in margin. *R. rufulum* has a magenta reaction in KOH and strongly striated margin. *Tabebuia rosea* is reported as a new host for a *Rhytidhysteron* species.

Rhytidhysteron esperanzae **Cobos-Villagrán, R.Valenz. & Raymundo sp. nov**
Mycobank No: 839086
Fig. 3

Diagnosis. Different from most *Rhytidhysteron* species by having greyish-green ascomata with greenish-grey to yellow epithecium in the presence of KOH, and large and wide ascospores (45–47 × 17–19 µm).

Type. ***Holotype*****:** Mexico. Oaxaca, Sierra de Juárez, Chinantla, Santiago Comaltepec Municipality, La Esperanza, Carretera Oaxaca-Tuxtepec Km 51, 17°37'55"N, –96°22'01"W, 1600 m a.s.l., 23 May 2017, T. Raymundo 6579 (ENCB). GenBank: LSU MW9394457, ITS MZ056795.

Etymology. The epithet refers to the locality "La Esperanza" where the species was found.

Description. *Ascomata* hysterothecial to apothecial, (2–)3–4.5 mm long, (1.2–)2–3 mm wide, (1–)1.7–2.4 mm high, superficial, solitary, rarely gregarious, boat-shaped hysterothecia, elongated, straight or flexuous, with sharp ends, opening in a discoid shape when ripe or with humidity, exposing the hymenium, taking the apothecial shape of 3–4 mm in diameter, brown (6D7), dull-green (30E4) to black. *Margin* involute, perpendicularly striate, greyish green (30C4) to dull green (30D4). *Exciple* integrated in two layers, the first carbonaceous, glabrous, 60–220 µm wide, thinning in the apical part, the middle part and the base are thicker, composed of pseudoparenchymal cells of *textura globulosa-angularis* (isodiametric cells), 11 × 10 µm, thick-walled, 3 µm wide, the second slightly pigmented to hyaline, thin-walled. *Pseudoparaphyses* up to 4 µm wide, filamentous, capitate, apical part wider, straight, hyaline, with a septum, enclosed in a gelatinous matrix, strongly anastomosed above the asci. *Epithecium* dark green (30F4) to black, becoming yellow (2A7) in the presence of 10% KOH. *Asci* (250–)265–270 × (18–)19–20 µm, bitunicate, cylindrical, rounded apex, hyaline, uniseriate, octosporic, thick-walled, with a short pedicel. *Ascospores* of (42–)45–47(–49) × (15–)17–19(–23) µm, ($\bar{x}$ = 45 × 17.2 µm, n = 30), ellipsoidal to spindle-shaped, rounded or pointed at both ends, reddish-brown to brown when mature, with three transverse septa, constricted at the septa, thick-walled and smooth.

Distribution. Known from a single locality in a forest in La Esperanza, Mexico.

Ecology. Dead stems and twigs in tropical cloud forest dominated by *Oreomunnea mexicana* Standl. J.-F. Leroy (Juglandaceae).

Specimens examined. Mexico. Oaxaca. Sierra de Juárez, Santiago Comaltepec Municipality, La Esperanza, Carretera Oaxaca-Tuxtepec Km 51, 17°37'55"N, –96°22'01"W, 1600 m a.s.l., 22 May, 2017, R. Valenzuela 17206 (ENCB); 23 May

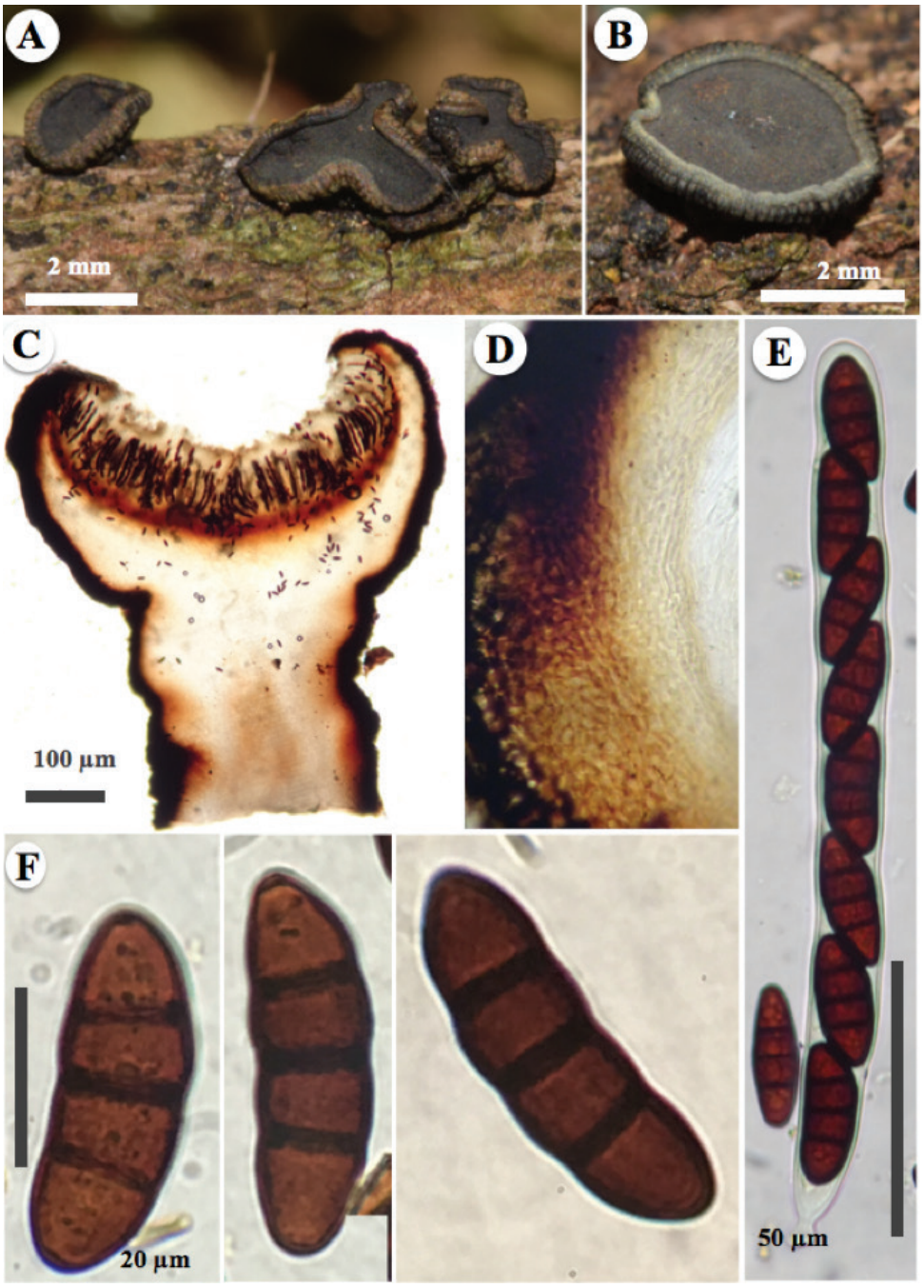

Figure 3. *Rhytidhysteron esperanzae* (Holotype, T. Raymundo 6579) **A** appearance of ascomata apothecial on host **B** ascomata apothecial close-up, greyish-green to dull green and striated margin and dark green to black epithecium **C–F** microscopical features stained with alcohol (70%) and KOH (10%) reagent **C** ascomata apothecial cross-section with alcohol (70%) **D** exciple of isodiametric cells (*textura globulosa-angularis*), close-up **E** asci **F** ascospores.

2017, A. Cobos-Villagrán 498 (ENCB); 25 May 2017, E. Campero 3 (ENCB), 30 April 2018, A. Cobos-Villagrán 1119 (ENCB), A. Gay AG30041814 (ENCB).

Notes. *Rhytidhysteron esperanzae*, is characterised by a brown, dull-green to black exciple and dark green to black epithecium that, in reaction with 10% KOH, changes to yellow colouration. This colouration with KOH is very different than those of of *R. rufulum* and *R. neorufulum* which are magenta and violet, respectively. *R. esperanzae* have larger ascospores than *R. rufulum* (22.4–30.4 × 8–9.6 µm) and *R. mexicanum* (34–40 × 10–12 µm). Ecologically, this new species grows in a tropical cloud forest dominated by *Oreomunnea mexicana* Standl. J.-F. Leroy (Juglandaceae).

Rhytidhysteron mesophilum **Cobos-Villagrán, R. Valenz., Hdz.-Rdz., Calvillo-Medina & Raymundo sp. nov.**
Mycobank No: 839097
Fig. 4

Diagnosis. Differs from *Rhytidhysteron rufulum* by its green-yellowish pruina on the margins, size of asci (267–282 × 15.5–16 µm) and larger ascospores (40–44 × 12–14 µm).

Type. Molango de Escamilla Municipality, Laguna Atezca, 20°48'32"N, –98°44'52"W, 1281 m a.s.l., 01 June 2018, A. Trejo 74 (ENCB). GenBank: LSU MW9394461, ITS MZ056799.

Etymology. The epithet refers to the type of vegetation (mountain mesophilic forest) it was collected from.

Description. *Ascomata* hysterothecial to apothecial, 2.5–4 mm long, 1.0–1.5 mm wide, 1.4–1.7 mm high, superficial or erumpent, gregarious, rarely solitary, with small hysterothecial ascomata, ellipsoid to oblong and black when young, then boat-shaped hysterothecia, with some constriction in the middle part, flexuous, open in apothecioid ascomata, dark green (30F3–4), dull green (30E3–4), greyish green (30E6–7), deep green (30D-E8) to yellowish green (30B-C8) when mature, forming small ascomata within disc in old specimens. *Margin* involute, perpendicularly striate, marks are not roughness, rather irregular slits, with yellowish green (30B-C8) pruina. *Exciple* integrated in two layers, the first carbonaceous, glabrous, green yellowish, 62.5–75 µm thick, in the middle part widening more (112.5–125 µm), composed of pseudoparenchymal cells of *textura prismatica* (isoradiating cells), the second composed of cells hyaline, thin-walled. *Pseudoparaphyses* 2.0–2.5 µm up to 3.0 µm wide, filamentous, capitate, hyaline, without septa, branched towards the apex, enclosed in a gelatinous matrix, strongly anastomosed above the asci. *Epithecium* reddish orange (7B8) to orange red (8A8), becoming greyish magenta (13D6) in the presence of 10% KOH. *Asci* 267–282 × 15.5–16 µm, bitunicate, cylindrical, hyaline, uniseriate, octosporic, thick-walled, with a sinuous base. *Ascospores* (38–)40–44(–46) × 12–14 µm, ($\overline{x}$= 44.2 × 13.6, n = 30), ellipsoidal to oblong, light brown in colour, with three transverse septa, constricted at the septa, with a thick and smooth wall.

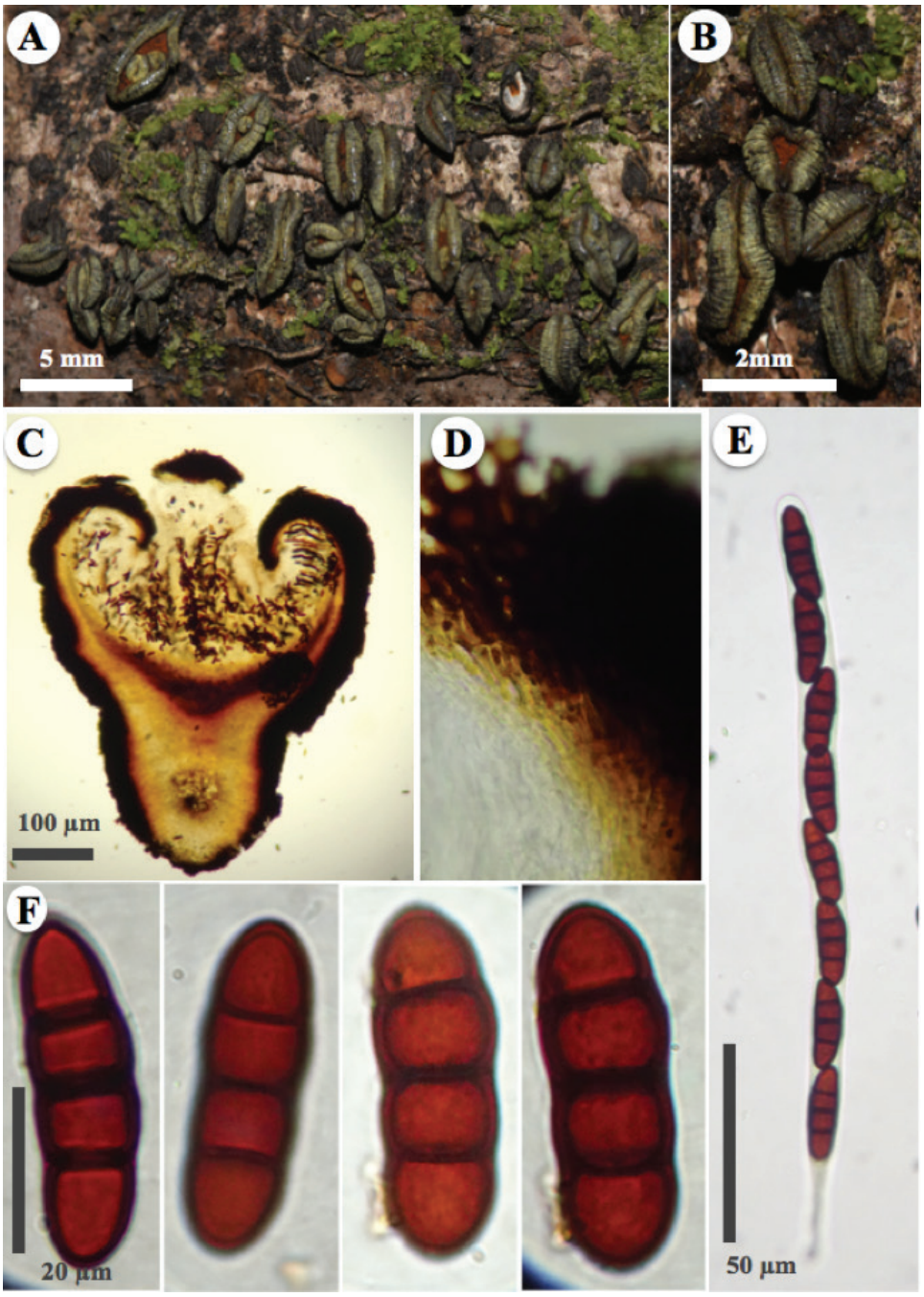

Figure 4. *Rhytidhysteron mesophilum* (Holotype, A. Trejo 74) **A** appearance of ascomata hysterothecial on host **B** ascomata hysterothecial close-up, striated margin with yellowish green pruina and reddish orange to orange red epithecium **C–F** microscopical features stained with alcohol (70%) and KOH (10%) reagent **C** ascomata hysterothecial cross-section with alcohol (70%) **D** exciple of iso-radiating cells (*textura prismatica*), close up **E** asci **F** ascospores.

Distribution. Known from a single locality in Laguna de Atezca, Molango de Escamilla, Hidalgo, Mexico.

Ecology. Dead stems in tropical cloud forest.

Specimens examined. Mexico. Hidalgo, Molango de Escamilla Municipality, Laguna Atezca, 20°48'32"N, –98°44'52"W, 1281 m a.s.l., 01 June 2018; C. Herrera 40 (ENCB), A. Cobos-Villagrán 1800 (ENCB).

Notes. *Rhytidhysteron mesophilum* is characterised by a dark green, dull green, greyish green, deep green to yellowish green hysterothecium, forming small ascomata within disc in old specimens. This fungus could be confused with *R. esperanzae* because both are found in tropical cloud forest (mesophilic forests) and have similar ascospores. However, *R. mesophilum* is distinguished by a reddish orange to orange red epithecium, while in *R. esperanzae*, the epithecium is dark green to black. *R. mesophilum* also resembles *R. columbiense* by the presence of a yellowish green (30B-C8) pruina in the margin, but the ascospores are larger (38–52 × 13–18 µm) and the epithecium is brown to dark brown in the second species.

A dichotomous key is presented with the species of *Rhytidhysteron* accepted by Index Fungorum (2021), including the three new species proposed in this work. The key includes the recently described *R. mexicanum* Cobos-Villagrán, Raymundo, Calvillo-Medina & R. Valenz and *R. hongheense* Wanas. It should be noted that *R. fuscum* (Ellis & Everh.) J.L. Bezerra & Kimbr. and *R. minor* (Cooke) A. Pande are not considered because the first belongs to the genus *Tryblidiella* and the second is a *nom. inval.*, because the basionym was not indicated and bibliographic reference omitted (Art. 41.5, see Art. 41.7, Melbourne).

Key to the known species of *Rhytidhysteron*

1 Ascospores submuriform **2**

– Ascospores transversely septate, 1–5 septa **3**

2 Ascospores with 3–5 transverse and 1–3 longitudinal septa, 20–25 × 7.5–10 µm, epithecium brown-red, on *Cylindropuntia fulgida*; type: USA ..... ***R. opuntiae*** **(J.G. Br.) M.E. Barr**

– Ascospores with 3 transverse septa mainly and rarely with 3 transverse septa and 1 longitudinal septum, 20–33 × 9–13 µm, epithecium reddish orange, on *Dodonaea viscosa*, type: China ..... ***R. hongheense*** **Wanas.**

3 Ascospores 1–septate **4**

– Ascospores 3–5 septate **5**

4 Epithecium ferruginous brown, ascospores 22–32 × 10–16 µm, on *Buxus sempervirens*, *Diospyros* spp. or *Ilex* spp.; type: France ..... ***R. hysterinum*** **(Dufour) Samuels & E. Müll.**

– Epithecium orange, ascospores 24.8–29(–31) × 8.8–10(–11.2) µm, on *Acacia* spp.; type: Mexico ..... ***R. neohysterinum*** **Cobos-Villagrán, Hdz.-Rdz., R. Valenz. & Raymundo**

5 Five septa in mature ascospores, 30–46 × 12–20 µm, epithecium yellowish orange, on *Pinus* spp.; type: Finland ..... ***R. dissimile*** **(P. Karst.) Magnes**

– Three septa in mature ascospores ..... **f**

6	Ascospores 12–15 × 5–6 µm, exciple brownish green, epithecium brown, on monocotyledonous; type: Sri Lanka ..... ***R. beccarianum*** **(Ces.) Bat. & Valle**
–	Ascospores longer than 15 µm **7**
7	Ascospores between 16 to 30 µm long **8**
–	Ascospores longer than 30 µm **22**
8	Ascomata with exciple and/or margin in several tones of green **9**
–	Ascomata with exciple and margin reddish brown to black **10**
9	Ascomata with exciple and margin vivid green, perpendicularly striate, ascospores 20–30 × 7–9 µm, constricted at the central septum, on angiosperm; type: Brazil..... ***R. viride*** **Speg.**
–	Ascomata dark brown to black with yellowish green on the margin, smooth, not striate, ascospores 23–28 × 8–11 µm, slightly constricted at the central septum, on *Chromolaena odorata*; type: Thailand ..... ***R. chromolaenae*** **Mapook & K.D. Hyde**
10	Epithecium with yellow, orange, red or green colour in some development stage..... **11**
–	Epithecium brown to black in young and mature specimens..... **18**
11	Epithecium yellowish green, margin perpendicularly striate, ascospores 20.3–30.4 × 7.6–10.1 µm, on *Prosopis jungiflora*; type: USA..... ***R. prosopidis*** **Peck**
–	Epithecium with yellow, orange or red colour **12**
12	Ascomata hysterotecial, epithecium yellow, margin smooth, ascospores (19–)28–29(–31) × (8–)10–12(–13) µm constricted at the central septum, on *Tectona grandis*; type: Thailand..... ***R. tectonae*** **Doilom & K.D. Hyde**
–	Ascomata apothecial **13**
13	Epithecium with red tones in young or mature specimens **14**
–	Epithecium with orange tones in young or mature specimens..... **16**
14	Epithecium vivid red or cinnabar red, ascospores 19.0–24.7 × 7.6–11.4 µm, constricted at the septa, on *Quercus* sp.: type: India..... .....***R. quercinum*** **(B.G. Desai & V.N. Pathak) M.P. Sharma & Rawla**
–	Epithecium dark red to black..... **15**
15	Growing on mangrove tree, epithecium dark red to dark brown, ascospores 21–28 × 7.5–8.5 µm; type: Thailand .....***R. mangrovei*** **Vin. Kumar & K.D. Hyde**
–	Growing mainly on Fabaceae, not on mangroves, epithecium orange red, red, dark red to black, 22.4–30.4 × 8–9.6 µm, type: Puerto Rico..... ..... ***R. rufulum*** **(Spreng.) Speg.**
16	Ascospores 28–30 × 10–12 µm, on angiosperm, type: Paraguay..... .....***R. discolor*** **(Speg.) Speg.**
–	Ascospores smaller than 28 µm **17**
17	Ascospores 6.2–9 µm broad, on *Bruguiera* sp. and *Chromolaena odorata*; type:Thailand.....***R. bruguierae*** **Dayarathne**
–	Ascospores 9–11 µm, on angiosperm; type: Thailand..... ..... ***R. erioi*** **Ekanayaka & K.D. Hyde**
18	Margin perpendicularly striate **19**
–	Margin smooth to slightly striate **20**

19 Ascospores 25–27 µm broad, on angiosperm; type: Australia ..... ***R. scortechinii* Sacc. & Berl.**

– Ascospores 28–30(–32) µm broad, on *Magnolia grandiflora*; type: China ..... ***R. magnoliae* N.I. de Silva, Lumyong S & K.D. Hyde**

20 Ascomata apothecial, ascospores 26–29(–31) × 9–11 (–13) µm, on *Tabebuia rosea* DC.; type: Mexico ..... ***R. cozumelense* Cobos-Villagrán, R.Valenz., Hdz-Rdz., Calvillo-Medina & Raymundo**

– Ascomata hysterotecial **21**

21 Ascospores 25–28 × 9–11 µm, hamathecium release magenta pigment in KOH, on angiosoperm; type: China ..... ***R. camporesii* Ekanayaka & K.D. Hyde**

– Ascospores 20–28(-31) × 7.5–12 µm, hamathecium do not release pigment in KOH, on angiosoperm; type: Thailand ..... ***R. thailandicum* Thambugala & K.D. Hyde**

22 Ascospores 30–40 µm **23**

– Ascospores longer than 40 µm **26**

23 Margin perpendicularly striate, epithecium yellowish green to pistachio green when fresh, light green to pale green when dry, 34–40 × 10–12 µm, on angiosperm; type: Mexico ..... ***R. mexicanum* Cobos-Villagrán, Raymundo, Calvillo-Medina & R. Valenz.**

– Margin smooth, epithecium yellow, reddish orange or black **24**

24 Epithecium yellow, orange to reddish orange, ascospores 27–34 × (6.5–)7–10.6 (–12.5) µm, on angiosperm; type: Thailand ..... ***R. neorufulum* Thambugala & K.D. Hyde**

– Epithecium black **25**

25 Ascospores 10–12 µm broad, constricted at the central septum, on angiosperm; type: Paraguay ..... ***R. guaraniticum* Speg.**

– Ascospores 13–14 µm broad, constricted at the septa, on *Scutia indica*; type: India ..... ***R. indicum* (Anahosur) M.P. Sharma & K.S. Thind**

26 Exciple black, epithecium black, ascospores 40–45 × 15–20 µm, on angiosperm; type: Brazil ..... ***R. brasiliense* Speg.**

– Exciple or margin with green tones **27**

27 Exciple and margin dark green, dull green, greyish green, deep green to yellowish green when mature, epithecium reddish orange to orange red, ascospores (38–)40–44(–46) × 12–14 µm, on angiosperm; type: Mexico ..... ***R. mesophilum* Cobos-Villagrán, R. Valenz., Hdz.-Rdz., Calvillo-Medina & Raymundo**

– Exciple brown, dark brown to black **28**

28 Margin with a yellowish-green pruina, epithecium brown to dark brown, ascospores 38–52 × 13–18 µm, on angisoperm; type: Colombia ..... ***R. columbiense* Soto-Medina & Lücking**

– Margin greyish green to dull green, epithecium dark green (30F4) to black, ascospores (42–)45–47(–49) × (15–)17–19(–23) µm, on angiosperm; type: Mexico ..... ***R. esperanzae* Cobos-Villagrán, R.Valenz. & Raymundo**

Discussion

The genus *Rhytidhysteron* is a highly diverse group with a mainly Pantropical distribution (Samuels and Müller 1979). The morphological characteristics that have, so far, helped in the segregation of the species are: shape and border of the hysterothecium, ornamentation of the exciple, colour and reaction of the epithecium, and size of the ascospores which only, in some cases, have helped delimiting species, as in the case of *Rhytidhysteron columbiense* Soto-Medina & Lücking and *R. neohysterinum* Cobos-Villagrán, Hern-Rodr., R. Valenz. & Raymundo.

Therefore, species in which the size of spores overlap, have been clarified by molecular methods and the use of molecular markers, such as ITS, LSU, elongation factor 1 alpha (TEF1), amongst others. For example, in the case of *R. rufulum*, catalogued as a species complex based on morphology, the fungal barcodes have been helpful in describing different species that are morphologically similar (Boehm et al. 2009b; Murillo et al. 2009; Yacharoen et al. 2015; Doilom et al. 2016; Thambugala et al. 2016; Soto-Medina and Lücking 2017). In recent years, part of the taxonomy has been resolved using collections from different countries around the globe. For example, in Thailand, *R. neorufulum* and *R. thailandicum* were described in the work of Thambugala et al. 2016. In the same year, Doilom et al. (2016) described *R. tectone* on *Tectona grandis* L. (Verbenaceae) also from Thailand.

In recent years, eight new species were described: Kumar et al. (2019) described *R. mangrovei* Vinit & K.D. Hyde, isolated from dead mangrove branches; Dayarathne et al. (2020) described *R. bruguierae* Dayarathne, also isolated from mangrove branches *Bruguiera* Lam. (Rhizophoraceae); Hyde et al. (2020) described *R. camporesii* Ekanayaka & K.D. Hyde and *R. erioi* Ekanayaka & K.D. Hyde; Mapook et al. (2020) described *R. chromolaenae* Mapook & K.D. Hyde, isolated from branches of *Chromolaena odorata* (L.) King & Robinson (Asteraceae); Wanasinghe et al. (2021) described *R. hongheense* Wanas. isolated from dead twigs of *Dodonaea* Mill. (Sapindaceae); and in Mexico, Cobos-Villagrán et al. (2020) described *R. neohysterinum* Cobos-Villagrán, Hdez.-Rdz., R. Valenz. & Raymundo and Cobos-Villagrán et al. (2021) *R. mexicanum* Cobos-Villagrán, Raymundo, Calvillo-Medina & R. Valenz. With this new study, three more species have been described from Mexico.

In the present study, we observed that *R. cozumelense* is phylogenetically close to *R. hongheense*, *R. camporesii* and *R. chromolaenae*. The four species are similar in terms of ascospore size in the range of 23–30 × 8–13 µm and have a margin smooth to slightly striate. *R. hongheense* has slightly longer ascospores (20–33 × 9–13 µm). However, they have ascomata of contrasting sizes. *R. chromolaenae* forms smaller navicular hysterothecia, 750–885 µm diam., with orange epithecium, turning purple in KOH and is described from Chiang Rai Province, Thailand (Mapook et al. 2020). *R. camporesii* has hysterothecial ascomata of 800–1100 µm long with black epithecium that changes to magenta in KOH and it is described from Yunnan Province, China (Hyde et al. 2020). Finally, *R. hongheense* has ascomata hystherothecial 1200–2000 µm long with reddish-orange epithecium and it is described from Honghe County, Yunnan Province, China (Wanasinghe et al. 2021). *R. cozumelense* produces longer ascomata, hysterothecial to

apothecial, 2500 to 3500 µm long with reddish brown to black epithecium that changes to greyish magenta in KOH and it grows on *Tabebuia rosea* DC. (Bignoniaceae).

R. esperanzae is phylogenetically close to *R. mexicanum*, both species described from Mexico presenting similar hysterothecial to apothecial ascomata, sizes of 2000–4500 × 1200–2500 µm and a perpendicularly striate margin. However, they differ by the colour of the ascomata and the epithecium: in *R. esperanzae*, the ascomata is brown, the exciple dull-green to black, and the epithecium dark green to black, with a yellow reaction in KOH. In contrast, in *R. mexicanum*, the exciple is completely black and the epithecium yellowish green to pistachio green when fresh, light green, pale green to lemon yellow when dry, becoming ocher to yellow gold in KOH. Another difference is the size of the ascospores which are longer and wider in *R. esperanzae*: they are (42–)45–47(–49) × (15–)17–19(–23) µm, while in *R. mexicanum*, they are 34–40(–44) × 10–12(–15) µm (Cobos-Villagrán et al. 2021).

On the other hand, *R. mesophilum* is characterised by navicular hysterothecia, striated margin with green-yellowish pruina, reddish orange to orange red epithecium that changes to greyish magenta in KOH, and long ascospores. It is related phylogenetically to *R. tectonae* and *R. rufulum*. However, it is morphologically different, including in the size and colour of the hysterothecium, colour of the epithecium, colouration in the reaction with 10% KOH and the size of asci and ascospores. The hysterothecia of *R. tectonae* are 1225–3365 µm long, with a smooth margin, yellow epithecium without reaction in KOH, ascospores (19–)28–29(–31) × (8–)10–12(–13) µm and the species grows on *Tectona grandis* L., in Chiang Rai, Thailand (Doilom et al. 2016). In *R. rufulum*, the size of the ascomata ranges from 1500–2000 µm long, the exciple is black, the epithecium brown, orange, or reddish, changing to magenta in KOH, and the ascospores are 21–32(–39) × 8–9.6 µm (Kutorga and Hawksworth 1997; Almeida et al. 2014; Thambugala et al. 2016; Cobos-Villagrán et al. 2020). In contrast, the hysterothecia of *R. mesophilum* are 2500–4000 µm long, the epithecium orange, changing to greyish magenta in KOH, and the ascospores (38–)40–44(–46) × 12–14 µm, therefore much longer and wider.

In Mexico, the tropical dry forest is the best represented vegetation with four *Rhytidhysteron* species: *R. cozumelense*, *R. neorufulum*, *R. rufulum* and *R. neohysterinum*. This is followed by the xerophilous scrub with *R. thailandicum*, *R. rufulum* and *R. neohysterinum*, and only *R. mexicanum* in *Quercus* forest. Finally, in this study, we describe *R. esperanzae* and *R. mesophilum* in a tropical cloud forest, which is a vulnerable ecosystem and therefore these species are in danger of extinction. With the present study, the number of *Rhytidhysteron* species known from Mexico reaches a total of eight and together with Thailand, they form the countries with the most species diversity of the genus.

Acknowledgements

Dr. T. Raymundo and Dr. R. Valenzuela gratefully acknowledge the financial support received from CONACYT and IPN of Project 252934, and Projects SIP-20210315 and SIP-20210661, respectively. Dr. C. Hernández Rodríguez, Dr. L. Villa Tanaca,

Dr. L. E. Mateo Cid and Dr. A. Pérez Valdespino thank IPN for financial support for their research of the Projects SIP 20200782, SIP-20210508, SIP-20210885 and SIP-20210609, respectively. Dr. Calvillo Medina thanks CONACYT Postdoctoral scholarship (005352). Cobos Villagrán thanks Posgrado en Biociencias, Escuela Nacional de Ciencias Biológicas, IPN. The authors gratefully acknowledge the Sistema Nacional de Investigadores (CONACYT) and COFAA (IPN).

References

Almeida DAC, Gusmão LFP, Miller AN (2014) Brazilian Semi-Arid Ascomycetes I: new and interesting records of hysteriaceous ascomycetes. Mycosphere 5(2): 379–391. https://doi.org/10.5943/mycosphere/5/2/11

Boehm EWA, Mugambi GK, Miller AN, Huhndorf SM, Marincowitz S, Spatafora JW, Schoch CL (2009a) A molecular phylogenetic reappraisal of the Hysteriaceae, Mytilinidiaceae and Gloniaceae (Pleosporomycetidae, Dothideomycetes) with keys to world species. Studies in Mycology 64: 49–83. https://doi.org/10.3114/sim.2009.64.03

Boehm EWA, Schoch CL, Spatafora JW (2009b) On the evolution of the Hysteriaceae and Mytilinidiaceae (Pleosporomycetidae, Dothideomycetes, Ascomycota) using four nuclear genes. Mycological Research 113: 461–479. https://doi.org/10.1016/j.mycres.2008.12.001

Bouckaert R, Heled J, Kühnert D, Vaughan T, Wu C-H, Xie D, Suchard MA, Rambaut A, Drummond AJ (2014) BEAST 2: A software platform for Bayesian Evolutionary analysis. PLOS Computational Biology 10: e1003537. https://doi.org/10.1371/journal.pcbi.1003537

Calvillo-Medina RP, Cobos-Villagrán A, Raymundo T (2020) *Periconia citlaltepetlensis* sp. nov. (Periconiaceae, Pleosporales): a psychrotolerant fungus from high elevation volcanic glacier (Mexico). Phytotaxa 459(3): 235–247. https://doi.org/10.11646/phytotaxa.459.3.5

Chander J, Singla N, Kundu R, Handa U, Spoorthy RCY (2017) Phaeohyphomycosis caused by *Rhytidhysteron rufulum* and review of literature. Mycopathologia 182: 403–407. https://doi.org/10.1007/s11046-016-0064-x

Chowdhary A, Guarro J, Randhawa HS, Gené J, Cano J, Jain RK, Kumar S, Khanna G (2008) A rare case of chromoblastomycosis in a renal transplant recipient caused by a non-sporulating species of *Rhytidhysteron*. Medical Mycology 46: 163–166. https://doi.org/10.1080/13693780701630420

Cifuentes J, Villegas M, Pérez-Ramírez L (1986) Hongos. In: Lot A, Chiang F (Eds) Manual de Herbario. Consejo Nacional de la Flora de México AC, Ciudad de México, 55–64.

Cobos-Villagrán A, Hernández-Rodríguez C, Valenzuela R, Villa-Tanaca L, Calvillo-Medina RP, Mateo-Cid LE, Martínez-Pineda M, Raymundo T (2020) El género *Rhytidhysteron* (Dothideomycetes, Ascomycota) en México. Acta Botanica Mexicana 127: e1675. https://doi.org/10.21829/abm127.2020.1675

Cobos-Villagrán A, Raymundo T, Calvillo-Medina RP, Valenzuela R (2021) *Rhytidhysteron mexicanum* sp. nov. (Dothideomycetes, Ascomycota) from the Sierra of Guadalupe, Trans Mexican Volcanic Belt. Phytotaxa 479(3): 275–286. https://doi.org/10.11646/phytotaxa.479.3.4

Dayarathne MC, Jones EG, Maharachchikumbura SSN, Devadatha B, Sarma VV, Khongphinitbunjong K, Chomnunti P, Hyde KD (2020) Morpho-molecular characterization of

microfungi associated with marine based habitats. Mycosphere 11(1): 1–188. https://doi.org/10.5943/mycosphere/11/1/1

De Silva NI, Tennakoon DS, Thambugala KM, Karunarathna SC, Lumyong S, Hyde KD (2020) Morphology and multigene phylogeny reveal a new species and a new record of *Rhytidhysteron* (Dothideomycetes, Ascomycota) from China. Asian Journal of Mycology 3(1): 295–306. https://doi.org/10.5943/ajom/3/1/4

Doilom M, Dissanayake AJ, Wanasinghe DN, Boonmee S, Liu JK, Bhat DJ, Taylor JE, Bahkali AH, McKenzie EHC, Hyde KD (2016) Microfungi on *Tectona grandis* (teak) in northern Thailand. Fungal Diversity 82: 107–182. https://doi.org/10.1007/s13225-016-0368-7

Frandsen PB, Calcott B, Mayer C, Lanfear R (2015) Automatic selection of partitioning schemes for phylogenetic analyses using iterative k-means clustering of site rates. BMC Evolutionary Biology 15(1): 1–17. https://doi.org/10.1186/s12862-015-0283-7

García E (1981) Modificaciones al sistema de clasificación climática de Köppen (para la República Mexicana). Instituto de Geogeográfia, Universidad Nacional Autónoma de México. Ciudad de México-México, 252 pp.

García-Martínez YA, Heredia Abarca G, Guzmán-Guillermo J, Valenzuela R, Raymundo T (2021) Hongos asociados al mangle rojo *Rhizophora mangle* (Rhizophoraceae) en la Reserva de la Biosfera Isla Cozumel, Quintana Roo, México. Acta Botanica Mexicana 128: e1792. https://doi.org/10.21289/abm128.2021.1792

GenBank (2020) from the NCBI databases. http://www.ncbi.nlm.nih.gov/genbank/ [Accessed on 24.06.2021]

Hall TA (1999) BioEdit: a user-friendly biological sequence alignment editor and analysis program for Windows 95/98/NT. Nucleic Acids Symposium Series 41: 95–98. http://brownlab.mbio.ncsu.edu/JWB/papers/1999hall1.pdf

Hyde KD, Jones EBG, Liu JK, Ariyawansa HA, Boehm E, Boonmee S, Braun U, Chomnunti P, Crous PW, Dai DQ, Diederich P, Dissanayake AJ, Doilom M, Doveri F, Hongsanan S, Jayawardena R, Lawrey JD, Li YM, Liu YX, Lücking R, Monkai J, Muggia L, Nelsen MP, Pang KL, Phookamsak R, Senanayake I, Shearer CA, Seutrong S, Tanaka K, Thambugala KM, Wijayawardene NN, Wikee S, Wu HX, Zhang Y, Aguirre-Hudson B, Alias SA, Aptroot A, Bahkali AH, Bezerra JL, Bhat JD, Camporesi E, Chukeatirote E, Gueidan C, Hawksworth DL, Hirayama K, De Hoog S, Kang JC, Knudsen K, Li WJ, Li X, Liu ZY, Mapook A, McKenzie EHC, Miller AN, Mortimer PE, Phillips AJL, Raja HA, Scheuer C, Schumm F, Chomnunti JE, Tian Q, Tibpromma S, Wanasinghe DN, Wang Y, Xu JC, Yan J, Yacharoen S, Zhang M (2013) Families of Dothideomycetes. Fungal Diversity 63: 1–313. https://doi.org/10.1007/s13225-013-0263-4

Huelsenbeck JP, Ronquist F (2001) Mr Bayes: Bayesian inference of phylogeny. Bioinformatics 17(8): 754–755. https://doi.org/10.1093/bioinformatics/17.8.754

Hyde KD, Dong Y, Phookamsak R, Jeewon R, Bhat DJ, Jones EBG, Liu N-G, Abeywickrama PD, Mapook A, Wei D, Perera RH, Manawasinghe IS, Pem D, Bundhun D, Karunarathna A, Ekanayaka AH, Bao D-F, Li J, Samarakoon MC, Chaiwan N, Lin C-G, Phutthacharoen K, Zhang S-N, Senanayake IC, Goonasekara ID, Thambugala KM, Phukhamsakda C, Tennakoon DS, Jiang H-B, Yang J, Zeng M, Huanraluek N, Liu J-K, Wijesinghe SN, Tian Q, Tibpromma S, Brahmanage RS, Boonmee S, Huang S-K, Thiyagaraja V, Lu Y-Z, Jayawardena RS, Anand G, Devadatha B, Niranjan M, Sarma VV, Liimatainen K, Aguirre-Hudson,

B, Niskanen T, Overall A, Mendes-Alvarenga RL, Baptista-Gibertoni T, Pfliegler WP, Horváth E, Imre A, Alves AM, da Silva-Santos AC, Vieira-Tiago P, Bulgakov TS, Wanasinghe DN, Bahkali AH, Doilom M, Elgorban AM, Maharachchikumbura SSN, Rajeshkumar C, Haelewaters D, Mortimer PE, Zhao Q, Lumyong S, Xu J, Sheng J (2020) Fungal diversity notes 1151–1276: taxonomic and phylogenetic contributions on genera and species of fungal taxa. Fungal Diversity 100: 5–277. https://doi.org/10.1007/s13225-020-00439-5

Index Fungorum (2021) Index Fungorum. http://www.indexfungorum.org/names/Names.asp [Accessed on 24.06.2021]

INEGI (2008) Prontuario de información geográfica municipal de los Estados Unidos Mexicanos. Santiago Comaltepec, Oaxaca. http://www3.inegi.org.mx/contenidos/app/mexicocifras/datos_geograficos/20/20458.pdf [Accessed on 11.03.2021]

INEGI (2009) Prontuario de información geográfica municipal de los Estados Unidos Mexicanos. Molango de Escamilla, Hidalgo. http://www3.inegi.org.mx/contenidos/app/mexicocifras/datos_geograficos/13/13042.pdf [Accessed on 11.03.2021]

INEGI (2013) Conociendo Quintana Roo, México. Instituto Nacional de Estadística y Geografía. http://internet.contenidos.inegi.org.mx/contenidos/productos/prod_serv/contenidos/espanol/bvinegi/productos/estudios/conociendo/QUINTANA_ROO.pdf [Accessed on 11.03.2021]

Katoh K, Misawa K, Kuma K, Miyata T (2002) MAFFT: a novel method for rapid multiple sequence alignment based on fast Fourier transform. Nucleic Acids Research 30(14): 3059–3066. https://doi.org/10.1093/nar/gkf436

Katoh K, Standley DM (2013) MAFFT multiple sequence alignment software version 7: improvements in performance and usability. Molecular Biology and Evolution 30(4): 772–780. https://doi.org/10.1093/molbev/mst010

Katoh K, Rozewicki J, Yamada, KD (2017) MAFFT online service: multiple sequence alignment, interactive sequence choice and visualization. Briefings in Bioinformatics: bbx108. https://doi.org/10.1093/bib/bbx108

Kumar V, Cheewangkoon R, Thambugala KM, Jones GEB, Brahmanage RS, Doilom M, Jeewon R, Hyde KD (2019) *Rhytidhysteron mangrovei* (Hysteriaceae), a new species from mangroves in Phetchaburi Province, Thailand. Phytotaxa 401: 166–178. https://doi.org/10.11646/phytotaxa.401.3.2

Kutorga E, Hawksworth DL (1997) A reassessment of the genera referred to the family Patellariaceae (Ascomycota). Systema Ascomycetum 15: 1–110.

Lanfear R, Calcott B, Kainer D, Mayer C, Stamatakis A (2014) Selecting optimal partitioning schemes for phylogenomic datasets. BMC Evolutionary Biology 14(1): 82. https://doi.org/10.1186/1471-2148-14-82

Lanfear R, Frandsen PB, Wright AM, Senfeld T, Calcott B (2017) Partition Finder 2: new methods for selecting partitioned models of evolution for molecular and morphological phylogenetic analyses. Molecular Biology and Evolution 34(3): 772–773. https://doi.org/10.1093/molbev/msw260.

Maddison WP, Maddison DR (2017) Mesquite: a modular system for evolutionary analysis. Version 3.31. http://mesquiteproject.org

Mahajan VK, Sharma V, Prabha N, Thakur K, Sharma NL, Rudramurthy SM, Chauhan PS, Mehta KS, Abhinav C (2014) A rare case of subcutaneous phaeohyphomycosis caused by a

Rhytidhysteron species: a clinico-therapeutic experience. International Journal of Dermatology 53: 1485–1489. https://doi.org/10.1111/ijd.12529

Mapook A, Hyde KD, McKenzie EHC, Jones EBG, Bhat DJ, Jeewon R, Stadler M, Samarakoon MC, Malaithong M, Tanunchai B, Buscot F, Wubet T, Purahong W (2020) Taxonomic and phylogenetic contributions to fungi associated with the invasive weed *Chromolaena odorata* (Siam weed). Fungal Diversity 101: 1–175. https://doi.org/10.1007/s13225-020-00444-8

Mishra K, Das S, Goyal S, Gupta C, Rai G, Ansari MA, Singal A (2014) Subcutaneous mycoses caused by *Rhytidhysteron* species in an immunocompetent patient. Medical Mycology Case Reports 5: 32–34. https://doi.org/10.1016/j.mmcr.2014.07.002

Müller K, Quandt D, Müller J, Neinhuis C (2005) PhyDE-Phylogenetic data editor. Program distributed by the authors, version 10.0. https://www.phyde.de

Murillo C, Federico JA, Julieta C, Thorsten L, Giselle T (2009) Molecular data indicate that *Rhytidhysteron rufulum* (ascomycetes, Patellariales) in Costa Rica consists of four distinct lineages corroborated by morphological and chemical characters. Mycological Research 113: 405–416. https://doi.org/10.1016/j.mycres.2008.09.003

Posada D (2008) jModelTest: phylogenetic model averaging. Molecular Biology and Evolution 25: 1253–1256. https://doi.org/10.1093/molbev/msn083

Rambaut A, Suchard MA, Xie D, Drummond AJ (2014) Tracer v1.6. http://beast.bio.ed.ac.uk/Tracer [Accessed on 27.06.2021]

Rashmi M, Kushveer JS, Sarma VV (2019) A worldwide list of endophytic fungi with notes on ecology and diversity. Mycosphere 10(1): 798–1079. https://doi.org/10.5943/mycosphere/10/1/19

Samuels GJ, Müller E (1979) Life-history studies of Brazilian ascomycetes. 7. *Rhytidhysteron rufulum* and the genus *Eutryblidiella*. Sydowia 31: 277–291.

Schoch CL, Crous PW, Groenewald J, Barres B, Boehm E, de Gruyter J, de Hoog G, Dixon LJ, Fournier J, Grube M, Gueidan C, Harada Y, Hatakeyama S, Hirayama K, Hosoya T, Hyde KD, Jones EBG, Kohlmeyer J, Lucking R, Lumbsch H, Lutzoni F, Marvanova L, Mbatchou J, Miller A, Mugambi G, Muggia L, Nelson M, Nelson P, Owensby C, Phongpaichit S, Pointing S, Pujade-Renaud V, Raja H, Rivas-Plata E, Robbertse B, Ruibal C, Sakayaroj J, Sano T, Selbmann L, Shearer C, Shirouzu T, Slippers B, Suetrong S, Tanaka K, Volkmann-Kohlmeyer B, Wood A, Woudenberg J, Yonezawa H, Zhang Y, Spatafora J (2009) A class wide phylogenetic assessment of Dothideomycetes. Studies in Mycology 64: 1–15. https://doi.org/10.3114/sim.2009.64.01

Schoch CL, Seifert KA, Huhndorf SM, Robert V, Spouge JL, Levesque CA, Chen W, Fungal Barcoding Consortium (2012) Nuclear ribosomal internal transcribed spacer (ITS) region as a universal DNA barcode marker for Fungi. Proceedings of the National Academy of Sciences. 109(16): 6241–6246. https://doi.org/10.1073/pnas.1117018109

Soto-Medina E, Lücking R (2017) A new species of *Rhytidhysteron* (Ascomycota: Patellariaceae) from Colombia, with a provisional working key to known species in the world. Revista de la Academia Colombiana de Ciencias Exactas, Físicas y Naturales 41: 59–63. https://doi.org/10.18257/raccefyn.423

Spegazzini C (1881) Fungi argentini additis nonnullis brasiliensibus montevideensibusque. Pugillus IV. Anales de la Sociedad Científica Argentina 12(4): 174–189. [nos 155–193].

Thambugala KM, Hyde KD, Eungwanichayapant PD, Romero AI, Liu Z-Y (2016) Additions to the genus *Rhytidhysteron* in Hysteriaceae. Cryptogamie Mycologie 37: 99–116. https://doi.org/10.7872/crym/v37.iss1.2016.99

Vilgalys R, Hester M (1990) Rapid genetic identification and mapping of enzymatically amplified ribosomal DNA from several *Cryptococcus* species. Journal of Bacteriology 172: 4238–4246. https://doi.org/10.1128/jb.172.8.4238-4246.1990

White TJ, Bruns T, Lee S, Taylor J (1990) Amplification and direct sequencing of fungal ribosomal RNA genes for phylogenetics. In: Innis MA, Gelfand DH, Sninsky JJ, White TJ (Eds) PCR Protocols: a guide to methods and applications. Academic Press, San Diego, 315–322. https://doi.org/10.1016/B978-0-12-372180-8.50042-1

Wijayawardene NN, Hyde KD, Al-Ani LKT, Tedersoo L, Haelewaters D, Rajeshkumar KC, Zhao RL, Aptroot A, Leontyev DV, Saxena RK, Tokarev YS, Dai DQ, Letcher PM, Stephenson SL, Ertz D, Lumbsch HT, Kukwa M, Issi IV, Madrid H, Phillips AJL, Selbmann L, Pfliegler WP, Horváth E, Bensch K, Kirk PM, Kolaříková K, Raja HA, Radek R, Papp V, Dima V, Ma J, Malosso E, Takamatsu S, Rambold G, Gannibal PB, Triebel D, Gautam AK, Avasthi S, Suetrong S, Timdal E, Fryar SC, Delgado G, Réblová M, Doilom M, Dolatabadi S, Pawłowska J, Humber RA, Kodsueb R, Sánchez-Castro I, Goto BT, Silva DKA, de Souza FA, Oehl F, da Silva GA, Silva IR, Błaszkowski J, Jobim K, Maia LC, Barbosa FR, Fiuza PO, Divakar PK, Shenoy BD, Castañeda-Ruiz RF, Somrithipol S, Lateef AA, Karunarathna SC, Tibpromma S, Mortimer PE, Wanasinghe DN, Phookamsak R, Xu J, Wang Y, Tian F, Alvarado P, Li DW, Kušan I, Matočec N, Maharachchikumbura SSN, Papizadeh M, Heredia G, Wartchow F, Bakhshi M, Boehm E, Youssef N, Hustad VP, Lawrey JD, Santiago ALCMA, Bezerra JDP, Souza-Motta CM, Firmino AL, Tian Q, Houbraken J, Hongsanan S, Tanaka K, Dissanayake AJ, Monteiro JS, Grossart HP, Suija A, Weerakoon G, Etayo J, Tsurykau A, Vázquez V, Mungai P, Damm U, Li QR, Zhang H, Boonmee S, Lu YZ, Becerra AG, Kendrick B, Brearley FQ, Motiejūnaitė J, Sharma B, Khare R, Gaikwad S, Wijesundara DSA, Tang LZ, He MQ, Flakus A, Rodriguez-Flakus P, Zhurbenko MP, McKenzie EHC, Stadler M, Bhat DJ, Liu JK, Raza M, Jeewon R, Nassonova ES, Prieto M, Jayalal RGU, Erdoğdu M, Yurkov A, Schnittler M, Shchepin ON, Novozhilov YK, Silva-Filho AGS, Liu P, Cavender JC, Kang Y, Mohammad S, Zhang LF, Xu RF, Li YM, Dayarathne MC, Ekanayaka AH, Wen TC, Deng CY, Pereira OL, Navathe S, Hawksworth DL, Fan XL, Dissanayake LS, Kuhnert E, Grossart HP, Thines M (2020) Outline of fungi and fungus-like taxa. Mycosphere 11(1): 1060–1456, https://doi.org/10.5943/mycosphere/11/1/8

Wu G, Feng B, Xu J, Zhu XT, Li YC, Zeng NK, Hosen MI, Yang Z (2014) Molecular phylogenetic analyses redefine seven major clades and reveal 25 new generic lineages in the fungal family Boletaceae. Fungal Diversity 69: 93–115. https://doi.org/10.1007/s13225-014-0283-8

Yacharoen S, Tian Q, Chomnunti P, Boonmee S, Chukeatirote E, Bhat JD, Hyde KD (2015) Patellariaceae revisited. Mycosphere 6: 290–326. https://doi.org/10.5943/mycosphere/6/3/7

Zhang Z, Schwartz S, Wagner L, Miller W (2000) A greedy algorithm for aligning DNA sequences. Journal of Computational Biology 7: 203–214. https://doi.org/10.1089/10665270050081478

MycoKeys 83: 145–160 (2021)
doi: 10.3897/mycokeys.83.69909
https://mycokeys.pensoft.net

RESEARCH ARTICLE

A peer-reviewed open-access journal
MycoKeys
Launched to accelerate biodiversity research

Morphological and phylogenetic evidence for recognition of two new species of *Hyphoderma* (Basidiomycota) from southern China, with a key to all Chinese *Hyphoderma*

Qian-Xin Guan[1,3], Yi-Fei Li[3], Chang-Lin Zhao[1,2,3]

1 *Key Laboratory for Forest Resources Conservation and Utilization in the Southwest Mountains of China, Ministry of Education, Southwest Forestry University, Kunming 650224, China* **2** *Yunnan Academy of Biodiversity, Southwest Forestry University, Kunming 650224, China* **3** *College of Biodiversity Conservation, Southwest Forestry University, Kunming 650224, China*

Corresponding author: Chang-Lin Zhao (fungi@swfu.edu.cn)

Academic editor: R. Henrik Nilsson | Received 9 June 2021 | Accepted 28 August 2021 | Published 20 September 2021

Citation: Guan Q-X, Li Y-F, Zhao C-L (2021) Morphological and phylogenetic evidence for recognition of two new species of *Hyphoderma* (Basidiomycota) from southern China, with a key to all Chinese *Hyphoderma*. MycoKeys 83: 145–160. https://doi.org/10.3897/mycokeys.83.69909

Abstract

Wood-inhabiting fungi play crucial roles as decomposers in forest ecosystems and, in this study, two new wood-inhabiting corticioid fungi, *Hyphoderma puerense* and *H. tenuissimum* **spp. nov.**, are proposed, based on a combination of morphological features and molecular evidence. *Hyphoderma puerense* is characterised by effused basidiomata with smooth to floccose hymenial surface, a monomitic hyphal system with clamped generative hyphae and ellipsoid basidiospores. *Hyphoderma tenuissimum* is characterised by resupinate basidiomata with tuberculate to minutely-grandinioid hymenial surface, septate cystidia and cylindrical to allantoid basidiospores. Sequences of ITS and nLSU rRNA markers of the studied samples were generated and phylogenetic analyses were performed with Maximum Likelihood, maximum parsimony and Bayesian Inference methods. These analyses showed that the two new species clustered into *Hyphoderma*, in which *H. puerense* grouped with *H. moniliforme* and *H. tenuissimum* formed a singleton lineage. In addition, an identification key to Chinese *Hyphoderma* is provided.

Keywords

Corticioid fungi, diversity, Hyphodermataceae, molecular phylogeny, taxonomy, Yunnan Province

Introduction

Fungi are eukaryotic microorganisms that play fundamental ecological roles as decomposers and mutualists of plants and animals. They drive carbon cycling in forest soils, mediate mineral nutrition of plants and alleviate carbon limitations of other soil organisms (Tedersoo et al. 2014). Fungi form an ecologically important branch of the tree of life, based on their distinct and diverse characters (James et al. 2020).

Hyphoderma Wallr. was typified by *H. setigerum* (Fr.) Donk (Donk 1957) and the genus is characterised by resupinate to effuse-reflexed basidiomata of ceraceous consistency and a smooth to tuberculate or hydnoid hymenophore. *Hyphoderma* species are characterised by a monomitic (rarely dimitic) hyphal structure with clamp connections on generative hyphae, presence of cystidia or not, suburniform to subcylindrical to cylindrical basidia and ellipsoid to subglobose, smooth, thin-walled basidiospores (Wallroth 1833; Bernicchia and Gorjón 2010). Currently, about 105 species have been accepted in *Hyphoderma* worldwide (Donk 1957; Nakasone 2008; Wu et al. 2010; Baltazar et al. 2016; Martín et al. 2018; Guan and Zhao 2021a, 2021b; Ma et al. 2021). Index Fungorum (http://www.indexfungorum.org; accessed on 16 July 2021) and MycoBank (https://www.mycobank.org; accessed on 16 July 2021) register 199 specific and infraspecific names in *Hyphoderma*.

Hyphoderma has been studied using molecular data, particularly the internal transcribed spacer (ITS) region and the large subunit nuclear ribosomal RNA gene (nLSU). Larsson (2007) showed that *H. obtusum* J. Erikss. and *H. setigerum* clustered into the Meruliaceae Rea and formed a sister taxon to *Hypochnicium polonense* (Bres.) Å. Strid. Telleria et al. (2012) proposed a new species, *Hyphoderma macaronesicum* Tellería, M. Dueñas, Beltrán-Tej., Rodr.-Armas & M.P. Martín and then discussed the relationships with the closely-related taxa in *Hyphoderma*. Research into the *Hyphoderma setigerum* complex showed that *H. pinicola* Yurch. & Sheng H. Wu represented a fifth species in this complex (Yurchenko and Wu 2014b). A revised family-level classification of the Polyporales revealed that four *Hyphoderma* species grouped into the residual polyporoid clade, belonging to Hyphodermataceae in that they grouped with three related genera in Meripilaceae: *Meripilus* P. Karst., *Physisporinus* P. Karst. and *Rigidoporus* Murrill (Justo et al. 2017).

In this study, two undescribed species of corticioid fungi from forest ecosystems were collected in the Yunnan Province, China. We present morphological and molecular phylogenetic evidence that support the recognition of two new species in *Hyphoderma*, based on the nuclear ribosomal internal transcribed spacer region (ITS1, 5.8S and ITS2) and the nuclear ribosomal nLSU (28S) gene.

Materials and methods

Morphology

The studied specimens are deposited at the Herbarium of Southwest Forestry University (SWFC), Kunming, Yunnan Province, P.R. China. Macromorphological descriptions are based on field notes and photos captured in the field and lab. Colour terminology fol-

lows Petersen (Petersen 1996). Micromorphological data were obtained from the dried specimens when observed under a light microscope following Dai (2012). The following abbreviations are used: **KOH** = 5% potassium hydroxide water solution, **CB** = Cotton Blue, **CB–** = acyanophilous, **IKI** = Melzer's Reagent, **IKI–** = both inamyloid and indextrinoid, **L** = mean spore length (arithmetic average for all spores), **W** = mean spore width (arithmetic average for all spores), **Q** = variation in the L/W ratios between the specimens studied and **n** = a/b (number of spores (a) measured from given number (b) of specimens).

Molecular phylogeny

The CTAB rapid plant genome extraction kit-DN14 (Aidlab Biotechnologies Co., Ltd, Beijing) was used to obtain genomic DNA from the dried specimens following the manufacturer's instructions (as done in Zhao and Wu 2017). The nuclear ribosomal ITS region was amplified with the primers ITS5 and ITS4 (White et al. 1990). The nuclear ribosomal LSU gene was amplified with the primers LR0R and LR7 (Vilgalys and Hester 1990; Rehner and Samuels 1994). The PCR procedure for ITS was as follows: initial denaturation at 95 °C for 3 min followed by 35 cycles at 94 °C for 40 s, 58 °C for 45 s and 72 °C for 1 min and a final extension of 72 °C for 10 min. The PCR procedure for nLSU was as follows: initial denaturation at 94 °C for 1 min followed by 35 cycles at 94 °C for 30 s, 48 °C for 1 min and 72 °C for 1.5 min and a final extension of 72 °C for 10 min. The PCR products were purified and sequenced at Kunming Tsingke Biological Technology Limited Company, Kunming, Yunnan Province, P.R. China. All newly-generated sequences were deposited in NCBI GenBank (Table 1).

The sequences were aligned in MAFFT version 7 (Katoh et al. 2019) using the G-INS-i strategy. The alignment was adjusted manually using AliView version 1.27 (Larsson 2014). Each dataset was aligned separately at first and then the ITS1, 5.8S, ITS2 and nLSU regions were combined with Mesquite version 3.51. The combined dataset was deposited in TreeBASE (submission ID 28564). *Climacocystis borealis* (Fr.) Kotl. and Pouzar and *Diplomitoporus crustulinus* (Bres.) Domański were selected as outgroup (Fig. 1) as inspired by a previous study (Justo et al. 2017).

Maximum parsimony analysis in PAUP* version 4.0a169 (http://phylosolutions.com/paup-test/) was applied to the combined ITS1+5.8S+ITS2+nLSU dataset. All characters were equally weighted and gaps were treated as missing data. Trees were inferred using the heuristic search option with TBR branch swapping and 1,000 random sequence additions. Max-trees were set to 5,000, branches of zero length were collapsed and all parsimonious trees were saved. Clade robustness was assessed using bootstrap (BT) analysis with 1,000 pseudoreplicates (Felsenstein 1985). Descriptive tree statistics – tree length (TL), composite consistency index (CI), composite retention index (RI), composite rescaled consistency index (RC) and composite homoplasy index (HI) – were calculated for each maximum parsimonious tree generated. The combined dataset was also analysed using Maximum Likelihood (ML) in RAxML-HPC2 through the CIPRES Science Gateway (Miller et al. 2012). Branch support (BS) for the ML analysis was determined by 1,000 bootstrap pseudoreplicates.

Table 1. List of species, specimens and GenBank accession numbers of sequences used in this study.

Species name	Specimen No.	GenBank accession No.		References
		ITS	LSU	
Climacocystis borealis	FD-31	KP135308	KP135210	Justo et al. (2017)
Diplomitoporus crustulinus	FD-137	KP135299	KP135211	Justo et al. (2017)
Hyphoderma amoenum	USO 286622	HE577030	—	Telleria et al. (2012)
H. assimile	CBS 125852	MH863808	MH875272	Vu et al. (2019)
H. cremeoalbum	NH 11538	DQ677492	DQ677492	Larsson (2007)
H. crystallinum	CLZhao 9338	MW917161	MW913414	Guan and Zhao (2021a)
	CLZhao 9374	MW917162	MW913415	Guan and Zhao (2021a)
	CLZhao 10224	MW917163	MW913416	Guan and Zhao (2021a)
	CLZhao 11723	MW917164	MW913417	Guan and Zhao (2021a)
	CLZhao 15841	MW917165	MW913418	Guan and Zhao (2021a)
	CLZhao 18459	MW917166	MW913419	Guan and Zhao (2021a)
H. definitum	GEL 2898	—	AJ406509	Yurchenko and Wu (2014)
	NH 12266	DQ677493	DQ677493	Larsson (2007)
H. fissuratum	CLZhao 6731	MT791331	MT791335	Ma et al. (2021)
	CLZhao 6726	MT791330	MT791334	Ma et al. (2021)
H. floccosum	CLZhao 17129	MW301683	MW293733	Guan and Zhao (2021b)
	CLZhao 17296	MW301686	MW293736	Guan and Zhao (2021b)
	CLZhao 16492	MW301688	MW293734	Guan and Zhao (2021b)
	CLZhao 17215	MW301687	MW293735	Guan and Zhao (2021b)
H. granuliferum	KHL 12561	JN710545	JN710545	Yurchenko and Wu (2014)
H. incrustatum	KHL 6685	—	AY586668	Yurchenko and Wu (2014)
H. litschaueri	NH 7603	DQ677496	DQ677496	Larsson (2007)
	FP-101740-Sp	KP135295	KP135219	Floudas and Hibbett (2015)
H. macaronesicum	MA:Fungi:16099	HE577027	—	Yurchenko and Wu (2014)
	TFC:Mic.15981	HE577028	—	Yurchenko and Wu (2014)
H. medioburiense	NH 10950	DQ677497	DQ677497	Larsson (2007)
H. membranaceum	CLZhao 5844	MW917167	MW913420	Guan and Zhao (2021a)
	CLZhao 6971	MW917168	MW913421	Guan and Zhao (2021a)
H. microporoides	CLZhao 6857	MW917169	MW913422	Guan and Zhao (2021a)
	CLZhao 8695	MW917170	MW913422	Guan and Zhao (2021a)
H. moniliforme	Wu 0211–42	KC928282	—	Yurchenko and Wu (2015)
	Wu 0211–46	KC928284	KC928285	Yurchenko and Wu (2015)
H. mopanshanense	CLZhao 6498	MT791329	MT791333	Ma et al. (2021)
	CLZhao 6493	MT791328	MT791332	Ma et al. (2021)
H. nemorale	TNM F3931	KJ885183	KJ885184	Yurchenko and Wu (2015)
	Wu 9508–14	KC928280	KC928281	Yurchenko and Wu (2015)
H. nudicephalum	Wu 9307–29	AJ534269	—	Nilsson et al. (2003)
	Wu 9508–225	AJ534268	—	Nilsson et al. (2003)
H. obtusiforme	KHL 1464	JN572909	—	Yurchenko and Wu (2014)
	KHL 11105	JN572910	—	Yurchenko and Wu (2014)
H. obtusum	JS 17804	—	AY586670	Yurchenko and Wu (2014)
H. occidentale	KHL 8469	—	AY586674	Yurchenko and Wu (2014)
	KHL 8477	DQ677499	DQ677499	Larsson (2007)
H. paramacaronesicum	MA:Fungi:87736	KC984399	—	Martín et al. (2018)
	MA:Fungi:87737	KC984405	—	Martín et al. (2018)
H. pinicola	Wu 0108–32	KJ885181	KJ885182	Yurchenko and Wu (2014)
	Wu 0108–36	KC928278	KC928279	Yurchenko and Wu (2014)
H. prosopidis	E09/58–9	HE577029	—	Yurchenko and Wu (2015)
H. puerense	**CLZhao 9476***	**MW443045**	—	**Present study**
	CLZhao 9583	**MW443046**	**MW443051**	**Present study**
H. roseocremeum	NH 10545	—	AY586672	Yurchenko and Wu (2014)
H. setigerum	FCUG 1200	AJ534273	—	Nilsson et al. (2003)
H. setigerum	FCUG 1688	AJ534272	—	Nilsson et al. (2003)
H. sinense	CLZhao 7963	MW301679	MW293730	Guan and Zhao (2021b)
	CLZhao 17811	MW301682	MW293732	Guan and Zhao (2021b)
	CLZhao 7981	MW301680	MW293731	Guan and Zhao (2021b)
Hyphoderma sp.	KUC20121102–21	KJ668522	—	Unpublished
	KUC11052	KJ714002	—	Jang et al. (2015)
	Wu 0311–25	KR868735	—	Unpublished
	Wu 0310–6	KR868736	—	Unpublished
	Wu 0808–87	KR868737	—	Unpublished
	GEL3689	DQ340327	—	Unpublished
H. subsetigerum	Wu 9304–18	AJ534277	—	Nilsson et al. (2003)
	Wu 9202–15	AJ534278	—	Nilsson et al. (2003)

Species name	Specimen No.	GenBank accession No.		References
		ITS	LSU	
H. subsetigerum	HHB11620	GQ409521	—	Yurchenko and Wu (2014)
	CFMR MJL1536	GQ409522	—	Yurchenko and Wu (2014)
H. tenuissimum	**CLZhao 6930**	**MW443047**	**MW443052**	**Present study**
	CLZhao 7003	**MW443048**	**MW443053**	**Present study**
	CLZhao 7221*	**MW443049**	**MW443054**	**Present study**
	CLZhao 16210	**MW443050**	**MW443055**	**Present study**
H. transiens	NH 12304	DQ677504	DQ677504	Larsson (2007)
H. variolosum	CBS 734.91	MH862320	MH873992	Vu et al. (2019)
	CBS 735.91	MH862321	MH873993	Vu et al. (2019)
Hypochnicium erikssonii	NH 9635	—	DQ677508	Larsson (2007)
H. geogenium	NH 10910	—	DQ677509	Larsson (2007)
	MA-Fungi 48308	FN552534	JN939576	Telleria et al. (2010)
H. michelii	MA-Fungi 79155	NR119742	NG060635	Telleria et al. (2010)
H. punctulatum	FP101698sp	KY948827	KY948860	Justo et al. (2017)
H. sphaerosporum	RLG15138sp	KY948803	KY948861	Justo et al. (2017)
H. wakefieldiae	MA-Fungi 7675	FN552531	JN939577	Telleria et al. (2010)
Physisporinus subcrocatus	Dai 15917	KY131870	KY131926	Wu et al. (2017)
P. subcrocatus	Dai 12800	KY131869	KY131925	Wu et al. (2017)
P. tibeticus	Cui 9588	KY131873	KY131929	Wu et al. (2017)
	Cui 9518	KY131872	KY131928	Wu et al. (2017)
Rigidoporus eminens	Dai 17200	MT279690	MT279911	Wu et al. (2017)
R. undatus	Miettinen-13591	KY948731	KY948870	Justo et al. (2017)

New species is shown in bold; * type material.

MrModeltest 2.3 (Nylander 2004) was used to determine the best-fit evolution model for each dataset (ITS1+5.8S+ITS2+nLSU) for Bayesian Inference (BI). BI was calculated with MrBayes version 3.2.7a (Ronquist et al. 2012). Four Markov chains were run for two runs from random starting trees for 3 million generations (Fig. 1). The first 25% of all generations was discarded as burn-in. A majority rule consensus tree was computed from the remaining trees. Branches were considered as significantly supported if they received a maximum likelihood bootstrap support value (BS) of > 70%, a maximum parsimony bootstrap support value (BT) of > 70% or a Bayesian posterior probability (BPP) of > 0.95.

Results

Molecular phylogeny

The ITS1+5.8S+ITS2+nLSU dataset comprised sequences from 86 fungal specimens representing 46 taxa. The dataset had an aligned length of 2,034 characters, of which 1,360 characters were constant, 131 were variable and parsimony-uninformative and 543 (35%) were parsimony-informative. Maximum parsimony analysis yielded 108 equally parsimonious trees (TL = 3,317, CI = 0.3361, HI = 0.6946, RI = 0.7051 and RC = 0.2370). The best model of nucleotide evolution for the ITS1+5.8S+ITS2+nLSU dataset estimated and applied in the Bayesian analysis was found to be GTR+I+G. Bayesian analysis and ML analysis resulted in a similar topology as in the MP analysis. The Bayesian analysis had an average standard deviation of split frequencies = 0.008952 (BI) and the effective sample size (ESS) across the two runs is double the average ESS (avg. ESS) = 1,771. The Bayesian tree is shown here (Fig. 1).

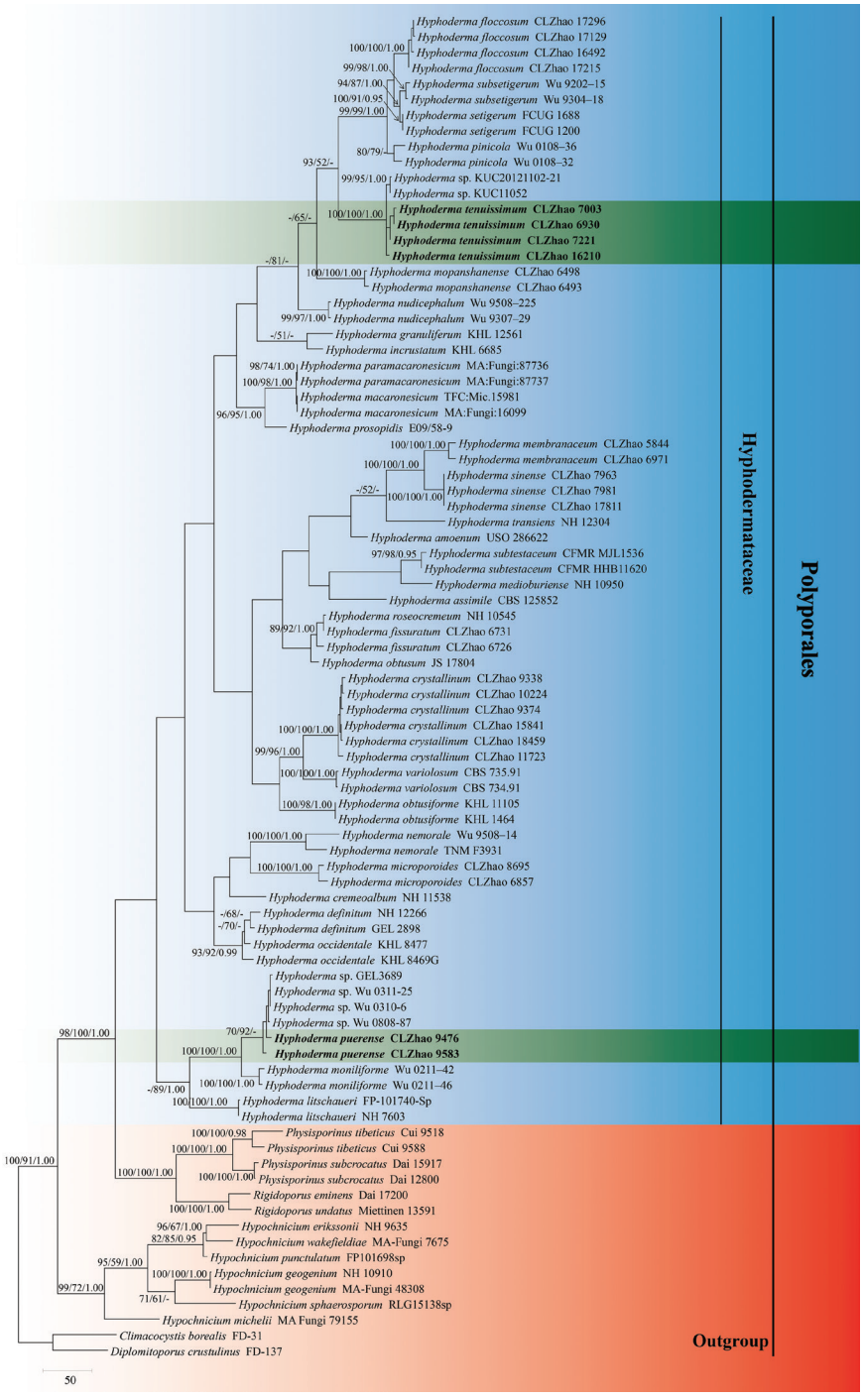

Figure 1. Maximum parsimony strict consensus tree illustrating the phylogeny of the two new species and related species in *Hyphoderma*, based on ITS1+5.8S+ITS2+nLSU sequences. Branches are labelled with maximum likelihood bootstrap values > 70%, parsimony bootstrap values > 50% and Bayesian posterior probabilities > 0.95, respectively.

The phylogram inferred from ITS1+5.8S+ITS2+nLSU sequences (Fig. 1) highlights the two undescribed species in *Hyphoderma*; *H. puerense* as a sister to *H. moniliforme* and *H. tenuissimum* that forms an independent monophyletic lineage (100% parsimony bootstrap support, 100% likelihood bootstrap support and 1.00 BPP).

Taxonomy

***Hyphoderma puerense* C.L. Zhao & Q.X. Guan, sp. nov.**
MycoBank No: 838411
Figs 2, 3

Holotype. China. Yunnan Province, Puer, Jingdong County, Huilianghe Village, GPS co-ordinates 24°04'45"N, 100°56'32"E, altitude 1246 m a.s.l., on fallen angiosperm branch, leg. C.L. Zhao, 4 January 2019, CLZhao 9476 (SWFC).

Etymology. *puerense* (Lat.): referring to the locality (Puer) of the specimens.

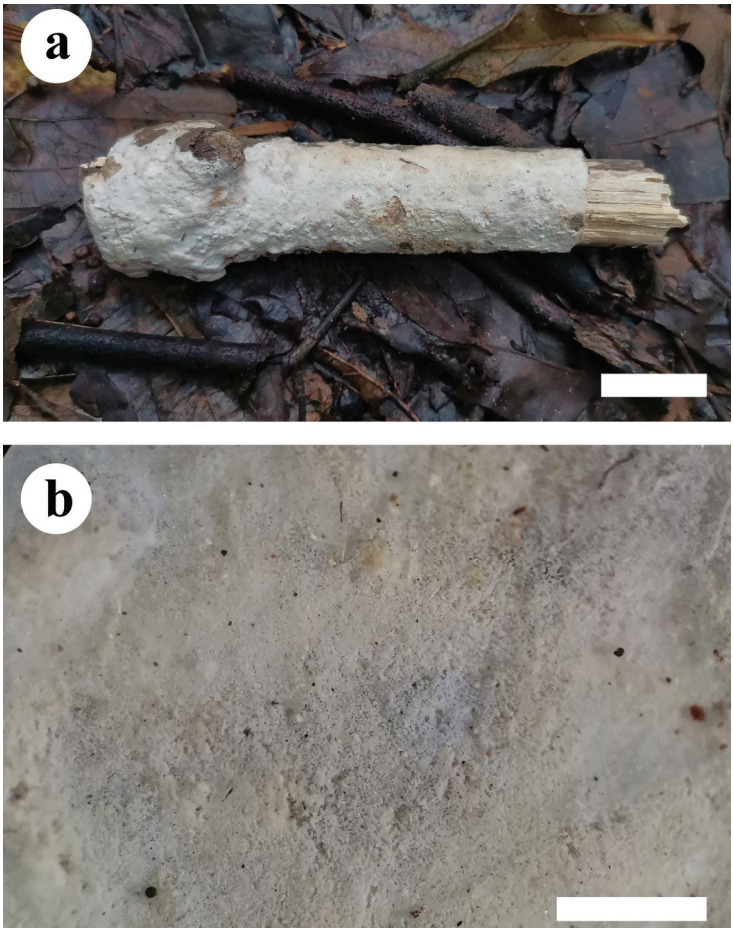

Figure 2. Basidiomata of *Hyphoderma puerense* (holotype). Scale bars: 2 cm (**a**); 1 mm (**b**).

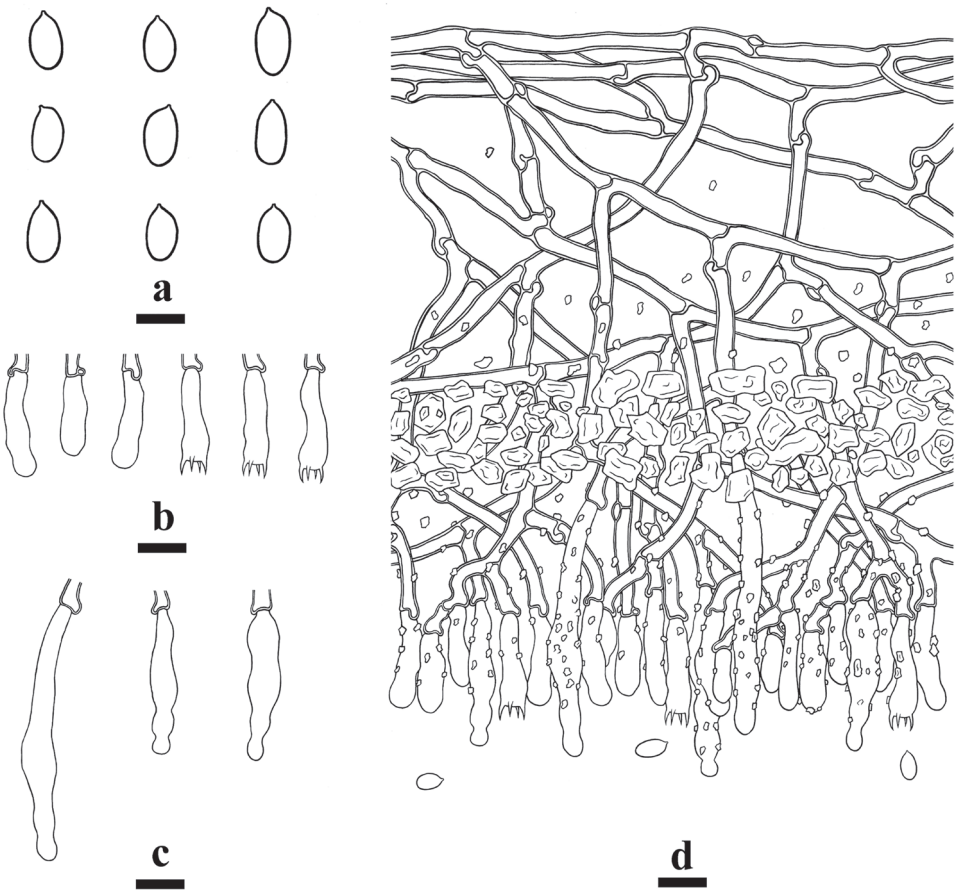

Figure 3. Microscopic structures of *Hyphoderma puerense* (holotype) **a** basidiospores **b** basidia and basidioles **c** cystidia **d** a section of hymenium. Scale bars: 5 μm (**a**); 10 μm (**b–d**).

Description. Basidioma annual, resupinate, adnate, byssoid, without odour and taste when fresh, up to 15 cm long, 3 cm wide, 100–260 μm thick. Hymenial surface smooth to floccose, cream when fresh, cream to slightly buff on drying. Margin sterile, thinning out, narrow, cream.

Hyphal system monomitic, generative hyphae with clamps, colourless, thick-walled, frequently branched, interwoven, 2.5–4.5 μm in diameter; IKI-, CB-; tissues unchanged in KOH; subhymenial hyphae densely covered by crystals.

Cystidia tubular, encrusted with small crystals, 25–97 × 5.5–9.5 μm.

Basidia clavate to subcylindrical, slightly constricted in the middle to somewhat sinuous, with 4 sterigmata and a basal clamp, 20–30 × 4.5–6 μm.

Basidiospores ellipsoid, colourless, thin-walled, smooth, IKI-, CB-, (5.5–)6–7.5(–8) × 3–4.5(–5) μm, L = 6.53 μm, W = 3.71 μm, Q = 1.73–1.79 (n = 60/2).

Habitat and ecology. Climate of the sample collection site is subtropical monsoon climate area, the forest type is evergreen angiosperm forest and samples were collected on fallen angiosperm branches.

Additional specimens examined. China. Yunnan Province, Puer, Jingdong County, Huilianghe Village, GPS co-ordinates 24°04'45"N, 100°56'32"E, altitude 1246 m a.s.l., on fallen angiosperm branch, leg. C.L. Zhao, 5 January 2019, CLZhao 9583 (SWFC).

***Hyphoderma tenuissimum* C.L. Zhao & Q.X. Guan, sp. nov.**
MycoBank No: 838412
Figs 4, 5

Holotype. China. Yunnan Province, Chuxiong, Zixishan Forestry Park, GPS co-ordinates 25°01'26"N, 101°24'37"E, altitude 2313 m a.s.l., on fallen angiosperm branch, leg. C.L. Zhao, 1 July 2018, CLZhao 7221 (SWFC).

Etymology. *tenuissimum* (Lat.): referring to the thin basidiomata.

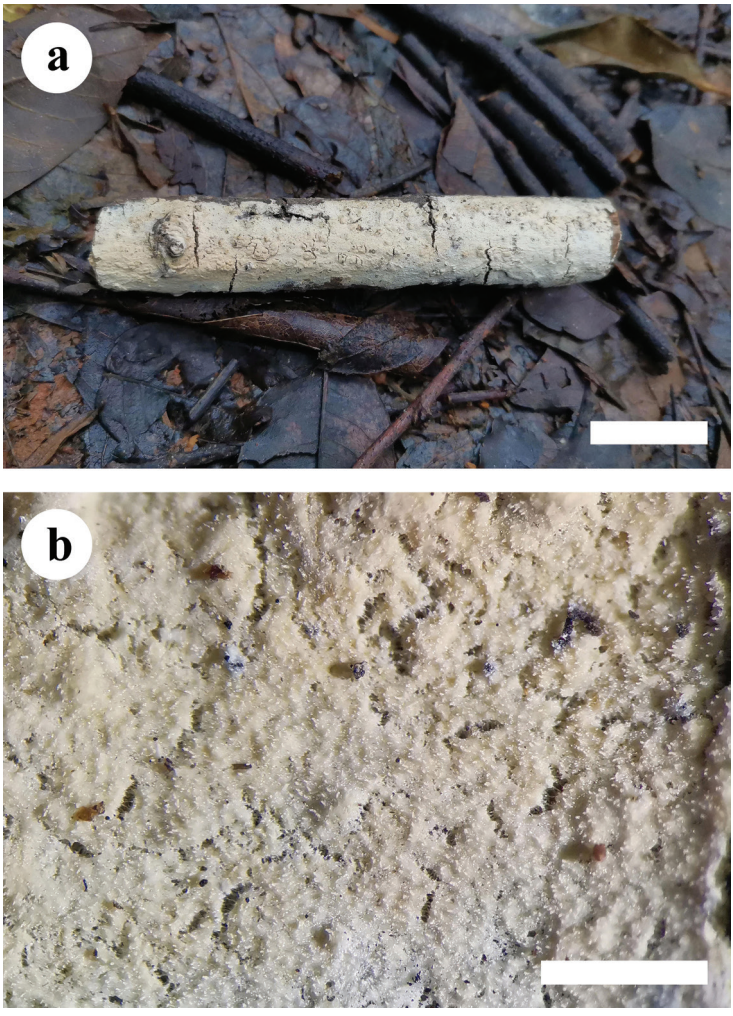

Figure 4. Basidiomata of *Hyphoderma tenuissimum* (holotype). Scale bars: 2 cm (**a**); 1 mm (**b**).

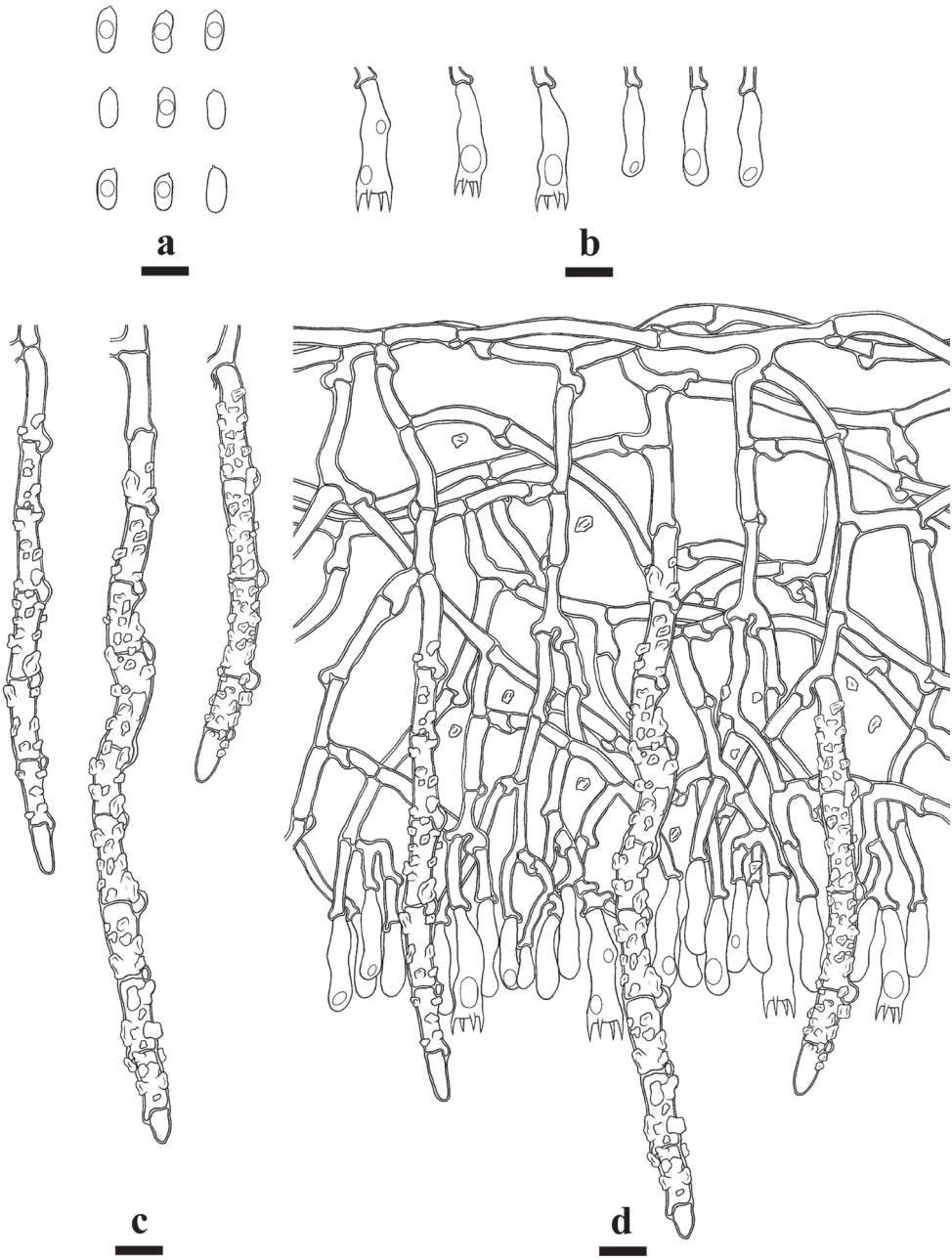

Figure 5. Microscopic structures of *Hyphoderma tenuissimum* (holotype) **a** basidiospores **b** basidia and basidioles **c** cystidia **d** a section of hymenium. Scale bars: 10 μm (**a–d**).

Description. Basidioma annual, resupinate, adnate, membranaceous when fresh, hard membranaceous upon drying, up to 20 cm long, 3 cm wide, 30–100 μm thick. Hymenial surface tuberculate to minutely-grandinioid, slightly buff when fresh, buff upon drying, cracking. Margin sterile, slightly buff, 1 mm wide.

Hyphal system monomitic, generative hyphae with clamps, colourless, thick-walled, frequently branched, interwoven, 3–5 µm in diameter, IKI-, CB-; tissues unchanged in KOH.

Cystidia large, cylindrical, with 4–12 clamped septa, with abundant encrustations, 50–220 × 6.5–13 µm.

Basidia clavate to subcylindrical, constricted, somewhat sinuous, with 4 sterigmata and a basal clamp connection, 17–31 × 4.5–8 µm.

Basidiospores cylindrical, colourless, thin-walled, smooth, with oil drops inside, IKI–, CB–, 7–10.5(–11) × 3–4.5(–5) µm, L = 8.75 µm, W = 4.15 µm, Q = 2.02–2.18 (n = 120/4).

Habitat and ecology. Climate of the sample collection site is subtropical monsoon climate area, the forest type is evergreen angiosperm forest and samples were collected on fallen angiosperm branches.

Additional specimens examined. China. Yunnan Province, Chuxiong, Zixishan National Forestry Park, GPS co-ordinates 25°01'26"N, 101°24'37"E, altitude 2263 m a.s.l., on fallen angiosperm branch, leg. C.L. Zhao, 1 July 2018, CLZhao 6930, CLZhao 7003 (SWFC); Wenshan, Pingba Town, Wenshan National Nature Reserve, GPS co-ordinates 23°18'19"N, 104°42'47"E, altitude 1976 m a.s.l., on fallen angiosperm branch, leg. C.L. Zhao, 25 July 2019, CLZhao 16210 (SWFC).

Discussion

In the present study, two new species, *Hyphoderma puerense* and *H. tenuissimum* are described, based on phylogenetic analyses and morphological characters.

Phylogenetically, the two new taxa were found to belong to *Hyphoderma*, in which *H. puerense* forms a sister species to *H. moniliforme* and *H. tenuissimum* forms an independent monophyletic lineage (100% BS, 100% BP and 1.00 BPP).

Morphologically, *Hyphoderma puerense* is similar to *H. obtusiforme* J. Eriksss. & Å. Strid and *H. obtusum* in having a smooth hymenium, non-septate cylindrical cystidia and ellipsoid basidiospores. However, *H. obtusiforme* differs from *H. puerense* by both larger basidia (30–40 × 8–9 µm) and basidiospores (10–14 × 5–7 µm; Eriksson and Ryvarden 1975). *Hyphoderma obtusum* also differs from *H. puerense* by larger basidia (30–35 × 6–8 µm) and basidiospores (8–9 × 5–6.5 µm; Eriksson 1958). *Hyphoderma puerense* is similar to *H. roseocremeum* (Bres.) Donk in having smooth hymenium and non-septate cylindrical cystidia. However, *Hyphoderma roseocremeum* differs through the presence of larger basidiospores (8–12 × 3–4 µm; Bernicchia and Gorjón 2010).

Morphologically, *Hyphoderma tenuissimum* is similar to *H. floccosum* C.L. Zhao & Q.X. Guan, *H. mopanshanense*, *H. nudicephalum* Gilb. & M. Blackw., *H. pinicola*, *H. setigerum* and *H. subsetigerum* Sheng H. Wu in having septocystidia and cylindrical basidiospores. However, *Hyphoderma floccosum* differs from *H. tenuissimum* by having a floccose hymenial surface and tubular cystidia (Guan and Zhao 2021b); *H. mopanshanense* is separated from *H. tenuissimum* by having porulose to pilose hymenial surface and smaller basidia (15–18.5 × 3–4.5 µm; Ma et al. 2021); *H. nu-*

dicephalum differs from *H. tenuissimum* in the nature of the septocystidial apex (lacking encrustation; swollen up to 14 µm; Gilbertson and Blackwell 1988); *H. pinicola* is separated from *H. tenuissimum* by having basidia with two sterigmata and larger basidiospores (13–16 × 4–4.5 µm; Yurchenko and Wu 2014b); *H. setigerum* differs by having a combination of thin basidiomata with very long septocystidia (Bernicchia and Gorjón 2010); and *H. subsetigerum* differs from *H. tenuissimum* by having narrower basidia (20–30 × 4.5–5.5 µm) and smaller basidiospores (6–8 × 2.8–3.2 µm; Wu 1997).

Nilsson et al. (2003) highlighted the phylogeography of *Hyphoderma setigerum* (Basidiomycota) in the Northern Hemisphere in a study based on molecular analysis, morphological studies and crossing tests. Nine preliminary taxa were shown to exist inside the *H. setigerum* complex; in the present study, *H. tenuissimum* belongs to the *H. setigerum* complex, based on the morphological character of long septocystidia and phylogenetic evidence. A previous study indicated the importance of vicariance in the evolution of this species complex (Nilsson et al. 2003) and our study shows that the specimens of *H. tenuissimum* are collected in Zixishan National Forestry Park (GPS co-ordinates 25°01'26"N, 101°24'37"E), Chuxiong, Yunnan Province, China, which is distinct from *H. setigerum* s. str. (Norway: Oppland and Finland: Pohjois-Häme). The present samples of *H. subsetigerum* and *H. nudicephalum* were collected in Yunnan Province, China, but neither of these taxa groups together closely with *H. tenuissimum* (Fig. 1).

In the current phylogenetic tree, two partially annotated GenBank sequences (KJ668522 and KJ714002) of *Hyphoderma* sp. (South Korea) cluster closely with four sequences of the new species *Hyphoderma tenuissimum*, although whether they really belong to this species remains to be assessed. It is certainly conceivable that they do, which would mean that *Hyphoderma tenuissimum* has been collected and sequenced at least six times in Asia. Regarding the new taxon *H. puerense* (Fig. 1), four partially annotated GenBank sequences (KR868735, KR868736, KR868737 and DQ340327) form a reasonably well-supported clade together with our two specimens of *H. puerense.* We interpret this to mean that all six taxa represent *H. puerense*. All of the samples in this clade are from Asia, which supports the point of the importance of vicariance in the evolution in this genus.

Key to 30 accepted species of *Hyphoderma* in China

1 Cystidia absent **2**
– Cystidia present **5**
2 Hymenial surface grandinioid ..... ***H. acystidiatum***
– Hymenial surface smooth **3**
3 Basidiospores > 10.5 µm in length ..... ***H. densum***
– Basidiospores < 10.5 µm in length **4**
4 Hymenophore cracked; basidiospores > 8.5 µm in length ..... ***H. fissuratum***
– Hymenophore uncracked; basidiospores < 8.5 µm in length ..... ***H. sibiricum***
5 Hymenophore smooth **6**
– Hymenophore tuberculate, porulose, grandinioid or odontoid **15**

6 Two types of cystidia present **7**
– One type of cystidia present **8**
7 Moniliform cystidia absent ..... ***H. microcystidium***
– Moniliform cystidia present ..... ***H. sinense***
8 Hymenophore uncracked **9**
– Hymenophore cracked **11**
9 Basidiospores > 11 µm in length ..... ***H. definitum***
– Basidiospores < 11 µm in length **10**
10 Basidiospores > 8.5 µm in length ..... ***H. microporoides***
– Basidiospores < 8.5 µm in length ..... ***H. puerense***
11 Cystidia moniliform **12**
– Cystidia cylindrical **13**
12 Basidiospores > 9 µm in length ..... ***H. litschaueri***
– Basidiospores < 9 µm in length ..... ***H. moniliforme***
13 Basidiospores ellipsoid < 10 µm in length ..... ***H. rimulosum***
– Basidiospores cylindrical > 10 µm in length **14**
14 Basidiospores > 12 µm in length ..... ***H. cremeum***
– Basidiospores < 12 µm in length ..... ***H. subclavatum***
15 Hymenophore odontoid or grandinioid **16**
– Hymenophore tuberculate, porulose **19**
16 Hymenophore odontoid **17**
– Hymenophore grandinioid **18**
17 Basidiospores < 4.5 µm in width ..... ***H. transiens***
– Basidiospores > 4.5 µm in width ..... ***H. formosanum***
18 Basidiospores larger 7–10.5 × 3–4.5 µm ..... ***H. tenuissimum***
– Basidiospores smaller 6–8 × 2.8–3.2 µm ..... ***H. subsetigerum***
19 Cystidia of two types **20**
– Cystidia of one type **23**
20 Septate cystidia absent **21**
– Septate cystidia present **22**
21 Basidiospores < 4 µm in width ..... ***H. variolosum***
– Basidiospores > 4 µm in width ..... ***H. crystallinum***
22 Basidia 2-sterigmata, basidiospores > 13 µm in length ..... ***H. pinicola***
– Basidia 4-sterigmata, basidiospores < 13 µm in length ..... ***H. floccosum***
23 Septate cystidia present **24**
– Septate cystidia absent **25**
24 Hymenophore porulose to pilose, basidia < 5 µm in width .... ***H. mopanshanense***
– Hymenophore tuberculate, basidia > 5 µm in width ..... ***H. setigerum***
25 Hymenophore porulose ..... ***H. obtusiforme***
– Hymenophore tuberculate, colliculose ***26***
26 Cystidia < 30 µm in length ..... ***H. cremeoalbum***
– Cystidia > 30 µm in length **27**
27 Basidia > 30 µm in length **28**
– Basidia < 30 µm in length **29**

28 Hymenophore cracking, cystidia < 10 μm in width..... ***H. medioburiense***
– Hymenophore not cracking, cystidia > 10 μm in width ..... ***H. clavatum***
29 Hymenophore colliculose..... ***H. nemorale***
– Hymenophore tuberculate ..... ***H. membranaceum***

Acknowledgements

The research was supported by the Yunnan Fundamental Research Project (Grant No. 202001AS070043) and Science Research Foundation of Yunnan Provincial Department of Education Project (Project No. 2021Y275).

References

Baltazar JM, Silveira RMB, Rajchenberg M (2016) Type studies of J. Rick's corticioid homobasidiomycetes (Agaricomycetes, Basidiomycota) housed in the Herbarium Anchieta (PACA). Phytotaxa 255(2): 101–132. https://doi.org/10.11646/phytotaxa.255.2.1

Bernicchia A, Gorjón SP (2010) Fungi Europaei 12: Corticiaceae s.l. Alassio: Edizioni Candusso.

Dai YC (2012) Polypore diversity in China with an annotated checklist of Chinese polypores. Mycoscience 53(1): 49–80. https://doi.org/10.1007/s10267-011-0134-3

Donk MA (1957) Notes on resupinate Hymenomycetes IV. Fungus 27: 1–29.

Eriksson J (1958) Studies in the Heterobasidiomycetes and Homobasidiomycetes – Aphyllophorales of Muddus National Park in North Sweden. Symbolae Botanicae Upsalienses 16(1): 1–172.

Eriksson J, Ryvarden L (1975) The Corticiaceae of North Europe; Fungiflora: Oslo, Norway, Volume 3, 288–546.

Felsenstein J (1985) Confidence intervals on phylogenetics: An approach using bootstrap. Evolution 39: 783–791. https://doi.org/10.1111/j.1558-5646.1985.tb00420.x

Floudas D, Hibbett DS (2015) Revisiting the taxonomy of *Phanerochaete* (Polyporales, Basidiomycota) using a four gene dataset and extensive ITS sampling. Fungal Biology 119(80): 679–719. https://doi.org/10.1016/j.funbio.2015.04.003

Gilbertson RL, Blackwell M (1988) Some new or unusual corticioid fungi from the Gulf Coast region. Mycotaxon 33: 375–386.

Guan QX, Zhao CL (2021a) Taxonomy and phylogeny of the wood-inhabiting fungal genus *Hyphoderma* with descriptions of three new species from East Asia. Journal of Fungi 7(4): e308. https://doi.org/10.3390/jof7040308

Guan QX, Zhao CL (2021b) Two new corticioid species, *Hyphoderma sinense* and *H. floccosum* (Hyphodermataceae, Polyporales), from southern China. Mycosystema 40(03): 447–461. https://doi.org/10.13346/j.mycosystema.200382

James TY, Stajich JE, Hittinger CT, Rokas A (2020) Toward a fully resolved fungal tree of life. Annual Review of Microbiology 74(1): 291–313. https://doi.org/10.1146/annurev-micro-022020-051835

Jang Y, Jang S, Min M, Hong JH, Lee H, Lee H, Lim YW, Kim JJ (2015) Comparison of the diversity of basidiomycetes from dead wood of the Manchurian fir (*Abies holophylla*) as

evaluated by fruiting body collection, mycelial isolation, and 454 sequencing. Microbial Ecology 70(3): 634–645. https://doi.org/10.1007/s00248-015-0616-5

Justo A, Miettinen O, Floudas D, Ortiz-Santana B, Sjökvist E, Linder D, Nakasone K, Niemelä T, Larsson K, Ryvarden L, Hibbetta DS (2017) A revised family-level classification of the Polyporales (Basidiomycota). Fungal Biology 121(9): 798–824. https://doi.org/10.1016/j.funbio.2017.05.010

Katoh K, Rozewicki J, Yamada KD (2019) MAFFT online service: multiple sequence alignment, interactive sequence choice and visualization. Briefings in Bioinformatics 20(4): 1160–1166. https://doi.org/10.1093/bib/bbx108

Larsson A (2014) AliView: a fast and lightweight alignment viewer and editor for large data sets. Bioinformatics 30(22): 3276–3278. http://dx.doi.org/10.1093/bioinformatics/btu531

Larsson KH (2007) Re-thinking the classification of corticioid fungi. Mycological Research 111(9): 1040–1063. https://doi.org/10.1016/j.mycres.2007.08.001

Ma X, Huang RX, Zhang Y, Zhao CL (2021) *Hyphoderma fissuratum* and *H. mopanshanense* spp. nov. (Polyporales) from southern China. Mycoscience 62(1): 36–41. https://doi.org/10.47371/Mycosci.2020.08.004

Martín MP, Zhang LF, Fernández-López J, Dueñas M, Rodríguez-Armas JL, Beltrán-Tejera E, Telleria MT (2018) *Hyphoderma paramacaronesicum* sp. nov. (Meruliaceae, Polyporales, Basidiomycota), a cryptic lineage to *H. macaronesicum*. Fungal Systematics and Evolution 2: 57–68. https://doi.org/10.3114/fuse.2018.02.05

Miller MA, Pfeiffer W, Schwartz T (2012) The CIPRES Science Gateway: enabling high-impact science for phylogenetics researchers with limited resources. Association for Computing Machinery 39: 1–8. https://doi.org/10.1145/2335755.2335836

Nakasone KK (2008) Type studies of corticioid Hymenomycetes described by Bresadola. Cryptogamie Mycologie 29(3): 231–257. https://doi.org/10.1002/yea.1629

Nilsson RH, Hallenberg N, Nordén B, Maekawa N, Wu SH (2003) Phylogeography of *Hyphoderma setigerum* (Basidiomycota) in the Northern Hemisphere. Mycological Research 107(6): 645–652. https://doi.org/10.1017/S0953756203007925

Nylander JAA (2004) MrModeltest v.2. Program Distributed by the Author. Evolutionary Biology Centre, Uppsala University, Uppsala.

Petersen JH (1996) The Danish Mycological Society's colour-chart. Foreningen til Svampekundskabens Fremme, Greve.

Rehner SA, Samuels GJ (1994) Taxonomy and phylogeny of *Gliocladium* analysed from nuclear large subunit ribosomal DNA sequences. Mycological Research 98(6): 625–634. https://doi.org/10.1016/S0953-7562(09)80409-7

Ronquist F, Teslenko M, van der Mark P, Ayres DL, Darling A, Hohna S, Larget B, Liu L, Suchard MA, Huelsenbeck JP (2012) MrBayes 3.2: efficient Bayesian phylogenetic inference and model choice across a large model space. Systematic Biology 61(3): 539–542. https://doi.org/10.1093/sysbio/sys029

Tedersoo L, Bahram M, Põlme S, Kõljalg U, Yorou NS, Wijesundera R, Ruiz LV, Vasco-Palacios AM, Thu PQ, Suija A, Smith ME, Sharp C, Saluveer E, Saitta A, Rosas M, Riit T, Ratkowsky D, Pritsch K, Põldmaa K, Piepenbring M, Phosri C, Peterson M, Parts K, Pärtel K, Otsing E, Nouhra E, Njouonkou AL, Nilsson RH, Morgado LN, Mayor J, May TW, Majuakim L, Lodge DJ, Lee SS, Larsson K-H, Kohout P, Hosaka K, Hiiesalu I, Henkel

TW, Harend H, Guo L-d, Greslebin A, Grelet G, Geml J, Gates G, Dunstan W, Dunk C, Drenkhan R, Dearnaley J, De Kesel A, Dang T, Chen X, Buegger F, Brearley FQ, Bonito G, Anslan S, Abelland S, Abarenkov K (2014) Global diversity and geography of soil fungi. Science 346: 1256688. https://doi.org/10.1126/science.1256688

Telleria MT, Dueñas M, Beltrán-Tejera E, Rodríguez-Armas JL, Martín MP (2012) A new species of *Hyphoderma* (Meruliaceae, Polyporales) and its discrimination from closely related taxa. Mycologia 104(5): 1121–1132. https://doi.org/10.3852/11-344

Telleria MT, Duenas M, Melo I, Hallenberg N, Martin MP (2010) A re-evaluation of *Hypochnicium* (Polyporales) based on morphological and molecular characters. Mycologia 102(6): 1426–1436. https://doi.org/10.3852/09-242

Vilgalys R, Hester M (1990) Rapid genetic identification and mapping of enzymatically amplified ribosomal DNA from several *Cryptococcus* species. Journal of Bacteriology 172(8): 4238–4246.

Vu D, Groenewald M, Vries M, Gehrmann T, Stielow B, Eberhardt U, Al-Hatmi A, Groenewald JZ, Cardinali G, Houbraken J, Boekhout T, Crous PW, Robert V, Verkley GJM (2019) Large-scale generation and analysis of filamentous fungal DNA barcodes boosts coverage for kingdom Fungi and reveals thresholds for fungal species and higher taxon delimitation. Studies in Mycology 92: 135–154. https://doi.org/10.1016/j.simyco.2018.05.001

Wallroth CFW (1833) Flora Cryptogamica Germaniae 2 Algas et fungos. Norimbergae [Nüremberg], Schragius [J.L. Schrag], 923 pp.

White TJ, Bruns T, Lee S, Taylor J (1990) Amplification and direct sequencing of fungal ribosomal RNA genes for phylogenetics. In: Innis MA, Gefand DH, Sninsky JJ, White JT (Eds) PCR Protocols: A Guide to Methods and Applications. Academic Press, San Diego, 18: 315–322. https://doi.org/10.1016/B978-0-12-372180-8.50042-1

Wu F, Chen JJ, Ji XH, Vlasák J, Dai YC (2017) Phylogeny and diversity of the morphologically similar polypore genera *Rigidoporus*, *Physisporinus*, *Oxyporus* and *Leucophellinus*. Mycologia 109(5): 749–765. doi:10.1080/00275514.2017.1405215

Wu SH (1997) New species of *Hyphoderma* from Taiwan. Mycologia 89: 132–140. https://doi.org/10.1080/00275514.1997.12026764

Wu SH, Nilsson HR, Chen CT, Yu SY, Hallenberg N (2010) The white-rotting genus *Phanerochaete* is polyphyletic and distributed throughout the phlebioid clade of the Polyporales (Basidiomycota). Fungal Diversity 42(1): 107–118. https://doi.org/10.1007/s13225-010-0031-7

Yurchenko E, Wu SH (2014) *Hyphoderma pinicola* sp. nov. of *H. setigerum* complex (Basidiomycota) from Yunnan, China. Botanical Studies 55: 71–78. https://doi.org/10.1186/s40529-014-0071-5

Yurchenko E, Wu SH (2015) *Hyphoderma moniliforme* and *H. nemorale* (Basidiomycota) newly recorded from China. Mycosphere 6(1): 113–121. https://doi.org/10.5943/mycosphere/6/1/11

Zhao CL, Wu ZQ (2017) *Ceriporiopsis kunmingensis* sp. nov. (Polyporales, Basidiomycota) evidenced by morphological characters and phylogenetic analysis. Mycological Progress 16(1): 93–100. https://doi.org/10.1007/s11557-016-1259-8

MycoKeys 83: 161–180 (2021)
doi: 10.3897/mycokeys.83.72325
https://mycokeys.pensoft.net

RESEARCH ARTICLE

A peer-reviewed open-access journal
MycoKeys
Launched to accelerate biodiversity research

Morphology and molecular study of three new Cordycipitoid fungi and its related species collected from Jilin Province, northeast China

Jia-Jun Hu[1,2], Gui-Ping Zhao[2], Yong-Lan Tuo[2], Dan Dai[2], Di-Zhe Guo[2,3], Gu Rao[2], Zheng-Xiang Qi[2], Zhen-Hao Zhang[2], Yu Li[2], Bo Zhang[2]

1 *School of Life Science, Northeast Normal University, Changchun City, 130024, Jilin Province, China* **2** *Engineering Research Centre of Edible and Medicinal Fungi, Ministry of Education, Jilin Agricultural University, Changchun City, 130118, Jilin Province, China* **3** *Hebei Normal University of Science and Technology, Qinghuangdao City, 066004, Hebei Province, China*

Corresponding authors: Bo Zhang (zhangbofungi@126.com), Yu Li (yuli966@126.com)

Academic editor: Thorsten Lumbsch | Received 29 July 2021 | Accepted 29 August 2021 | Published 27 September 2021

Citation: Hu J-J, Zhao G-P, Tuo Y-L, Dai D, Guo D-Z, Rao G, Qi Z-X, Zhang Z-H, Li Y, Zhang B (2021) Morphology and molecular study of three new Cordycipitoid fungi and its related species collected from Jilin Province, northeast China. MycoKeys 83: 161–180. https://doi.org/10.3897/mycokeys.83.72325

Abstract

Cordyceps species are notable medicinal fungi in China, which are pathogenic on insects and exhibit high biodiversity in tropical and subtropical regions. Recently, three new *Cordyceps* species, *Cordyceps changchunensis* and *Cordyceps jingyuetanensis* growing on pupae of Lepidoptera and *Cordyceps changbaiensis* growing on larvae of Lepidoptera, were found in Jilin Province, China and are described, based on morphological and ecological characteristics. These three new species are similar to the *Cordyceps militaris* group, but are distinctly distinguishable from the known species. *Cordyceps changchunensis*, characterised by its small and light yellow to orange stromata which is occasionally forked, covered with white mycelium at the base of stipe, globose to ovoid perithecia, is macroscopically similar to *Cordyceps militaris*. *Cordyceps changbaiensis* is clearly discriminated from other *Cordyceps* species by its white to orange and branched stromata, clavate to cylindrical fertile apical portion, immersed and globose to ovoid perithecia. Moreover, unbranched, clavate and orange to light red stromata, almond-shaped to ovoid and immersed perithecia separate *Cordyceps jingyuetanensis* from other *Cordyceps* species. nrITS, nrLSU and EF-1α sequences were undertaken and phylogenetic trees, based on Maximum Likelihood and Bayesian Inference analysis showed that the three new species clustered with *Cordyceps militaris*, but formed individual clades, as well as confirmed the results of our morphological study.

Keywords

Cordyceps, host, new species, phylogenetic study, relationship

Introduction

The family Cordycipitaceae belongs to Hypocreales with plant-, animal- and fungus-based nutrition modes (Sung et al. 2007; Vega et al. 2009). The species of Cordycipitaceae are a wide variety which infect invertebrates and, in the tropics and subtropics, are known to have the highest species diversity (Kobayasi 1941, 1982). According to current data, over 900 species of Cordycipitoid fungi are reported worldwide (Yan and Bau 2015; Zha et al. 2018). In China, more than 146 species are recorded (Yan and Bau 2015).

Cordycipitoid fungi were first described in 1753 as *Clavaria militaris* L., later being recognised as *Cordyceps militaris* (L.) Fr. The genus *Cordyceps* Fr. was established by Fries in 1818, encompassing over 450 species (Kobayasi 1982; Luangsa-ard et al. 2007). Compared with a large number of species, subdivisions into infrageneric groups, for example, subgenera and sections, have been proposed in the *Cordyceps* classification, traditionally based on morphological and ecological characters (Stensrud et al. 2005). The classification of *Cordyceps*, based on the studies of Kobayasi (1941, 1983), three subgenera, *C.* subg. *Cordyceps*, *C.* subg. *Ophiocordyceps* and *C.* subg. *Neocordyceps* were recognised. Subg. *Cordyceps* was characterised by the production of either immersed or superficial perithecia, which are approximately at right angles to the surface of stroma and ascospores break into part-spores at maturity. Mains proposed a different viewpoint, two subgenera, *C.* subg. *Cryptocordyceps* and *C.* subg. *Racemella*, were added (Mains 1958). Based on nrITS, nrSSU, nrLSU, EF-1α, RPB1, RPB2, TUB and ATP6 sequences, the phylogenetic study implied that the Cordycipitoid fungi belong to six genera (*Cordyceps* Fr., *Metacordyceps* G.H. Sung, J.M. Sung, Hywel-Jones & Spatafora, *Tyrannicordyceps* Kepler & Spatafora, *Elaphocordyceps* G.H. Sung & Spatafora, *Ophiocordyceps* Petch and *Polycephalomyces* Kobayasi) across three families, Cordycipitaceae, Clavicipitaceae and Ophiocordycipitaceae (Sung et al. 2007; Yan and Bau 2015).

The host of Cordycipitoid fungi is varied and the fungi are always parasitic on larvae of swifts, pupae of Lepidoptera, spiders etc. Cordycipitoid fungi have a strong relationship with the environment and its host (Zha et al. 2019).

In this study, three new species of *Cordyceps* are reported, based on morphology and molecular studies. Furthermore, the relationship between the host and *Cordyceps* species is analysed.

Material and methods

Sampling and morphological studies

The specimens were photographed in situ. The size of the stromata was measured when fresh. After examination and description of the fresh macroscopic characters, the specimens were dried in an electric drier at 40–45 °C.

Descriptions of macroscopic characters were based on field notes and photographs. The colours correspond to the "Flora of British fungi: colour identification chart" (Royal Botanic Garden 1969). The dried specimens were rehydrated in 94% ethanol for microscopic examination and then mounted in 3% potassium hydroxide (KOH), 1% Congo Red, Cotton Blue and Melzer's Reagent (Torres et al. 2005), along with a Zeiss Axio Lab. A1 microscope for observation. For each species, a minimum of 40 part-spores was measured from two different ascocarps, part-spores are given as length × width (l × w). The specimens examined are deposited in the Herbarium of Mycology of Jilin Agricultural University (HMJAU).

DNA extraction, PCR amplification and sequencing

Total DNA was extracted from dried specimens using the NuClean Plant Genomic DNA Kit (Kangwei Century Biotechnology Company Limited, Beijing, China). Sequences of the internal transcribed spacer region (ITS), nuclear large ribosomal subunits (LSU) and translation elongation factor 1-alpha (EF-1α) were used for phylogenetic analysis. The ITS sequence was amplified using the primer pair ITS4 and ITS5 (White et al. 1990), LSU sequence was amplified using the primer pair LROR and LR7 (Stensrud et al. 2005) and EF-1α sequence was amplified using the primer pair 983F and 2218R (Castlebury et al. 2004).

Reaction programmes followed Yan and Bau (2015), Castillo et al. (2018) and Ban et al. (2015), respectively. PCR products were visualised via UV light after electrophoresis on 1% agarose gels stained with ethidium bromide and purified using Genview High-Efficiency Agarose Gels DNA Purification Kit (Gen-View Scientific Inc., Galveston, TX, USA). The purified PCR products were sent to Sangon Biotech Limited Company (Shanghai, China) for sequencing using the Sanger method. The new sequences were deposited in GenBank.

Data analysis

Based on the results of BLAST and morphological similarities, the sequences obtained and related to these samples are listed in Table 1. A dataset comprising of sequences from this study, 31 representative sequences showing the highest similarity to *Cordyceps* spp. and the outgroup *Metacordyceps taii* (Z.Q. Liang & A.Y. Liu) G.H. Sung, J.M. Sung, Hywel-Jones & Spatafora, *Metarhizium yongmunense* (G.H. Sung, J.M. Sung & Spatafora) Kepler, S.A. Rehner & Humber, *Nigelia martiale* (Speg.) Luangsa-ard & Thanakitp., *Ophiocordyceps* spp. and *Tolypocladium ophioglossoides* (J.F. Gmel.) C.A. Quandt, Kepler & Spatafora, retrieved from GenBank, were aligned with using ClustalX (Thompson et al. 1997), MACSE V2.03 (Ranwez et al. 2018) and MAFFT (Katoh and Standley 2013), then manually adjusted in BioEdit (Hall 1999). The datasets were aligned first and then, nrITS, nrLSU and EF-1α sequences were combined with Mesquite. The tree construction procedure was performed in PAUP* ver-

Table 1. Voucher information and GenBank accession numbers of ITS, LSU and EF-1α DNA sequences of *Cordyceps changchunensis*, *Cordyceps changbaiensis*, *Cordyceps jingyuetanensis* and related species used in this study.

Species name	Specimen/Strain number	Host/Substratum	GenBank accession numbers			References
			ITS	LSU	EF-1α	
Akanthomyces lecanii	CBS101247	Homopteran	JN049836	AF339555	DQ522359	(Kepler et al. 2012)
A. tuberculatus	NBRC106949	Lepidoptera	JN943318	JN941400	MF416490	(Kepler et al. 2017; Schoch et al. 2012)
Blackwellomyces cardinalis	CBS113414	Lepidoptera	MH862930	MH874497	EF469059	(Sung et al. 2007; Vu et al. 2019)
B. pseudomilitaris	NBRC101411	Lepidoptera	JN943308	JN941395	MT017849	(Mongkolsamrit et al. 2020; Schoch et al. 2012)
Cordyceps bassiana	IFO4848	Lepidoptera	AB027382	AB027382	MN401498	(Khonsanit et al. 2020; Nikoh and Fukatsu 2000)
C. bifusispora	ARS5690/EFCC8260	Lepidoptera	AY245627	EF468807	EF468747	(Kuo et al. 2005; Sung et al. 2007)
C. brongniartii	NBRC101395	Lepidopteran pupae	JN943298	JN941382	JF416009	(Kepler et al. 2012; Schoch et al. 2012)
C. cateniobliqua	CBS153.83	Lepidoptera	MH861560		MT017860	(Vu et al. 2019)
C. changbaiensis	**HMJAU48255**	**Lepidoptera**	**MW893252**	**MW893277**	**MZ616772**	**This study**
C. changbaiensis	**HMJAU48260**	**Lepidoptera**	**MW893270**	**MW893272**	**MZ616774**	**This study**
C. changchunensis	**HMJAU48251**	**Lepidoptera**	**MW893249**	**MW893274**	**MZ616769**	**This study**
C. changchunensis	**HMJAU48252**	**Lepidoptera**	**MW893250**	**MW893275**	**MZ616775**	**This study**
C. changchunensis	**HMJAU48259**	**Lepidoptera**	**MW893251**	**MW893276**	**MZ616773**	**This study**
C. chiangdaoensis	BCC75734/TBRC7274	Coleopteran larvae	KT261394	MF140732	KT261404	(Mongkolsamrit et al. 2018; Tasanathai et al. 2016)
C. coleopterorum	CBS110.73	Coleoptera	AY624177	JF415988	JF416028	(Kepler et al. 2012; Luangsa-Ard et al. 2005)
C. exasperata	MCA2155	Lepidoptera		MF416542	MF416486	(Kepler et al. 2017)
C. farinosa	CBS111113	Lepidoptera	AY624181	MF416554	MF416499	(Kepler et al. 2017; Luangsa-Ard et al. 2005)
C. fumosorosea	CBS244.31	Coleoptera	AY624182	MF416557	MF416503	(Kepler et al. 2017; Luangsa-Ard et al. 2005)
C. hepialidicola		Lepidoptera	AF315649			Unpublished
C. jingyuetanensis	**HMJAU48253**	**Lepidoptera**	**MW893253**	**MW893278**	**MZ616770**	**This study**
C. jingyuetanensis	**HMJAU48261**	**Lepidoptera**	**MW893271**	**MW893273**		**This study**
C. kyushuensis	HMAS78115	Lepidoptera	EF368021	EF468813	EF468754	(Sung et al. 2007; Wang et al. 2008)
C. militaris	OSC93623	Lepidopteran pupae	JN049825	AY184966	DQ522332	(Sung et al. 2007)
C. militaris	**HMJAU48256**	**Lepidopteran pupae**	**MW888227**	**MW893279**		**This study**
C. morakotii	BCC55820/TBRC7276	Hymenoptera	KT261389	MF140731	KT261399	(Mongkolsamrit et al. 2018; Tasanathai et al. 2016)
C. ninchukispora	BCC30937	Lepidoptera	FJ765274	FJ765242	MF416477	(Kepler et al. 2017)
C. ningxiaensis	HMJAU25074	Diptera	KF309668	KF309671		(Yan and Bau 2015)
C. polyarthra	6578	Lepidoptera	AJ536548			Unpublished
C. pruinosa	ARSEF5413	Lepidoptera	JN049826	MK761215	DQ522351	(Kepler et al. 2012; Zha et al. 2019)
C. qingchengensis	MFLU17-1022	Lepidoptera	KY423506	MK761211	MK770630	(Zha et al. 2019)
C. rosea	Spat09-053	Lepidoptera		MF416536	MF416480	(Kepler et al. 2017)
C. roseostromata	ARSEF4870	Larva, not specified	AY245637	AF339523		(Kuo et al. 2005; Sung et al. 2001)
C. scarabaeicola	ARSEF5689	Coleoptera	JN049827	AF339524	DQ522335	(Kepler et al. 2012; Sung et al. 2007)
C. scarabaeicola	Arsef5689	Coleoptera	JN049827	AF339524		(Kepler et al. 2012; Sung et al. 2001)
Cordyceps sp.	**HMJAU48254**	**Lepidoptera**	**MW888228**	**MW893280**	**MZ616771**	**This study**

Species name	Specimen/Strain number	Host/Substratum	GenBank accession numbers			References
			ITS	LSU	EF-1α	
C. spegazzinii	ARSEF7850	Diptera	DQ196435	DQ196435	GU734752	(Torres et al. 2005)
C. taishanensis	A-1	Lepidoptera	FJ008927			Unpublished
C. tenuipes	TBRC7266	Lepidoptera	MF140742		MF140828	(Mongkolsamrit et al. 2018; Vu et al. 2019)
Isaria cicadae	GACP07071701	Hemiptera	KX017277	MK761212	MT268245	(Zhi et al. 2021)
I. japonica	BCC2808	Lepidoptera	AY624199			(Luangsa-Ard et al. 2005)
Metarhizium yongmunense	EFCC2131	Lepidoptera	JN049856	EF468833	EF468770	(Kepler et al. 2012; Sung et al. 2007)
Metacordyceps taii	ARSEF5714	Lepidoptera	JN049829	AF543787	AF543775	(Sung et al. 2007)
Nigelia martiale	HMAS197472(S)	Coleoptera	JN049881	JF415975	JF416016	(Kepler et al. 2012)
Ophiocordyceps acicularis	OSC12858/ OSC110987	Coleoptera	JN049820	DQ518757	DQ522326	(Kepler et al. 2012)
O. clavata	NBRC106961	Coleoptera	JN943327	JN941414	MH879672	(Schoch et al. 2012)
O. gracilis	EFCC8572	Lepidoptera	HM142942	EF468811	EF468751	(Sung et al. 2007; Zhong et al. 2010)
O. rubiginosoperitheciata	NBRC106966	Coleoptera	JN943344	JN941437		(Schoch et al. 2012)
O. sinensis	ARSEF6282	Lepidopteran pupae	HM595981	HM595885	EF468767	(Chan et al. 2011; Sung et al. 2007)
Tolypocladium ophioglossoides	NBRC106331	*Elaphomyces* sp.	JN943320	JN941408		(Schoch et al. 2012)

sion 4.0b10 (Swofford 2002) as described by Jiang et al. (Jiang et al. 2011). All characters were equally weighted and gaps were treated as missing data.

MrModeltest 2.3 was used to determine the best fitting substitution model for each dataset for Bayesian Inference, which was calculated with MrBayes 3.2.6 with a general time-reversible DNA substitution model and a gamma distribution rate variation across sites (Ronquist and Huelsenbeck 2003). Four Markov chains were run for two runs from random starting trees for four million generations until the split deviation frequency value was < 0.01 and trees were sampled every 100 generations. raxmlGUI 2.0 (Edler et al. 2020) was used for Maximum Likelihood (ML) analysis with 1,000 bootstrap replicates using the GTRGAMMA algorithm to perform a tree inference and search for optimal topology (Vizzini et al. 2015).

Results

Phylogenetic analysis

The phylogenetic tree, based on ITS from Bayesian analysis, included sequences from 46 fungal samples representing 43 taxa and the results are shown in Fig. 1. According to the phylogenetic tree, the three new species gather into one branch with *C. militaris*, *C. roseostromata* Kobayasi & Shimizu, *C. taishanensis* B. Liu, P.G. Yuan & J.Z. Cao, *C. kyushuensis* A. Kawam. and *C. hepialidicola* Kobayasi & Shimizu, but the species *C. jingyuetanensis* does not gather into one branch by itself. Meanwhile, the genus *Cordyceps* was divided into three independent clades. Furthermore, *Cordyceps* and *Akanthomyces* Lebert are a sister clade to *Blackwellomyces* Spatafora & Luangsa-ard.

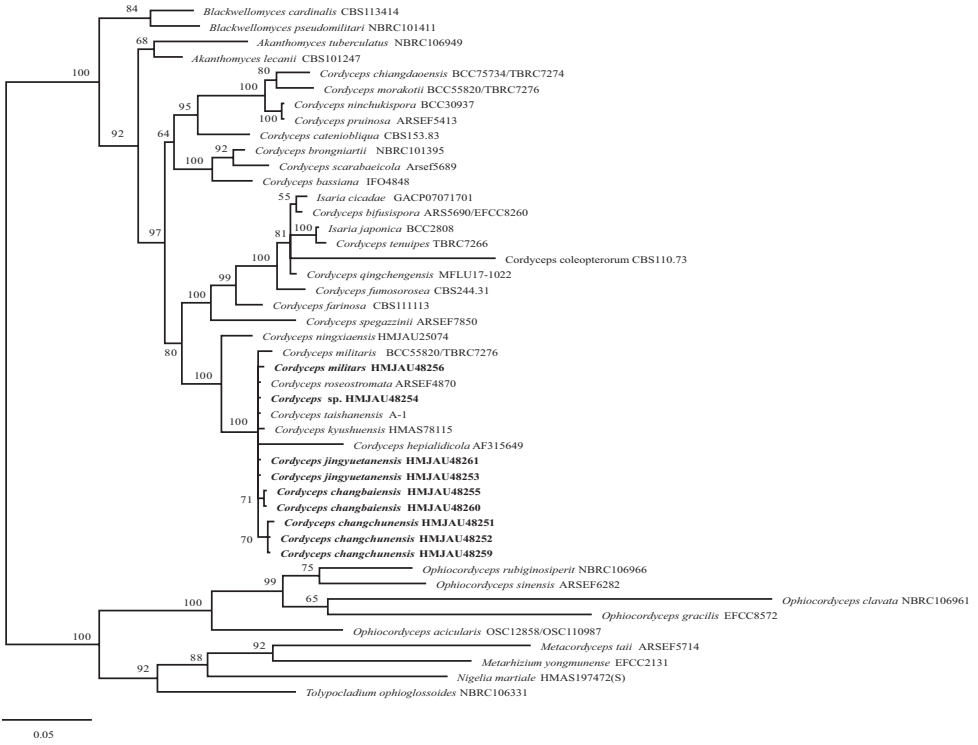

Figure 1. Phylogenetic tree of Cordycepitiod fungi, based on ITS from Bayesian analysis; self-examined sequences are shown in bold.

For these reasons, the combined ITS, LSU and EF-1α dataset including 121 fungal samples representing 48 taxa was used for analysis and the results are shown in Fig. 2. In these data, the three new species are in three independent clades included in the *C. militaris* complex, *C. jingyuetanensis* was close to *C. hepialidicola* Kobayasi & Shimizu and is different from Fig. 1. From the phylogenetic tree (Fig. 2), the species of *Cordyceps* are mainly divided into three independent clades. Moreover, the family Cordycipitaceae clustered into three clades and the genus *Akanthomyces* formed a sister clade to the genus *Cordyceps*.

Taxonomy

Cordyceps changchunensis **J.J. Hu, Bo Zhang & Y. Li, sp. nov.**
MycoBank No: 839249
Figs 3, 4

Holotype. China. Jilin Province: Changchun City, Jingyuetan National Forest Park, 43.77°N, 125.47°E, 27 August 2018, Jia-Jun Hu, Bo Zhang & Gui-Ping Zhao (HMJAU 48251, holotype, GenBank Acc. nos.: ITS = MW893249, LSU = MW893274, EF-1α = MZ616769).

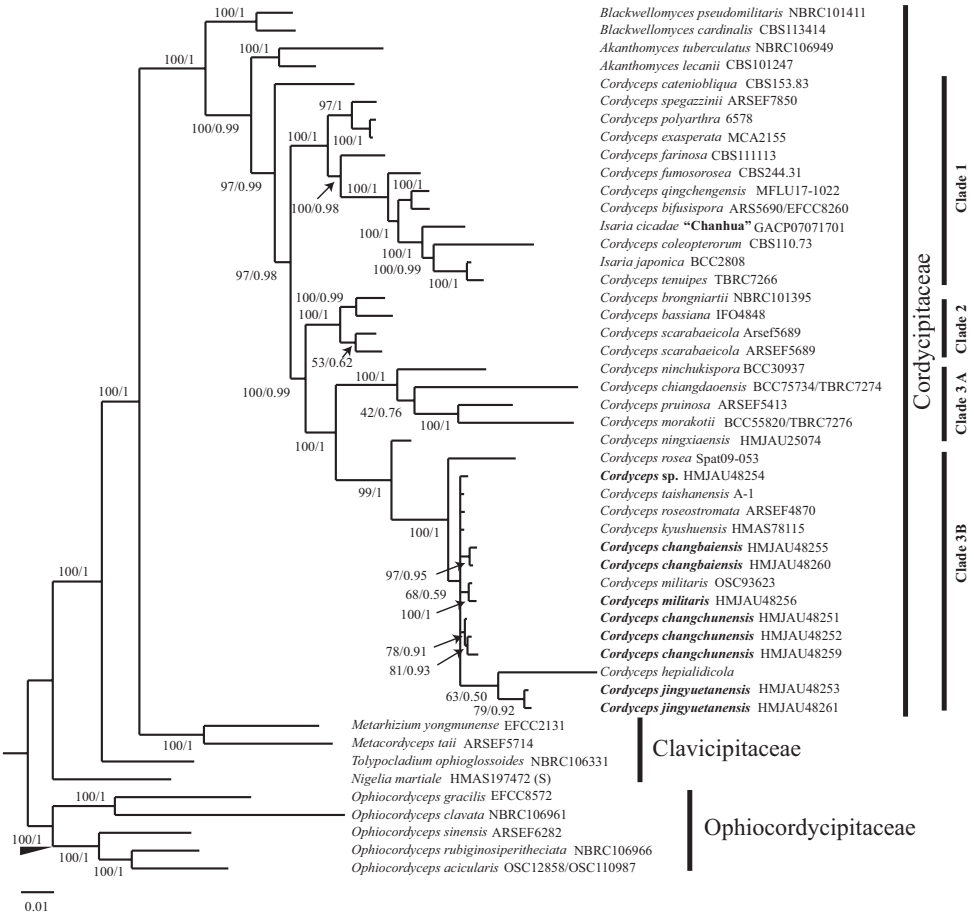

Figure 2. Phylogenetic tree of Cordycepitiod fungi, based on concatenated ITS, LSU and EF-1α from Bayesian analysis and Maximum Likelihood analysis; self-examined sequences are shown in bold.

Etymology. *changchunensis*: referring to Changchun, the location of the holotype.

Diagnosis. *Cordyceps changchunensis* can be easily differentiated from closely-related species *C. militaris* by its unique host, smaller stromata, immersed perithecia and larger part-spores (2.6–6 × 1.0–1.4 μm).

Description. Sexual Morph. Stromata 2.4–4.5 cm long, single or multiple, solitary to gregarious, arising from pupa; branched, sometimes single at base, then branched into two forks. **Fertile apical** portion, orange, clavate to globose, sometimes irregular, 2.0–3.5 cm long and 0.4–0.6 cm wide, distinctly distinguishable from the stipe. **Sterile stipe** fleshy, light yellow to orange, cylindrical, 1.3–3.3 cm long and ca. 0.4 cm wide, usually with white mycelium at the base. **Perithecia** immersed at right angles to the surface of the fruiting body, globose to ovoid, 180–600 × 180–520 μm, with a thick wall about 10–15 μm. **Asci** cylindrical, 80–300 × 2.5–5 μm, 8–spored, apex of ascus hemispherical, 3.0–4.0 × 2.0–3.0 μm.

Figure 3. Morphological characters of *Cordyceps changchunensis* (HMJAU 48251, holotype) **a, b, e** stromata and host of *Cordyceps changchunensis* **c** surface of fertile apex of ascostroma **d** host of *Cordyceps changchunensis* **f–h** apex of ascus **i–k** ascus **l–n** part-spores. Scale bars: 1 cm (**a, b**); 2 mm (**c, e**); 1 mm (**d**); 10 μm (**f–h**); 50 μm (**i–k**); 5 μm (**l–n**).

Part-spores oblong, 2.6–6 × 1.0–1.4 μm, smooth, hyaline in 3% KOH, thin-walled, inamyloid.

Asexual Morph. Unknown.

Host. Growing on pupae of Lepidoptera.

Other specimens examined. China. Jilin Province: Changchun City, Jingyuetan National Forest Park, 20 August 2015, Bo Zhang (HMJAU 48259, GenBank Acc. nos.: ITS = MW893251, LSU = MW893276, EF-1α = MZ616773); Changchun City, Jingyuetan National Forest Park, 18 August 2018, Bo Zhang (HMJAU 48252, isotype, GenBank Acc. nos.: ITS = MW893250, LSU = MW893275, EF-1α = MZ616775).

Distribution. China (Jilin Province).

Note. *C. changchunensis* is easily confused with *C. militaris* due to highly similar morphology and sharing the same habitat. Morphologically, the stromata of *C. militaris* are larger than *C. changchunensis*, single or gregarious, larger perithecia

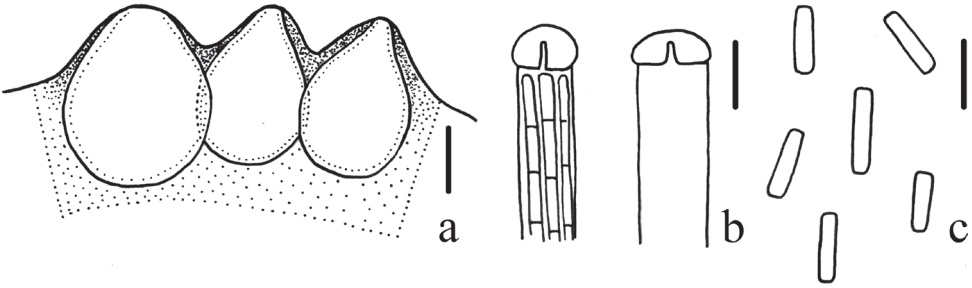

Figure 4. Microscopical characters of *Cordyceps changchunensis* (HMJAU 48251, holotype) **a** perithecia **b** apex of ascus **c** part-spores. Scale bars: 100 μm (**a**); 5 μm (**b, c**).

(500–1089 × 132–264 μm) and smaller part-spores (2–4 × 1 μm) (Li et al. 2015). In the phylogenetic analysis, the three specimens of *C. changchunensis* were placed in separate monophyletic lineages (BPP = 0.91, MLBS = 78%).

***Cordyceps changbaiensis* J.J. Hu, Bo Zhang & Y. Li, sp. nov.**
MycoBank No: 839250
Figs 5, 6

Holotype. China. Jilin Province, Yanbian Korean Autonomous Prefecture, Antu County, Changbai Mountain, 42.19°N, 128.18°E, 4 September 2019, Jia-Jun Hu & Bo Zhang (HMJAU 48255, holotype, GenBank Acc. nos.: ITS = MW893252, LSU = MW893277, EF-1α = MZ616772).

Etymology. *changbaiensis*: referring to Mt. Changbai, the location of the holotype.

Diagnosis. The species is characterised by orange to white and branched stromata, globose to ovoid perithecia and larger part-spores (3.0–7.0 × 1.0–1.4 μm).

Description. Sexual Morph. Stromata 2.4–5.2 cm long, single or multiple, solitary, arising from the head of the host insect covered with white mycelia. **Fertile apical** portion, orange, clavate to cylindrical, 0.6–1.5 cm long and 0.2–0.6 cm wide, obviously distinguishable from the stipe. **Sterile stipe** fleshy, white to light yellow, cylindrical, 1.8–3.7 cm long and 0.2–0.5 cm wide. **Perithecia** immersed to the surface of the fruiting body, globose to ovoid, 120–230 × 90–170 μm, with a thick wall about 15 μm. **Asci** cylindrical, 225–625 × 4–5 μm, 8–spored, apex of ascus hemispherical, 3.0–4.0 × 2.2–3.2 μm. **Part-spores** oblong, 3.0–7.0 × 1.0–1.4 μm, smooth, hyaline in 3% KOH, thin-walled, inamyloid.

Asexual Morph. Unknown.

Host. Growing on larvae of Lepidoptera.

Distribution. China (Jilin Province).

Other specimen examined. China. Jilin Province: Baishan City, Fusong County, Quanyang Town, 42.30°N, 127.29°E, 22 August 2021, Jia-Jun Hu, Bo Zhang & Gui-

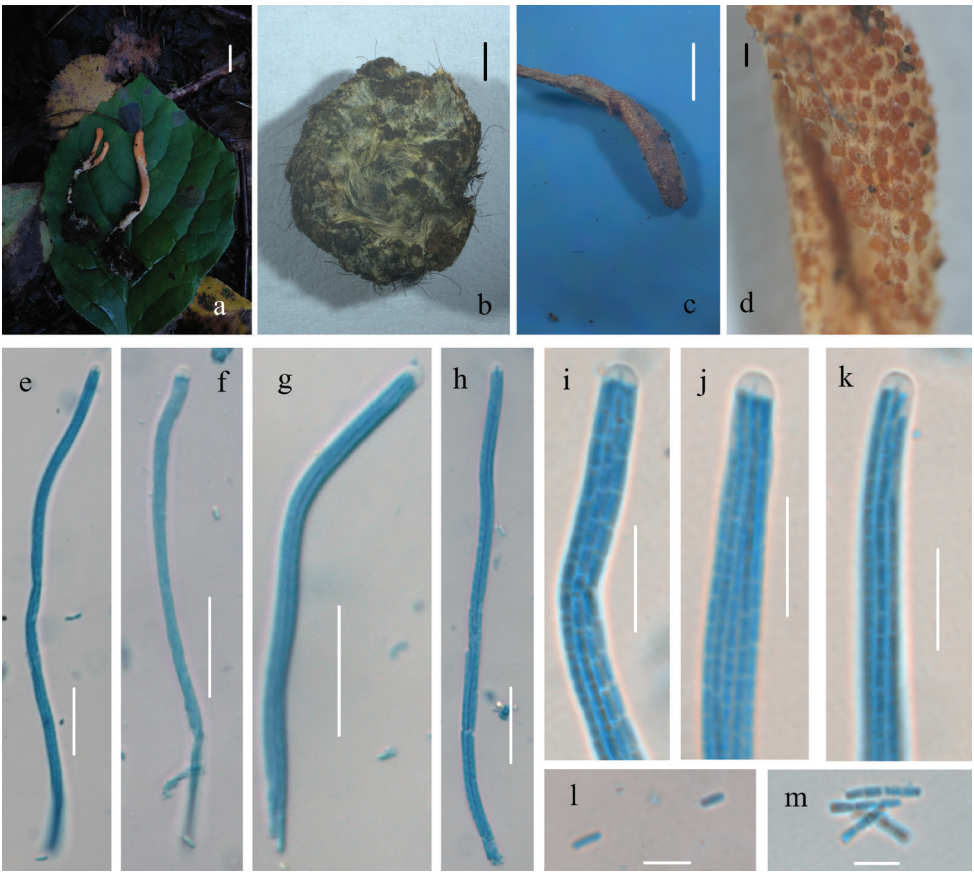

Figure 5. Morphological characters of *Cordyceps changbaiensis* (HMJAU 48255, holotype) **a** stromata and host of *Cordyceps changbaiensis* **b** host of *Cordyceps changbaiensis* **c, d** surface of fertile apex of ascostroma **e–h** ascus **i–k** apex of ascus **l–m** part-spores. Scale bars: 1 cm (**a**); 5 mm (**b–c**); 200 μm (**d**); 20 μm (**e–h**); 10 μm (**i–k**); 5 μm (**l–m**).

Ping Zhao (HMJAU 482260, isotype, GenBank Acc. nos.: ITS = MW893270, LSU = MW893272, EF-1α = MZ616774)

Note. *C. changbaiensis* has orange to white and branched stromata. Morphologically, *C. roseostromata* Kobayasi & Shimizu is similar to *C. changbaiensis* due to the single or branched stromata. *C. kyushuensis* A. Kawam. is also close to *C. changbaiensis* because of the host and the stromata being similar in colour. However, both *C. roseostromata* and *C. kyushuensis* have a larger perithecia and smaller part-spores. Furthermore, the stromata of *C. kyushuensis* is gregarious or fascicled and grows from the head or abdomen of the host (Li et al. 2015); *C. roseostromata* has pyriform perithecia and host on larva of Coleoptera (Kobayasi 1983). In the phylogenetic analysis, *C. changbaiensis* was placed in separate monophyletic lineages (BPP = 0.95, MLBS = 97%) and formed a sister relationship with *C. rosea*.

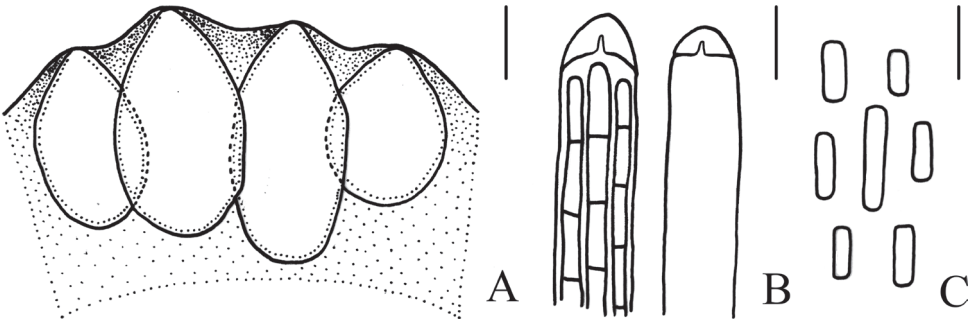

Figure 6. Microscopical characters of *Cordyceps changbaiensis* (HMJAU 48255, holotype) **a** perithecia **b** apex of ascus **c** part-spores. Scale bars: 100 μm (**a**); 5 μm (**b, c**).

Cordyceps jinyuetanensis **J.J. Hu, Bo Zhang & Y. Li, sp. nov.**
MycoBank No: 839251
Figs 7, 8

Holotype. China. Jilin Province: Changchun City, Jingyuetan National Forest Park, 43.80°N, 125.50°E, 27 August 2018, Jia-Jun Hu, Bo Zhang & Gui-Ping Zhao (HMJAU 48253, holotype, GenBank Acc. nos.: ITS = MW893253, LSU = MW893278, EF-1α = MZ616770).

Etymology. *jinyuetanensis*: referring to Jingyuetan National Forest Park, the location of the holotype.

Diagnosis. *C. jingyuetanensis* is different from other species by growing on pupae, orange to light red stromata, immersed and almond-shaped to ovoid perithecia.

Description. Sexual Morph. Stromata 4–4.5 cm long, multiple, solitary, arising from pupae of Lepidoptera. **Fertile apical** portion, orange to light red, clavate, 0.8–1.3 cm long and 0.1–0.2 cm wide, obviously distinguishable from the stipe. **Sterile stipe** fleshy, light yellow to orange, cylindrical, 2.7–3.7 cm long and 0.1–0.2 cm wide, usually with white mycelium at the base. **Perithecia** immersed to the surface of the fruiting body, almond-shaped to ovoid, 220–340 × 110–220 μm, with a thick wall about 15–20 μm. **Asci** cylindrical, 225–475 × 3–5 μm, 8-spored, apex of ascus hemispherical to irregular, 3.0–4.0 × 1.4–2.8 μm. **Part-spores** oblong, 2.8–5.0 × 1.0–1.4 μm, smooth, hyaline in 3% KOH, thin-walled, inamyloid.

Asexual Morph. Unknown.

Host. Growing on pupae of Lepidoptera.

Distribution. China (Jilin Province).

Other specimen examined. China. Jilin Province: Baishan City, Fusong County, Quanyang Town, 42.30°N, 127.29°E, 22 August 2021, Jia-Jun Hu, Bo Zhang & Gui-Ping Zhao (HMJAU 482261, isotype, GenBank Acc. nos.: ITS = MW893271, LSU = MW893273)

Note. A review of literature revealed that there are about 20 species of Cordycipitiod fungi growing on pupae, like the unusual medicinal fungi *O. sinensis* (Berk.)

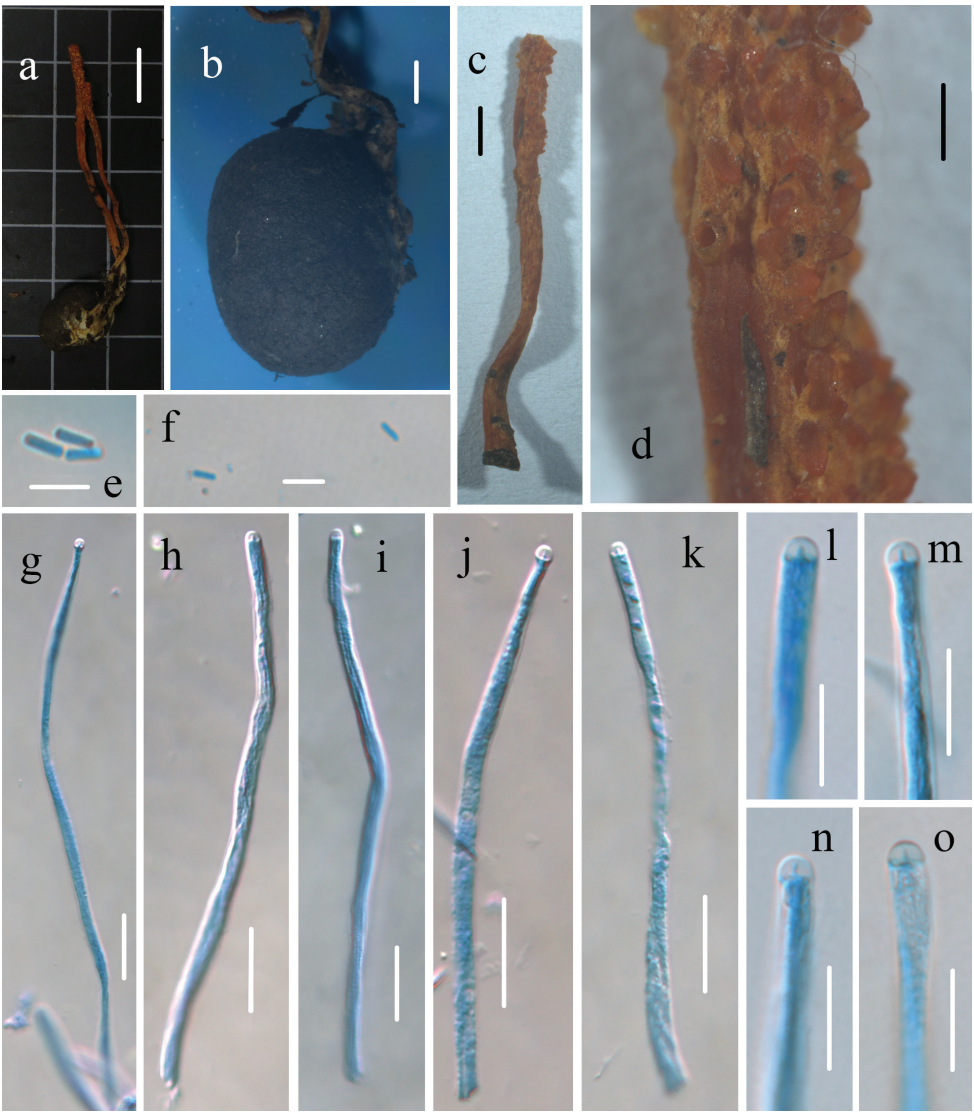

Figure 7. Morphological characters of *Cordyceps jingyuetanensis* (HMJAU 48253, holotype) **a** stromata and host of *Cordyceps jingyuetanensis* **b** host of *Cordyceps jingyuetanensis* **c, d** surface of fertile apex of ascostroma **e, f** part-spores **g–k** ascus **l–o** apex of ascus. Scale bars: 1 cm (**a**); 2 mm (**b, c**); 500 μm (**d**); 5 μm (**e, f**); 20 μm (**g–k**); 10 μm (**i–o**).

G.H. Sung, J.M. Sung, Hywel-Jones & Spatafora, *C. militaris*, *I. cicadae* Miq. and also like the two new species, *C. ningxiaensis* T. Bau & J.Q. Yan and *C. qingchengensis* L.S. Zha & T.C. Wen, reported from China in 2015 and 2019. Nevertheless, *C. jingyuetanensis* is different from these Cordycipitiod species; *C. ningxiaensis* grows

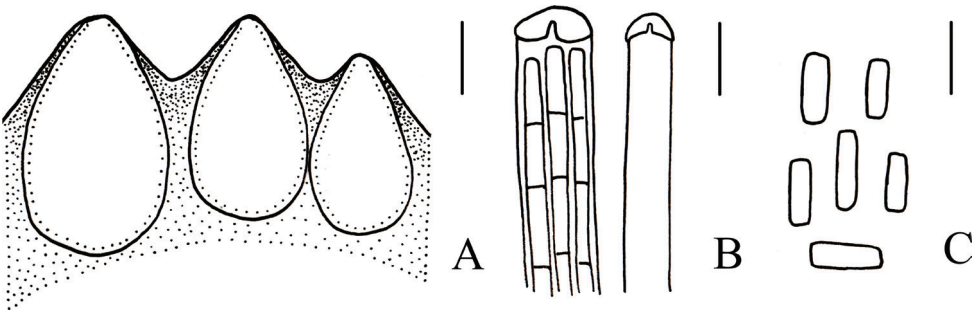

Figure 8. Microscopical characters of *Cordyceps jingyuetanensis* (HMJAU 48253, holotype) **a** perithecia **b** apex of ascus **c** part-spores. Scale bars: 100 μm (**a**); 5 μm (**b, c**).

on the pupae of Diptera, *I. cicadae* grows on the pupae of Hemiptera and the stromata of *C. qingchengensis* are yellow, single or branched on the top. *C. hepialidicola* Kobayasi & Shimizu from Japan is similar to *C. jingyuetanensis* in its phylogenetic relationship, but there are distinct morphological differences. Morphologically, the stromata of *C. hepialidicola* are multiple, branched on the top sometimes, grow from the head of larva of Hepialida or Lepidoptera, have larger perithecia (300–350 × 500 μm) and smaller part-spores (3–4 × 1 μm) (Kobayasi 1983). In the phylogenetic analysis, *C. changbaiensis* was placed in separate monophyletic lineages (BPP = 0.92, MLBS = 79%).

***Cordyceps militaris* (L.) Fr., Observ. mycol. (Havniae) 2: 317 (cancellans) (1818)**
Fig. 9

Specimens examined. China. Yunnan Province: Qujin City, Huize County, 26.24°N, 103.25°E, 30 July 2019, Jia-Jun Hu, Bo Zhang & Di-Zhe Guo (HMJAU 48256, GenBank Acc. nos.: ITS = MW888227, LSU = MW893279); Jilin Province: Changchun City, Jingyuetan National Forest Park, 43.80°N, 125.50°E, 25 August 2018, Jia-Jun Hu & Yong-Lan Tuo (HMJAU 48257); Changchun City, Jingyuetan National Forest Park, 43.80°N, 125.50°E, 25 August 2018, Jia-Jun Hu, Bo Zhang & Gui-Ping Zhao (HMJAU 48258); Tonghua City, Ji'an County, Wunvfeng National Forest Park, 41.28°N, 126.14°E, 25 August 2019, Yong-Lan Tuo (HMJAU 48262); Heilongjiang Province: Daxing'an Mountains, Shuanghe National Nature Reserve, 52.44°N, 125.40°E, 23 June 2019, Di-Zhe Guo (HMJAU 48263).

Note. *C. militaris* is a widely distributed species and also a well-known medicinal fungus in China. At this time, we collected samples from many different places. The morphological evidence shows no apparent differences between each other. However, the habitat is markedly different.

Table 2. Morphological comparisons of sexual states of *Cordyceps changchunensis*, *Cordyceps changbaiensis* and *Cordyceps jingyuetanensis*.

Species	Host	Stromata	Fertile part	Perithecia	Asci	Ascospores	Reference
Beauveria bassiana	Larvae of Lepidoptera	Single or several, unbranched, slender and cylindrical, brownish- yellow to yellowish	18.7–33. 3 × 2.8–8.0 mm	Elliptical, 610–720 × 230–320 µm, immersed to surface	Cylindrical, 230–590 × 3.5–4.0 µm with ascus cap 3.6–4.0 µm in diameter	Filamentous, 300–570 × 1.0 µm, not broken into part-spores	(Li et al. 2001)
Blackwellomyces pseudomilitaris	Larvae of Lepidoptera	Single or cluster, simple or branched, cylindrical, white to white-orange	15–30 × 0.9–3 mm	Elongate-ellipsoid or elongate-ovoid, 290–570 × 120–245 µm, superficial	Filiform, 290–410 × 5–6 µm	Filiform, 280–390 × 1 µm, not broken into part-spores	(Hywel-Jones 1994)
Cordyceps bifusispora	Larvae of Lepidoptera	Simple, cylindrical clavate, whitish	6 × 1.3 mm	Pyriform, with protruding apices, yellowish, 300 × 150–170 µm, immersed	Cylindrical, 200–220 × 3–4.5 µm	Bifusiform, 145–220 µm in length, central part filiform about 0.4 µm wide, terminal parts narrowly fusiform, about 30 × 1.6 µm and 3 septate	(Eriksson 1982)
C. kyushuensis	Larvae of Lepidoptera	Cluster, cylindrical, Light yellow to orange red	20–30 × 5–8 mm	Elliptical, 300–500 × 200–300 µm, half-buried	Cylindrical, 3–4.5 µm wide	Short cylindrical, part-spores 5–7 × 0.7–1 µm	(Guo and Li 2000; Li et al. 2015)
C. militaris	Lepidopteran pupae	Single or several, clavate, orange	10–20 × 3–5 mm	Conical, half-buried	Clavate, 300–400 × 4–5 µm	Filiform, part spores 2–3 × 1 µm	(Li et al. 2015)
C. ningxiaensis	Fly pupae (Diptera)	One to two in a group, clavate, orange	1.2–3 × 1.2–2.8 mm	Ellipsoid to ovoid, 288–400 × 103–240 µm, with a wall about 10 µm thick, loosely embedded at right angles to the surface	Cylindrical, 168–205 × (3.7–)4.1–5.5(–6.6) µm, with oblate spheroid or hemispherical refractive cap 3.4–3.8 × 2.9–3.4 µm at apex	Filiform, irregularly multiseptate, part-spores 3.6–7.8 × 1.0–1.4 µm	(Yan and Bau 2015)
C. polyarthra	Larvae of Lepidoptera	Cespitose, narrowly clavate, light yellow to reddish-brown		Ovoid, 250–450 × 125–250 µm, brown, with a definite wall 25 µm thick, embedded at right angles to the surface	Cylindrical, 150–260 × 3–4 µm, with a 1.5–2 µm thick cap	Filiform, part-spores 4–6 × 0.75–1 µm	(Mains 1958)
C. pruinosa	Larvae of Lepidoptera	Solitary or several, clavate, orange to red	2–8 × 1–3 mm	Ovoid to fusiform, 360–400 × 130–200 µm, crowded, red, ordinal in orientation, immersed	Cylindrical, 100–200 × 2.5–4 µm	Filiform, part-spores 4–6 × 1 µm	(Li et al. 2015)
C. qingchengensis	Lepidopteran pupae	Branched, yellow	7–9 × 2.0–2.5 mm	Ovoid but apex sharply pointed, 335–490 × 145–240 µm, partially immersed at right angle to the surface	Cylindrical, 180–200 × 2.4–4.0 µm wide, caps hemispherical, 1.8–2.2 × 2.5–3.2 µm	Filiform, 180–220 × 0.45–0.65 µm, not at all bifusiform and not broken into part-spores	(Zha et al. 2019)
C. roseostromata	Larva, not specified	Single or branched	1.2–5 × 1.5–2.2 mm	Pyriform, 280–300 × 140–160 µm, Superficial	3–3.5 × 2.5–3 µm	4–5 × 1 µm	(Kobayasi 1983)
C. changchunensis	Lepidopteran pupae	Single or multiple, clavate, orange	2.0–3.5 × 0.4–0.6 mm	Globose to ovoid, 180–600 × 180–520 µm, with a thick wall about 10–15 µm, partially immersed at right angles to the surface	Cylindrical, 80–300 × 2.5–5 µm, caps hemispheric, 3.0–4.0 × 2.0–3.0 µm at apex	Oblong, 2.6–6 × 1.0–1.4 µm	This study
C. changbaiensis	Larvae of Lepidoptera	Single or multiple, clavate, white to orange	0.6–1.5 × 0.2–0.6 mm	Globose to ovoid, 120–230 × 90–170 µm, with a thick wall about 15 µm, immersed to surface	Cylindrical, 225–625 × 4–5 µm, caps hemispherical, 3.0–4.0 × 2.2–3.2 µm at apex	Oblong, 3.0–7.0 × 1.0–1.4 µm	This study
C. jingyuetanensis	Lepidopteran pupae	Single or multiple, clavate, orange to light red	0.8–1.3 × 0.1–0.2 mm	Almond-shaped to ovoid, 220–340 × 110–220 µm, with a thick wall about 15–20 µm, immersed to surface	Cylindrical, 225–475 × 3–5 µm, caps hemispherical to irregular, 3.0–4.0 × 1.4–2.8 µm at apex	Oblong, 2.8–5.0 × 1.0–1.4 µm	This study

Figure 9. Macrocharacter of *Cordyceps militaris* **a–e** stromata and host of *Cordyceps militaris* (**a** collected from Daxing'an Mountains, Heilongjiang Province **b** collected from Ji'an County, Tonghua City, Jilin Province **c, e** collected from Changchun City, Jilin Province **d** collected from Qujin City, Huize County, Yunnan Province). Scale bars: 1 cm (**a–e**).

Key to reported species in this study

1	Stromata arise from pupae	**2**
–	Stromata arise from larvae	***Cordyceps changbaiensis***
2	Stromata branched into two forks sometimes	***Cordyceps changchunensis***
–	Stromata not branched	**3**
3	Part-spores over 3 μm	***Cordyceps jingyuetanensis***
–	Part-spores less than 3 μm	***Cordyceps militaris***

Discussion

In this study, three new species, collected from northeast China in the *Cordyceps militaris* group, are described. In previous work, about 38 species were recognised as

belonging to the *C. militaris* group (Yan and Bau 2015). ML and BI analysis recognised four well-supported clades, one is Cordycipitaceae, the others are Clavicipitaceae and Ophiocordycipitaceae (Fig. 2). Moreover, the Cordycipitaceae branch is mainly divided into three clades, the *Akanthomyces* clade near the *Cordyceps* clade, implies a closer biological relationship.

The previous studies have revealed that the genus *Cordyceps* was not monophylic (Artjariyasripong et al. 2001), the species of *Isaria* was nested within *Cordyceps* (Kepler et al. 2017) and our phylogenetic analysis also shows a similar result. *Cordyceps* clade consisted of three major subclades designated as clade 1, clade 2 and clade 3 (Fig. 2). Nearly all the subclades in *Cordyceps* clade were strongly supported.

Clade 1, including nine *Cordyceps* spp. and two *Isaria* spp. *I. cicadae*, based on Chinese sequences, gathers into one branch with *Cordyceps* species. What is known as *I. cicadae* in China, named on a Brazilian specimen, is of confused classification status, due to the teleomorph having remained undiscovered. In China, *C. cicadae* Massee has been regarded as a teleomorph of *I. cicadae* as well as a teleomorph of *O. sobolifera* (Hill ex Watson) G.H. Sung, J.M. Sung, Hywel-Jones & Spatafora and referred to as *C. sobolifera* (Hill ex Watson) Berk. & Broome. Until recently, the teleomorph was discovered in Mt. Jinggang, Jiangxi Province, China and both teleomorph and anamorph existed on some specimens, with the morphology of the anamorph consistent with those, "*I. cicadae*", harvested throughout southern China, significantly different from the type specimen of *I. cicadae*. For this reason, it was published as a new species named *C. chanhua* Z.Z. Li, F.G. Luan, Hywel-Jones, C.R. Li & S.L. Zhang (Zhi et al. 2021). Furthermore, *I. japonica* Yasuda reported from Japan, exhibits exceptionally high affinity with the genus *Cordyceps*. The teleomorph, however, still remains a mystery and a more intensive study is needed. Clade 2 consists of *C. scarabaeicola* Kobayasi, *C. bassiana* Z.Z. Li, C.R. Li, B. Huang & M.Z. Fan and *C. brongniartii* Shimazu. Yellow stromata seem to be a synapomorphic character of clade 2. Clade 3 included 15 *Cordyceps* spp. However, clade 3 did not form a monophyletic group. *C. ninchukispora* (C.H. Su & H.H. Wang) G.H. Sung, J.M. Sung, Hywel-Jones & Spatafora, *C. chiangdaoensis* Tasan., Thanakitp., Khons. & Luangsa-ard, *C. pruinosa* Petch and *C. morakotii* Tasan., Thanakitp. & Luangsa-ard gather into one branch. *Cordyceps* spp. of clade 3A all arise from pupae. Clade 3B includes 11 *Cordyceps* spp., seven known *Cordyceps* spp., one unidentified *Cordyceps* sp. and our three new species. Being visually similar to *Cordyceps militaris* seems to be a synapomorphic character of clade 3B.

About 60% of *Cordyceps* sensu lato species are recorded on two insect orders–Coleoptera and Lepidoptera (Shrestha et al. 2016). Host preferences have been variously implemented in taxonomic work, so this is also in *Cordyceps*. Host associations, when superimposed on phylogeny, suggested that some groups of taxa have conserved the endoparasite-host interactions to some extent; however, several host shifts have occurred during the evolution of *Cordyceps* (Stensrud et al. 2005). In *Cordyceps* species, hosts were considered as having low significance as a phylogenetic character, but are the most crucial feature in morphological aspects (Torres et al. 2005).

Acknowledgements

This study is funded by the National Key R & D of Ministry of Science and Technology (2018YFE0107800), the National Key R & D of Ministry of Science and Technology (2019YFD1001905-33), Jilin Province Science and Technology Development Plan Project (20190201256JC), Scientific and Technological Tackling Plan for the Key Fields of Xinjiang Production and Construction Corps (No. 2021AB004) and "111" programme (No. D17014). The authors are very thankful to Dr. Xue-Fei Li, Miss Hui-Ze Hu and Miss Fang-Fang Zhang from Engineering Research Centre of Edible and Medicinal Fungi, Ministry of Education, for help during this study.

References

Artjariyasripong S, Mitchell JI, HyweI-Jones NL, Jones EBG (2001) Relationship of the genus *Cordyceps* and related genera, based on parsimony and spectral analysis of partial 18S and 28S ribosomal gene sequences. Mycoscience 42: 503–517. https://doi.org/10.1007/BF02460949

Ban S, Sakane T, Nakagiri A (2015) Three new species of *Ophiocordyceps* and overview of anamorph types in the genus and the family Ophiocordyceptaceae. Mycological Progress 14: 1–12.

Castillo LP, Osorio A, Vargas N, Sanjuan T, Grajales A, Restrepo S (2018) Genetic diversity of the entomopathogenic fungus *Cordyceps tenuipes* in forests and butterfly gardens in Quindío, Colombia. Fungal Biology 122: 891–899. https://doi.org/10.1016/j.funbio.2018.05.003

Castlebury LA, Rossman AY, Sung G-H, Hyten AS, Spatafora JW (2004) Multigene phylogeny reveals new lineage for *Stachybotrys chartarum*, the indoor air fungus. Mycological Research 108: 864–872.

Chan WH, Ling KH, Chiu SW, Shaw PC, But PPH (2011) Molecular analyses of *Cordyceps gunnii* in China. Journal of Food and Drug Analysis 19: 18–25. https://doi.org/10.1310/hct1202-118

Edler D, Klein J, Antonelli A, Silvestro D (2020) raxmlGUI 2.0: a graphical interface and toolkit for phylogenetic analyses using RAxML. Methods in Ecology and Evolution 12: 373–377. https://doi.org/10.1111/2041-210X.13512

Eriksson O (1982) *Cordyceps bifusispora* spec. nov. Mycotaxon 15: 185–188.

Guo Y, Li C (2000) *Cordyceps kyushuensis* new to China. Mycosystem 19: 296.

Hall TA (1999) BioEdit: a user-friendly biological sequence alignment editor and analysis program for Windows 95/98/NT. Nucleic Acids Symposium Series 41: 95–98. https://doi.org/10.1021/bk-1999-0734.ch008

Hywel-Jones NL (1994) *Cordyceps khaoyaiensis* and *C. pseudomilitaris*, two new pathogens of lepidopteran larvae from Thailand. Mycological Research 98: 939–942. https://doi.org/10.1016/S0953-7562(09)80267-0

Jiang X, Yu H, Xiang M, Liu X, Liu X (2011) *Echinochlamydosporium variabile*, a new genus and species of Zygomycota from soil nematodes. Fungal Diversity 46: 43–51. https://doi.org/10.1007/s13225-010-0076-7

Katoh K, Standley DM (2013) MAFFT multiple sequence alignment software version 7: improvements in performance and usability. Molecular Biology and Evolution 30: 772–780. https://doi.org/10.1093/molbev/mst010

Kepler R, Sung GH, Ban S, Nakagiri A, Chen MJ, Huang B, Li Z, Spatafora J (2012) New teleomorph combinations in the entomopathogenic genus *Metacordyceps*. Mycologia 104: 182–197. https://doi.org/10.3852/11-070

Kepler RM, Luangsa-Ard JJ, Hywel-Jones NL, Quandt CA, Sung G-H, Rehner SA, Aime MC, Henkel TW, Sanjuan T, Zare R (2017) A phylogenetically-based nomenclature for Cordycipitaceae (Hypocreales). IMA Fungus 8: 335–353.

Khonsanit A, Luangsa-ard JJ, Thanakitpipattana D, Noisripoom W, Chaitika T, Kobmoo N (2020) Cryptic diversity of the genus *Beauveria* with a new species from Thailand. Mycological progress 19: 291–315.

Kobayasi Y (1941) The genus *Cordyceps* and its allies. Tokyo Bunrika Daigaku. Science Report 84: 73–75.

Kobayasi Y (1982) Keys to the taxa of the genera *Cordyceps* and *Torrubiella*. Transactions of the Mycological Society of Japan 23: 329–364.

Kobayasi Y (1983) *Cordyceps* species from Japan 6. Bulletin of the National Science Museum Tokyo Series B 9: 1–21.

Kuo HC, Su YL, Yang HL, Chen TY (2005) Identification of Chinese medicinal fungus *Cordyceps sinensis* by PCR-single-stranded conformation polymorphism and phylogenetic relationship. Journal of Agricultural and Food Chemistry 53: 3963–3968. https://doi.org/10.1021/jf0482562

Li Y, Li TH, Yang ZL, Bau T, Dai YC (2015) Atlas of Chinese macrofungal resources. Central China Farmers Publishing House, ZhengZhou, China, 93–109.

Li Z, Li C, Huang B, Fan M (2001) Discovery and demonstration of the teleomorph of *Beauveria bassiana* (Bals.) Vuill., an important entomogenous fungus. Chinese Science Bulletin 46: 751–753.

Luangsa-Ard JJ, Hywel-Jones NL, Manoch L, Samson RA (2005) On the relationships of *Paecilomyces* sect. *Isarioidea* species. Mycological Research 109: 581–589. https://doi.org/10.1017/S0953756205002741

Luangsa-ard JJ, Tasanathai K, Mongkolsamrit S, Hywel-Jones N (2007) Atlas of invertebrate-pathogenic fungi of Thailand. National Center of Genetic Engineering and Biotechnology, National Science and Technology Development, Thailand, 75 pp.

Mains E (1958) North American entomogenous species of *Cordyceps*. Mycologia 50: 169–222.

Mongkolsamrit S, Noisripoom W, Tasanathai K, Khonsanit A, Thanakitpipattana D, Himaman W, Kobmoo N, Luangsa-ard JJ (2020) Molecular phylogeny and morphology reveal cryptic species in *Blackwellomyces* and *Cordyceps* (Cordycipitaceae) from Thailand. Mycological Progress 19: 957–983.

Mongkolsamrit S, Noisripoom W, Thanakitpipattana D, Wutikhun T, Spatafora JW, Luangsa-Ard J (2018) Disentangling cryptic species with isaria-like morphs in Cordycipitaceae. Mycologia 110: 230–257. https://doi.org/10.1080/00275514.2018.1446651

Nikoh N, Fukatsu T (2000) Interkingdom host jumping underground: phylogenetic analysis of entomoparasitic fungi of the genus *Cordyceps*. Molecular Biology and Evolution 17: 629–638. https://doi.org/10.1093/oxfordjournals.molbev.a026341

Ranwez V, Douzery EJ, Cambon C, Chantret N, Delsuc F (2018) MACSE v.2: toolkit for the alignment of coding sequences accounting for frameshifts and stop codons. Molecular Biology and Evolution 35: 2582–2584.

Ronquist F, Huelsenbeck JP (2003) MrBayes 3: Bayesian phylogenetic inference under mixed models. Bioinformatics 19: 1572–1574. https://doi.org/10.1093/bioinformatics/btg180

Royal Botanic Garden E (1969) Flora of British Fungi: colour identification chart. HM Stationery Office.

Schoch CL, Seifert KA, Huhndorf S, Robert V, Spouge JL, Levesque CA, Chen W, Consortium FB (2012) Nuclear ribosomal internal transcribed spacer (ITS) region as a universal DNA barcode marker for Fungi. Proceedings of the National Academy of Sciences 109: 6241–6246. https://doi.org/10.1073/pnas.1117018109

Shrestha B, Tanaka E, Hyun MW, Han J-G, Kim CS, Jo JW, Han S-K, Oh J, Sung G-H (2016) Coleopteran and Lepidopteran hosts of the entomopathogenic genus *Cordyceps* sensu lato. Journal of Mycology 2016: e7648219. https://doi.org/10.1155/2016/7648219

Stensrud Ø, Hywel-Jones NL, Schumacher T (2005) Towards a phylogenetic classification of *Cordyceps*: ITS nrDNA sequence data confirm divergent lineages and paraphyly. Mycological Research 109: 41–56. https://doi.org/10.1017/S095375620400139X

Sung GH, Hywel-Jones NL, Sung JM, Luangsa-Ard JJ, Shrestha B, Spatafora JW (2007) Phylogenetic classification of *Cordyceps* and the clavicipitaceous fungi. Studies in Mycology 57: 5–59. https://doi.org/10.3114/sim.2007.57.01

Sung GH, Spatafora JW, Zare R, Hodge KT, Gams W (2001) A revision of *Verticillium* sect. *Prostrata*. II. Phylogenetic analyses of SSU and LSU nuclear rDNA sequences from anamorphs and teleomorphs of the Clavicipitaceae. Nova Hedwigia 72: 311–328. https://doi.org/10.1111/j.1756-1051.2001.tb00824.x

Swofford DL (2002) PAUP*: phylogenetic analysis using parsimony (*and other methods), version 4.0b10. Sinauer Associates, Sunderland. https://doi.org/10.1002/0471650129.dob0522

Tasanathai K, Thanakitpipattana D, Noisripoom W, Khonsanit A, Kumsao J, Luangsa-ard JJ (2016) Two new *Cordyceps* species from a community forest in Thailand. Mycological Progress 15: 28.

Thompson JD, Gibson TJ, Plewniak F, Jeanmougin F, Higgins DG (1997) The CLUSTAL X windows interface: flexible strategies for multiple sequence alignment aided by quality analysis tools. Nucleic Acids Research 25: 4876–4882. https://doi.org/10.1093/nar/25.24.4876

Torres MS, White J, Bischoff JF (2005) *Cordyceps spegazzinii* sp. nov., a new species of the *C. militaris* group. Mycotaxon 94: 253–263. https://doi.org/10.1016/j.micrel.2005.07.047

Vega FE, Goettel MS, Blackwell M, Chandler D, Jackson MA, Keller S, Koike M, Maniania NK, Monzon A, Ownley BH (2009) Fungal entomopathogens: new insights on their ecology. Fungal Ecology 2: 149–159. https://doi.org/10.1016/j.funeco.2009.05.001

Vizzini A, Antonin V, Sesli E, Contu M (2015) *Gymnopus trabzonensis* sp. nov. Omphalotaceae and *Tricholoma virgatum* var. *fulvoumbonatum* var. nov. Tricholomataceae, two new white-spored agarics from Turkey. Phytotaxa 226: 119–130. https://doi.org/10.11646/phytotaxa.226.2.2

Vu D, Groenewald M, De Vries M, Gehrmann T, Stielow B, Eberhardt U, Al-Hatmi A, Groenewald J, Cardinali G, Houbraken J (2019) Large-scale generation and analysis of filamentous fungal DNA barcodes boosts coverage for kingdom fungi and reveals thresholds for fungal species and higher taxon delimitation. Studies in Mycology 92: 135–154. https://doi.org/10.1016/j.simyco.2018.05.001

Wang L, Zhang W, Hu Ba, Chen Y, Qu L (2008) Genetic variation of *Cordyceps militaris* and its allies based on phylogenetic analysis of rDNA ITS sequence data. Fungal Diversity 31: 147–155. https://doi.org/10.1002/yea.1604

White TJ, Bruns T, Lee S, Taylor J (1990) Amplification and direct sequencing of fungal ribosomal RNA genes for phylogenetics. PCR protocols: a guide to methods and applications 18: 315–322.

Yan JQ, Bau T (2015) *Cordyceps ningxiaensis* sp. nov., a new species from Dipteran pupae in Ningxia Hui Autonomous Region of China. Nova Hedwig 100: 251–258. https://doi.org/10.1127/nova_hedwigia/2014/0222

Zha LS, Huang SK, Xiao YP, Boonmee S, Eungwanichayapant PD, McKenzie EH, Kryukov V, Wu XL, Hyde KD, Wen TC (2018) An evaluation of common *Cordyceps* (Ascomycetes) species found in Chinese markets. International Journal of Medicinal Mushrooms 20: 1149–1162. https://doi.org/10.1615/IntJMedMushrooms.2018027330

Zha LS, WEN TC, Huang SK, Boonmee S, Eungwanichayapant PD (2019) Taxonomy and biology of *Cordyceps qingchengensis* sp. nov. and its allies. Phytotaxa 416: 14–24. https://doi.org/10.11646/phytotaxa.416.1.2

Zhi LZ, Gang LF, L H-JN, Li ZS, Jun CM, Bo H, Sheng SC, An CZ, Ru LC, Jiu TY, Fei DJ (2021) Biodiversity of cordycipitoid fungi associated with *Isaria cicadae* Miquel II: Teleomorph discovery and nomenclature of chanhua, an important medicinal fungus in China. Mycosystema 40: 95–107. https://doi.org/10.13346/j.mycosystema.200119

Zhong X, Peng Q, Qi L, Lei W, Liu X (2010) rDNA-targeted PCR primers and FISH probe in the detection of *Ophiocordyceps sinensis* hyphae and conidia. Journal of Microbiological Methods 83: 188–193. https://doi.org/10.1016/j.mimet.2010.08.020

MycoKeys 83: 181–208 (2021)
doi: 10.3897/mycokeys.83.70925
https://mycokeys.pensoft.net

RESEARCH ARTICLE

A peer-reviewed open-access journal
MycoKeys
Launched to accelerate biodiversity research

Ophiostomatoid species associated with pine trees (*Pinus* spp.) infested by *Cryphalus piceae* from eastern China, including five new species

Runlei Chang[1], Xiuyu Zhang[1], Hongli Si[1], Guoyan Zhao[1], Xiaowen Yuan[2], Tengteng Liu[1], Tanay Bose[3], Meixue Dai[1]

1 *College of Life Sciences, Shandong Normal University, Jinan 250014, China* **2** *Kunyushan Forest Farm, Yantai 264112, China* **3** *Forestry and Agricultural Biotechnology Institute (FABI), Department of Biochemistry, Genetics & Microbiology, University of Pretoria, Pretoria 0002, South Africa*

Corresponding author: Meixue Dai (daimeixue@sdnu.edu.cn)

Academic editor: Nattawut Boonyuen | Received 1 July 2021 | Accepted 20 September 2021 | Published 13 October 2021

Citation: Chang R, Zhang X, Si H, Zhao G, Yuan X, Liu T, Bose T, Dai M (2021) Ophiostomatoid species associated with pine trees (*Pinus* spp.) infested by *Cryphalus piceae* from eastern China, including five new species. MycoKeys 83: 181–208. https://doi.org/10.3897/mycokeys.83.70925

Abstract

Cryphalus piceae attacks various economically important conifers. Similar to other bark beetles, *Cr. piceae* plays a role as a vector for an assortment of fungi and nematodes. Previously, several ophiostomatoid fungi were isolated from *Cr. piceae* in Poland and Japan. In the present study, we explored the diversity of ophiostomatoid fungi associated with *Cr. piceae* infesting pines in the Shandong Province of China. We isolated ophiostomatoid fungi from both galleries and beetles collected from our study sites. These fungal isolates were identified using both molecular and morphological data. In this study, we recovered 175 isolates of ophiostomatoid fungi representing seven species. *Ophiostoma ips* was the most frequently isolated species. Molecular and morphological data indicated that five ophiostomatoid fungal species recovered were previously undescribed. Thus, we proposed these five novel species as *Ceratocystiopsis yantaiensis*, *C. weihaiensis*, *Graphilbum translucens*, *Gr. niveum*, *and Sporothrix villosa*. These new ophiostomatoid fungi add to the increasing number of fungi known from China, and this evidence suggests that numerous novel taxa are awaiting discovery in other forests of China.

Keywords

Ceratocystiopsis, fungal symbionts, *Graphilbum*, nematode vector, *Ophiostoma*, *Sporothrix*

Introduction

Wingfield et al. (1993) coined the name "ophiostomatoid fungi" referring to a polyphyletic group of fungi that included several species from the orders *Microascales* and *Ophiostomatales*. These fungi are distinguished by spores generated in sticky droplets that aid in dispersion by arthropods (De Beer et al. 2013). The order *Microascales* includes three families, including *Ceratocystidaceae* (11 genera), *Gondwanamycetaceae* (2 genera), and *Graphiaceae* (1 genus) (De Beer et al. 2013). The *Ophiostomatales* was divided into two families: *Ophiostomataceae* (11 genera) and *Kathistaceae* (3 genera) (Hyde et al. 2020). Initially, De Beer and Wingfield (2013) identified 18 species complexes within the order *Ophiostomatales*. Later, the '*S. schenckii* – *O. stenoceras*' species complex was elevated to genus level as *Sporothrix* (De Beer et al. 2016). Subsequently, this genus was divided into six species complexes (De Beer et al. 2016). Following this, Linnakoski et al. (2016a), Yin et al. (2016), and Jankowiak et al. (2017b) identified the *O. clavatum*, *O. piceae* and *G. grandifoliae* species complexes, respectively. Currently, the order *Ophiostomatales* thus encompasses at least 26 species complexes (De Beer and Wingfield 2013; De Beer et al. 2016; Linnakoski et al. 2016a; Yin et al. 2016; Jankowiak et al. 2017b).

Ophiostomatoid fungi often form a symbiotic association with bark and ambrosia beetles who assist in the dispersal of their inocula (Klepzig and Six 2004). For example, *Ceratocystiopsis ranaculosus* colonizes the mycangium of *Dendroctonus frontalis* whereas *Ophiostoma minus* is carried phoretically on the exoskeleton (Hofstetter et al. 2015). In addition, an ophiostomatoid fungus can symbiotically associate with multiple beetle species. Recently, six ophiostomatoid fungi were isolated from *Monochamus alternatus* in China (Zhao et al. 2014; Wang et al. 2018). Among them, *Ophiostoma ips* was previously isolated from *Bursaphelenchus xylophilus* (Steiner & Buhrer) Nickle and *M. alternatus* Hope from North America and Korea, respectively (Wingfield 1987; Suh et al. 2013).

Beetle-associated ophiostomatoid fungi play pivotal roles in the ecosystem. As exemplified by *Endoconidiophora polonica* and *Sporothrix* sp. 1., these fungi can provide beetles with nourishment, help them overcome plant defenses, and increase their vitality (Hammerbacher et al. 2013; Zhao et al. 2013; Wadke et al. 2016). *Endoconidiophora polonica* uses plant defensive compounds such as stilbenes and flavonoids as a carbon source, whilst *Sporothrix* sp. 1. enhances the development and survival rate of arthropods such as *M. alternatus* (Zhao et al. 2013). This evidence confirms that ophiostomatoid fungi substantially influence the devastation caused by these arthropods in forestry contexts globally.

In Europe and Asia, *Cryphalus piceae* infests various species of *Abies*, *Pinus*, *Picea*, and *Larix* (Jankowiak and Kolarik 2010). This bark beetle predominantly affects stressed trees (Michalski and Mazur 1999), but can also attack healthy ones (Justesen et al. 2020). Previously, several fungal species were isolated from *Cr. piceae* infesting *Abies alba* and *A. veitchii*. This data included an assortment of ophiostomatoid fungi from the genera *Graphilbum*, *Grosmannia*, *Leptographium*, *Ophiostoma*, and *Sporothrix* from Poland (Jankowiak and Kolarik 2010; Jankowiak et al. 2017a) and Japan (Oh-

taka et al. 2002a; Ohtaka et al. 2002b), and hypocrealean species from the genus *Geosmithia* from Poland (Jankowiak and Bilanski 2018).

In China, knowledge regarding the diversity of ophiostomatoid fungi associated with *Cr. piceae* is currently limited. Between 2019 and 2020, we thus conducted surveys of numerous *Pinus* stands in China's Shandong province. During these surveys, we collected samples of wood and bark from afflicted trees that had beetle galleries. From these samples, 175 isolates of ophiostomatoid fungi were isolated. Analyses of molecular and morphological data revealed that our isolates belonged to seven different species of ophiostomatoid fungi. Among these, phylogenetic and morphological analyses confirmed that five of these taxa from China were previously undescribed. Here we described these species as *Ceratocystiopsis yantaiensis* sp. nov., *C. weihaiensis* sp. nov., *Graphilbum translucens* sp. nov., *Gr. niveum* sp. nov., and *Sporothrix villosa* sp. nov.

Materials and methods

Collection of beetles and isolation of fungi

From September 2019 to August 2020, multiple surveys were conducted in several *Pinus thunbergii* stands located near Weihai (37°30'07"N, 121°07'24"E) and Yantai (37°15'38"N, 121°44'39"E), and *Pinus densiflora* located near Qingdao (36°15'26"N, 121°38'07"E), Shandong Province of China. All these *Pinus thunbergii* and *Pinus densiflora* stands were infested by *Cr. Piceae* along with *Bursaphelenchus xylophilus* and *Monochamus alternatus*. Samples of wood and bark with beetle galleries were collected from affected trees. In the laboratory, adult beetles from these galleries were individually collected in 2 ml sterile collection tubes inside a laminar flow cabinet. Both galleries and beetles were stored at 4 ℃ until the isolation of fungi.

Beetles were identified using both morphological and molecular data. In the case of the latter, cytochrome oxidase subunit I (COI) was used as the marker gene region. Sequences of bark beetle were identified using the "animal identification [COI]" database available through BOLDSYSTEMS (https://v3.boldsystems.org/). Sequence similarity searches confirmed the identity of all bark beetles as *Cr. piceae*. Hence, two representative sequences of the bark beetle were submitted to GenBank under the accession numbers MZ778788 and MZ778789.

In total, 32 adult beetles and 89 galleries were used for the isolation of ophiostomatoid fungi. Fungal isolation was done using the method suggested by Chang et al. (2019). Fungal mycelia and/or spore masses from *Cr. piceae* galleries were transferred onto 2% malt extract agar (MEA, Qingdao Hope Bio-technology, Qingdao, China) medium amended 0.05% streptomycin (Sangon Biotech, Qingdao, China). In cases of no mycelia and/or spore masses, galleries were incubated in moist chambers at 25 °C in darkness for 4–6 weeks. Post incubation, conidia with spore masses emerging from the conidiophores were transferred onto MEA amended with 0.05% streptomycin. To isolate ophiostomatoid fungi from the beetles, adult *Cr. piceae* was crushed on a sterile

Table 1. Isolates of ophiostomatoid fungi isolated from *Cryphalus piceae* in this study.

Taxon	Species	Isolate	CGMCC	Tree host	Location	Sources	ITS	LSU	BT	EF	CAL
1	*Ceratocystiopsis yantaiensis* sp. nov.	SNM582		*Pinus thunbergii*	Yantai	Gallery	MW989410	MZ819923	MZ019522	MZ853079	–
		SNM650[T]	3.20247	*P. thunbergii*	Yantai	Gallyer	MW989411	MZ819924	MZ019523	MZ853080	–
2	*Ceratocystiopsis weihaiensis* sp. nov.	SNM634		*P. thunbergii*	Weihai	Gallery	MW989412	MZ819925	MZ019524	MZ853081	–
		SNM649[T]	3.20246	*P. thunbergii*	Weihai	Gallery	MW989413	MZ819926	MZ019525	MZ853082	–
3	*Graphilbum translucens* sp. nov.	SNM101		*P. thunbergii*	Weihai	Gallery	MW989414	–	MZ019526	MZ019544	MZ781969
		SNM104		*P. densiflora*	Qingdao	Gallery	MW989415	–	MZ019527	MZ019545	MZ781970
		SNM144[T]	3.20263	*P. thunbergii*	Weihai	Gallery	MW989416	–	MZ019528	MZ019546	MZ781971
4	*Graphilbum niveum* sp. nov.	SNM100		*P. densiflora*	Qingdao	Gallery	MW989417	–	MZ019529	MZ019547	MZ418998
		SNM145[T]	3.50268	*P. thunbergii*	Weihai	Beetle	MW989418	–	MZ019530	MZ019548	MZ418997
5	*Graphium pseudormiticum*	SNM159		*P. thunbergii*	Weihai	Gallery	MW989419	–	–	MZ019549	–
6	*Ophiostoma ips*	SNM20		*P. thunbergii*	Weihai	Gallery	MW989420	–	MZ019531	–	–
		SNM44		*P. thunbergii*	Weihai	Gallery	MW989421	–	MZ019532	–	–
		SNM110		*P. thunbergii*	Weihai	Gallery	MW989422	–	MZ019533	–	–
		SNM120		*P. thunbergii*	Weihai	Gallery	MW989423	–	MZ019534	–	–
		SNM121		*P. thunbergii*	Weihai	Gallery	MW989424	–	MZ019535	–	–
7	*Sporothrix villosa* sp. nov.	SNM162		*P. thunbergii*	Weihai	Beetle	MW989425	–	MZ019536	MZ853075	MZ019540
		SNM182		*P. thunbergii*	Weihai	Beetle	MW989426	–	MZ019537	MZ853076	MZ019541
		SNM185		*P. thunbergii*	Weihai	Gallery	MW989427	–	MZ019538	MZ853077	MZ019542
		SNM188[T]	3.20264	*P. thunbergii*	Weihai	Beetle	MW989428	–	MZ019539	MZ853078	MZ019543

surface using a pair of forceps, thereafter, this crushed beetle was placed on the surface of MEA amended 0.05% streptomycin. To purify the fungal isolates, hyphal tips from fungal colonies were transferred onto fresh MEA plates.

All fungal isolates were submitted to the microbial culture collection of Shandong Normal University, Jinan, Shandong, China (SNM; for accession numbers see Table 1). Ex-holotypes cultures of ophiostomatoid fungi described in this study were deposited in the China General Microbiological Culture Collection Center (CGMCC; http://www.cgmcc.net/english/catalogue.html), Beijing, China. Holotype specimens (dry cultures) were deposited in the Herbarium Mycologicum, Academiae Sinicae (HMAS), Beijing, China.

DNA extraction, PCR amplification and sequencing

All fungal isolates obtained in this study were initially grouped based on colony morphology. For preliminary identification, at least two representative isolates from each group were identified using molecular techniques. For the novel species described in the present study, all isolates were sequenced to confirm their identity.

The PrepMan ultra sample preparation reagent (Applied Biosystems, Foster City, CA) was used for extracting the total genomic DNA from five-day-old cultures, following the manufacturer's protocols. The complete ITS region, and partial large subunit (LSU) of the nuclear ribosomal RNA (rRNA) gene, and partial β-tubulin (BT), elongation factor 1-α (EF), and calmodulin (CAL) genes were amplified using primers ITS1F/ITS4 (White et al. 1990; Gardes and Bruns 1993), LR0R/LR5 (Vilgalys and Hester 1990), Bt2a (or T10)/Bt2b (Glass and Donaldson 1995), EF2F/EF2R (Jacobs

et al. 2004; Marincowitz et al. 2015), and CL2F/CL2R (Duong et al. 2012), respectively.

Each 25 µl PCR reaction included 12.5 µl 2 × Taq Master Mix (buffer, dNTPs, and Taq; Vazyme Biotech Co., Ltd, China), 0.5 µl each of forward and reverse primers, 10.5 µl PCR grade water, and 1 µl of DNA template. PCR amplifications were conducted with an initial denaturation at 95 °C for 3 min, followed by 30 cycles of 95 °C for 60 sec; annealing temperature was 55 °C for 60 sec for all primers; 72 °C for 1 min; and final elongation at 72 °C for 10 min.

All PCR products were sequenced by Sangon Biotech, Qingdao, Shandong Province, China. The sequences were assembled using Geneious v. 7.1.4 (Biomatters, Auckland, New Zealand). The BLAST algorithm (Altschul et al. 1990) available through the NCBI GenBank was used for the preliminary identification of the taxa. All sequences were submitted to GenBank and the accession numbers are listed in Table 1.

Phylogenetic analyses

For phylogenetic analyses, separate datasets were prepared for all four gene regions (ITS, BT, EF and CAL). Each of these datasets included sequences generated in this study, and those that were retrieved from the GenBank (including the ex-type sequences, Suppl. material 3: Table S1). We recovered a high number of isolates representing the same species from *O. ips* (141 isolates) and *S. gossypina* species complex (24 isolates). Therefore, datasets for these two species complexes included sequences from four representative isolates. The gene areas that are available in public databases substantially vary amongst genera and species complexes of ophiostomatoid fungi. As a result, we chose gene regions for our study based on previous research. These are as follows: ITS, BT, EF and CAT for *Graphilbum* (Jankowiak et al. 2020), ITS and BT for *O. ips* species complex (Wang et al. 2020), ITS, LSU and BT for *Ceratocystiopsis* (Nel et al. 2021), ITS, BT and CAL for *Sporothrix* (De Beer et al. 2016; Wang et al. 2018), and ITS and EF for *Graphium* (Chang et al. 2019). The datasets were aligned using MAFFT v. 7 (Katoh and Standley 2013). If needed, alignments were manually edited using MEGA v. 6.06 (Tamura et al. 2013). All aligned sequence datasets were deposited to TreeBase (Acc. No. 28127).

Programs used for maximum likelihood (ML) and Bayesian inference (BI) analyses were accessed through the CIPRES Science Gateway v. 3.3 (Miller et al. 2010). For all datasets, jModelTest v. 2.1.6 (Darriba et al. 2012) was used for selecting appropriate substitution models. Maximum likelihood analyses were done through RaxML v. 8.2.4 (Stamatakis 2014) using the GTR substitution model and 1000 bootstrap replicates. Bayesian inference analyses were done using MrBayes v. 3.2.6 (Ronquist et al. 2012). Four MCMC chains were run from a random starting tree for five million generations and trees were sampled every 100th generation. One-fourth of the sampled trees were discarded as burn-in and the remaining trees were used for constructing majority rule consensus trees. MEGA-X was used for conducting maximum parsimony (MP) analyses with 1000 bootstrap replicates (Kumar et al. 2018) where gaps were treated as a fifth character.

Growth and morphological studies

For each new fungal species, an ex-type along with another isolate identified through phylogenetic analyses were selected for growth study. Isolates were initially sub-cultured on 2% MEA and incubated for seven days at 25 °C in darkness. Thereafter, 5 mm agar plugs were placed at the center of 90 mm Petri dishes and three replicate plates per isolate were incubated at 5, 10, 15, 20, 25, 30 and 35 °C (± 0.5 °C) in darkness. The colony diameter of each isolate was measured at an interval of two days up to the tenth day.

Microscopic structures of the ophiostomatoid fungi were measured and photographed using a Zeiss Axio Imager Z2 (CarlZeiss, Germany). Fifty measurements for each taxonomically informative structure were made, such as conidiophore and conidia. The measurements are presented in the format (minimum–) mean minus standard deviation-mean plus standard deviation (–maximum).

Results

Collection of beetles and isolation of fungi

In the present study, 175 isolates of ophiostomatoid fungi were recovered. Among these, 148 were isolated from galleries, whereas 28 were from beetles. Based on the collection sites, 16, 63, and 96 isolates were recovered from Yantai, Qingdao, and Weihai, respectively.

Phylogenetic analyses

Preliminary identification of the ophiostomatoid fungi recovered in this study showed that the isolates resided in the genera *Ceratocystiopsis* (4 isolates), *Graphilbum* (5 isolates), *Graphium* (1 isolate), *Ophiostoma* (141 isolates), and *Sporothrix* (24 isolates).

Species residing in the genus *Ceratocystiopsis* were analyzed using ITS, LSU, and BT gene regions. In the phylogenies of *Ceratocystiopsis*, four isolates of *Ceratocystiopsis* clustered into two distinct monophyletic clades (Figs 1 and 2). Taxon 1 (two isolates) and Taxon 2 (two isolates) were found to be sisters to *C. manitobensis* and *C. minuta*, respectively (Figs 1 and 2).

Species residing in the genus *Graphilbum* were analyzed using ITS, BT, CAL, and EF gene regions. The taxon sampling differed substantially amongst the gene regions due to the lack of sequences. In the phylogenetic analyses, our five isolates of *Graphilbum* clustered into two distinct clades (Figs 3–5). The three isolates of Taxon 3 nested within clades that included *Gr. acuminatum*, *Gr. anningense*, and *Gr. puerense* (Figs 3–5). In the ITS, CAL, and EF trees, the two isolates of Taxon 4 were found to be closely related to *Gr. crescericum* (Figs 3–5). In contrast, Taxon 4 emerged as the sister species to *Gr. kesiyae* in the BT tree (Fig. 4). This is due to the lack of BT gene sequences for *Gr. crescericum*.

The identity of the isolate residing in *Graphium* was confirmed using ITS and EF gene regions. In the phylogenies, the single isolate of Taxon 5 emerged as a previously described species, *G. pseudormiticum* (Suppl. material 1).

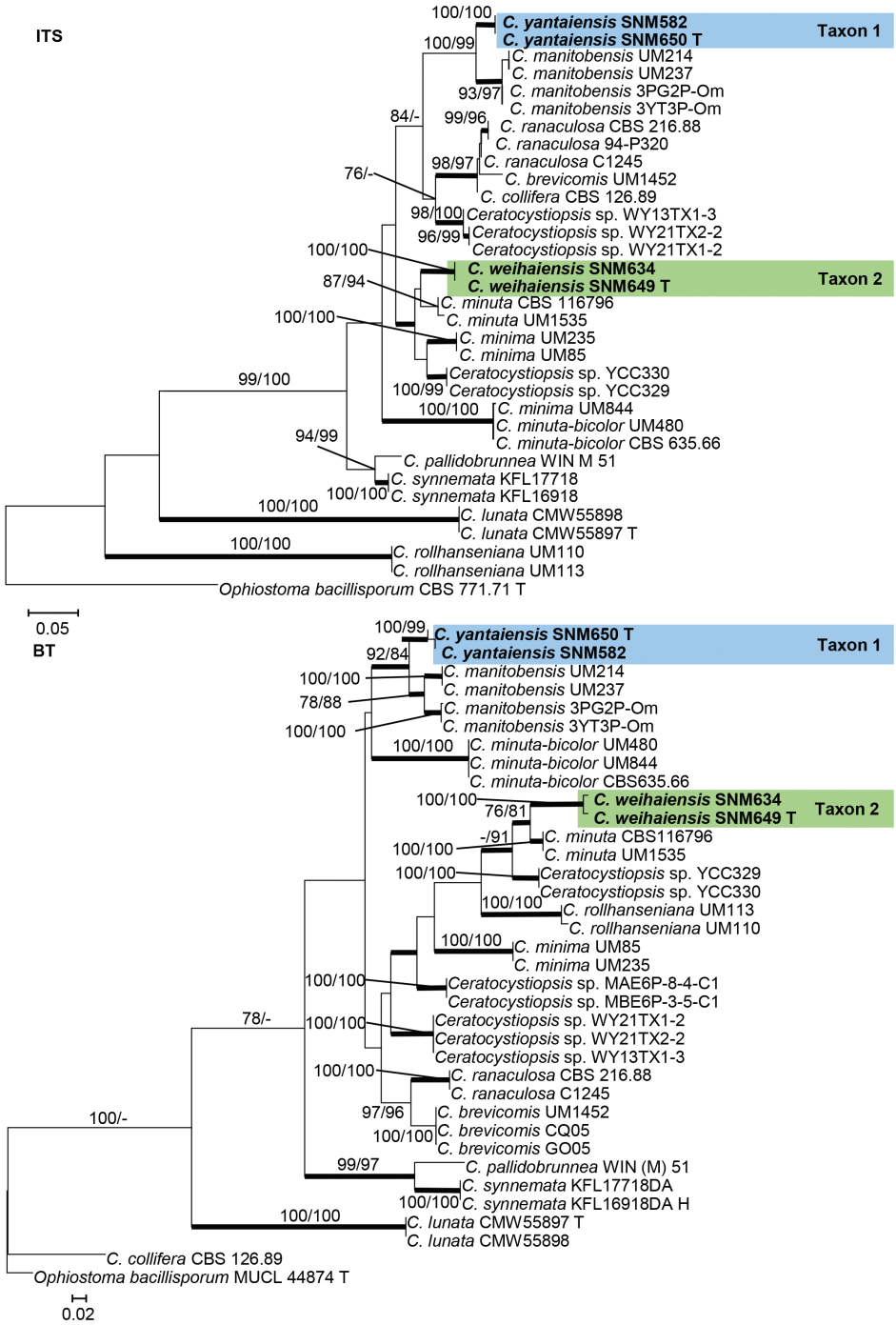

Figure 1. Maximum likelihood phylogeny of *Ceratocystiopsis* using complete ITS and partial BT gene regions. The isolates recovered in this study are highlighted in color and in bold font. ML and MP bootstrap support values ≥ 75 are indicated at the nodes as ML/MP. Bold branches indicate posterior probabilities values ≥ 0.9. T indicates ex-type cultures.

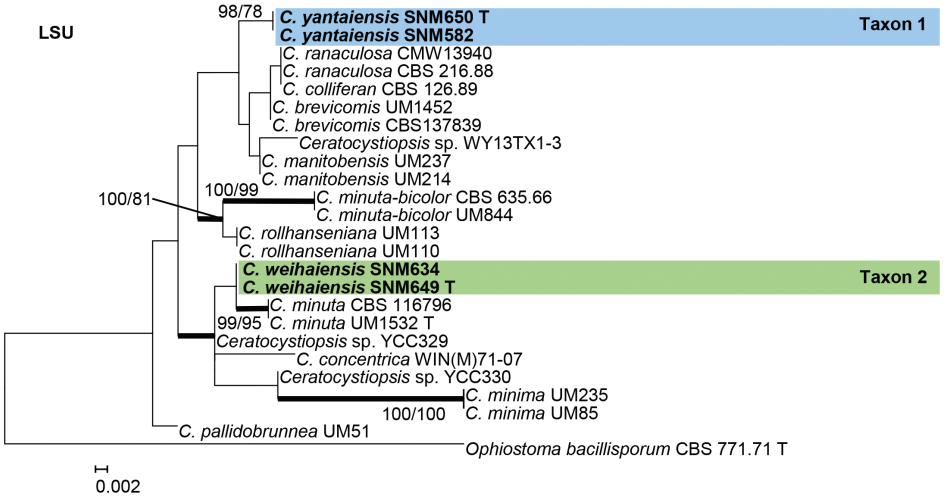

Figure 2. Maximum likelihood phylogeny of *Ceratocystiopsis* using partial LSU gene regions. The isolates recovered in this study are highlighted in color and in bold font. ML and MP bootstrap support values ≥ 75 are indicated at the nodes as ML/MP. Bold branches indicate posterior probabilities values ≥ 0.9. T indicates ex-type cultures.

Species resided in the *O. ips* species complex were analyzed using ITS and BT gene regions. In the ITS and BT trees, our isolates of Taxon 6 (141 isolates) formed monophyletic clades with *O. ips* (Suppl. material 2).

Isolates from the *S. gossypina* species complex were analyzed using ITS, BT, and CAL gene regions. In the phylogenetic analyses, our isolates of Taxon 7 were found to be closely related to two fungal isolates from China that were previously identified as *S. cf. abietina* (Figs 6–8).

Taxonomy

1. *Ceratocystiopsis yantaiensis* R.L. Chang & X.Y. Zhang, sp. nov.
Fig. 9
MycoBank No: 839252

Holotype. China. Shandong province: Kunyushan National Forest Park, Yantai city, from the gallery of *Cryphalus piceae* on *Pinus thunbergii*, 2 Sep. 2020, R. L. Chang (HMAS249924-holotype; SNM650 = CGMCC3.20247 – ex-holotype culture).

Additional cultures checked. China. Shandong province: Kunyushan National Forest Park, Yantai city, from the gallery of *Cryphalus piceae* on *Pinus thunbergii*, 2 Sep. 2020, R. L. Chang (SNM582).

Etymology. The name refers to Yantai City, where this fungus was isolated.

Diagnosis. *Ceratocystiopsis yantaiensis* differs from closely related species by the production of smaller conidia.

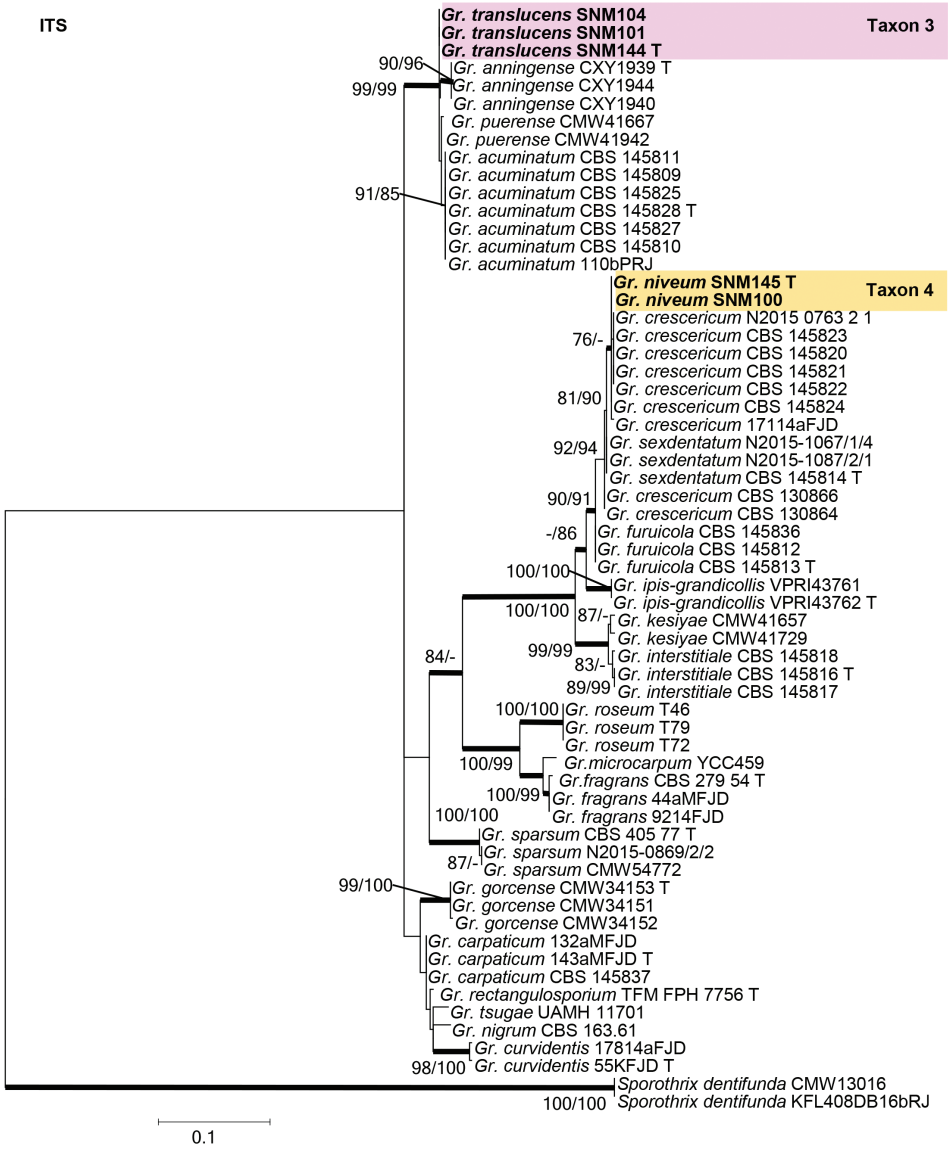

Figure 3. Maximum likelihood phylogeny of *Graphilbum* using complete ITS region. The isolates recovered in this study are highlighted in color and in bold font. ML and MP bootstrap support values ≥ 75 are indicated at the nodes as ML/MP. Bold branches indicate posterior probabilities values ≥ 0.9. T indicates ex-type cultures.

Description. Sexual morph is unknown. Asexual state hyalorhinocladiella-like: the conidiophores directly arising singly from the vegetative hyphae, measuring (2.4–) 4.7–26.7 (–46.4) µm × (0.8–) 1.0–1.5 (–1.8) µm (Fig. 9d, e); or a short basal cell which continues to develop short lateral and terminal extensions from conidiogenous sites at their apices or discrete basal cells that produce 1–5 branches, which then branch irregularly and form conidiogenous cells at their apices, measuring (12.2–)

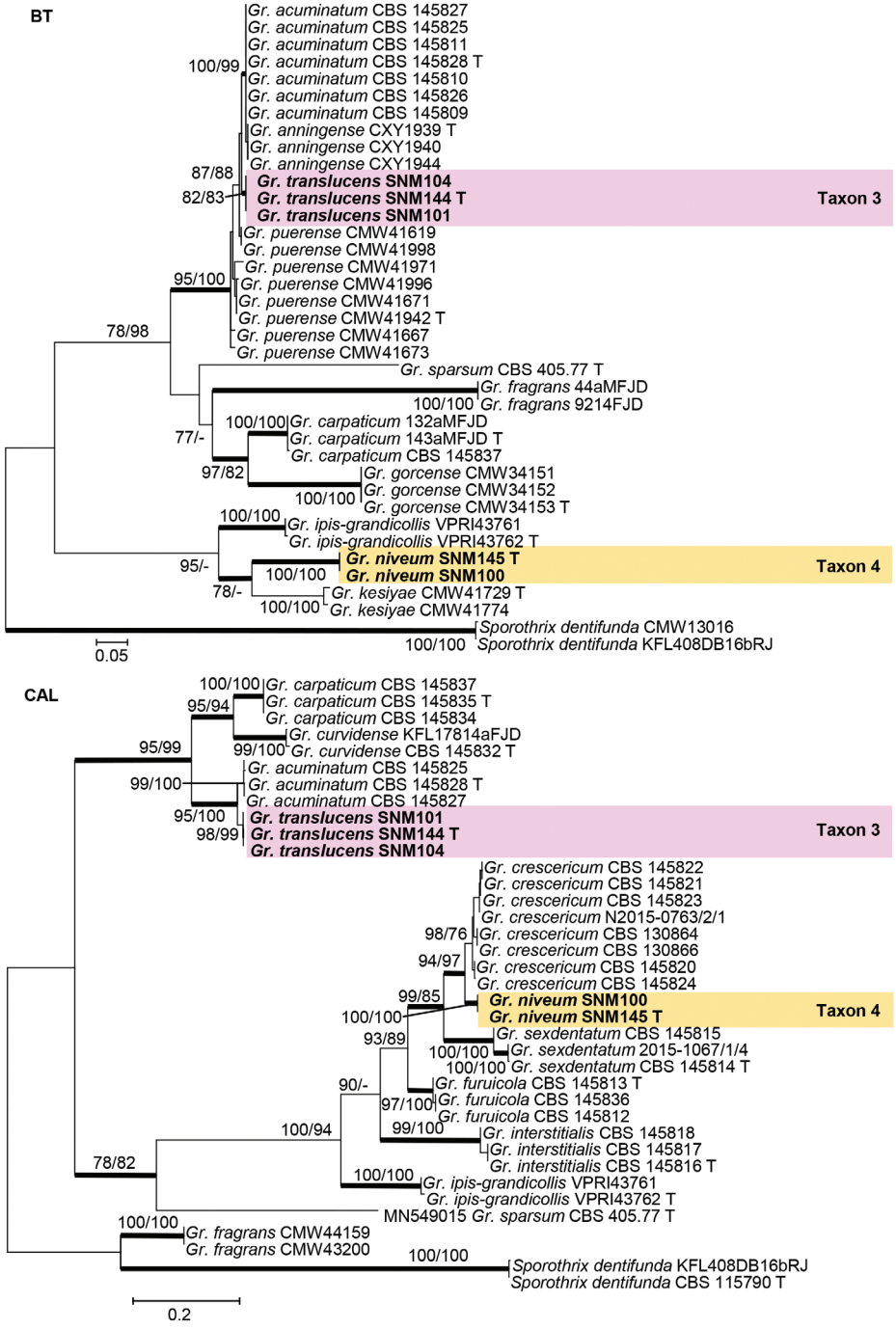

Figure 4. Maximum likelihood phylogeny of *Graphilbum* using partial BT and partial CAL gene regions. The isolates recovered in this study are highlighted in color and in bold font. ML and MP bootstrap support values ≥ 75 are indicated at the nodes as ML/MP. Bold branches indicate posterior probabilities values ≥ 0.9. T indicates ex-type cultures.

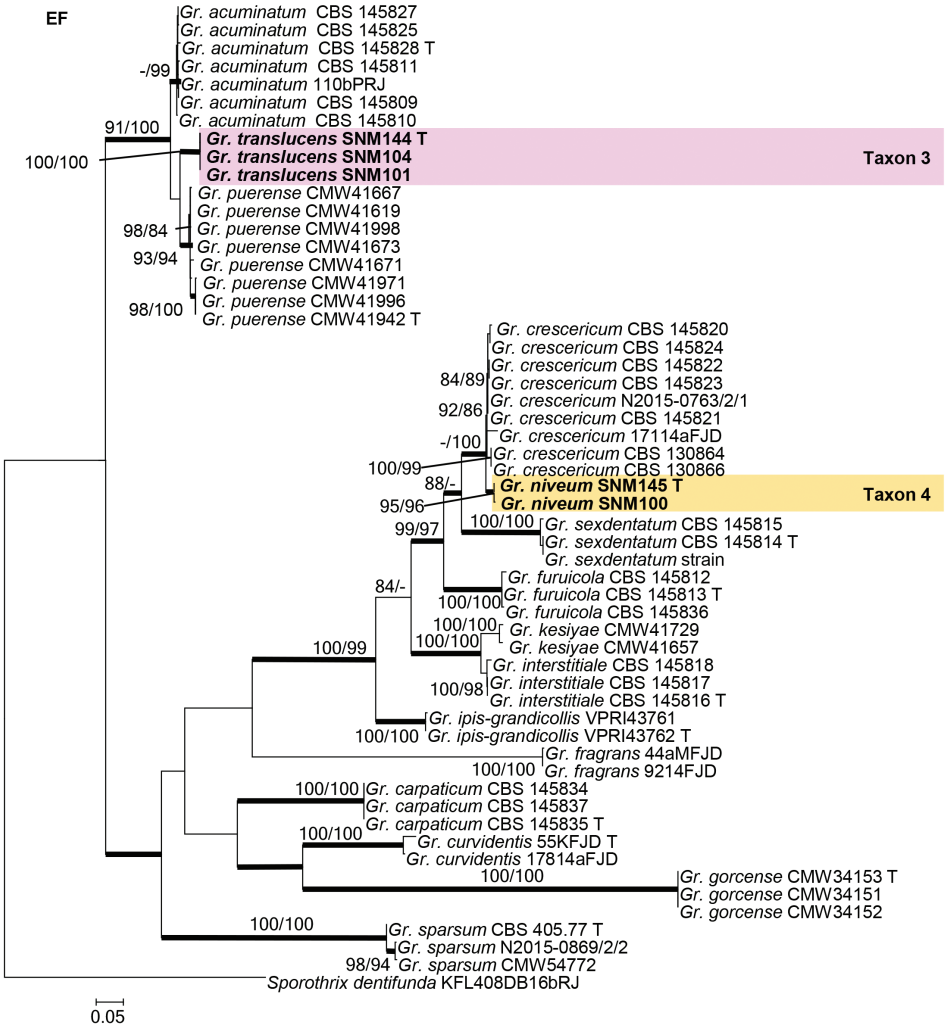

Figure 5. Maximum likelihood phylogeny of *Graphilbum* using partial EF gene region. The isolates recovered in this study are highlighted in color and in bold font. ML and MP bootstrap support values ≥ 75 are indicated at the nodes as ML/MP. Bold branches indicate posterior probabilities values ≥ 0.9. T indicates ex-type cultures.

6.2–10.2 (–50.7) µm long (Fig. 9b, c); conidiogenous cells measuring (4.7–) 6.2–10.2 (–12.4) × (0.7–) 0.9–1.3(–1.5) µm (Fig. 9b, c); conidia hyaline, smooth, unicellular, short oblong, with rounded ends, measuring (1.1–) 1.4–2.2 (–2.7) × (0.8–) 0.9–1.2 (–1.5) µm (Fig. 9b-e).

Culture characteristics. The Colonies are light brown in color on MEA (Fig. 9a). Mycelia are white, superficially growing on the agar. The optimal temperature for growth was 30–35 °C, reaching 43.0 mm diam in 10 days. No growth was observed at 5 °C.

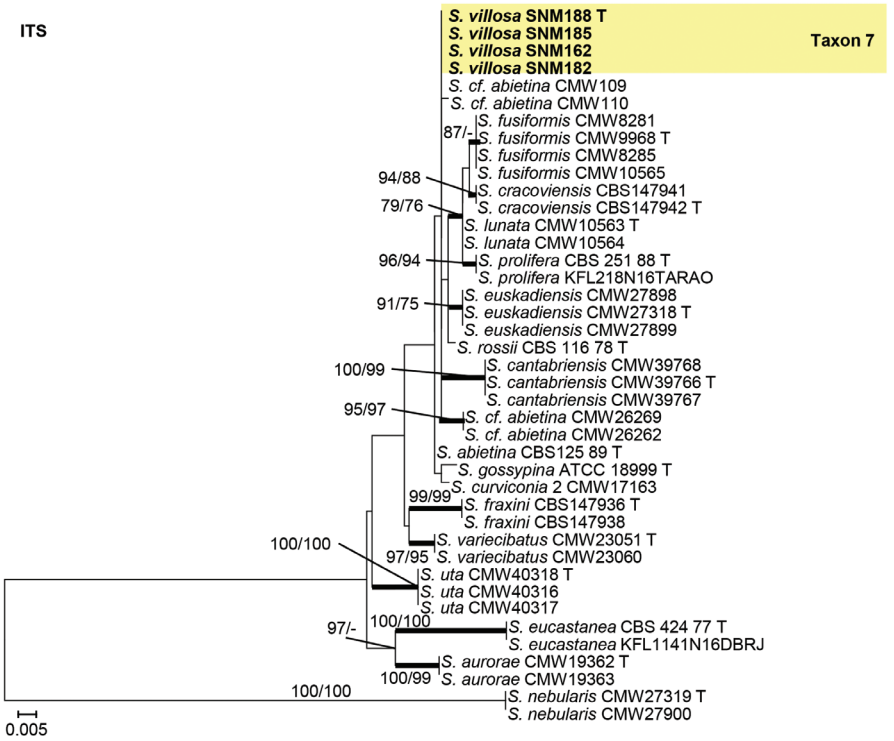

Figure 6. Maximum likelihood phylogeny of *Sporothrix gossypina* species complex using complete ITS region. The isolates recovered in this study are highlighted in color and in bold font. ML and MP bootstrap support values ≥ 75 are indicated at the nodes as ML/MP. Bold branches indicate posterior probabilities values ≥ 0.9. T indicates ex-type cultures.

Distribution. Currently known from Yantai City in Shandong Province, China.

Note. *Ceratocystiopsis yantaiensis* is phylogenetically close to *C. manitobensis*, but formed a distinct clade on both ITS, LSU, and BT trees (Figs 1 and 2). Two types of hyalorhinocladiella-like asexual state were also observed in *C. manitobensis* (Hausner et al. 2003). Conidia of *C. yantaiensis* and *C. manitobensis* are similar in morphology, but there is a difference in size (1.1–2.7 × 0.8–1.5 vs. 3.0–5.5 × 1.0–2.0 μm, Fig. 9b-e).

2. *Ceratocystiopsis weihaiensis* R.L. Chang & X.Y. Zhang, sp. nov.

Fig. 10

MycoBank No: 839253

Holotype. China. Shandong province: Zhujiajuan village, Huancui District, Weihai City, from the gallery of *Cryphalus piceae* on *Pinus thunbergii*, 2 Sep. 2019, R. L. Chang (HMAS 249923-holotype; SNM649 = CGMCC3.20246 – ex-holotype culture).

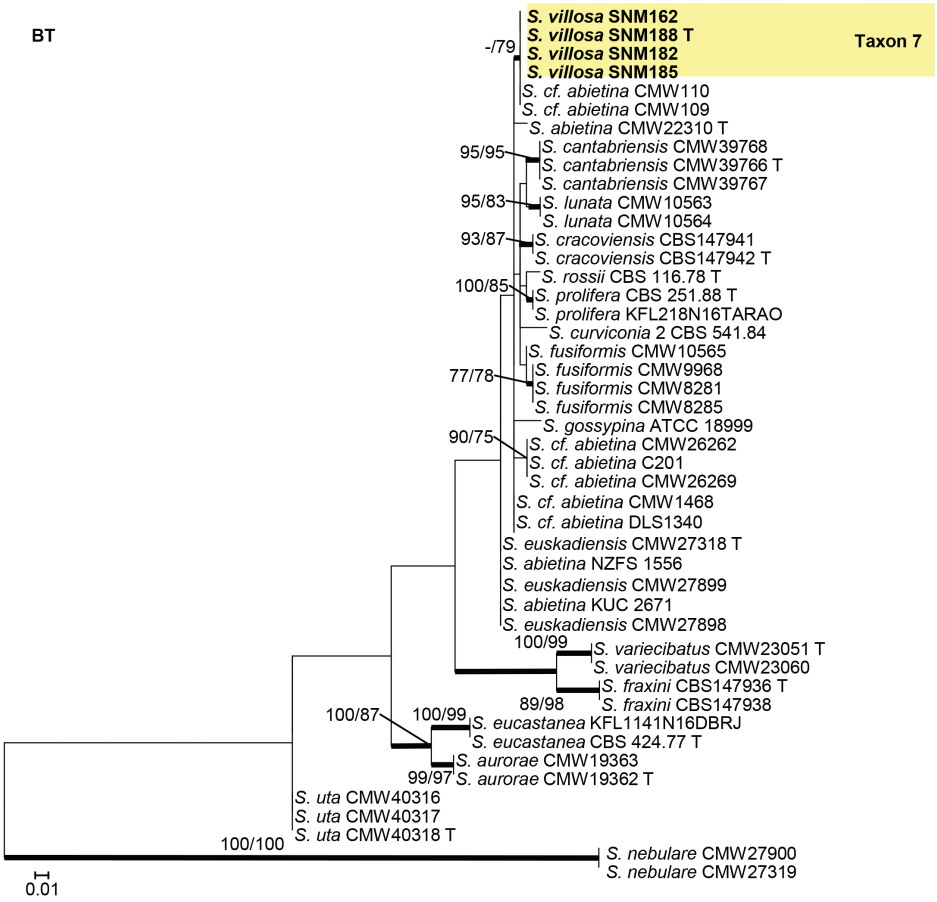

Figure 7. Maximum likelihood phylogeny of *Sporothrix gossypina* species complex using partial BT gene region. The isolates recovered in this study are highlighted in color and in bold font. ML and MP bootstrap support values ≥ 75 are indicated at the nodes as ML/MP. Bold branches indicate posterior probabilities values ≥ 0.9. T indicates ex-type cultures.

Additional cultures checked. China. Shandong province: Zhujiajuan village, Huancui District, Weihai City, from the gallery of *Cryphalus piceae* on *Pinus thunbergii*, 2 Sep. 2019, R. L. Chang (SNM634).

Etymology. The name refers to Weihai City, where this fungus was isolated.

Diagnosis. Compared to other closely related species, the conidia of *C. weihaiensis* are smaller.

Description. Sexual morph is unknown. Asexual state hyalorhinocladiella-like: the conidiophores directly arise singly from the vegetative hyphae, measuring (2.6–) 10.9–29.2 (–44.6) μm × (0.7–) 0.9–1.3 (–1.6) μm (Fig. 10b-e); conidia hyaline, smooth, unicellular short oblong, with rounded ends or clavate, ellipsoidal to ovoid measuring (1.5–) 2.0–2.6 (–2.9) × (0.7–) 0.9–1.2 (–1.5) μm (Fig. 10b-e).

Figure 8. Maximum likelihood phylogeny of *Sporothrix gossypina* species complex using partial CAL gene region. The isolates recovered in this study are highlighted in color and in bold font. ML and MP bootstrap support values ≥ 75 are indicated at the nodes as ML/MP. Bold branches indicate posterior probabilities values ≥ 0.9. T indicates ex-type cultures.

Culture characteristics. The colonies are light brown in color on MEA (Fig. 10a). Mycelia white, submerged in the agar. The optimal temperature for growth is 30 °C, reaching 46.0 mm diam in 10 days. Growth is slower at 35 °C, 27 mm diam in 10 days.

Distribution. Currently known from Weihai City in Shandong Province, China.

Note. *Ceratocystiopsis weihaiensis* is phylogenetically close to *C. minuta*, but formed a distinct monophyletic clade on both ITS and BT trees (Figs 1 and 2). In the phylogenetic study of *C. minuta* by Plattner et al. (2009) using ITS, LSU, and BT gene regions, the authors suggested that this taxon is possibly an assemblage of multiple species. Therefore, they designated the strain RJ705 from Poland as the neotype. Later, strain RJ705 = UAMH 11218 = WIN(M) 1532 was considered as the lectotype for *C. minuta* (Reid and Hausner 2010).

Ceratocystiopsis minuta and most other *Ceratocystiopsis* species have a hyalorhinocladiella-like asexual state (Plattner et al. 2009; De Beer and Wingfield 2013). The conidia of *C. weihaiensis* and *C. minuta* are similar in gross morphology. The *C. weihaiensis* differs from *C. minuta* in having short conidia size (1.5–2.9 × 0.7–1.5 vs. 2–4 × 1–2 µm, Fig. 10b-e) (Reid and Hausner 2010).

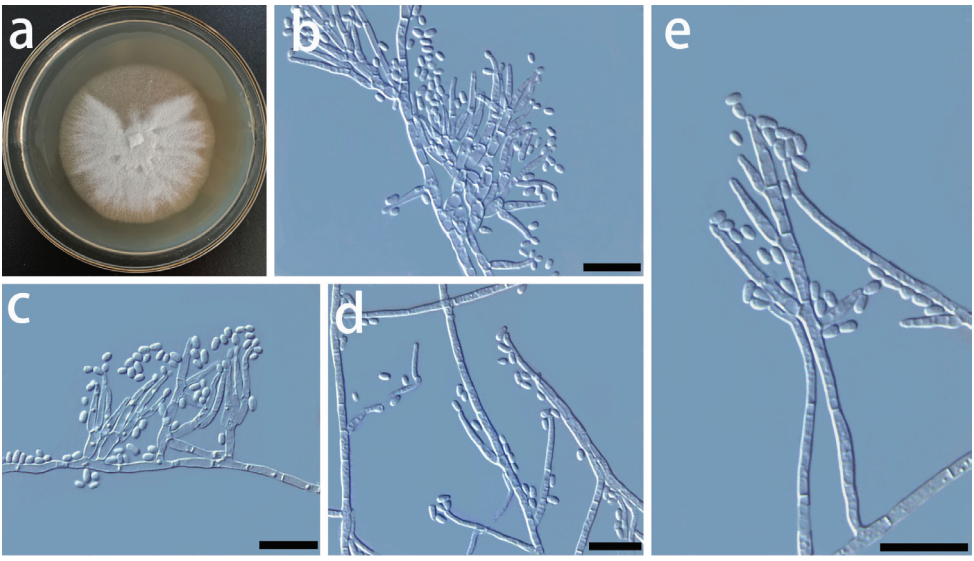

Figure 9. Morphological characters of asexual structures of *Ceratocystiopsis yantaiensis* sp. nov. **a** fourteen-day-old culture on MEA **b, c** type 1 conidiophores and conidia **d-e** type 2 conidiophores and conidia. – Scale bars: 10 μm.

3. *Graphilbum translucens* R.L. Chang & X.Y. Zhang, sp. nov.

Fig. 11
MycoBank No: 839254

Holotype. China. Shandong province: Zhujiajuan village, Huancui District, Weihai City, from the gallery of *Cryphalus piceae* on *Pinus thunbergii*, 10 Oct. 2019, R. L. Chang (HMAS 249925-holotype; SNM144 = CGMCC 3.20263 – ex-holotype culture).

Additional cultures checked. China. Shandong province: Laojiangou village, Laoshan District, Qingdao City, from the gallery of *Cryphalus piceae* on *Pinus densiflora*, 2, Aug. 2020, R. L. Chang (SNM104).

Etymology. The name refers to the translucent appearance of the colony on MEA.

Diagnosis. *Graphilbum translucens* can be distinguished from other closely related species, *Gr. puerense* and *Gr. acuminatum*, by the shorter hyalorhinocladiella-like conidiophores, smaller conidia and no pesotum-like asexual state.

Description. Sexual morph is unknown. Asexual state hyalorhinocladiella-like: the conidiophores directly arising from the vegetative hyphae, measuring (3.6–) 8.6–42.2 (–72.3) μm × (0.9–) 1.1–1.7 (–2.0) μm (Fig. 11b-e); conidia hyaline, smooth, unicellular short oblong, with rounded ends or ellipsoidal to ovoid, measuring (2.1–) 2.4–3.5 (–4.1) × (0.8–) 1.3–2.0 (–2.7) μm (Fig. 11b-e).

Culture characteristics. The colonies are light brown in color on MEA (Fig. 11a). Mycelia are partially submerged in the agar. The optimal temperature for growth is 30 °C, reaching 74.0 mm diam in 5 days. Growth slower at 35°C, 24 mm diam in 5 days. No growth was observed at 5 °C.

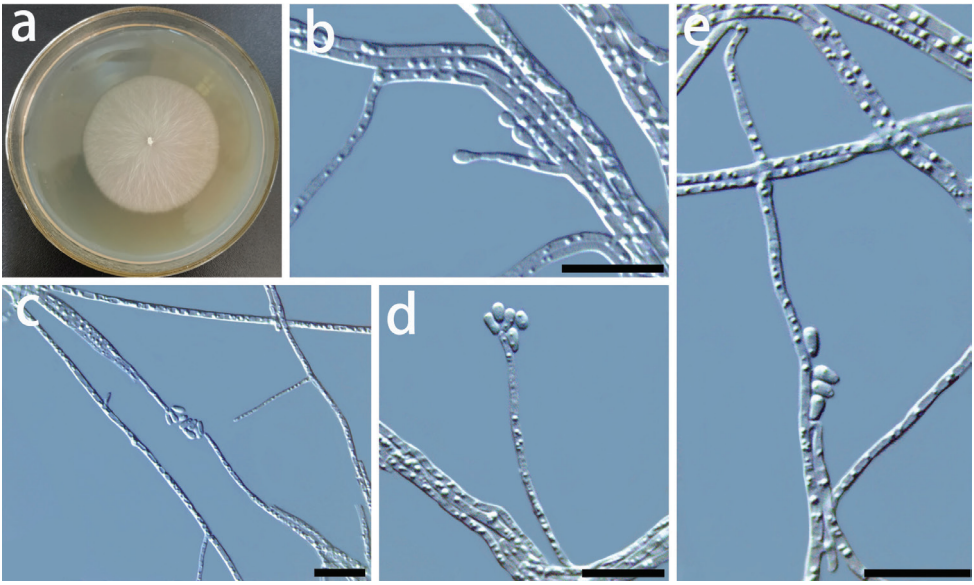

Figure 10. Morphological characters of asexual structures of *Ceratocystiopsis weihaiensis* sp. nov **a** fourteen-day-old culture on MEA **b-e** conidiophores and conidia. – Scale bars: 10 μm.

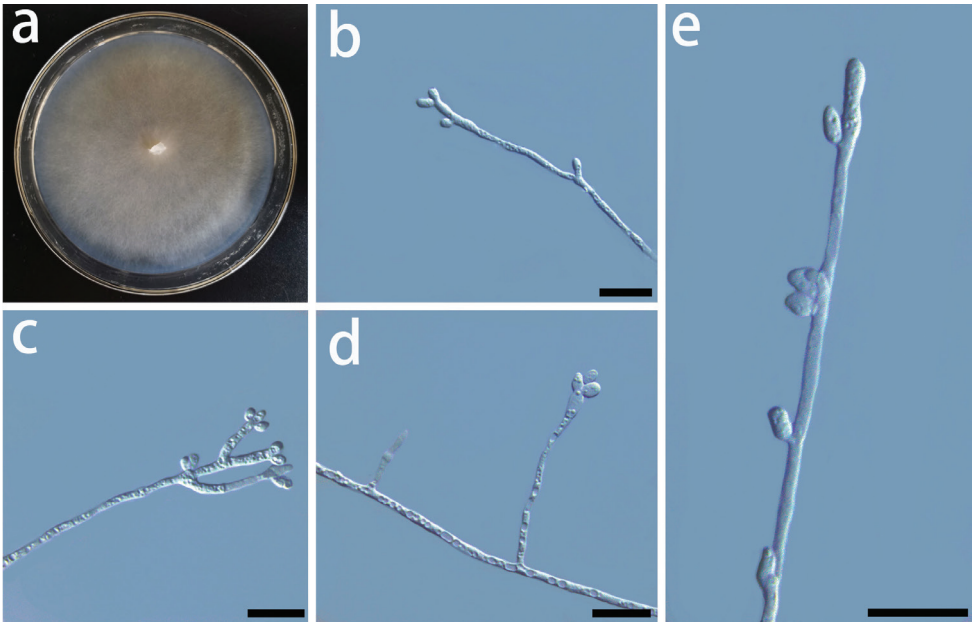

Figure 11. Morphological characters of asexual structures of *Graphilbum translucens* sp. nov. **a** fourteen-day-old culture on MEA **b-e** conidiophores and conidia. – Scale bars: 10 μm.

Distribution. Currently known from Qingdao City and Weihai City in Shandong Province, China.

Note. Based on morphology coupled with single-gene (ITS, EF, BT, and CAL) phylogenies, *Graphilbum translucens* is phylogenetically close to *Gr. puerense* and *Gr. acuminatum*. In the ITS tree, *Gr. translucens* grouped with *Gr. puerense* (Fig. 3) and *Gr. acuminatum* whereas it formed distinct clades in the BT and EF trees (Figs 4 and 5). The hyalorhinocladiella-like asexual state was observed in *Gr. translucens* and *Gr. puerense*, but it is absent in *Gr. acuminatum* (Chang et al. 2017; Jankowiak et al. 2020). The conidiophores of *Gr. translucens* are shorter than the *Gr. puerense* (Chang et al. 2017). Conidia of *Gr. translucens* and *Gr. puerense* form hyalorhinocladiella-like asexual states that are similar in shape, yet the conidia size of *Gr. translucens* is smaller than *Gr. puerense* (2.1–4.1 × 0.8–2.7 vs. 3.5–12 × 1–3 μm, Fig. 11b-e) (Chang et al. 2017). Unlike *Gr. puerense* and *Gr. acuminatum*, a pesotum-like asexual state was not observed among the isolates of *Gr. translucens* recovered in this study.

4. *Graphilbum niveum* R.L. Chang & X.Y. Zhang, sp. nov.

Fig. 12
MycoBank No: 840197

Holotype. China. Shandong province: Zhujiajuan village, Huancui District, Weihai City, from *Cryphalus piceae* on *Pinus thunbergii*, 10 Oct. 2019, R. L. Chang (HMAS 350268-holotype; SNM145 = CGMCC3.20423– ex-holotype culture).

Additional cultures checked. China. Shandong province: Laojiangou village, Laoshan District, Qingdao City, from the gallery of *Cryphalus piceae* on *Pinus densiflora*, 2, Aug. 2020, R. L. Chang (SNM100).

Etymology. The name refers to the white mycelia that appear on the MEA after 14 days.

Diagnosis. *Graphilbum niveum* differs from the closely related species *Gr. crescericum* by its shorter conidiophore and conidia.

Description. Sexual morph is unknown. Asexual state hyalorhinocladiella-like: the conidiophores directly arising from the vegetative hyphae, or produce 1–3 branches, which then branch irregularly and form conidiogenous cells at their apices, measuring (14.0–) 21.7–36.7 (–56.0) μm (Fig. 12c-e); conidiogenous cell hyaline, discrete, measuring (6.2–)8.4–13.8 (–18.7) μm × (0.7–) 0.9–1.3 (–1.8) μm (Fig. 12c -e); conidia hyaline, smooth, unicellular oblong to ovoid, with rounded ends, measuring (2.2–) 2.6–3.4 (–4.1) × (0.8–) 1.0–1.6 (–1.8) μm (Fig. 12b-e).

Culture characteristics. Colonies at first translucent to light brown in color on MEA (7 days). Thereafter, turning white in colour after 14 days (Fig. 12a). Mycelia are partially submerged in the agar. The optimal temperature for growth is 25 °C, reaching 61.0 mm diam in 8 days. The growth is relatively slower at 5 and 35 °C, reaching 2.7 mm and 9.1 mm diam in 8 days, respectively.

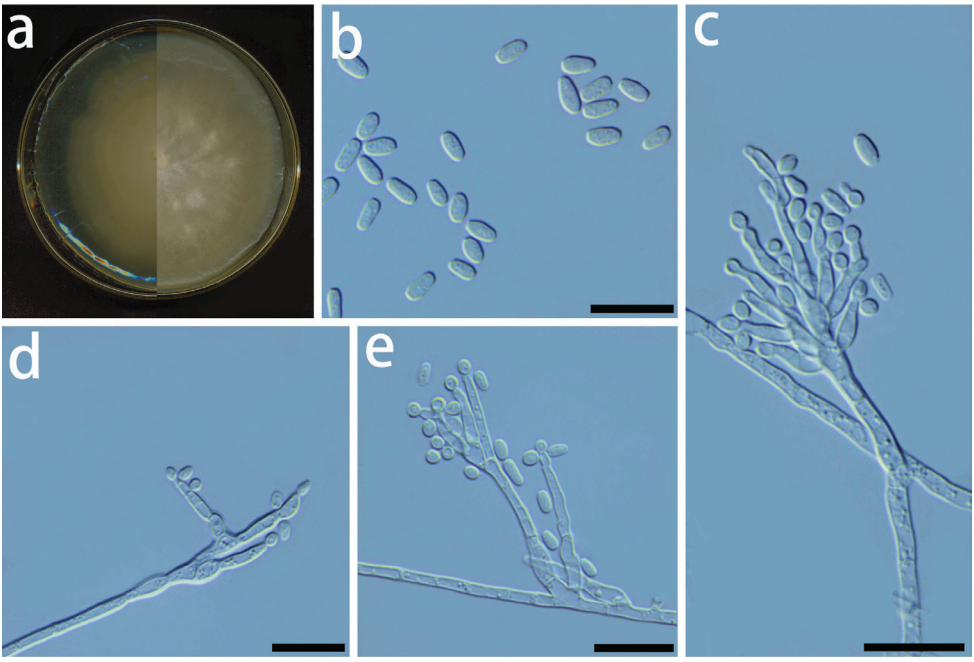

Figure 12. Morphological characters of asexual structures of *Graphilbum niveum* sp. nov. **a** left: seven-day-old culture on MEA; right: twenty-day-old culture on MEA **b** *Conidia* **c-e** conidiophores and conidia. – Scale bars: 10 μm.

Distribution. Currently known from Qingdao and Weihai City in Shandong Province, China.

Note. Phylogenetic analyses based on each ITS, EF, and CAL tree shows that *Gr. niveum* is phylogenetically close to *Gr. crescericum* (Figs 3–5). In the ITS tree (Fig. 3), *Gr. niveum* clustered with *Gr. crescericum* whereas they a distinct clade in the EF and CAL trees (Figs 4 and 5). In both these species, the asexual structure is hyalorhinocladiella-like. Nonetheless, the conidiophore of *Gr. niveum* is shorter than *Gr. crescericum* (14.0–56.0 vs. 16.3–69.9 μm) (Romón et al. 2014b). Additionally, the conidia of *Gr. niveum* and *Gr. crescericum* are similar in shape, but differ in sizes. The conidia of *Gr. niveum* (2.2–4.1 × 0.8–1.8 μm) are substantially smaller than those of *Gr. crescericum* (4.4–6.2 × 1.7–3.3 μm). Furthermore, the colony color of *Gr. niveum* is light brown at first, whereas that of *Gr. crescericum* is white (Romón et al. 2014b).

Graphilbum niveum emerged as a sister to *Gr. kesiyae* in the BT tree. This is because sequences for the BT gene region were unavailable for *Gr. crescericum*. *Graphilbum kesiyae* has both pesotum-like and hyalorhinocladiella-like asexual states, whereas *Gr. niveum* exclusively has the latter one. Furthermore, *Gr. niveum*'s conidiogenous cells and conidia are smaller than those of *Gr. kesiyae* (Chang et al. 2017).

7. *Sporothrix villosa* R.L. Chang & X.Y. Zhang, sp. nov.
Fig. 13
MycoBank No: 839255

Holotype. China. Shandong province: Zhujiajuan village, Huancui District, Weihai City, from *Cryphalus piceae* on *Pinus thunbergii*, 10 Oct. 2019, R. L. Chang (HMAS 249926-holotype; SNM188 = CGMCC 3.20264– ex-holotype culture).

Additional cultures checked. China. Shandong province: Zhujiajuan village, Huancui District, Weihai City, from *Cryphalus piceae* on *Pinus thunbergii*, 10 Oct. 2019, R. L. Chang (SNM162); China. Shandong province: Zhujiajuan village, Huancui District, Weihai City, from *Cryphalus piceae* on *Pinus thunbergii*, 10 Oct. 2019, R. L. Chang (SNM182).

Etymology. The name refers to the velvety colony morphology of this fungus on MEA.

Diagnosis. *Sporothrix villosa* differ from *S. abietina* by the production of smaller conidia and slow growth rate on MEA at 35 °C.

Description. Sexual morph is unknown. Asexual state sporothrix-like: the conidiophores directly arising from the vegetative hyphae, measuring (3.2–) 6.8–23.8 (–53.6) μm × (0.5–) 0.8–1.3 (–1.5) μm (Fig. 13b, d and e); conidia hyaline, smooth, unicellular oblong to ovoid, with rounded ends, measuring (1.2–) 1.8–2.6 (–4.1) × (0.7–) 0.8–1.1 (–1.4) μm (Fig. 13c).

Culture characteristics. The colonies are white in color on MEA. Mycelia were submerged in the agar. The optimal temperature for growth is 25 °C, reaching 21.1 mm diam in 10 d. Growth is extremely slow at 35°C 3 mm diam in 10 days. No growth was observed at 5 °C.

Distribution. Currently known from Weihai City in Shandong Province, China.

Note. *Sporothrix villosa* is closely related to two fungal isolates recovered from China in CAL tree, and another two isolates recovered from the USA in ITS and BT trees, which were previously identified as *S. cf. abietina*. This taxon is phylogenetically distinct from all other species in the *S. gossypina* species complex (Figs 6–8). Six et al. (2011) classified all the isolates from China, Canada, the USA, New Zealand, Korea, and South Africa that were close to the ex-type cultures on the BT tree as *S. abietina*. However, these selected isolates did not form a monophyletic clade. Later, in the phylogenies using BT and CAL gene-regions, these isolates of *S. abietina* did not cluster with the ex-type isolates of *S. abietina*. Therefore, these isolates were provisionally identified as *S. cf. abietina* (Romón et al. 2014a; Romón et al. 2014b). Our phylogenetic analyses indicated that isolates classified as *S. abietina* (Six et al. 2011) plausibly included several phylogenetic distinct species. In this study, *Sporothrix villosa* recovered produced a sporothrix-like asexual morph similar to other species in the complex. Furthermore, the conidia of *S. villosa* (Fig. 13c) are smaller than those of *S. abietina* (1.2–4.1 × 0.7–1.4 vs. 4–7.5 × 1–2 μm) (Marmolejo and Butin 1990). Unlike *S. abietina*, *S. villosa* can grow slowly at 35 °C.

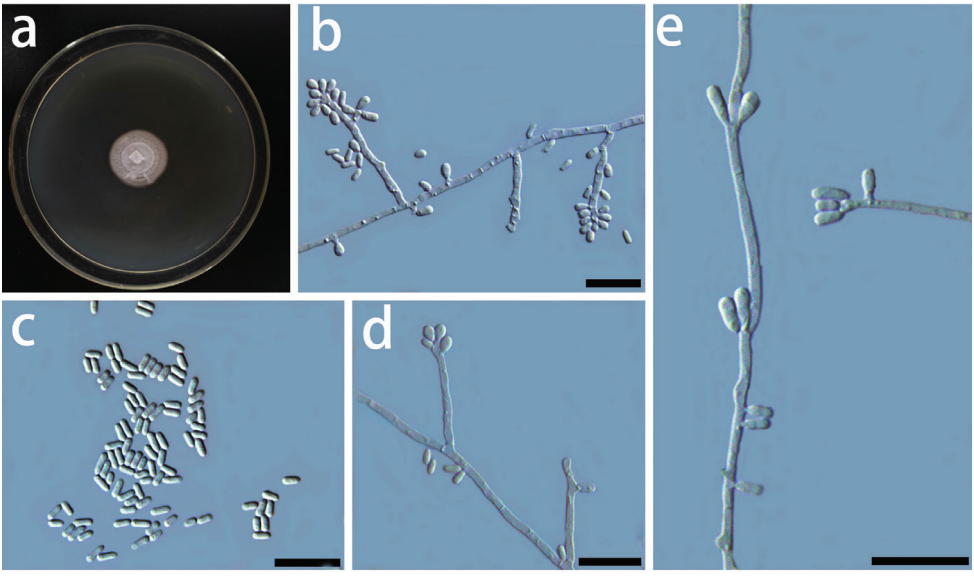

Figure 13. Morphological characters of asexual structures of *Sporothrix villosa* sp. nov. **a** fourteen-day-old culture on MEA **b-e** conidiophores and conidia. – Scale bars: 10 μm.

Discussion

In the present study, we collected *Cryphalus piceae* and their galleries from various pine forests located near Qingdao, Weihai, and Yantai cities in the Shandong province of China. From these beetles and galleries, we recovered 175 isolates of ophiostomatoid fungi representing seven well-defined genera. These genera were *Ceratocystiopsis*, *Graphilbum*, *Graphium*, *Ophiostoma*, and *Sporothrix*. Based on molecular and morphological data, the data indicated that five of the ophiostomatoid fungal species recovered in this study were previously undescribed. Hence, we newly described these ophiostomatoid species as *C. yantaiensis*, *C. weihaiensis*, *Gr. translucens*, *Gr. niveum*, and *S. villosa*.

Ophiostoma ips was one of the most frequently isolated ophiostomatoid fungi in China and this study (Lu et al. 2009; Chang et al. 2017; Wang et al. 2018; Chang et al. 2019). Across China, this fungus was also found associated with various species of mites and bark beetles (Chang et al. 2017). As reported for *Sporothrix* sp.1, in the symbiotic relationship between *M. alternatus-B. xylophilus*-ophiostomatoid fungi, *O. ips* substantially influences the survival and reproduction of the other two partners (Niu et al. 2012; Zhao et al. 2013). Earlier, *O. ips* was also isolated from *M. alternatus*, but its specific function in this symbiotic relationship is still unknown (Zhao et al. 2018). Therefore, it is not unreasonable to hypothesize that this symbiotic fungus also influences the life history and population of its vector and associated nematode.

Cryphalus piceae vectors diverse groups of fungi and nematodes. At least sixty fungal species have been found associated with this beetle. Globally, the diversity of fungi

that are associated with *Cr. piceae* varies greatly (Ohtaka et al. 2002a; Ohtaka et al. 2002b; Jankowiak and Kolarik 2010; Jankowiak et al. 2017a; Jankowiak and Bilanski 2018). In Europe, several *Geosmithia* species were found associated with *Cr. piceae* (Jankowiak and Kolarik 2010; Kolařík and Jankowiak 2013; Jankowiak and Bilanski 2018). However, we did not recover any *Geosmithia* in this study. In Poland and Japan, the most frequently isolated ophiostomatoid fungi derived from *Cr. piceae* was *O. piceae*, *Leptographium europhioides* and *O. subalpinum*, respectively (Ohtaka et al. 2002b; Yamaoka et al. 2004; Jankowiak and Kolarik 2010). However, in our study, the dominant fungal species was *O. ips*. A similar trend was also reported from other ophiostomatoid fungi-bark beetle relationships, such as those with *Ips typographus* and *Dendroctonus valens* (Taerum et al. 2013; Chang et al. 2019). This data suggests that the relationship between bark beetles and their fungal associates is casual.

This shift in the diversity of ophiostomatoid fungi that are associated with bark beetles is possibly influenced by both climatic factors and host tree species. Previously, Linnakoski et al. (2016b) indicated that temperature can significantly influence the diversity of fungi that are associated with bark beetles. This is not an unreasonable hypothesis because the climatic conditions in China, Japan, and Poland are considerably different, which may influence the fungal diversity associated with various species of bark beetles from these regions. In China, we isolated these ophiostomatoid fungi from *Cr. piceae* infecting pine trees, whereas in Japan and Poland, hosts included various species of *Abies* (Ohtaka et al. 2002a; Ohtaka et al. 2002b; Yamaoka et al. 2004; Jankowiak and Kolarik 2010). Besides climate, this difference in the host tree species could have also influenced the diversity of symbiotic fungi associated with *Cr. piceae*.

Ophiostomatoid fungi are an enigmatic taxonomic group (De Beer et al. 2013). As reported previously and in the present study, the morphological differences between the species are often slim (De Beer and Wingfield 2013; Chang et al. 2019). Additionally, marker genes used for phylogenetic identification frequently vary between species complexes (Linnakoski et al. 2016a; Yin et al. 2019). Isolates of ophiostomatoid fungi recovered from *Cr. piceae* in Japan were exclusively identified using morphological characters (Ohtaka et al. 2002a; Ohtaka et al. 2002b; Yamaoka et al. 2004). On the other hand, those from Poland were either based on ITS sequences (Jankowiak and Kolarik 2010) or ITS, LSU, BT and EF sequences (Jankowiak et al. 2017a). Therefore, the chances of misidentification are high, which can also influence the reported diversity of ophiostomatoid fungi associated with *Cr. piceae* from these regions.

In the last decade, more than a hundred ophiostomatoid fungi have been reported from China. Among these, almost half were previously undescribed species (Yin et al. 2016; Chang et al. 2017; Wang et al. 2018; Chang et al. 2019; Chang et al. 2020; Wang et al. 2020). Owing to climate change, the economic damage caused by these bark beetles and nematodes has exponentially increased in China (Li 2013; Tang et al. 2021), initiating studies focusing on the biology and control of these beetles (Sun et al. 2013). These studies simultaneously cataloged the diversity of symbiotic fungi associated with these beetles, influencing fungal species discovery (Sun et al. 2013; Zhao and Sun 2017).

In this study, we recovered seven species of ophiostomatoid fungi, including five previously undescribed species from the Shandong province of China. The previous study from Shandong province reported two new ophiostomatoid fungi associated with *B. xylophilus* and *M. alternatus* collected from two pine species (Wang et al. 2018). Thus far, more than 10 bark beetle species have been reported from this province (Bai 1985; Zhu et al. 1991). Prior to this study, no attempts were made to isolate ophiostomatoid fungi from the Shandong province of China. Therefore, in the future, follow-up surveys and isolations from other bark beetle species from the province will likely allow the discovery of several novel ophiostomatoid fungi.

Acknowledgments

This work is supported by the 'Startup Fund' awarded to Runlei Chang by Shandong Normal University. We are very grateful to Mr. Huade Zhang and Dr. Kaijian Teng for their assistance in collecting samples in Weihai and Yantai cities, Shandong province, China. The authors are grateful to the anonymous reviewers for their valuable comments on earlier versions of this manuscript. Prof Almuth Hammerbacher (Forestry and Agricultural Biotechnology Institute, University of Pretoria) provided substantial assistance in revising this manuscript, for which we are most grateful.

References

Altschul SF, Gish W, Miller W, Myers EW, Lipman DJ (1990) Basic local alignment search tool. J Mol Biol 215: 403–410. https://doi.org/10.1016/s0022-2836(05)80360-2

Bai J (1985) Several beetle species in Shandong provine and their control method (in Chinese). Shandong Forestry Science and Technology 54: 69–72.

Chang R, Duong T, Taerum S, Wingfield M, Zhou X, Yin M, De Beer Z (2019) Ophiostomatoid fungi associated with the spruce bark beetle *Ips typographus*, including 11 new species from China. Persoonia 42: 50–74. https://doi.org/10.3767/persoonia.2019.42.03

Chang R, Duong TA, Taerum SJ, Wingfield MJ, Zhou X, de Beer ZW (2017) Ophiostomatoid fungi associated with conifer-infesting beetles and their phoretic mites in Yunnan, China. MycoKeys 28: 19–64. https://doi.org/10.3897/mycokeys.28.21758

Chang R, Duong TA, Taerum SJ, Wingfield MJ, Zhou X, de Beer ZW (2020) Ophiostomatoid fungi associated with mites phoretic on bark beetles in Qinghai, China. IMA Fungus 11: e15. https://doi.org/10.1186/s43008-020-00037-9

Darriba D, Taboada GL, Doallo R, Posada D (2012) jModelTest 2: more models, new heuristics and parallel computing. Nature Methods 9: e772–772. https://doi.org/10.1038/nmeth.2109

De Beer ZW, Duong TA, Wingfield MJ (2016) The divorce of *Sporothrix* and *Ophiostoma*: solution to a problematic relationship. Stud Mycol 83: 165–191. http://dx.doi.org/10.1016/j.simyco.2016.07.001

De Beer ZW, Seifert KA, Wingfield MJ (2013) The ophiostomatoid fungi: their dual position in the Sordariomycetes. In: Seifert KA, De Beer ZW, Wingfield MJ (Eds) The Ophiostomatoid Fungi: Expanding Frontiers. CBS, Utrecht, The Netherlands, 1–19.

De Beer ZW, Wingfield MJ (2013) Emerging lineages in the Ophiostomatales. In: Seifert KA, De Beer ZW, Wingfield MJ (Eds) The Ophiostomatoid Fungi: Expanding Frontiers. CBS, Utrecht, The Netherlands, 21–46.

Duong TA, De Beer ZW, Wingfield BD, Wingfield MJ (2012) Phylogeny and taxonomy of species in the *Grosmannia serpens* complex. Mycologia 104: 715–732. http://dx.doi.org/10.3852/11-109

Gardes M, Bruns TD (1993) ITS primers with enhanced specificity for basidiomycetes-application to the identification of mycorrhizae and rusts. Molecular Ecology 2: 113–118. https://doi.org/10.1111/j.1365-294X.1993.tb00005.x

Glass NL, Donaldson GC (1995) Development of primer sets designed for use with the PCR to amplify conserved genes from filamentous Ascomycetes. Applied and Environmental Microbiology 61: 1323–1330. https://doi.org/10.1128/AEM.61.4.1323-1330.1995.

Hammerbacher A, Schmidt A, Wadke N, Wright LP, Schneider B, Bohlmann J, Brand WA, Fenning TM, Gershenzon J, Paetz C (2013) A common fungal associate of the spruce bark beetle metabolizes the stilbene defenses of Norway spruce. Plant Physiology 162: 1324–1336. https://doi.org/10.1104/pp.113.218610

Hausner G, Eyjólfsdóttir GG, Reid J (2003) Three new species of *Ophiostoma* and notes on *Cornuvesica falcata*. Canadian Journal of Botany 81: 40–48. https://doi.org/10.1139/b03-009

Hofstetter RW, Dinkins-Bookwalter J, Davis TS, Klepzig KD (2015) Symbiotic associations of bark beetles. In: Vega FE, Hofstetter RW (Eds) Bark beetles: Biology and ecology of native and invasive species. Academic Press, San Diego, 209–245. https://doi.org/10.1016/B978-0-12-417156-5.00006-X

Hyde K, Norphanphoun C, Maharachchikumbura S, Bhat DJ, Jones E, Bundhun D, Chen YJ, Bao D-F, Boonmee S, Calabon M, Chaiwan N, Kandawatte T, Dai D-Q, Dayarathne M, Devadatha B, Dissanayake A, Dissanayake L, Doilom M, Dong W, Zhang S (2020) Refined families of Sordariomycetes. Mycosphere 11: e1058. https://doi.org/10.5943/mycosphere/11/1/7

Jacobs K, Bergdahl DR, Wingfield MJ, Halik S, Seifert KA, Bright DE, Wingfield BD (2004) *Leptographium wingfieldii* introduced into North America and found associated with exotic *Tomicus piniperda* and native bark beetles. Mycological Research 108: 411–418. https://doi.org/10.1017/S0953756204009748

Jankowiak R, Bilanski P (2018) *Geosmithia* species associated with fir-infesting beetles in Poland. Acta Mycologica 53 pp. https://doi.org/10.5586/am.1115

Jankowiak R, Kolarik M (2010) Fungi associated with the fir bark beetle *Cryphalus piceae* in Poland. Forest Pathology 40: 133–144. doi:10.1111/j.1439-0329.2009.00620.x

Jankowiak R, Solheim H, Bilański P, Marincowitz S, Wingfield MJ (2020) Seven new species of *Graphilbum* from conifers in Norway, Poland, and Russia. Mycologia 112: 1–23. https://doi.org/10.1080/00275514.2020.1778375

Jankowiak R, Strzałka B, Bilański P, Kacprzyk M, Lukášová K, Linnakoski R, Matwiejczuk S, Misztela M, Rossa R (2017a) Diversity of Ophiostomatales species associated with conifer-

infesting beetles in the Western Carpathians. European Journal of Forest Research 136: 939–956. https://doi.org/10.1007/s10342-017-1081-0

Jankowiak R, Strzałka B, Bilański P, Linnakoski R, Aas T, Solheim H, Groszek M, de Beer ZW (2017b) Two new *Leptographium* spp. reveal an emerging complex of hardwood-infecting species in the Ophiostomatales. Antonie van Leeuwenhoek 110: 1537–1553. https://doi.org/10.1007/s10482-017-0905-8

Justesen MJ, Hansen AK, Thomsen IM, Byriel DB, Ro-Poulsen H, Ravn HP (2020) Contributions to the knowledge on biology and phenology of *Cryphalus piceae* (Coleoptera: Curculionidae: Scolytinae). Scandinavian Journal of Forest Research 35: 468–475. https://doi.org/10.1080/02827581.2020.1797868

Katoh K, Standley DM (2013) MAFFT multiple sequence alignment software version 7: improvements in performance and usability. Mol Biol Evol 30: 772–780. https://doi.org/10.1093/molbev/mst010

Klepzig KD, Six DL (2004) Bark beetle-fungal symbiosis: context dependency in complex associations. Symbiosis (Rehovot) 37: 189–205.

Kolařík M, Jankowiak R (2013) Vector Affinity and Diversity of Geosmithia Fungi Living on Subcortical Insects Inhabiting Pinaceae Species in Central and Northeastern Europe. Microbial Ecology 66: 682–700. https://doi.org/10.1007/s00248-013-0228-x

Kumar S, Stecher G, Li M, Knyaz C, Tamura K (2018) MEGA X: molecular evolutionary genetics analysis across computing platforms. Mol Biol Evol 35: 1547–1549. https://doi.org/10.1093/molbev/msy096

Li Y (2013) Causes of *Tomicus Piniperda* L. disaster in Yuxi of Yunnan province and countermeasures of prevention and control (in Chinese). Forest Resources Management 3: 40–42.

Linnakoski R, Jankowiak R, Villari C, Kirisits T, Solheim H, de Beer ZW, Wingfield MJ (2016a) The *Ophiostoma clavatum* species complex: a newly defined group in the Ophiostomatales including three novel taxa. Antonie van Leeuwenhoek 109: 987–1018. https://doi.org/10.1007/s10482-016-0700-y

Linnakoski R, Mahilainen S, Harrington A, Vanhanen H, Eriksson M, Mehtätalo L, Pappinen A, Wingfield MJ (2016b) Seasonal succession of fungi associated with *Ips typographus* beetles and their phoretic mites in an outbreak region of Finland. PloS ONE 11: e0155622. https://doi.org/10.1371/journal.pone.0155622

Lu M, Zhou XD, De Beer ZW, Wingfield MJ, Sun JH (2009) Ophiostomatoid fungi associated with the invasive pine-infesting bark beetle, *Dendroctonus valens*, in China. Fungal Diversity 38: 133–145.

Marincowitz S, Duong TA, De Beer ZW, Wingfield MJ (2015) *Cornuvesica*: A little known mycophilic genus with a unique biology and unexpected new species. Fungal Biology 119: 615–630. http://dx.doi.org/10.1016/j.funbio.2015.03.007

Marmolejo J, Butin H (1990) New conifer-inhabiting species of *Ophiostoma* and *Ceratocystiopsis* (Ascomycetes, Microascales) from Mexico. Sydowia 42: 193–199.

Michalski J, Mazur A (1999) Bark Beetles. A practical guide for foresters. (Korniki. Praktyczny przewodnik dLa leśników). (in Polish). Oficyna Edytorska Wydawnictwo Świat, Warszawa 125: 215–215. https://doi.org/10.1046/j.1439-0418.2001.0502b.x

Miller MA, Pfeiffer W, Schwartz T (2010) Creating the CIPRES Science Gateway for inference of large phylogenetic trees. Gateway Computing Environments Workshop (GCE).

Institute of Electrical and Electronics Engineers, New Orleans, LA, 1–8 pp. https://doi.org/10.1109/GCE.2010.5676129

Nel WJ, Wingfield MJ, de Beer ZW, Duong TA (2021) Ophiostomatalean fungi associated with wood boring beetles in South Africa including two new species. Antonie van Leeuwenhoek. https://doi.org/10.1007/s10482-021-01548-0

Niu H, Zhao L, Lu M, Zhang S, Sun J (2012) The ratio and concentration of two monoterpenes mediate fecundity of the pinewood nematode and growth of its associated fungi. PloS one 7: e31716 https://doi.org/10.1371/journal.pone.0031716

Ohtaka N, Masuya H, Kaneko S, Yamaoka Y (2002a) Two *Ophiostoma* species associated with bark beetles in wave-regenerated *Abies veitchii* forests in Japan. Mycoscience 43: 0151–0157. https://doi.org/10.1007/s102670200022

Ohtaka N, Masuya H, Kaneko S, Yamaoka Y, Ohsawa M (2002b) Ophiostomatoid fungi associated with bark beetles on *Abies veitchii* in wave-regenerated forests. Journal of Forest Research 7: 145–151. https://doi.org/10.1007/BF02762603

Plattner A, Kim J-J, Reid J, Hausner G, Lim YW, Yamaoka Y, Breuil C (2009) Resolving taxonomic and phylogenetic incongruence within species *Ceratocystiopsis minuta*. Mycologia 101: 878–887. https://doi.org/10.3852/08-132

Reid J, Hausner G (2010) The epitypification of *Ophiostoma minutum*, now *Ceratocystiopsis minuta*. Mycotaxon 113: 463–474. https://doi.org/10.5248/113.463

Romón P, De Beer ZW, Fernández M, Diez J, Wingfield BD, Wingfield MJ (2014a) Ophiostomatoid fungi including two new fungal species associated with pine root-feeding beetles in northern Spain. Antonie van Leeuwenhoek 106: 1167–1184. https://doi.org/10.1007/s10482-014-0286-1

Romón P, De Beer ZW, Zhou XD, Duong TA, Wingfield BD, Wingfield MJ (2014b) Multigene phylogenies of Ophiostomataceae associated with Monterey pine bark beetles in Spain reveal three new fungal species. Mycologia 106: 119–132. https://doi.org/10.3852/13-073

Ronquist F, Teslenko M, van der Mark P, Ayres DL, Darling A, Höhna S, Larget B, Liu L, Suchard MA, Huelsenbeck JP (2012) MrBayes 3.2: efficient Bayesian phylogenetic inference and model choice across a large model space. Systematic biology 61: 539–542. https://doi.org/10.1093/sysbio/sys029

Six D, Beer ZW, Duong T, Carroll A, Wingfield M (2011) Fungal associates of the lodgepole pine beetle, *Dendroctonus murrayanae*. Antonie van Leeuwenhoek 100: 231–244. https://doi.org/10.1007/s10482-011-9582-1

Stamatakis A (2014) RAxML version 8: a tool for phylogenetic analysis and post-analysis of large phylogenies. Bioinformatics 30: 1312–1313. https://doi.org/10.1093/bioinformatics/btu033

Suh DY, Hyun MW, Kim JJ, Son SY, Kim SH (2013) *Ophiostoma ips* from pinewood nematode vector, Japanese pine sawyer beetle (*Monochamus alternatus*), in Korea. Mycobiology 41: 59–62. https://doi.org/10.5941/MYCO.2013.41.1.59

Sun J, Lu M, Gillette NE, Wingfield MJ (2013) Red turpentine beetle: innocuous native becomes invasive tree killer in china. Annu Rev Entomol 58: 293–311. https://doi.org/10.1146/annurev-ento-120811-153624

Taerum SJ, Duong TA, De Beer ZW, Gillette N, Sun JH, Owen DR, Wingfield MJ (2013) Large shift in symbiont assemblage in the invasive red turpentine beetle. PloS ONE 8: e78126. http://dx.doi.org/10.1371/journal.pone.0078126

Tamura K, Stecher G, Peterson D, Filipski A, Kumar S (2013) MEGA6: molecular evolutionary genetics analysis version 6.0. Mol Biol Evol 30: 2725–2729. https://doi.org/10.1093/molbev/mst197

Tang X, Yuan Y, Li X, Zhang J (2021) Maximum entropy modeling to predict the impact of climate change on pine wilt disease in China. Frontiers in Plant Science 12. https://doi.org/10.3389/fpls.2021.652500

Vilgalys R, Hester M (1990) Rapid genetic identification and mapping of enzymatically amplified ribosomal DNA from several *Cryptococcus* species. Journal of Bacteriology 172: 4238–4246. https://doi.org/10.1128/jb.172.8.4238-4246.1990

Wadke N, Kandasamy D, Vogel H, Lah L, Wingfield BD, Paetz C, Wright LP, Gershenzon J, Hammerbacher A (2016) The bark-beetle-associated fungus, *Endoconidiophora polonica*, utilizes the phenolic defense compounds of its host as a carbon source. Plant Physiology 171: 914–931.

Wang H, Lun Y, Decock C, Lu Q, Liu H, Zhang X (2018) Ophiostomatoid fungi associated with pines infected by *Bursaphelenchus xylophilus* and *Monochamus alternatus* in China, including three new species. MycoKeys 39: 1–27. https://doi.org/10.3897/mycokeys.39.27014

Wang Z, Liu Y, Wang H, Meng X, Liu X, Decock C, Zhang X, Lu Q (2020) Ophiostomatoid fungi associated with *Ips subelongatus*, including eight new species from northeastern China. IMA Fungus 11: e3. https://doi.org/10.1186/s43008-019-0025-3

White TJ, Bruns T, Lee S, Taylor JW (1990) Amplification and direct sequencing of fungal ribosomal RNA genes for phylogenetics. In: Innis MA, Gelfand DH, Sninsky JJ, White TJ (Eds) PCR protocols: a guide to methods and applications. Academic Press, San Diego (California), 315–322. https://doi.org/10.1016/B978-0-12-372180-8.50042-1

Wingfield MJ (1987) Fungi associated with the pine wood nematode, *Bursaphelenchus Xylophilus*, and cerambycid beetles in Wisconsin. Mycologia 79: 325–328. https://doi.org/10.1080/00275514.1987.12025713

Wingfield MJ, Seifert KA, Webber JF, Society AP (1993) *Ceratocystis* and *Ophiostoma*: taxonomy, ecology, and pathogenicity. American Phytopathological Society,

Yamaoka Y, Masuya H, Ohtaka N, Goto H, Kaneko S, Kuroda Y (2004) *Ophiostoma* species associated with bark beetles infesting three *Abies* species in Nikko, Japan. Journal of Forest Research 9: 67–74. https://doi.org/10.1007/s10310-003-0056-9

Yin M, Wingfield MJ, Zhou X, Linnakoski R, de Beer ZW (2019) Taxonomy and phylogeny of the *Leptographium olivaceum* complex (Ophiostomatales, Ascomycota), including descriptions of six new species from China and Europe. MycoKeys 60: 93–123. https://doi.org/10.3897/mycokeys.60.39069

Yin ML, Wingfield MJ, Zhou XD, De Beer ZW (2016) Multigene phylogenies and morphological characterization of five new *Ophiostoma* spp. associated with spruce-infesting bark beetles in China. Fungal Biology 120: 454–470. http://dx.doi.org/10.1016/j.funbio.2015.12.004

Zhao L, Ahmad F, Lu M, Zhang W, Wickham JD, Sun J (2018) Ascarosides promote the prevalence of ophiostomatoid fungi and an invasive pathogenic nematode, *Bursaphelenchus xylophilus*. Journal of Chemical Ecology 44: 701–710. https://doi.org/10.1007/s10886-018-0996-3

Zhao L, Lu M, Niu H, Fang G, Zhang S, Sun J (2013) A native fungal symbiont facilitates the prevalence and development of an invasive pathogen-native vector symbiosis. Ecology 94: 2817–2826. https://doi.org/10.1890/12-2229.1

Zhao L, Mota M, Vieira P, Butcher RA, Sun J (2014) Interspecific communication between pinewood nematode, its insect vector, and associated microbes. Trends in Parasitology 30: 299–308. nhttp://dx.doi.org/10.1016/j.pt.2014.04.007

Zhao L, Sun J (2017) Pinewood nematode *Bursaphelenchus xylophilus* (Steiner and Buhrer) Nickle. In: Wan F, Jiang M, Zhan A (Eds) Biological Invasions and Its Management in China: Volume 2. Springer Singapore, Singapore, 3–21. https://doi.org/10.1007/978-981-10-3427-5_1

Zhu C, Liu S, Lu X (1991) Species diversity and treatment of beetles in Shandong province (in Chinese). Shandong Forestry Science and Technology 2: 53–56.

Supplementary material 1

Ophiostomatoid fungi associated with *Cryphalus piaceae* in Shandong province in eastern China

Authors: Runlei Chang, Xiuyu Zhang, Hongli Si, Guoyan Zhao, Xiaowen Yuan, Tengteng Liu, Tanay Bose, Meixue Dai

Data type: molecular data

Explanation note: Maximum likelihood phylogeny of *Graphium* using complete ITS and partial EF gene regions. The isolates recovered in this study are highlighted in color and in bold font. ML and MP bootstrap support values ≥ 75 are indicated at the nodes as ML/MP. Bold branches indicate posterior probabilities values ≥ 0.9. T indicates ex-type cultures.

Link: https://doi.org/10.3897/mycokeys.83.70925.suppl1

Supplementary material 2

Figure S2

Authors: Runlei Chang, Xiuyu Zhang, Hongli Si, Guoyan Zhao, Xiaowen Yuan, Tengteng Liu, Tanay Bose, Meixue Dai

Data type: phylogenetic data

Explanation note: Maximum likelihood phylogeny of *Ophiostoma ips* species complex using complete ITS and partial BT gene regions. The isolates recovered in this study are highlighted in color and in bold font. ML and MP bootstrap support values ≥ 75 are indicated at the nodes as ML/MP. Bold branches indicate posterior probabilities values ≥ 0.9. T indicates ex-type cultures.

Link: https://doi.org/10.3897/mycokeys.83.70925.suppl2

Supplementary material 3

Table S1

Authors: Runlei Chang, Xiuyu Zhang, Hongli Si, Guoyan Zhao, Xiaowen Yuan, Tengteng Liu, Tanay Bose, Meixue Dai

Data type: phylogenetic data

Explanation note: List of ophiostomatioid fungi used for phylogenetic analyses. T = ex-type culture.

Link: https://doi.org/10.3897/mycokeys.83.70925.suppl3